Characterisation of Transcription Factor SPL15, an Integrator of Multiple Flowering Time Pathways

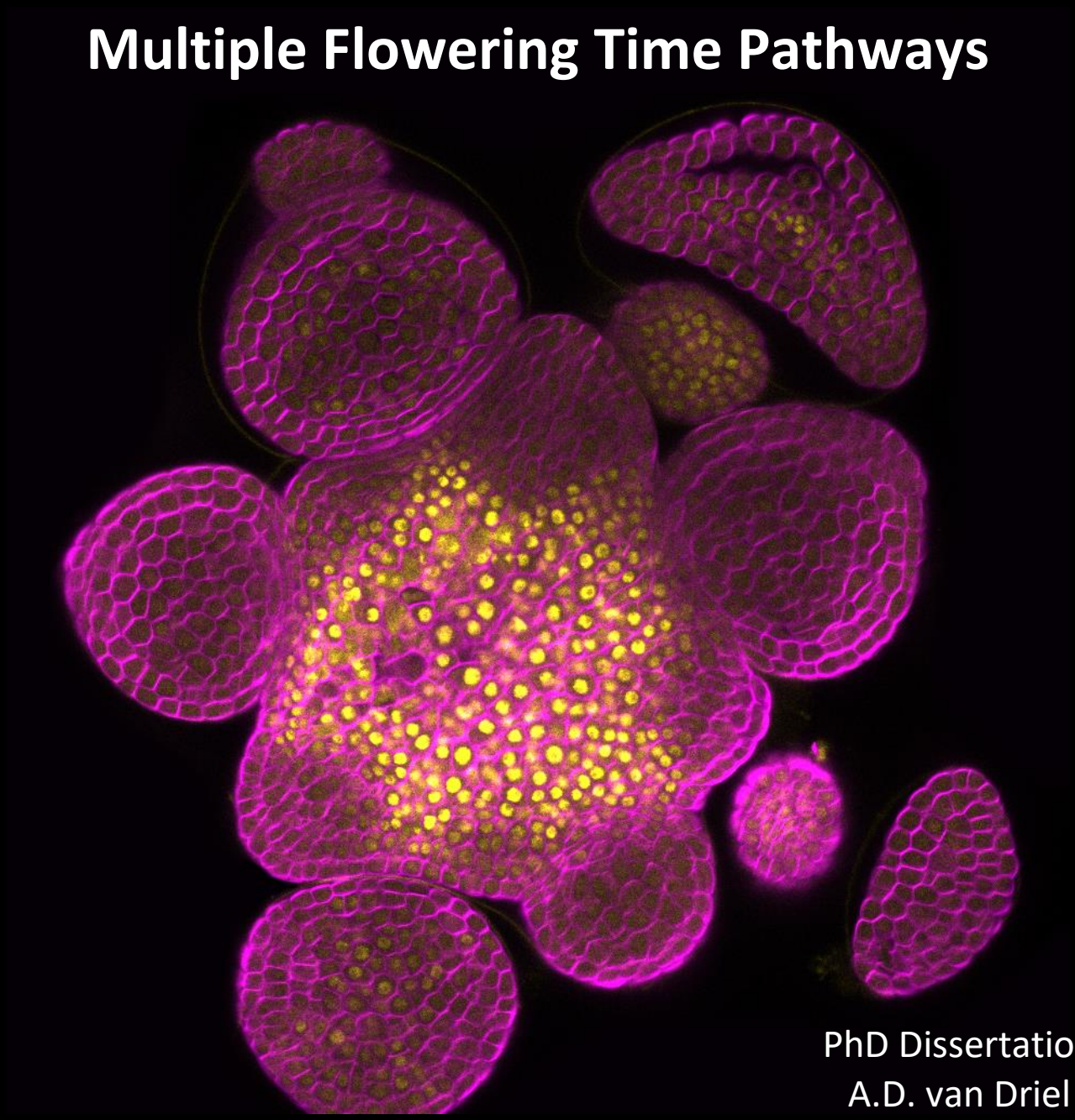

PhD Dissertation
A.D. van Driel

Cologne, 2020

Characterisation of Transcription Factor SPL15, an Integrator of Multiple Flowering Time Pathways

Inaugural - Dissertation

zur

Erlangung des Doktorgrades

der Mathematisch-Naturwissenschaftlichen Fakultät

der Universität zu Köln

vorgelegt von

Annabel Dirksita van Driel

aus Gorinchem, die Niederlande

Köln, 2020

Berichterstatter:	**Prof. Dr. George Coupland**
	Prof. Dr. Ute Höcker
Prüfungsvorsitzender:	**Prof. Dr. Martin Hülskamp**
Tag der Disputation:	**28. August 2020**

Die vorliegende Arbeit wurde am Max-Planck-Institut für Pflanzenzüchtungsforschung in Köln in der Abteilung für Entwicklungsbiologie der Pflanzen (Direktor Prof. Dr. G. Coupland), Arbeitsgruppe Prof. Dr. George Coupland durchgeführt.

The work described in this thesis was conducted at the Max Planck Institute for Plant Breeding Research in the Department of Plant Developmental Biology (Director: Prof. Dr. George Coupland) under the supervision of Prof. Dr. George Coupland.

Abstract

The transition from vegetative to reproductive development in plants is tightly controlled to ensure their reproductive success. Plants integrate many different environmental signals to flower at the appropriate time, and complex regulatory networks underlie this decision.

In *Arabidopsis thaliana,* the model organism for plant molecular research, the timing of floral transition is influenced by environmental cues, which include temperature and day length, and by internal factors, including the age of the plant and the levels of the phytohormone gibberellin. During the transition, Arabidopsis switches from producing leaves to producing flowers, a process that includes morphological and identity changes in the shoot apical meristem (SAM). In favourable environmental conditions, such as floral inductive long-days, Arabidopsis accelerates the floral transition and quickly bolts and flowers. In the absence of floral inductive signals, these plants still undergo the floral transition, but do so later after producing many more leaves.

The transcription factor SQUAMOSA PROMOTER BINDING PROTEIN LIKE 15 (SPL15) promotes flowering in non-inductive conditions. SPL15 integrates signals from multiple floral induction pathways at the shoot apical meristem and is proposed to directly activate transcription of two other genes with a prominent function in flowering: *FRUITFULL* (*FUL*), which encodes a MADS box transcription factor, and *MICRORNA172b* (*MIR172B*), which encodes a short non-coding RNA. However, the precise role of SPL15 in floral induction remains unknown.

To gain understanding of the importance of SPL15 targets and other downstream components, I genetically assessed their contribution to floral induction. I found that *FUL* and *MIR172B* were important for SPL15 function during floral induction. However, in their absence, increased expression of SPL15 still induced early bolting of the inflorescence, but could not induce floral development. These analyses suggested that SPL15 regulates more target genes than *FUL* and *MIR172B* during the floral transition. Subsequently, I identified the binding sites of SPL15 in the *FUL* promoter, and studied the effect of mutating them. This revealed that SPL15 is not the only SPL protein that recognises these sites to regulate floral transition. I therefore propose that during vegetative growth, other SPLs bind there to repress the expression of *FUL*.

Lastly, I set out to identify additional putative target genes of SPL15 by two complementary transcriptome analyses. The resulting high confidence list of putative target genes of SPL15 showed that SPL15 likely regulates several other genes with described functions in floral induction. In addition, SPL15 regulates a set of genes with functions in cell proliferation, which might be relevant for the morphological changes occurring in the SAM during the floral transition.

Altogether this thesis has contributed to a better understanding of how SPL15 regulates different stages of the floral transition in *A. thaliana* under non-inductive conditions.

Zusammenfassung

In Pflanzen ist der Übergang von vegetativer zu reproduktiver Entwicklung streng kontrolliert, um den Fortpflanzungserfolg sicherzustellen. Um zur richtigen Zeit zu blühen integrieren Pflanzen eine Vielzahl verschiedener Umweltfaktoren und dieser Entscheidung liegen komplexe regulatorische Netzwerke zugrunde.

Im *Arabidopsis thaliana*, dem Modellorganismus der molekulare Pflanzenforschung, wird der Zeitpunkt dieses floralen Übergangs von Umwelteinflüssen wie Temperatur und Tageslänge, sowie von endogenen Faktoren wie dem Alter der Pflanze und dem Gehalt an Phytohormon Gibberellin beeinflusst. Während des Übergangs schwenkt Arabidopsis von der Blatt- zur Blütenproduktion um, ein Prozess der mit morphologischen Veränderungen im Sprossapikalmeristem (SAM); jenem Gewebe, das Stammzellen für die Sprossbildung beherbergt. Unter günstigen Umweltbedingungen, wie z. B. an blühinduzierenden langen Tagen, beschleunigt Arabidopsis den floralen Übergang, schießt und beginnt schnell mit der Blüte. In Abwesenheit induktiver Signale verzögert sich dieser Prozess, letztendlich führt er aber auch in Pflanzen unter ungünstigen Bedingungen zur Blüte.

Der Transkriptionsfaktor SQUAMOSA PROMOTER BINDING PROTEIN LIKE 15 (SPL15) wird für die Blüte unter solchen nicht-induktiven Bedingungen benötigt. SPL15 integriert dabei die Signale mehrerer floraler Induktionswege im SAM. Die Transkription zweier weiterer Gene mit herausragender Funktion in der Blüte wird direkt von SPL15 aktiviert: *FRUITFULL* (*FUL*) und *MICRORNA172b* (*MIR172B*). Bisher bleibt es jedoch unklar, wie genau SPL15 die Blüte induziert.

Um die Bedeutung von SPL15 Zielen und anderen nachgeschalteten Komponenten zu verstehen, habe ich deren SPL15-vermittelten Beitrag zur Blühinduktion genetisch analysiert. Ich fand heraus, dass *FUL* und *MIR172B* für die SPL15-Funktion in der Blühinduktion von großer Bedeutung waren, dass aber selbst in ihrer Abwesenheit eine Überexpression von SPL15 ausreichte um ein Schießen, nicht jedoch die Blüte, zu induzieren. Diese Analysen legen nahe, dass SPL15 zusätzliche Zielgene reguliert, um den floralen Übergang zu fördern.

Anschließend untersuchte ich den Effekt von Mutationen in mutmaßlichen SPL15-Bindestellen im *FUL*-Promotor. Dies zeigte, dass diese Bindestellen im FUL-Promotor nicht einzig von SPL15 verwendet werden, sondern dass vermutlich andere SPLs während des vegetativen Wachstums die Expression von FUL unterdrücken.

Zu guter Letzt machte ich mich daran, neue Zielgen-Kandidaten von SPL15 durch Transkriptomanalyse zu identifizieren. Die daraus resultierende Liste hoher Konfidenz mit möglichen SPL15 Zielen zeigte, dass wahrscheinlich mehrere weitere von SPL15 regulierte Gene eine beschriebene Funktion in der Blüteninduktion besitzen. Außerdem könnte SPL15 direkt eine Reihe von Genen mit Funktion in der Zellproliferation regulieren, was für die morphologischen Veränderungen im SAM während des Übergangs zur Blüte relevant sein könnte.

Zusammengefasst trägt diese Doktorarbeit zu einem vertieften und differenzierteren Verständnis bei, wie SPL15 den floralen Übergang unter nicht-induktiven Bedingungen in Arabidopsis reguliert.

Table of Contents

Chapter 1:
Introduction

Gene regulatory networks in plant development

Gene regulatory networks control complex processes in plants

Organisms occur in most diverse shapes, sizes and colours. Plants have evolved highly specialised reproductive structures, life histories and survival strategies to optimize their fitness. Millions of years of natural selection in angiosperms has led to the evolution of complex gene regulatory networks (GRNs) that control plant growth and development (Gehrke & Shubin, 2016; Howard & Davidson, 2004; Kaufmann, Pajoro, *et al.*, 2010; Levine & Davidson, 2005). These GRNs consist of regulatory molecules such as proteins and non-coding RNAs that control gene expression. Proteins can interact with each other and with gene-regulatory regions to control gene expression patterns that govern plant development and its responsiveness to the environment. Cues from the environment can alter the activity of GRNs to initiate developmental programmes, such as reproductive development, to cease growth or seed germination. These processes are tightly controlled and often include parallel signalling pathways and redundant gene functions.

The transition from vegetative to reproductive growth in plants is one of the processes controlled by complex GRNs and these have been extensively studied in the model plant *Arabidopsis thaliana* (Arabidopsis) also known as thale cress (D. Chen *et al.*, 2018; Dong *et al.*, 2012; Schmid *et al.*, 2003). In Arabidopsis, the reproductive transition involves major changes in organ development, from the production of leaves to the production of flowers. The shoot apical meristem (SAM) contains a population of stem cells that produces these aboveground organs and also undergoes morphological changes during the transition from a vegetative to reproductive identity. This transition occurs after exposure to inductive external cues, but Arabidopsis plants will eventually flower even in the absence of these cues.

In this introduction, I will first describe in detail the GRNs that underlie the different floral induction pathways and finally, I will introduce how this thesis contributes to a deeper understanding of the regulation of floral induction.

The floral transition in *Arabidopsis thaliana*

Life history and floral transition in *Arabidopsis thaliana*

Arabidopsis is a facultative long-day plant, which means that the floral transition occurs earlier when it grows in long days (late spring/summer), but also occurs in short days (autumn). Arabidopsis is an annual plant that will cease growth after flowering after which it senesces and dies. Therefore, it has only one chance to successfully undergo floral transition, and its fitness is dependent on appropriate timing of this transition. Once Arabidopsis undergoes the floral transition, it is fully committed to flowering. During this transition, the SAM changes shape, size and starts to exclusively produce floral primordia, instead of leaf primordia (Fig. 1.2).

Floral induction in Arabidopsis is a tightly regulated process that involves complex GRNs and is coordinated by several floral integrator proteins, which include FLOWERING LOCUS T (FT), SUPPRESSOR OF OVEREXPRESSION OF CONSTANS 1 (SOC1) and SQUAMOSA PROMOTER BINDING PROTEIN-LIKE 15 (SPL15; Fig. 1.1; Andrés & Coupland, 2012; Hyun *et al.*, 2016; Jung *et al.*, 2012; Lee *et al.*, 2000; Lee *et al.*, 2006). These floral integrators are points of convergence of various external and internal floral-induction cues.

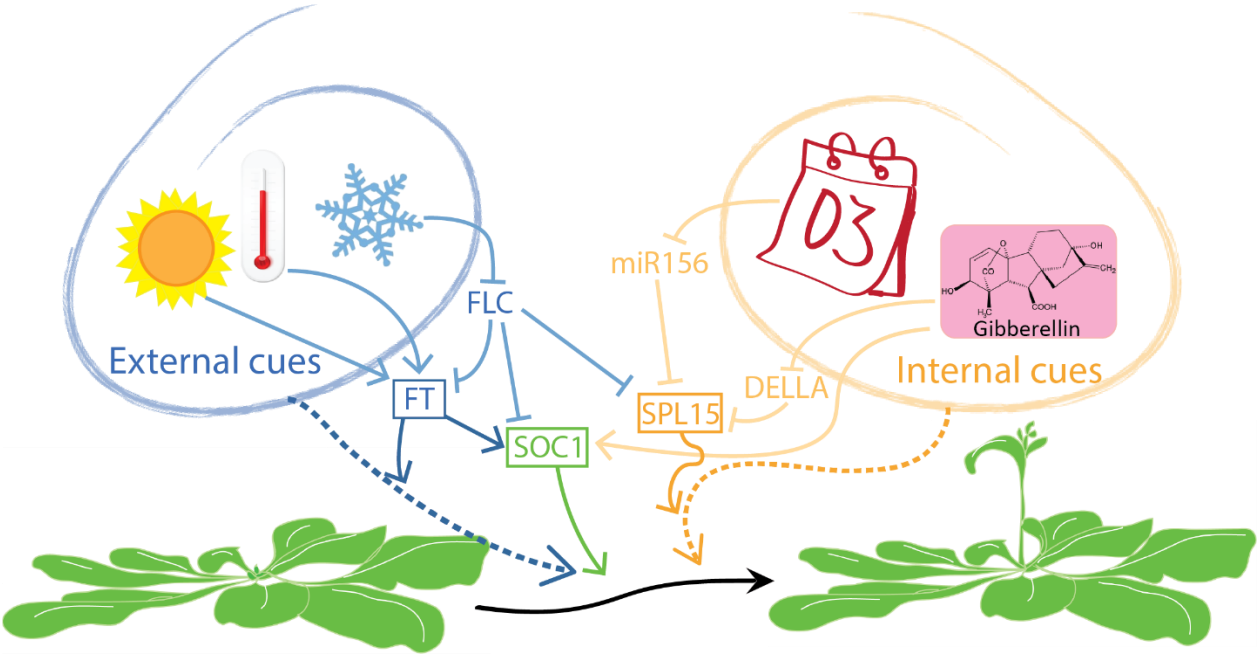

Figure 1.1. Diagram of floral induction in Arabidopsis by external and internal cues. Floral integrators are marked with a box.

They orchestrate the activation of genes that promote floral induction, the repression of genes that repress floral induction, as well as the expression of genes that specify the reproductive identity of the floral meristem. When these floral meristem identity genes, such as *APETALA1* (*AP1*) or *LEAFY* (*LFY*) are expressed, the transition of the SAM from a vegetative to a reproductive identity is complete, and subsequently only floral primordia will be produced (Fig. 1.2; Ferrándiz *et al.*, 2000; Huala & Sussex, 1992; Parcy *et al.*, 2002; Simon *et al.*, 1996, Torti *et al.*, 2012).

The floral repressor APETALA 2 (AP2), and possibly other AP2-LIKE family members, such as TARGET OF EAT (TOE) 1-3, SCHNARCHZAPFEN (SNZ) and SCHLAFMÜTZE (SMZ), strongly repress expression of the floral meristem identity genes (Fig. 1.2; Krogan *et al.*, 2012; Yant *et al.*, 2010). AP2 also directly represses the floral integrator *SOC1*, the floral promoter *FRUITFULL* (*FUL*), and *MICRORNA172B* (*MIR172B* (Yant *et al.*, 2010). To overcome this repression by AP2, the floral integrators act on *FUL* and *MIR172* genes that are also repressors of *AP2* expression. FUL directly represses transcription of *AP2, SNZ* and possibly other *AP2-Ls,* whereas *MIR172* post-transcriptionally inhibits all of the *AP2-Ls* (Fig. 1.2; Aukerman & Sakai, 2003; Balanzà *et al.*, 2018; Xuemei Chen, 2004; Zhu & Helliwell, 2011). FUL also promotes the expression of *LFY*, which in turn, activates *AP1* and its homologue *CAULIFLOWER* in floral meristems (Fig. 1.2; Balanzà *et al.*, 2014, 2018; Ferrándiz *et al.*, 2000; Goslin *et al.*, 2017; Mandel & Yanofsky, 1995a, 1995b; Serrano-Mislata *et al.*, 2017). Moreover, many other floral integrators also directly transcriptionally activate *LFY* and *AP1* (C. Liu *et al.*, 2008; Scott D. Michaels, Ditta, *et al.*, 2003; Ruiz-García *et al.*, 1997; Teper-Bamnolker & Samach, 2005; A. Yamaguchi *et al.*, 2009). AP1-function is restricted to determinate floral meristems, where it regulates floral organ specification (Busch *et al.*, 1999; Gregis *et al.*, 2006, 2009; C. Liu *et al.*, 2009; Weigel & Meyerowitz, 1993). Floral induction thus includes a change in the balance between floral repressors and floral promoters (Fig. 1.2).

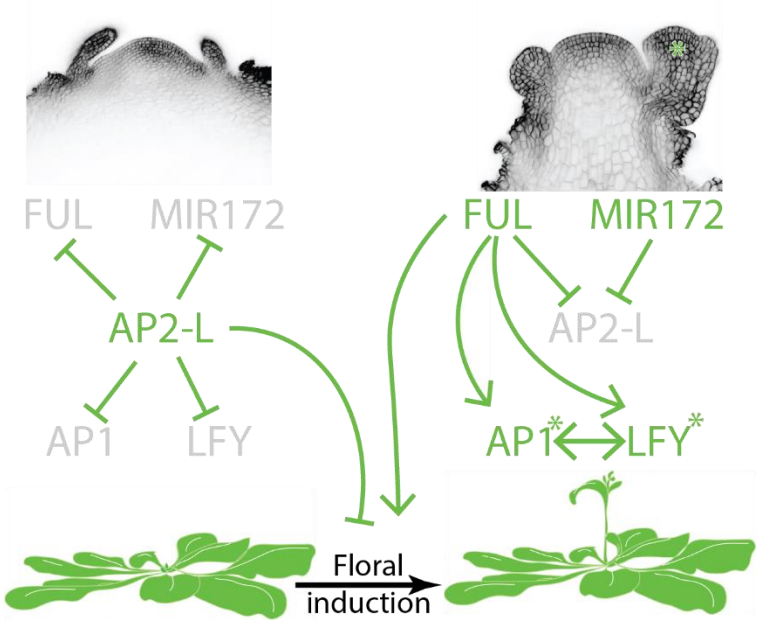

Figure 1.2. Diagram of the floral transition in *Arabidopsis.* The images show the morphology of a vegetative and an inflorescence SAM. Below are simplified interactions occur before floral induction (left) and at the end of floral induction (right). Asterisks indicate expression specific to the floral meristem as indicated in the top right image.

Floral induction is accelerated upon exposure to specific permissive conditions. The integration of environmental cues allows the plant to respond rapidly to appropriate conditions. Arabidopsis will still induce flowering in the absence of such cues, due to default endogenous signals. External cues include day length (photoperiod), vernalization (exposure to a period of extended cold), ambient temperature, and biotic and abiotic stresses (Fig. 1.1). Endogenous cues include levels of the phytohormone gibberellin (GA) as well as an internal timer of the plant's age, termed the age pathway (Fig. 1.1).

Gene regulatory networks underlying floral induction in *Arabidopsis thaliana:* external cues

Photoperiod and the importance of *FLOWERING LOCUS T*

Photoperiod, or day length, is one of the most important external cues for plants. Photoperiod marks the seasons of the year, and unlike temperature, changes in photoperiod are highly consistent between years. It is thus a reliable timer for floral induction during a specific season. A long photoperiod accelerates the transition from vegetative to reproductive growth in Arabidopsis.

The plant circadian clock provides the timing mechanism for day length measurement. This internal clock consists of multiple transcription-factor loops that cause the circadian expression of output genes (Oakenfull & Davis, 2017; Shim *et al.*, 2017a). The activity of some of these output genes is influenced by light and depending on when and if their expression peaks at a certain time during the photoperiod defines whether its protein will be active or not (external coincidence model; Andrés & Coupland, 2012; Shim *et al.*, 2017b).

One of the output genes that shows a circadian expression pattern is *CONSTANS* (*CO*), which encodes an important B-box transcription factor involved in the promotion of flowering under long-day (LD) conditions (Putterill *et al.*, 1995; Suárez-López *et al.*, 2001). *co* mutants flower later in LD conditions, but not under SD conditions (Koornneef *et al.*, 1991; Putterill *et al.*, 1995; Reeves & Coupland, 2001). *CO* mRNA is present under LDs and short days (SDs) but its protein only accumulates under LDs, explaining why it promotes flowering only under LDs (Suárez-López *et al.*, 2001; Valverde *et al.*, 2004). This difference occurs because CO protein stability is regulated by the action of photoreceptors and the ubiquitin ligase complex including CONSTITUTIVE PHOTOMORPHOGENIC 1 (COP1)-SUPPRESSOR OF PHYTOCHROME A 1 (SPA1; Hoecker & Quail, 2001; Jang *et al.*, 2008; Laubinger *et al.*, 2006; Valverde *et al.*, 2004). *CO* mRNA expression is highest between approximately 12 h and 20 hours after dawn (Jang *et al.*, 2008; Suárez-López *et al.*, 2001). Under non-inductive SD conditions, the *CO* mRNA level is therefore high when it is already dark, and as the COP1-SPA1 ubiquitin ligase complex is active in the dark, CO protein will be degraded (Jang *et al.*, 2008; Laubinger *et al.*, 2006). However, in LD conditions, light extends into the part of the day when *CO* mRNA levels are high, and activated photoreceptors, such as Cryptochromes and Phytochrome A, inactivate the COP1-SPA1 complex allowing CO protein to accumulate. CO can then activate the transcription of its target genes, such as the floral promoters *FT* and its paralogue *TWINSISTER OF FT* (*TSF;* Kardailsky *et al.*, 1999; Kobayashi *et al.*, 1999; A. Yamaguchi *et al.*, 2005). Because of the dynamics of CO protein accumulation, *FT* is only

expressed at the end of the day in LD conditions. Upon expression, this small protein moves from the leaves through the vasculature towards the SAM (Corbesier *et al.*, 2007; Jaeger & Wigge, 2007). At the SAM, FT can interact with the bZIP transcription factor FD (Abe *et al.*, 2005, 2019; Wigge *et al.*, 2005). FD binds to the promoters of several flowering genes, such as *SOC1, FUL* and *AP1,* and is proposed to recruit FT to these promoters to activate their transcription in the shoot meristem (Abe *et al.*, 2005; Collani *et al.*, 2019; Romera-Branchat *et al.*, 2020; Samach *et al.*, 2000; Teper-Bamnolker & Samach, 2005; Yoo *et al.*, 2005). Thus, activation of *FT* transcription in the leaf by exposure to LDs results in the transcriptional activation of flowering genes in the meristem, and these ultimately switch the vegetative meristem to an inflorescence meristem.

High ambient temperature and accelerated floral induction

Arabidopsis grown under high ambient temperature (27°C) flowers earlier than when its grown under ambient temperatures (approximately 20°C; Balasubramanian *et al.*, 2006; Capovilla *et al.*, 2015). This acceleration of flowering is mediated by *FT.* Exposure to high ambient temperature under SD conditions causes early flowering, overcoming the requirement for exposure to LDs.

The bHLH transcription factor PHYTOCHROME-INTERACTING FACTOR 4 (PIF4) directly induces the transcription of *FT* in response to high temperatures under SDs and this causes early flowering (Koini *et al.*, 2009; Kumar *et al.*, 2012). *pif4* mutants are late flowering in higher ambient temperature, and consistently, these plants have a lower expression level of *FT* and its paralogue *TSF* (Fernández *et al.*, 2016; Vinicius Costa Galvão *et al.*, 2015).

However, PIF4 is not the only factor that can induce earlier flowering under high ambient temperatures. For example, the phytohormone GA also plays a role in accelerating flowering under high ambient temperature, because reduced GA levels lead to a delay in flowering under these conditions (Balasubramanian *et al.*, 2006).

Moreover, the MADS-domain transcription factors FLOWERING LOCUS M (FLM) and SHORT VEGETATIVE PHASE (SVP) also play a role in accelerated flowering under high ambient temperature. SVP is a potent inhibitor of flowering and it represses expression of *FT* and *TSF*, among others (Jeong *et al.*, 2007). *svp* mutants are earlier flowering in general and do not show additional acceleration of flowering under higher temperatures (Lee *et al.*, 2013). In wild-type plants growing under high ambient temperatures, SVP does not accumulate and no longer represses *FT* and *TSF*, allowing plants to flower earlier under these conditions (Lee *et al.*, 2013). The floral repressor FLM is alternatively spliced in a temperature-dependent

manner, which affects the interaction between FLM and SVP. At low ambient temperatures, the dominant splice form of FLM is FLM-β and this form binds to SVP and together they repress flowering (Lee *et al.*, 2013; Posé *et al.*, 2013). However, under high ambient temperature, the FLM-β form becomes less abundant as it is alternatively spliced and its transcripts are subjected to degradation, relieving the repressive effects of FLM on its targets (Capovilla *et al.*, 2017; Sureshkumar *et al.*, 2016). An additional member of the SQUAMOSA PROMOTER BINDING-LIKE (SPL) transcription factor family, SPL3, was also shown to have a function in ambient temperature-induced flowering, but not specifically under high ambient temperature (Kim *et al.*, 2012).

Vernalization, a prolonged period of cold that promotes floral induction

Many plant species, including certain Arabidopsis accessions, require a period of low temperature characteristic of winter to induce flowering. This process is termed vernalization and in *A. thaliana* promotes flowering by inducing the stable repression of floral repressor *FLOWERING LOCUS C* (*FLC*; Amasino, 2004; Bastow *et al.*, 2004; Michaels & Amasino, 2000).

FLC binds directly to genes that promote flowering in Arabidopsis, such as *SOC1, SPL15, FD* and *FT*, and represses their expression until the plant is exposed to vernalization (Deng *et al.*, 2011; Helliwell *et al.*, 2006; Mateos *et al.*, 2017; Searle *et al.*, 2006) . In some species, vernalization is absolutely required before plants become competent to respond to floral inductive cues (Albani *et al.*, 2012; Mylne *et al.*, 2004; Wang *et al.*, 2009). In Arabidopsis, most accessions flower eventually without vernalization, even if they have strong FLC activity (Clarke & Dean, 1994; Wollenberg & Amasino, 2012).

During vernalization, the *FLC* locus is epigenetically silenced. This occurs by altering methylation levels of histone 3 at the *FLC* locus, mediated by protein complexes, including POLYCOMB REPRESSIVE COMPLEX 2 (PRC2; Bastow *et al.*, 2004; De Lucia *et al.*, 2008; Sung & Amasino, 2004; Wood *et al.*, 2006). During exposure to cold, VIVIPAROUS1/ABSCISIC ACID INSENSITIVE3-LIKE1 (VAL1) recruits a deacetylase, which downregulates *FLC* expression (Qüesta *et al.*, 2016). At the same time an anti-sense transcript called *COOLAIR,* which is encoded close to the *FLC* locus, assists in the transcriptional downregulation of *FLC* (Csorba *et al.*, 2014). Following *FLC* downregulation, its locus is recognised by PRC2 (De Lucia *et al.*, 2008; Yuan *et al.*, 2016), which removes the histone 3 marks associated with active gene expression, and deposits repressive histone marks (Angel *et al.*, 2011; De Lucia *et al.*, 2008; Qüesta *et al.*, 2016; Yang *et al.*, 2017). At this point the *FLC* locus is stably silenced and upon exposure to inductive conditions flowering is induced through *FT* and the photoperiodic pathway.

Several late-flowering mutants were originally identified and proposed to delay flowering by impairing autonomous flowering. These genes included *LUMINIDEPENDENS* (*LD*), *FLOWERING CONTROL LOCUS A* (*FCA*), *FLOWERING LOCUS D* (*FLD*), *FLOWERING LOCUS K* (*FLK*), *FPA* and *FVE* (Chen *et al.*, 2005; Koornneef *et al.*, 1991; Lee *et al.*, 1994; Lim *et al.*, 2004). All of these genes were later shown to affect flowering time by maintaining *FLC* mRNA at low levels in early-flowering accessions that do not require vernalization (Chen *et al.*, 2005; Lim *et al.*, 2004; Michaels, He *et al.*, 2003; Sanda & Amasino, 1996). The proteins encoded by these genes were found to play a general role in chromatin remodelling, RNA-mediated gene repression and other aspects of gene expression, and to contribute to many biological processes, including germination (Auge *et al.*, 2018; Bäurle & Dean, 2008; Chiang *et al.*, 2009; He & Amasino, 2005; Lee *et al.*, 2014; Simpson, 2004; Veley & Michaels, 2008; Wu *et al.*, 2020).

Stress-induced floral induction

Abiotic and biotic stress can affect floral induction in Arabidopsis. These stresses include nutrient deficiency, drought, salt-exposure, high irradiation and pathogen infection. Most of these environmental stresses cause earlier flowering, often via phytohormones related to stress, such as abscisic acid (ABA) and salicylic acid (SA; Martínez *et al.*, 2004; Riboni *et al.*, 2013, 2016). In a nutrient-deficient environment, Arabidopsis plants flower earlier than plants grown in a nutrient-rich soil (Kolář & Seňková, 2008). This has been proposed to be due to limited nitrate availability, which causes early flowering independently of photoperiod or the flowering-promoting phytohormone GA (Marín *et al.*, 2011). However, moderate nitrate limitation causes a slight delay in flowering by suppressing *SOC1* and reducing GA levels (Gras *et al.*, 2018; Olas *et al.*, 2019).

GIGANTEA (GI) is a clock-dependent positive regulator of *CO* expression and has also been implicated in early floral induction in plants experiencing drought (Riboni *et al.*, 2013, 2016). These reports described that *GI* upregulation caused increased expression of *CO* and subsequently of *FT* and thus, earlier flowering. However, early flowering only occurred when ABA, which is involved in drought responses, was present. ABA also repressed *SOC1* expression under drought conditions, illustrating the complex regulation of flowering under these stress conditions (Riboni *et al.*, 2016).

UV-C light radiation also affects floral induction in Arabidopsis. This stressful light condition causes an upregulation of SA-response genes and subsequent earlier flowering in wild-type plants, but not in plants where SA signalling is disrupted (Martínez *et al.*, 2004). Treatment with UV-C light caused a higher

expression of *CO* and consequently, a higher expression of *FT.* Plants disrupted in SA signalling also flowered later than wild-type plants, and because SA is important for plant resistance and defence, these results suggest that an interplay exists between floral induction and plant defence (Delaney *et al.*, 1994; Martínez *et al.*, 2004). Consistent with this, Arabidopsis plants were shown to flower earlier following infection with two different pathogens (Korves & Bergelson, 2003).

Although most stress conditions cause earlier flowering, salt-stress delays the floral transition. Plants grown in high-salt conditions show slower growth and development (Achard *et al.*, 2006). Floral induction in these plants was also delayed and this was due to the integration of stress signals by DELLA proteins (Achard *et al.*, 2006). DELLA proteins are involved in GA signalling, and the GA signalling pathway affects the expression of *FT* and *TSF* under LD conditions (Galvão *et al.*, 2012). Furthermore, a NAC transcription factor involved in salt responses is also involved in the downregulation of *FT* and this was suggested to be mediated by GA (Kim *et al.*, 2007, 2008). It is still unclear however, whether this delay in flowering is due to slower growth of the whole plant, or whether it results from an active process that inhibits flowering. However, it was shown that the floral inhibitor BROTHER OF FT (BFT) might compete with FT for binding to FD under salt stress (Ryu *et al.*, 2014). This would lead to a delay in flowering because FT can no longer induce flowering in complex with FD.

Gene regulatory networks underlying floral induction in *Arabidopsis thaliana:* internal cues

Gibberellin and its role in flowering under non-inductive conditions

The promotive effects of GA on floral induction of *A. thaliana* have been known for over 60 years, when it was shown that in addition to an effect of GA on stem elongation, external application of GA also induces earlier flowering under SDs (Lang, 1957). Since then, many reports have described roles for GA in floral induction (Bao *et al.*, 2020). GA signalling functions by the binding of GA to the GIBBERELLIN INSENSITIVE DWARF 1 (GID1) receptors (Griffiths *et al.*, 2006; Shimada *et al.*, 2008). This binding leads to conformational changes in the receptor and allows it to bind to DELLA proteins causing proteasome-mediated degradation of the DELLA protein (Dill *et al.*, 2004; Murase *et al.*, 2008; Shimada *et al.*, 2008; Silverstone *et al.*, 2001). These DELLA proteins physically interact with a wide range of transcription factors and positively or negatively influence their activity. The degradation of these DELLA proteins in the presence of GA thus alters the activity of DELLA-interacting transcription factors (Hauvermale *et al.*, 2012; Peng *et al.*, 1997).

Mutations that impair GA biosynthesis almost prevent flowering under SDs, and slightly delay flowering under LD conditions (Blázquez *et al.*, 1998; Galvão *et al.*, 2012; Hisamatsu & King, 2008; Wilson *et al.*, 1992). Therefore, GA is considered to contribute to flowering under LD conditions, but to be most important for flowering in SD conditions (Galvão *et al.*, 2012; Hisamatsu & King, 2008; Wilson *et al.*, 1992). Under LD conditions, GA is involved in the expression of *FT* and *TSF* by degrading DELLA proteins that inhibit CO function, which is not relevant under SD conditions (Moon *et al.*, 2003; Porri *et al.*, 2012; Wang *et al.*, 2016; Xu *et al.*, 2016). Under SD conditions, GA activates the transcription of *SOC1* and *LFY* (Blázquez *et al.*, 1998; Blazquez & Weigel, 2000; Borner *et al.*, 2000; Moon *et al.*, 2003; Wilson *et al.*, 1992). Under these conditions, the levels of GA in the SAM rise steeply before the floral transition, correlating with the expression of floral meristem identity genes such as *LFY* (Eriksson *et al.*, 2006).

Plants that overexpress *MICRORNA156* (*MIR156;* from the age pathway, further explained below) show a reduced flowering response to GA under SD conditions. MiR156 post transcriptionally downregulates its SPL transcription factor targets, indicating the importance of these SPLs in GA-mediated flowering under SD conditions (Yu *et al.*, 2012). One of these SPLs, SPL9 plays a role in floral induction and was shown to interact with multiple DELLA proteins (Wang *et al.*, 2009; Yu *et al.*, 2012). The interaction of SPL9 with the

DELLA protein REPRESSOR OF GA (RGA) stimulated the transcriptional activity of SPL9 and was required for timely production of floral organs (Yamaguchi *et al.*, 2014). In contrast, the SPL9 ortholog and floral integrator SPL15 also interacts directly with DELLA proteins, but here they inhibit the transcriptional activity of SPL15 (Hyun *et al.*, 2016). Although GA application can induce earlier flowering in SD conditions, this response no longer occurs in the *spl15* knock out mutant. This thus indicates that GA regulates flowering in SD conditions at least partly through SPL15.

Endogenously timing the appropriate flowering time: the age pathway and *MICRORNA156*

The age pathway is another endogenous flowering pathway and is related to the GA pathway. This pathway is increasingly activated as plants age, through the transcriptional repression of a group of *MICRORNA* (*MIR*) genes.

These *MIR* genes encode microRNAs (miRNAs), which are non-coding RNA molecules of about 21–22 nucleotides long. miRNAs post-transcriptionally inhibit their target mRNAs by inducing mRNA degradation or by interfering with mRNA translation (Bartel, 2004; Gandikota *et al.*, 2007; Jeong *et al.*, 2013). The mature miRNA sequences of *MIR156* (encoded by eight *MIR* genes) and *MIR157* (*MIR157*; encoded by four genes) are similar and differ in only three nucleotides (Reinhart *et al.*, 2002). The expression of these *MIR* genes is high in the cotyledons and first leaves produced and gradually declines in leaves produced later in shoot development (Wu & Poethig, 2006). This decrease is partly due to an increase in photosynthates, and exogenous application of sugar causes an accelerated decrease in the expression of these *MIRs* (Yang *et al.*, 2013; Yu *et al.*, 2013). In addition, the loci of *MIR156A* and *C* are silenced by the accumulation of methylated histone 3 at the loci during ageing (Xu *et al.*, 2016).

MIR156 and MIR157 are complementary to the mRNAs of 11 members of a family of SPL transcription factors (Rhoades *et al.*, 2002; Schwab *et al.*, 2005). Many of these SPLs play roles in development and are involved in the vegetative phase change (VPC) or the subsequent floral transition (Cardon *et al.*, 1997; Usami *et al.*, 2009; Wang *et al.*, 2009; Wu & Poethig, 2006). The VPC is the transition from a juvenile vegetative plant to an adult vegetative plant involving a gradual change in leaf morphology, trichome distribution and the acquisition of floral competence, *i.e.* the ability to respond to floral inductive signals (Poethig, 2013). Arabidopsis plants that overexpress *MIR156* undergo the VPC late and these plants also flower later than wild-type plants (Schwab *et al.*, 2005; Wu *et al.*, 2009; Wu & Poethig, 2006). Conversely, plants that express a mimicry target for *MIR156* undergo the VPC earlier and flower earlier than wild-type plants (Franco-Zorrilla *et al.*, 2007; Todesco *et al.*, 2010; Wu *et al.*, 2009). Many of the *MIR156*-targeted SPLs play a role in floral induction and directly target genes involved in flowering.

Introduction to SQUAMOSA PROMOTER BINDING PROTEIN-LIKE proteins (SPLs), including SPL15

SPL transcription factors and their roles in plant development

SPL transcription factors were originally identified as proteins that bound to the *Antirrhinum majus SQUAMOSA* promoter (*AP1* orthologue; Huijser *et al.*, 1992; Klein *et al.*, 1996). These proteins were detected in protein extracts from Antirrhinum inflorescences, but not in extracts from vegetative plants and they were termed SQUAMOSA PROMOTER BINDING PROTEINs (SBPs). Subsequently, related proteins were also identified in Arabidopsis and these were termed SBP-LIKEs, or SPLs (Cardon *et al.*, 1999; Cardon *et al.*, 1997).

SPLs are plant-specific transcription factors and the only transcription factors that possess an SBP DNA-binding domain (Cardon *et al.*, 1999). Twelve SPLs were originally identified in Arabidopsis*,* but it was found later on that at least 16 loci encoded proteins with an SBP-domain and the gene product of one additional locus shared similarities to SPLs, but lacked the SBP-domain (Birkenbihl *et al.*, 2005; Cardon *et al.*, 1999; Guo *et al.*, 2008). SPLs are conserved in all other higher plant species examined and regulate plant architecture and development (Chen *et al.*, 2010; Duan *et al.*, 2019; Hyun *et al.*, 2019; Li & Lu, 2014; Tripathi *et al.*, 2018; Wang & Zhang, 2017; Wei *et al.*, 2018). The DNA-binding SPLs recognise a core GTAC motif in their target promoters, although for some SPLs, the core GTAC motif might be supplemented with additional nucleotides (Birkenbihl *et al.*, 2005; Cardon *et al.*, 1999; Liang *et al.*, 2008; Lu *et al.*, 2013; Wang *et al.*, 2009; Wei *et al.*, 2012; Yamasaki *et al.*, 2009). In phylogenetic trees, SPLs cluster into multiple clades based on the sequences of their SBP domains (A. Y. Guo *et al.*, 2008; Preston & Hileman, 2013). SPL1, SPL12 and SPL14 group together and are not targeted by miR156. SPL1 and SPL12 have been described to function in thermotolerance of the inflorescence, and SPL14 has been implicated in plant resistance (Chao *et al.*, 2017; Jorgensen & Preston, 2014; Stone *et al.*, 2005).

SPL2 is targeted by miR156 and is most similar to SPL10 and SPL11. SPL2 is highly expressed in leaves, flowers and inflorescences (Jorgensen & Preston, 2014; Shikata *et al.*, 2009). It has been implicated to function in inflorescence development, fertility and in VPC, but similar to SPL10 and SPL11, SPL2 does not play a major role in the floral transition (Shikata *et al.*, 2009; Wang *et al.*, 2016; Xing *et al.*, 2010; Yao *et al.*, 2019). SPL10 was described to regulate lateral root outgrowth and root meristem size (Barrera-Rojas *et al.*, 2020; Gao *et al.*, 2018).

SPL3, 4 and 5 are the smallest SPL proteins and their sequences are highly similar (Wu & Poethig, 2006). They have been described to function redundantly in the floral transition, because single mutants of *spl3* did not have a phenotype different from wild-type plants, but a triple knockdown of these genes causes later flowering than Col-0 in LD conditions (Cardon *et al.*, 1997; Jung *et al.*, 2016; Wu & Poethig, 2006; Xu *et al.*, 2016). These SPLs are expressed in the SAM, downstream of the FT/FD pathway and bind to FD and contribute to its transcriptional activity (Jung *et al.*, 2016; Wang *et al.*, 2009). In addition, SPL3, SPL4 and SPL5 bind to the *FUL* promoter and SPL3 stimulates *FUL* expression (Wang *et al.*, 2009; Xie *et al.*, 2020; Yamaguchi *et al.*, 2009). Moreover, SPL3 binds directly to the *LEAFY* and *AP1* promoters and activates their expression (Yamaguchi *et al.*, 2009). Plants that overexpress *SPL3, SPL4* or *SPL5* genes that have been made insensitive to miR156 targeting from a 35S-promoter also flowered earlier than Col-0 in LD conditions (Wu & Poethig, 2006). In addition, expression of a miR156-resistant form of *SPL3* caused earlier flowering in SD conditions (Wang *et al.*, 2009).

Phylogenetically, SPL6, 7 and 8 cluster on their own and separate from all other SPLs, where SPL6 is targeted by miR156, but SPL7 and SPL8 are not. SPL6 functions in plant immunity, and although its expression increases over time, *SPL6* is not expressed in the SAM (Padmanabhan *et al.*, 2013; Xu *et al.*, 2016). SPL7 is involved in response to copper deficiency, and its role in copper signalling is necessary for fertility (Garcia-Molina *et al.*, 2014; Schulten *et al.*, 2019; Yan *et al.*, 2017). SPL8 plays an important role in plant fertility and development of the pollen sac and is highly expressed in the inflorescence (Jorgensen & Preston, 2014; Unte *et al.*, 2003; Xing *et al.*, 2013).

As previously mentioned, SPL9 clusters together with SPL15 and both proteins affect floral induction and leaf initiation rate (Hyun *et al.*, 2016; Schwarz *et al.*, 2008; Wang *et al.*, 2009). miR156-resistant SPL9 causes earlier flowering, but *spl9* mutants do not flower later than Col-0 in LD conditions (Hyun *et al.*, 2016; Wang *et al.*, 2009). SPL9 can bind to the promoters of *SOC1* and *FUL* and can upregulate transcription of *FUL* (Wang *et al.*, 2009). Moreover, SPL9 can bind directly to the *AP1* promoter and activate its transcription, and this transcriptional activation is stimulated by DELLA protein RGA within the GA pathway (Wang *et al.*, 2009; Yamaguchi *et al.*, 2014). In addition, SPL9 is involved in trichome distribution by directly regulating transcription factors involved in trichome development (Yu *et al.*, 2010).

SPL13 is encoded by two closely linked genes on chromosome five; *SPL13A* and *SPL13B* (also described as *SPL17* in the literature), which presumably, reflects a recent gene-duplication event (A. Y. Guo *et al.*, 2008). A role in seedling development was described for SPL13 and plants that expressed *MIR156*-resistant

SPL13A showed a delay in the production of the first true leaves after germination (R. C. Martin *et al.*, 2010).

SQUAMOSA PROMOTER BINDING PROTEIN-LIKE 15 integrates multiple flowering-time pathways in Arabidopsis

SPL15 plays roles in regulating leaf initiation rate, cell division in the leaf as well as flowering, where it integrates several different floral induction signals (Hyun *et al.*, 2016; Schwarz *et al.*, 2008; Usami *et al.*, 2009; Wei *et al.*, 2012). Unlike many of the other SPLs with a function in floral induction, SPL15 has a major role in non-inductive SD conditions (Hyun *et al.*, 2016). *spl15* mutants flower similarly to Col-0 in LD conditions and this is probably due to redundancy in the promotion of floral induction with the FT pathway. Transcription of *FT* is not impaired in an *spl15-1* mutant background, but the *spl15-1/ft-10/tsf-1* triple mutant shows a highly synergistic late-flowering phenotype in LD (Hyun *et al.*, 2016, 2019). This indicates that these pathways function in parallel in LD conditions, and that the FT pathway is the dominant pathway in these conditions.

It has previously been described that *SPL15* is a direct target of FLC (Deng *et al.*, 2011; Mateos *et al.*, 2017). This is less relevant in the early flowering Col-0 background as it only weakly expresses *FLC* and Col-0 does not require vernalization to flower (Johanson *et al.*, 2000; Michaels & Amasino, 1999). In accessions that require vernalization for flowering, *SPL15* transcription is likely inhibited by FLC until vernalisation occurs (Deng *et al.*, 2011; Hyun *et al.*, 2019). Supporting this, reduced *SPL15* mRNA levels are observed in a background where FLC is present, compared to *flc-3* mutants (Deng *et al.*, 2011). Moreover, a perennial relative of Arabidopsis, *Arabis alpina* (Pajares accession), has an absolute requirement for vernalization to flower. In these plants, the FLC orthologue PERPETUAL FLOWERING 1 (PEP1) also binds to the *SPL15* promoter (Mateos *et al.*, 2017). *A. alpina* plants undergo floral induction during vernalization and are dependent on SPL15 activity for full commitment to flowering after vernalization (Hyun *et al.*, 2019). Moreover, overexpression of *SPL15* by expression of *MIR156*-resistant *rSPL15* led to plants that require shorter vernalization periods to flower. Therefore, in plants that require vernalization, SPL15 plays an important role in defining the duration of vernalization required for the commitment to flower.

In addition to transcriptional repression through *FLC*, SPL15 is one of the 11 SPL proteins whose mRNA is targeted by miR156 (Rhoades *et al.*, 2002). During vegetative development, high levels of miR156 prevent efficient translation and induce cleavage of *SPL15* mRNA. However, as plants age, *MIR156* transcription

decreases and *SPL15* mRNA can be translated more efficiently, resulting in more SPL15 protein (Hyun *et al.*, 2016).

Lastly, GA is required for Arabidopsis to flower in SD conditions (Blazquez *et al.*, 1998; Galvão *et al.*, 2012; Michaels & Amasino, 1999; Wilson *et al.*, 1992). The GA pathway interferes with SPL15 protein function. Once *SPL15* mRNA is translated, SPL15 protein can be bound by DELLA proteins within the GA signalling pathway (Hyun *et al.*, 2016). At least two DELLA proteins, RGA and GIBBERELLIC ACID INSENSITIVE (GAI), can bind to SPL15 and prevent it from interacting with MEDIATOR subunits to promote transcription (Hyun *et al.*, 2016). Moreover, as described above, floral induction by GA in SD conditions partially depends on SPL15 (Hyun *et al.*, 2016). Once active, SPL15 binds to the promoters of *FUL* and *MIR172B* and activates their transcription in cooperation with SOC1 (Hyun *et al.*, 2016). This thesis further characterises the role of SPL15 in floral induction in Arabidopsis.

Aims of this thesis

The general aim of this thesis is to decipher the mechanisms by which SPL15 promotes the floral transition and to determine mechanistically how its central role in SD conditions is bypassed under LD conditions. SPL15 plays an important role in the integration of signals from the vernalization, age-related and GA floral-induction pathways. However, it remains unclear how the gene regulatory cascade downstream of SPL15 results in the transition from a vegetative meristem to a reproductive meristem. SPL15 has been proposed to function in a feedback loop and directly repress some of the precursor genes that encode for miR156, but also because it has unexplained effects on shoot growth (Schwarz *et al.*, 2008; Usami *et al.*, 2009; Wei *et al.*, 2012). Therefore, SPL15 probably has additional, yet uncharacterised targets. Moreover, even for established targets of SPL15, such as *FUL*, it is not clear to which GTAC motifs SPL15 binds and whether this binding is important for floral induction mediated by SPL15. Therefore, the primary aims of this project were 1) to use genetic approaches to determine the significance of SPL15 targets and downstream genes in floral induction, 2) to employ target promoter mutagenesis to understand how SPL15 induces transcription of the target-gene *FUL* and 3) to identify new candidate target genes of SPL15.

Chapter 2:

Genetic analysis of downstream factors of SPL15

Introduction

Flowering in plants is tightly regulated to guarantee successful reproduction. In Arabidopsis, flowering is predominantly induced when the daylength becomes longer (Mouradov *et al.*, 2002; Song *et al.*, 2018). In laboratory conditions, this response can be induced by growing plants under long-day (LD) conditions with 16 hours of light and 8 hours of darkness. Wild type plants such as Columbia-0 (Col-0) flower around 25 days after sowing in these controlled inductive conditions (Fig. 2.1A, B). Many mutations and alleles have

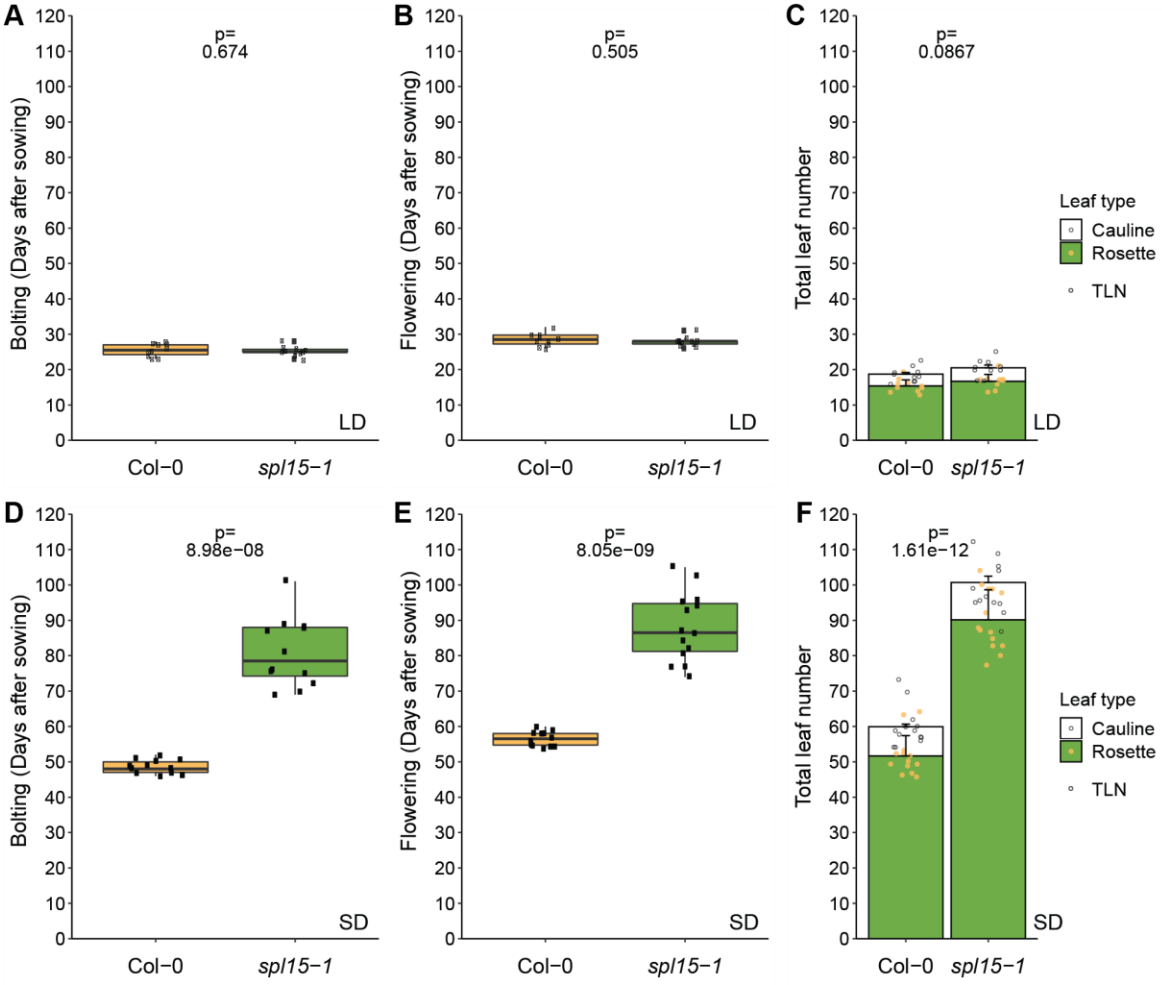

Figure 2.1. Flowering-time phenotype of Col-0 and *spl15-1* in LD and SD conditions. Time to bolting (**A**), flowering time (**B**) and total leaf number (**C**; TLN) of Col-0 and *spl15-1* in LD conditions (n = 10, *p* was calculated using the student's *t*-test). Time to bolting (**D**), flowering time (**E**) and TLN (**F**) of Col-0 and *spl15-1* in SD conditions (n = 13–14, *p* was calculated using the student's *t*-test). Bolting time was scored as the day on which the inflorescence extended 0.5 cm from the rosette and flowering time was scored as the day on which the first flower opened, anywhere on the plant.

been characterized that perturb this flowering response and cause plants to flower either earlier or later than the wild type, Col-0 (Andrés & Coupland, 2012).

When grown under non-inductive short-day (SD) conditions with 8 hours of light and 16 hours of darkness, Col-0 plants still flower after around 50–60 days of growth (Fig. 2.1 D, E), but much later than in LD conditions. Most flowering-time mutants in LDs also have a flowering-time phenotype in SD conditions, but some mutants have a much stronger phenotype in SD conditions. For instance, mutation of SQUAMOSA PROMOTER BINDING PROTEIN-LIKE 15 (SPL15) either does not affect flowering or only results in a mild late-flowering phenotype in LD conditions, but causes extremely late flowering in SD conditions (Fig. 2.1; Hyun *et al.*, 2016). *SPL15* mRNA can be detected in the shoot apical meristem (SAM) in LD and SD conditions, and in leaves in LD and presumably also in SD conditions (Nguyen *et al.*, 2017; Usami *et al.*, 2009). Moreover, VENUS-tagged SPL15 protein was detected in the SAM using confocal microscopy after about 12 days in LD conditions, and after 3 weeks in SD conditions (Fig. 2.2; Hyun *et al.*, 2016). SPL15 protein remains visible in the SAM during the transition to an inflorescence meristem and afterwards (Fig. 2.2).

In the absence of SPL15, flowering in SD conditions is delayed, which might in part be due to reduced expression of two important floral regulators: *FRUITFULL* (*FUL*) and *MICRORNA 172B* (*MIR172B*; Fig. 2.3A; Hyun *et al.*, 2016). These two genes were shown by ChIP-qPCR, to be directly targeted by SPL15 and therefore, the absence of SPL15-mediated transcriptional activation of *FUL* and *MIR172b* might be responsible for the delayed flowering time observed in *spl15-1* in SD conditions (Hyun *et al.*, 2016). *MIR172* post-transcriptionally inhibits members of the *APETALA 2-LIKE* (*AP2-L*) family, including *AP2* (Aukerman & Sakai, 2003; Zhu & Helliwell, 2011). These proteins are potent inhibitors of floral induction and they are downregulated to allow the on-set of flowering (Aukerman & Sakai, 2003; Xuemei Chen, 2004; Mathieu *et al.*, 2009). Therefore, SPL15 may induce flowering by activating *MIR172* expression to indirectly

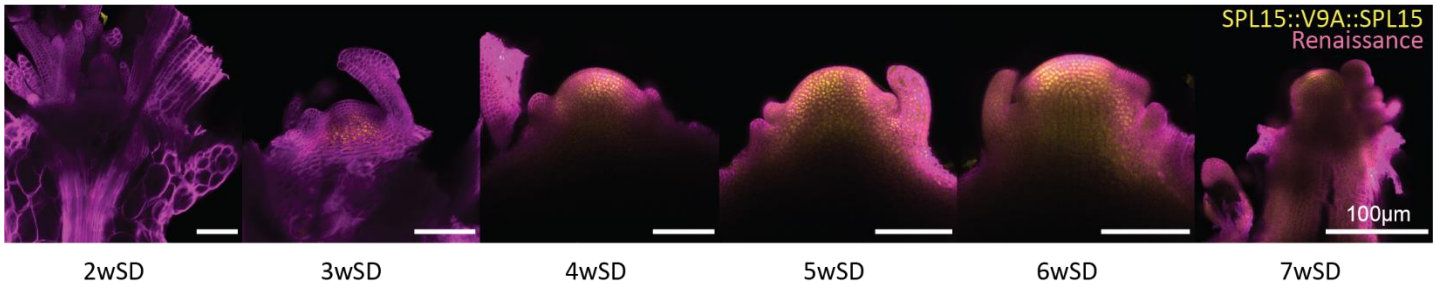

Figure 2.2. Confocal microscopy time course of shoot apical meristems expressing *pSPL15::VENUS::SPL15* in SD conditions. Confocal laser scanning micrographs of shoot apices of *pSPL15::VENUS::SPL15* at the indicated time points in SD conditions. Fluorescence from VENUS is artificially coloured in yellow and fluorescence from the Renaissance dye is artificially coloured in magenta. White scale bars represent 100 µm. A representative image of three samples is shown for each time point.

downregulate the *AP2-Ls* (Fig. 2.3A, B). In addition to *MIR172*, the direct SPL15-target *FUL* transcriptionally downregulates the *AP2*-L genes *SCHNARCHZAPFEN* (*SNZ*) and *AP2*, and furthermore, FUL directly binds to *TARGET OF EAT1* (*TOE1*) and *TOE3* (Balanzà *et al.*, 2018). SPL15 might thus also regulate flowering through the inhibition of AP2-Ls by transcriptionally activating *FUL.* On the other hand, AP2 also binds the *FUL* promoter, suggesting that a regulatory feedback loop connects AP2-Ls and *FUL* and *MIR172B* expression. A change in the balance between these factors will allow floral induction to occur (Fig 2.4A, B; Yant *et al.*, 2010). SPL15 might be one of the factors that is required to change the balance within this regulatory loop.

This chapter describes genetic approaches to analyse the contribution of *FUL* and *MIR172B* to the *spl15-1* flowering phenotype, and to investigate the influence of other *MIR172*-family members.

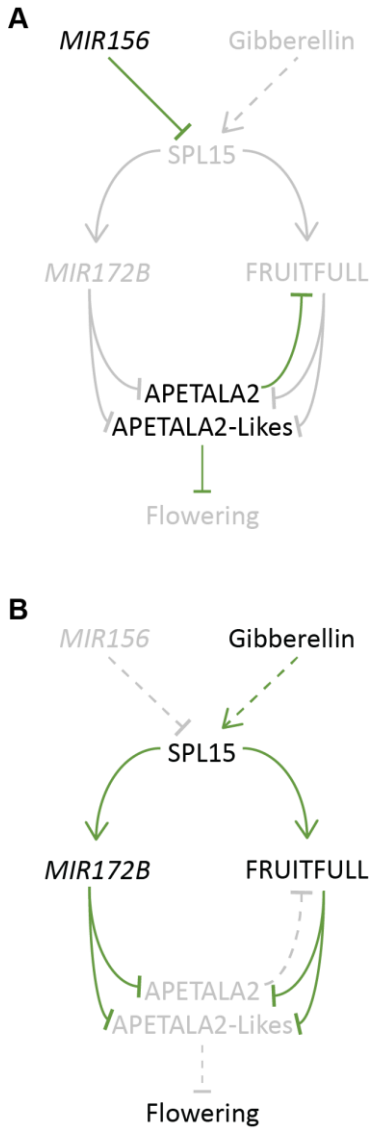

Figure 2.3. Model for the proposed interactions within the SPL15 floral induction pathway. A: Model for the interactions during the vegetative phase. **B:** Model for the interactions at the end of the floral transition. Interactions in green are those that occurring, black represents active genes/proteins and interactions/genes and proteins that are inactive are shown in grey (Balanzà *et al.*, 2018; Hyun *et al.*, 2016; G. Wu *et al.*, 2009).

Assessment of the genetic contribution of *ful-2* and *MIR172* to the *spl15-1* phenotype

The *ful-2*/*mir172b* double mutant phenocopies the *spl15-1* mutant in SD conditions, but not in LD conditions

To assess the extent to which mutations in *FUL* and *MIR172B* phenocopy the late-flowering phenotype of *spl15-1* in SD conditions, *ful-2*, *ful-2/mir172a-2, ful-2/mir172b-3* and *ful-2/mir172a-2/b-3* were grown in

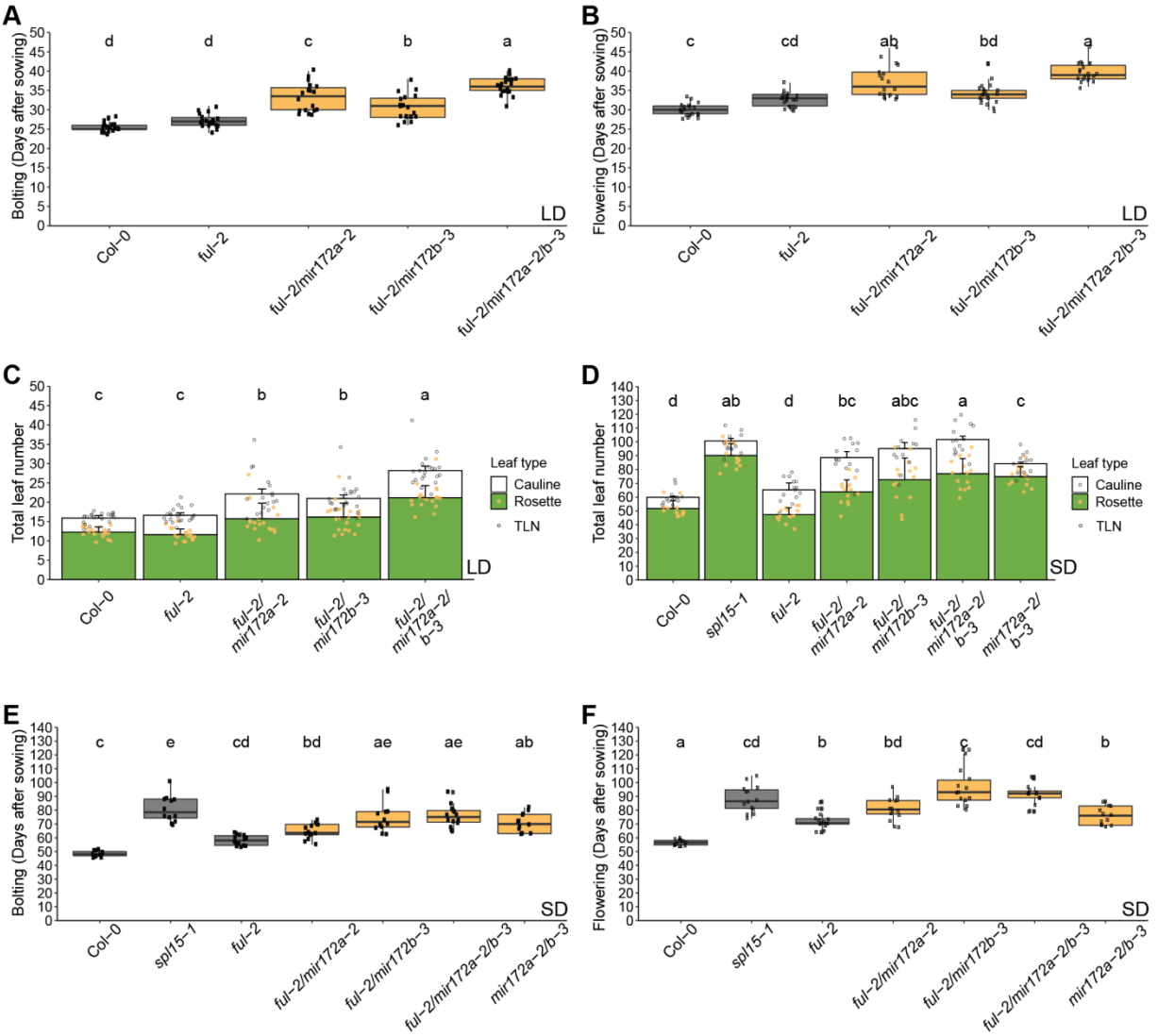

Figure 2.4. Flowering-time phenotype of Col-0, *ful-2, ful-2/mir172a-2, ful-2/mir172b-3 and ful-2/mir172a-2/b-3* in LD and SD conditions. Time to bolting (**A**), flowering time (**B**) and total leaf number (**C**; TLN) of the indicated genotypes in LD conditions (n = 19–21). TLN (**D**), time to bolting (**E**) and flowering time (**F**) of the indicated genotypes in SD conditions (n = 13–14). Bolting time was scored as the day on which the inflorescence extended 0.5 cm from the rosette, and flowering time was scored as the day on which the first flower opened, anywhere on the plant. Statistical differences were calculated with ANOVA followed by Tukey's HSD (honestly significant difference) test at $p < 0.01$.

LD and SD conditions and scored for flowering time. The *mir172a*-2 mutant combinations were included to test whether *mir172a-2* affects the phenotypes, and whether *MIR172A* also functions downstream of SPL15. In LD conditions, *ful-2/mir172a-2, ful-2/mir172b-3* and *ful-2/mir172a-2/b-3* all flower later than Col-0 (Fig. 2.4A–C). Although *spl15-1* plants were not included in this experiment, they normally bolt and flower at a similar time to Col-0, and are delayed by a maximum of 4 days compared with Col-0 (Fig. 2.1A-C). *FUL, MIR172A* and *MIR172B* clearly are important for floral induction in LD conditions as the double and triple mutants of these genes are bolting and flowering significantly later than Col-0 in these conditions.

In SD conditions, the differences in flowering time among the genotypes were considerably enhanced (Fig. 2.4D–F). *spl15-1* mutant plants flowered very late, and *ful-2/mir172b-3* and *ful-2/mir172a-2/b-3* phenocopied this flowering-time phenotype. This suggests that *ful-2* and *MIR172B* are both required for wild-type flowering in SD conditions and that they might play significant roles in the SPL15 floral induction pathway in SD conditions. However, the combination of *mir172a-2* with *ful-2* did not fully phenocopy the *spl15-1* phenotype, nor did it further enhance the *ful-2/mir172b-3* flowering phenotype in SD conditions. This suggests that *MIR172A* contributes less to SPL15 function than *MIR172B* in SD conditions. Although *ful-2/mir172b-3* and *ful-2/mir172a-2/b-3* phenocopied the late-flowering phenotype of *spl15-1* in terms of bolting and flowering in SD conditions, the rosette leaf number still differed between *spl15-1* and these genotypes. *spl15-1* plants had significantly more rosette leaves than *ful-2/mir172b-3* and *ful-2/mir172a-2/b-3* ($p < 0.01$). This suggests that the timing of bolting and flowering in *spl15-1* is caused by misregulation of *FUL* and *MIR172B* in SD conditions, but in terms of leaf number and perhaps leaf initiation rate, additional genes are misregulated. Moreover, the *ful*-2 mutation consistently led to an increase in the number of cauline leaves and this phenotype was further enhanced in plants containing an additional mutation in *MIR172A* and/or *MIR172B* ($p < 0.01$). No increase in the number of cauline leaves was observed in any plants with the wild-type *FUL* allele.

Overexpression of rSPL15 can partially restore flowering even in the absence of its direct targets FUL and MIR172B.

To further test whether *FUL* and *MIR172B* are the main target genes of SPL15, the overexpression line *pSPL15::VENUS::rSPL15* (*rSPL15*) was analysed. This line contains SPL15 fused to VENUS, and includes the entire up- and downstream intergenic regions of *SPL15.* In addition, the MIR156 target site was mutated, rendering *SPL15* resistant to MIR156-mediated repression. This line overexpresses SPL15 and flowers slightly earlier than Col-0. In this experiment, the early-flowering phenotype of the *rSPL15* line was tested

in backgrounds where *FUL*, *MIR172A* and *MIR172B* were no longer present. In LD conditions, *rSPL15* flowered slightly earlier than wild type, although not significantly (Fig. 2.5A-B; $p < 0.01$). In terms of total leaf number, however, *rSPL15* plants clearly possessed fewer leaves than Col-0 upon flowering (Fig. 2.5C). When *FUL* was mutated in the *rSPL15* background, flowering was significantly delayed by a few days compared to that of *rSPL15* (Fig.2.5A–C).

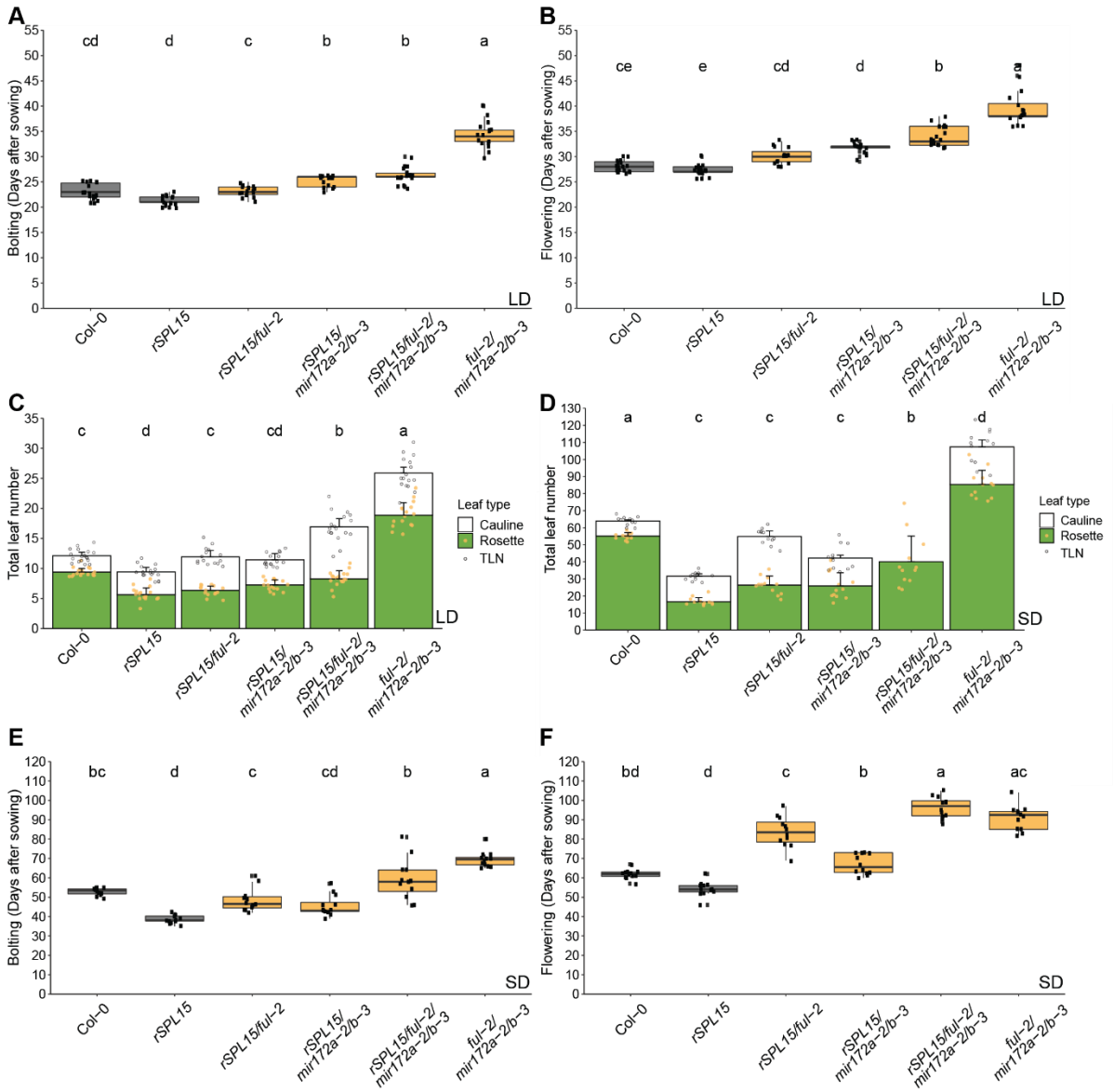

Figure 2.5. Flowering time phenotype of Col-0, *rSPL15*, *rSPL15*/*ful-2*, *rSPL15*/*mir172a-2/b-3*, *rSPL15*/*ful-2*/*mir172a-2/b-3* and *ful-2*/*mir172a-2/b-2* in LD and SD conditions. Time to bolting (**A**), flowering time (**B**) and total leaf number (**C**; TLN) of the indicated genotypes in LD conditions (n = 16-18). TLN (**D**), time to bolting (**E**) and flowering-time (**F**) of the indicated genotypes in SD conditions (n = 12). Bolting time was scored as the day on which the inflorescence extended 0.5 cm from the rosette, and flowering time was scored as the day on which the first flower opened, anywhere on the plant. Statistical differences were calculated with ANOVA followed by Tukey's HSD (honestly significant difference) test at $p < 0.01$. In figure D, statistical differences were based on rosette leaf number, not TLN, due to the absence of cauline leaf number data for *rSPL15*/*ful-2*/*mir172a-2/b-3*.

Combinations of *mir172a-2/b-3* and *ful-2/mir172a-2/b-3* with *rSPL15* further delayed the flowering-time phenotype of *rSPL15*, but compared to the *ful-2/mir172a-2/b-3* triple mutant, all these mutants were earlier flowering (Fig. 2.5A–C). This suggests that although the early-flowering phenotype of *rSPL15* is partially dependent on *FUL, MIR172A* and *MIR172B, rSPL15* can still induce flowering in LD conditions via other, yet unknown pathways.

In SD conditions, *rSPL15* was significantly earlier flowering than Col-0 in terms of leaf number or bolting time, but not in days to flower (Fig. 2.5D–F). Again, bolting was delayed by introgression of the *ful-2* and the *ful-2/mir172a-2/b-3* mutations into *rSPL15* (Fig. 2.5E). However, introgression of only *mir172a-2/b-3* did not greatly affect bolting time of *rSPL15*. Similar to LD conditions, *ful-2/mir172a-2/b-3* plants bolted latest in SD conditions, and this late-bolting phenotype could be partially rescued by introducing *rSPL15* (Fig. 2.5E).

Besides differences in bolting time, clear differences in flowering time and plant architecture were also observed (Fig2.6A). Although *rSPL15* plants were slightly, but not significantly earlier flowering in SD conditions, the differences between combinations of *rSPL15* with *ful-2* and *mir172a-2/b-3* were not as large as those for the bolting time of these genotypes in the same conditions (Fig. 2.5F). *rSPL15/mir172a-2/b-3* plants were not significantly later flowering than Col-0, but were later than *rSPL15* plants. *ful-2* had a prominent effect on the timing of flower opening, when combined with *rSPL15*. *rSPL15*/*ful-2* and *rSPL15*/*ful-2/mir172a-2/b-3* plants bolted very early in these conditions, and flowered as late *ful-2/mir172a-*

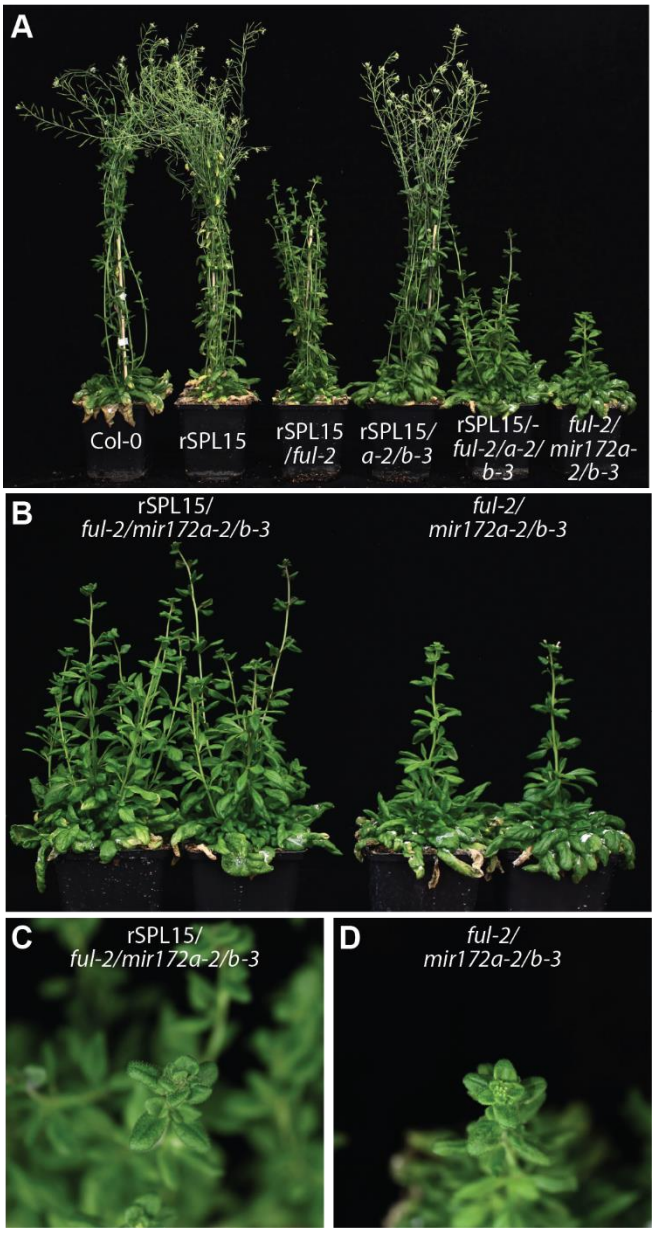

Figure 2.6. Images of Col-0, *rSPL15*, *rSPL15*/*ful-2*, *rSPL15*/*mir172a-2/b-3*, *rSPL15*/*ful-2/mir172a-2/b-3* and *ful-2/mir172a-2/b-3* in SD conditions. (**A**) The phenotype of all the plants included in the flowering-time experiment in Fig. 2.5D–F at 84SD. (**B**) Comparison of two representative *rSPL15*/*ful-2/mir172a-2/b-3* and two representative *ful-2/mir172a-2/b-3* plants at 84SD, illustrating the differences in architecture. (**C**) Detail of the inflorescence of a representative *rSPL15*/*ful-2/mir172a-2/b-3* plant illustrating the lack of floral buds. (**D**) Detail of the inflorescence of a representative *ful-2/mir172a-2/b-3* plant illustrating the presence of floral buds, similar to how they appear on Col-0 inflorescences.

2/b-3, indicating that *FUL, MIR172A* and *MIR172B* are epistatic to *rSPL15* in affecting flowering time (Fig. 2.5E-F). This is probably due to a delay in flower production, as can also be seen in Fig. 2.6B–D. *rSPL15/ful-2/mir172a-2/b-3* bolted early, but did not produce flowers until later, and these flowers opened as late those of as *ful-2/mir172a-2/b-3* plants. The inflorescences of *rSPL15/ful-2/mir172a-2/b-3* grew very tall before they produced visible floral buds (Fig 2.6C). By contrast, late-bolting and late-flowering *ful-2/mir172a-2/b-3* plants produced visible floral buds soon after the inflorescence was visible (Fig. 2.6D). Despite a large difference in bolting time, the flowers of these two genotypes opened at the same time, with plants of *rSPL15/ful-2/mir172a-2/b-3* being very tall with many inflorescences from the rosette, and those of *ful-2/mir172a-2/b-3* being relatively short with only the main inflorescence visible (Fig. 2.6B). The rosette leaf number of all lines that contained *rSPL15* was very low compared to that of Col-0 and *ful-2/mir172a-2/b-3.* On the basis of the morphological complexity of *rSPL15/ful-2/mir172a-2/b-3* plants, it was not possible to count the number of cauline leaves on these plants. These results suggest that SPL15 requires *FUL* and *MIR172A* and *B* for flowering but not for bolting. However, these factors are apparently necessary for floral induction and open flowers in *rSPL15* under SD conditions.

***mir172a, d* and *e* single mutations delay flowering in SD conditions**

Because the combination of mutations in *MIR172A* or *MIR172B* with *ful-2* had a small and large effect on flowering time, respectively, the flowering-time phenotype of *MIR172* single mutants was analysed in SD conditions to evaluate whether they showed flowering phenotypes similar to those of *spl15-1* (Fig. 2.4E–F). The flowering-time phenotype of these mutants was previously only analysed in LD conditions, and showed that *mir172a-2* had the largest effect on flowering compared to Col-0 (O'Maoileidigh *et al.,* in preparation). In SDs, however, *mir172a-2, mir172d-3* and *mir172e-1* were late flowering compared with Col-0 (Fig. 2.7A–C). The *mir172b-3* and *mir172c-1* single mutants did not have an altered flowering-time phenotype in these conditions. Because *MIR172E* expression was never observed in the SAM, and it was hypothesised that SPL15 mainly functions in the SAM, *MIR172E* was not included in any of the subsequent experiments (Hyun *et al.*, 2016; O'Maoileidigh *et al.,* in preparation).

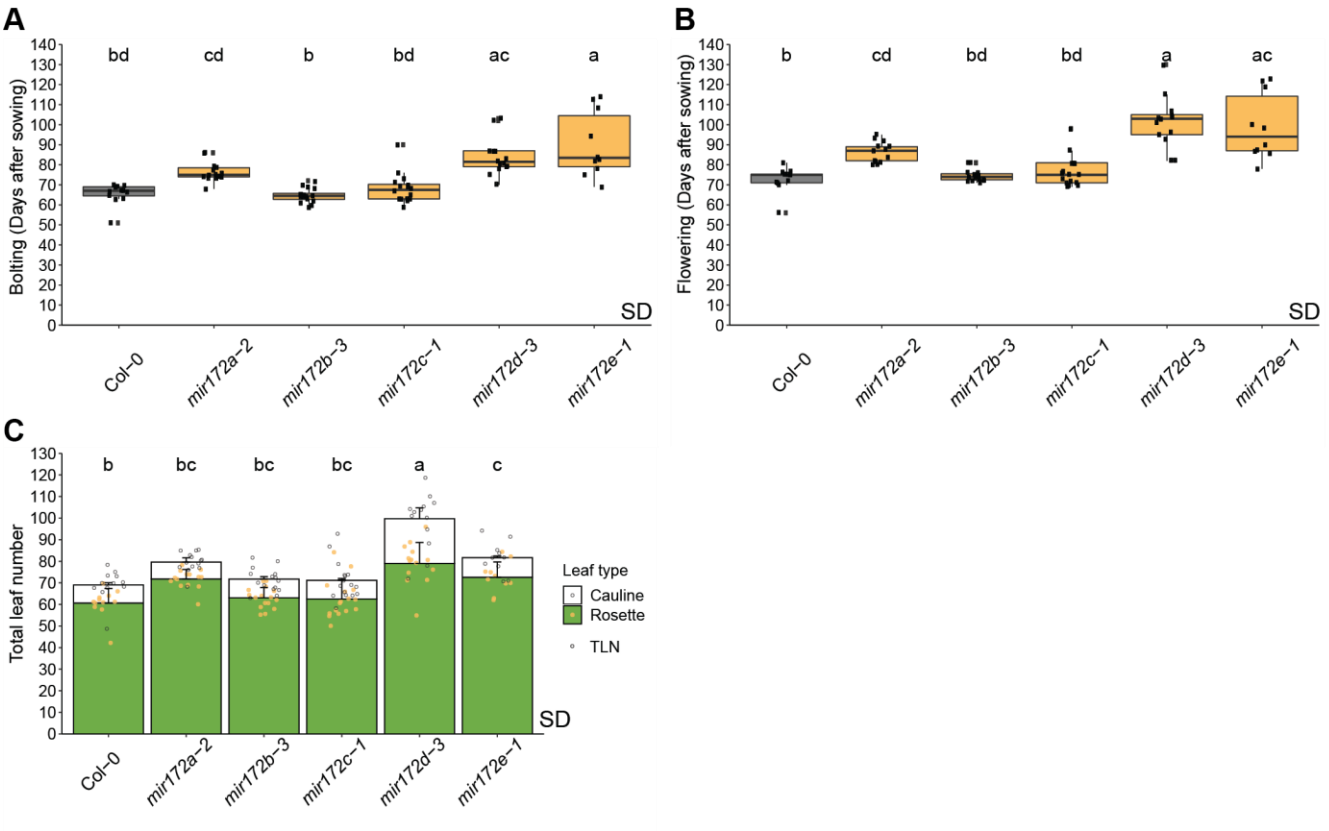

Figure 2.7. Flowering-time phenotype of Col-0 and all single mir172 mutants in SD conditions. Time to bolting (**A**), flowering time (**B**) and total leaf number (**C**; TLN) of the indicated genotypes in SD conditions (n = 10–16). Bolting time was scored as the day on which the inflorescence extended 0.5 cm from the rosette, and flowering time was scored as the day on which the first flower opened, anywhere on the plant. Statistical differences were calculated with ANOVA followed by Tukey's HSD (honestly significant difference) test at $p < 0.01$.

FUL accumulates in the shoot apical meristem of Col-0 prior to flowering in short-day conditions, but does not accumulate in *spl15-1* mutant shoot apical meristems

Because *FUL* is a direct target of SPL15, the effect of SPL15 on FUL protein expression and localisation was analysed in SD conditions. To this end, confocal microscopy of dissected SAMs of plants expressing *pSPL15::VENUS::SPL15* in Col-0, *pFUL::FUL::VENUS* in *ful-2* and *spl15-1/ful-2* was performed along a SD time course. As shown in Fig. 2.2, SPL15 was present in the SAM at 4wSD and remained expressed during and after the floral transition (Fig. 2.8A). For the complementation line *pFUL::FUL::VENUS*/*ful-2*, the results show that in SD conditions, FUL::VENUS became visible in the SAM at 5wSD in *ful-2* and remained in the SAM from that time point onwards (Fig. 2.8B, top). The signal appeared to spread over a larger area of the SAM and extended downwards into the stem. Furthermore, FUL::VENUS expression was observed on the abaxial sides of the floral primordia (Fig. 2.7, 7wSD). In *spl15-1* mutant plants, FUL::VENUS was not observed at any time point in the time course, nor were there any signs of floral induction in these plants

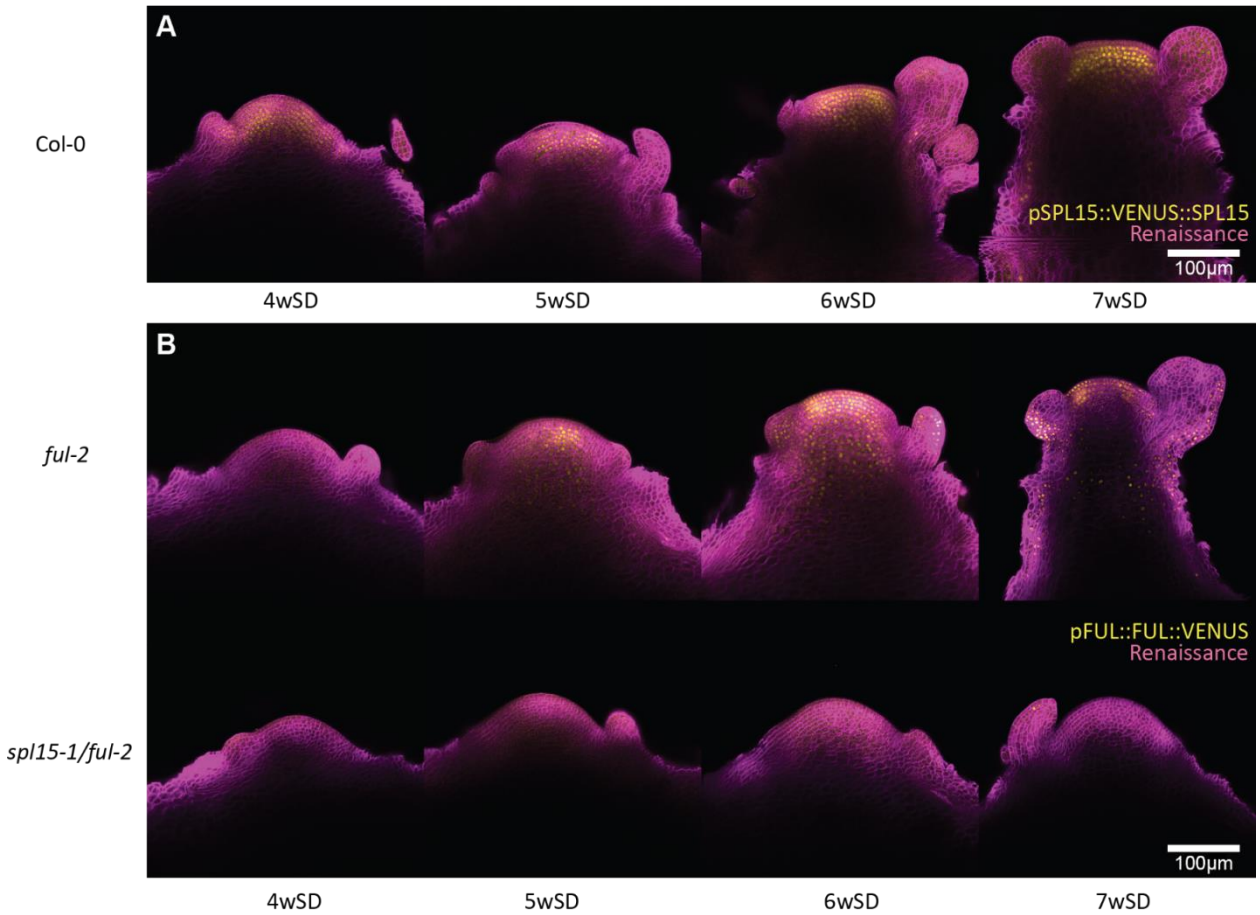

Figure 2.8. Confocal time-course of *pSPL15::VENUS::SPL15* in Col-0 and *pFUL::FUL::VENUS* expression in *ful-2* and *spl15-1* in SD conditions. (**A**) Confocal laser scanning micrographs of shoot apices of *pSPL15::VENUS::SPL15* at the indicated time points in SD conditions. (**B**) Confocal laser scanning micrographs of shoot apices of *pFUL::FUL::9AVENUS*/*ful-2* (top) and the same line in *spl15-1/ful-2* background (bottom) at the indicated time points in SD conditions. Fluorescence from VENUS is artificially coloured in yellow and fluorescence from the Renaissance dye is artificially coloured in magenta. The white scale bar represents 100 µm. A representative image of five samples is shown for each genotype and time point.

(Fig. 2.8B, bottom). This confirms the previously published *in situ* hybridization pattern of FUL in Col-0 and *spl15-1* and shows that expression of the FUL protein is coincident with that of *FUL* RNA. Moreover, these results confirm that in the absence of SPL15 (*spl15-1*), *FUL* is not expressed in the SAM, nor is there any FUL protein visible in the SAM at least up until 7wSD.

MIR172A, B and D accumulate in the shoot apical region over time in short-day conditions in Col-0 and *spl15-1* mutants.

MIR172B was previously shown to be a direct target of SPL15 (Hyun *et al.*, 2016). Moreover, *mir172a* and *mir172d* showed a late-flowering phenotype in SD conditions; therefore, I reasoned that in addition to *MIR172B, MIR172A* and *D* might also be direct or indirect targets of SPL15. To analyse the effect of SPL15 on the expression and localisation of these microRNAs (miRNAs), I used the MIR172 markers for *MIR172A, B* and *D* (O'Maoileidigh *et al.,* in preparation). In the marker constructs, the hairpin region of the *MIR172* gene was replaced by NLS::VENUS::GUS (referred to as VENUS::GUS), which resulted in a transcriptional fusion for each of these *MIRNA* genes. The *MIR172A* and *B* markers had already been combined with *spl15-1* previously, and I generated the MIR172D::VENUS:GUS*/spl15-1* line. The FUL::VENUS line and the *MIR172* marker lines were grown in SD conditions and their expression studied with confocal microscopy.

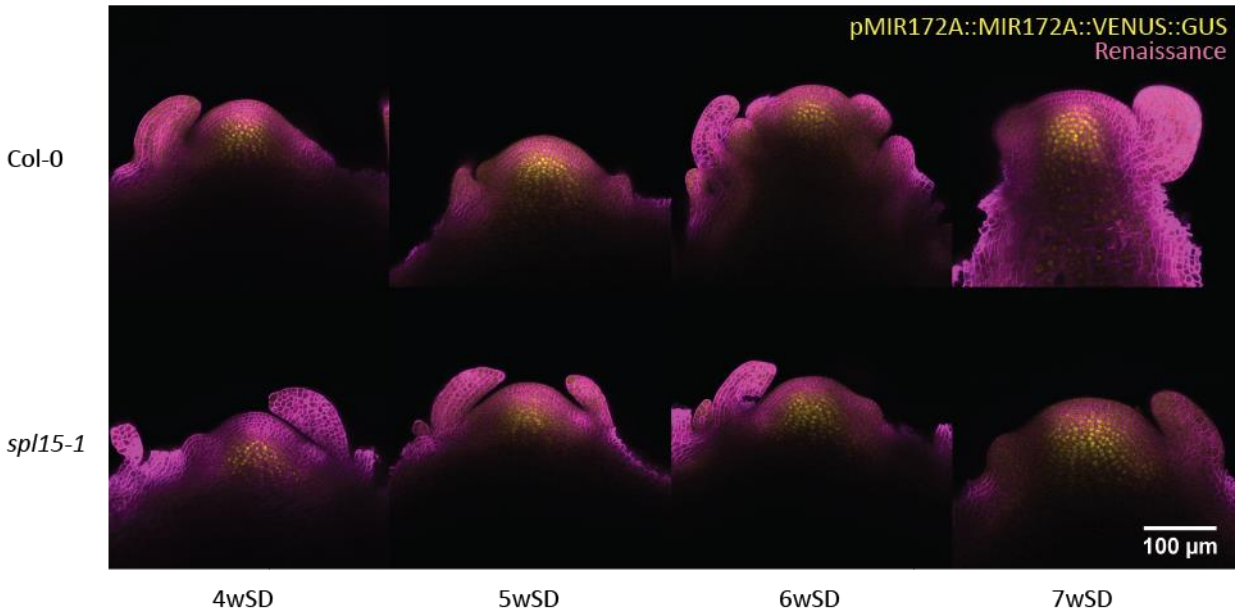

Figure 2. 9: Confocal time course of pMIR172A::MIR172A::VENUS::GUS expression in Col-0 and *spl15-1* in SD conditions. Confocal laser scanning micrographs of shoot apices of pMIR172A::MIR172A::NLS::VENUS::GUS (top) and the same line in the *spl15-1* background (bottom) at the indicated time points in SD conditions. Fluorescence from VENUS is artificially coloured in yellow and fluorescence from the Renaissance dye is artificially coloured in magenta. The white scale bar represents 100 µm. A representative image of five samples is shown for each genotype and time point.

All three markers were expressed in Col-0 SAMs after 4 weeks in SD conditions (Fig. 2.9–2.11). Expression of *pMIR172A::MIR172A::VENUS::GUS* was observed in the L3 of the SAM and below, and during the time-course, expression spread further down towards the stem, but not higher into the SAM than the L3 layer in Col-0 (Fig. 2.9, top). Although the morphology of these plants changed over time from a relatively flat SAM, to a domed SAM that bolted and produced buds, the pattern of expression of *MIR172A* remained relatively constant. Expression remained absent in the L1 and L2 layers and in floral primordia. The L1 layer of the meristem is the first layer of cells from the top of the meristem. The L2 layer is the layer of cells right below the L1 and the L3 are all layers of cells below the L2 until the cells start changing shape and size lower down in the SAM. As the floral transition progressed, *MIR172A* expression extended down the stem, but might also have been present at lower levels in the stem at earlier time points. The thickness of the samples at those stages might have prevented detection of the signal. In *spl15-1* mutants, *MIR172A* was already present at 4wSD, but also remained in the SAM throughout the time-course. The only difference from expression in Col-0 was that in *spl15-1* the SAM became larger over time, but did not begin to dome, bolt or produce any floral buds. The expression of *MIR172A* in this genotype did not change over time.

The expression of *pMIR172B::MIR172B::VENUS::GUS* did change over time in Col-0. At 4wSD, expression was localised to the central region of the SAM, in the lower part of the L3 (Fig. 2.10A, top). During doming of the SAM at 5wSD, the expression pattern of *MIR172B* enlarged together with an increase in the size of the SAM. When the SAM initiated the production of axillary shoots and started to bolt at 6wSD, expression of *MIR172B* extended downwards into the stem and the expression domain became broader. In some plants, expression was also observed in the L1 and L2 layer of the SAM at this stage, but at 7wSD, the *MIRNA* gene was expressed in these two layers in all plants analysed. Furthermore, at this time point there was a break in *MIR172B* expression in the SAM between the L2 and the lower region of L3 (Fig. 2.10A, top right). No *MIR172B* expression was observed in the floral buds. In *spl15-1* plants, the expression of *MIR172B* in the SAM remained constant in the lower region of the SAM, and the expression domain enlarged together with an increase in the size of the SAM (Fig. 2.10A, bottom). However, similar to *MIR172B* expression in Col-0, at 6- and 7wSD, VENUS signal was also detected in the L1 and L2 of the SAM. Similar to in Col-0 at 7wSD, there was a break in expression between those layers and the lower region of the L3. Therefore, although *spl15-1* plants did not undergo the floral transition in this time course, a change in expression of *MIR172B* was still observed as the SAM developed.

The expression of *MIR172A* and *B* was detectable in the SAM in Col-0 and *spl15-1* throughout the whole time-course. This suggests that even in the absence of SPL15, these two *MIRNA* genes produced *MIRNA* precursor and potentially also mature MIRNA172 in this spatio-temporal pattern. Data from a related flowering-time experiment indeed suggest that additional mutation of *MIR172A* or *B* in the *spl15-1* background led to even later flowering (Fig. 2.10B). Although this experiment was conducted in greenhouse SD conditions, which are controlled in daylength and temperature only, they demonstrate that the flowering time of *spl15-1* plants can be delayed further by these *MIR172* mutations.

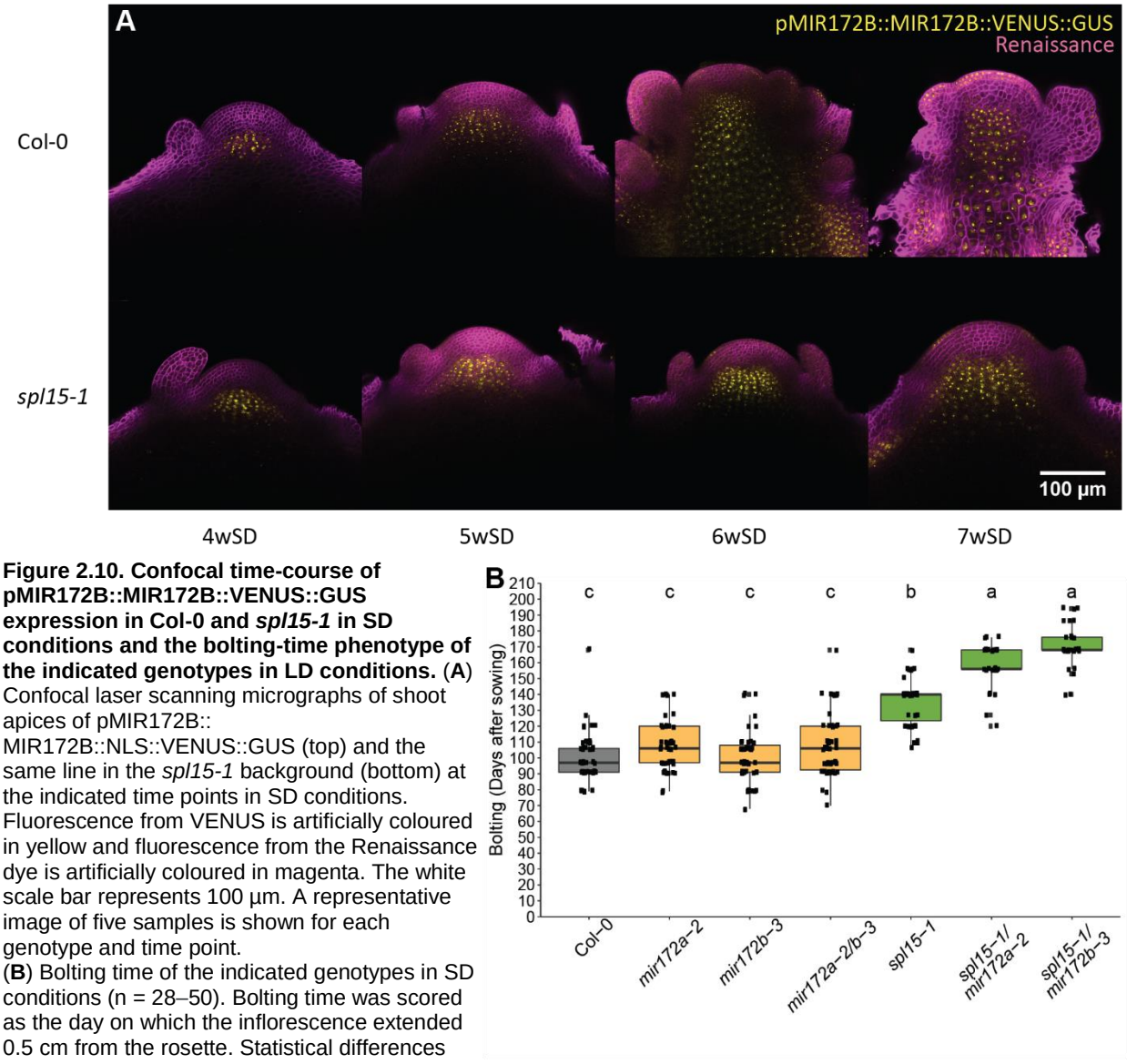

Figure 2.10. Confocal time-course of pMIR172B::MIR172B::VENUS::GUS expression in Col-0 and *spl15-1* in SD conditions and the bolting-time phenotype of the indicated genotypes in LD conditions. (**A**) Confocal laser scanning micrographs of shoot apices of pMIR172B:: MIR172B::NLS::VENUS::GUS (top) and the same line in the *spl15-1* background (bottom) at the indicated time points in SD conditions. Fluorescence from VENUS is artificially coloured in yellow and fluorescence from the Renaissance dye is artificially coloured in magenta. The white scale bar represents 100 µm. A representative image of five samples is shown for each genotype and time point.
(**B**) Bolting time of the indicated genotypes in SD conditions (n = 28–50). Bolting time was scored as the day on which the inflorescence extended 0.5 cm from the rosette. Statistical differences were calculated with ANOVA followed by Tukey's HSD (honestly significant difference) test at $p < 0.01$.

The other *MIRNA* gene in this assay, *MIR172D*, was expressed similarly to *MIR172B* in the early time points in Col-0. Expression of *pMIR172D::MIR172D::VENUS::*GUS was observed in a relatively small region low in the L3 layer and in a domain that enlarged with the increasing size of the SAM (Fig. 2.11, top, 4- and 5wSD). However, as the Col-0 SAM started to drastically change at 6wSD by producing axillary meristems and starting to bolt, the *MIR172D* expression pattern also drastically expanded. At 6- and 7wSD, the expression pattern not only became wider and extended all the way down into the stem, but also marked the flanks of the SAM as well as the complete L1 layer of the meristem. In some samples there was a gap in *MIR172D* expression between L1 and L3 at 6wSD, but in others there was not. At 7wSD, very strong expression was observed in the L1, and below the L1 all cells in the SAM showed signal, which was weaker than that in the L1 layer. *MIR172D* expression was also not detected in floral buds, except for in very young floral primordia. In *spl15-1* plants, the *MIR172D* expression pattern was similar to that in Col-0 at 4- and 5wSD and remained constant at 6- and 7wSD (Fig. 2.11, bottom). However, some VENUS signal was also detected in the L1 layer at 6wSD and even in all the layers above the localised expression region at 7wSD. Expression at 7wSD was different from the pattern in Col-0, where *MIR172D* was strongly expressed in the whole L1, because in *spl15-1*, the upper layers only expressed *MIR172D* in the centre of the top of the SAM.

In contrast to *FUL* expression in Col-0 and *spl15-1,* the *MIR172* markers were expressed at the earliest time point in both genotypes, which suggests that SPL15 is not required for their initial expression in the SAM.

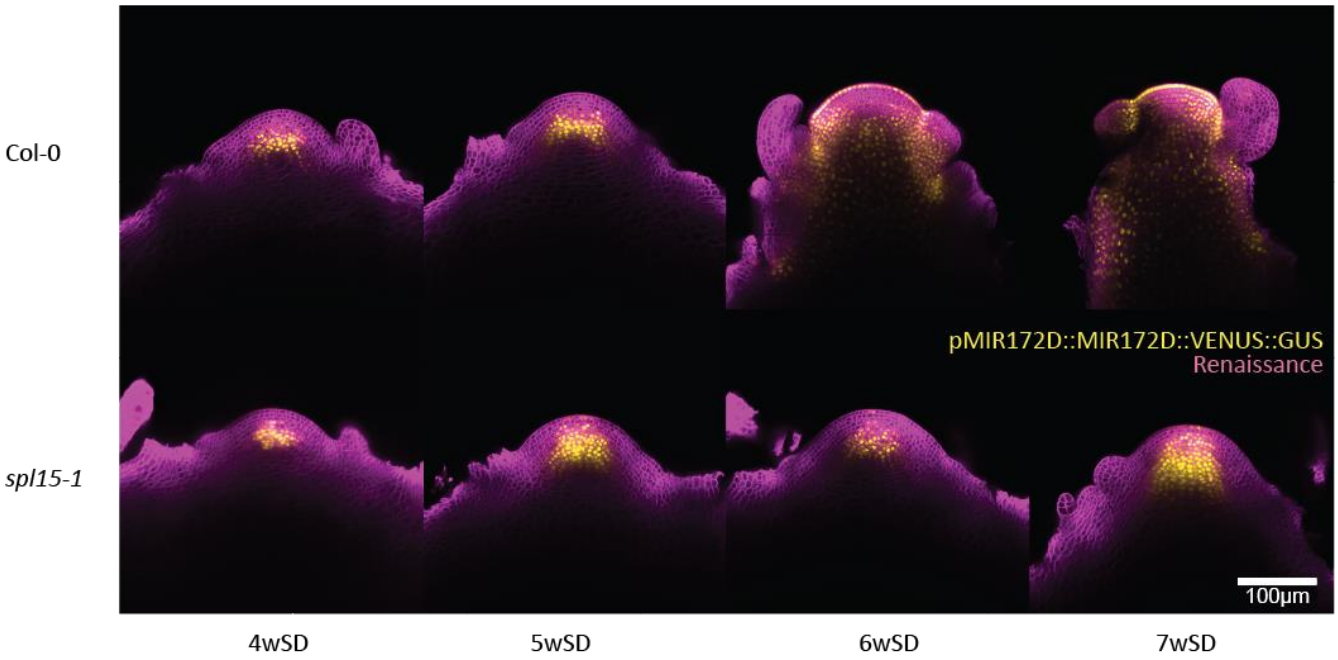

Figure 2.11. Confocal time course of pMIR172D::MIR172D::VENUS::GUS in Col-0 and *spl15-1* in SD conditions. Confocal laser scanning micrographs of shoot apices of pMIR172D::MIR172D::NLS::VENUS::GUS (top) and the same line in *spl15-1* background (bottom) at the indicated time points in SD conditions. Fluorescence from VENUS is artificially coloured in yellow and fluorescence from the Renaissance dye is artificially coloured in magenta. The white scale bar represents 100 µm. A representative image of five samples is shown for each genotype and time point.

In the shoot apical meristem, APETALA2 expression decreases over time and negatively correlates with SPL15 accumulation

APETALA2 is one of the targets of *MIR172* and is a floral repressor that is downregulated during the floral transition. Because SPL15 targets at least one of the *MIR172s,* namely *MIR172B,* and the MIR172s target *AP2*, it is plausible that expression of AP2 and SPL15 is inversely correlated in the SAM. To study this, I used confocal microscopy and dissected SAMs of plants that expressed pSPL15::VENUS::SPL15, pAP2::AP2::VENUS and pAP2::rAP2::VENUS, an AP2-line that is no longer targeted by MIR172. As described previously, SPL15 became visible in the meristem from 3wSD onwards (Fig. 2.12; first column). During the early time points SPL15 signal was relatively weak, but from 5wSD, became much stronger and was localised throughout the SAM. On the other hand, AP2 expression was clearly visible throughout the meristem from 3wSD until 6wSD (Fig. 2.12; middle column). Subsequently, AP2 expression disappeared from the SAM, but remained visible in the axillary and floral meristems (clearly visible at 7wSD). rAP2 plants flowered very late under SD conditions and consistent with this, rAP2 was expressed throughout the meristem during the whole time course until 10wSD (Fig. 2.12; right column). Although the expression of SPL15 and AP2 was indeed inversely

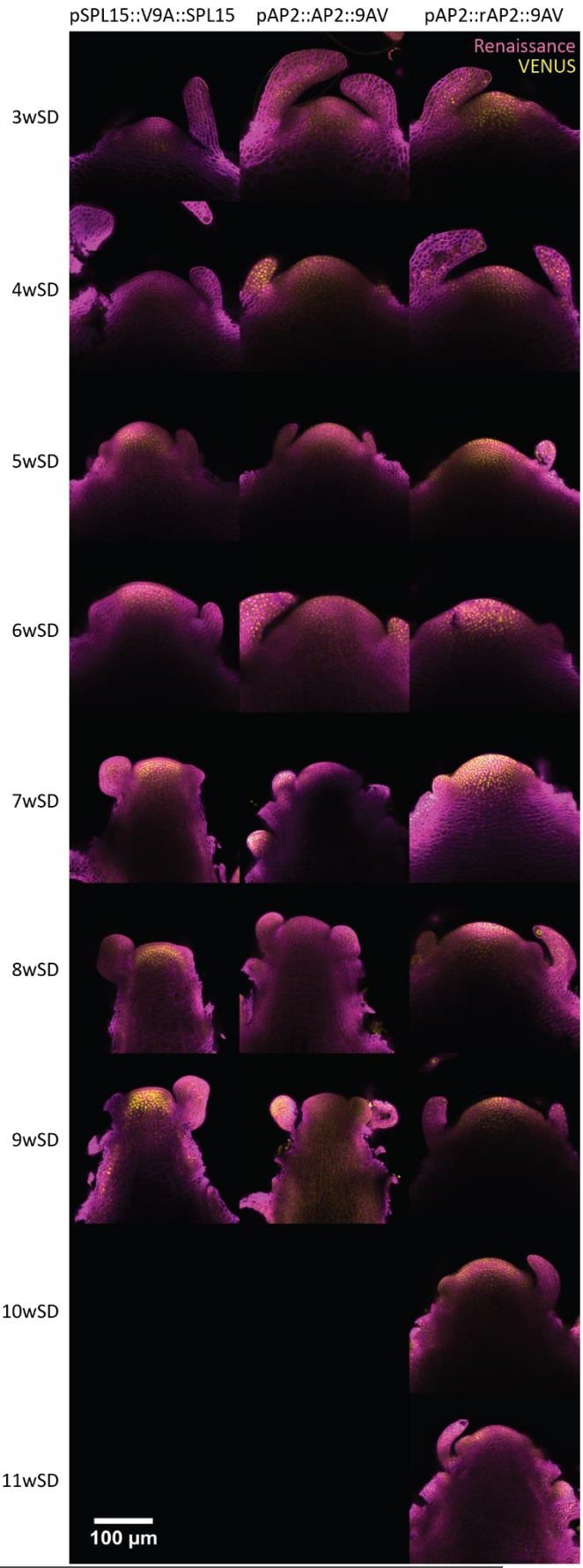

Figure 2.12. Confocal time course of pSPL15::VENUS::SPL15, pAP2::AP2::VENUS, pAP2::rAP2::VENUS expression in Col-0 in SD conditions. Confocal laser scanning micrographs of shoot apices of indicated fluorescent lines (top) at the indicated time points in SD conditions (left). Fluorescence from VENUS is artificially coloured in yellow and fluorescence from the Renaissance dye is artificially coloured in magenta. The white scale bar represents 100 µm. A representative image of four samples is shown per genotype and time point.

correlated in the SAM over time, SPL15 and AP2 were both clearly present in the SAM at several time points in this confocal time course (5- and 6wSD). Although these samples were not grown side by side, Figures 2.9–2.10 indicate that *MIR172A, B* and *D* are also expressed in the SAM from 4wSD. It is possible that from the time when SPL15 becomes expressed in the SAM and activates *FUL* expression, and perhaps further stimulates *MIR172* expression, it nevertheless takes another week for these factors to co-ordinately overcome floral inhibition of AP2 and potentially other AP2-Ls (Fig. 2.3). The consistently high expression of rAP2 in this confocal time course indicates that *MIR172* plays a crucial role in the repression of *AP2* in a spatial and temporal manner.

Mutations in *SPL15, FUL* and *MIR172A* and *B* delayed flowering, caused loss of apical dominance and a variety of other morphological phenotypes

To study how the flowering-time phenotype is affected when *FUL* and almost all the *MIR172* paralogues are mutated, I grew higher-order mutants of these genotypes, including *ful-2, mir172a-2/b-3/c-1/d-3, ful-2/mir172a-2/b-2/c-1/d-3* and *spl15-1/mir172a-2/b-3*, in LD conditions. The latter genotype was included to compare *ful-2/mir172a-2/b-2/c-1/d-3* and *spl15-1/mir172a-2/b-3* and to determine the effects of these mutations on the morphological phenotypes of the plants. The *mir172a-2/b-3/c-1/d-3* plants bolted and flowered later than *ful-2* and both these genotypes bolted and flowered later than Col-0 (Fig. 2.13A, B). The *ful-2/mir172a-2/b-2/c-1/d-3* genotype caused even later bolting and flowering, which was similar to the flowering-time phenotype of *spl15-1/mir172a-2/b-3* (Fig. 2.13A, B).

These data support the hypothesis that *FUL* and *MIR172* act in parallel, because their combined mutation enhances the delay in flowering and bolting time caused by mutation in either gene. Furthermore, the data also support the hypothesis that SPL15 directly and/or indirectly regulates *FUL* and *MIR172,* because additional mutation of *spl15* in a *ful/mir172* mutant background does not further delay flowering in LD conditions. The differences in TLN among genotypes were very similar to those in bolting and flowering time, although the TLN of *ful-2* was not significantly higher than that of Col-0 (Fig. 2.13C).

Plants with higher-order mutations that include *ful-2* and multiple *mir172* mutant alleles show severe defects in plant morphology and meristem determinacy

Besides the differences in flowering time, *ful-2/mir172a-2/b-2/c-1/d-3* and *spl15-1/mir172a-2/b-3* plants were morphologically very different. *ful-2* plants produce a tall inflorescence with more nodes, but when combined with *mir172a-2/b-3/c-1/d-3*, which produced a relatively short inflorescence, the plants become

very short (Fig. 2.13D; Balanzà *et al.*, 2018; Bemer *et al.*, 2017). Moreover, *ful-2* plants produce many axillary shoots on the inflorescence, but *mir172a-2/b-3/c-1/d-3* has many axillary shoots that derive from the rosette. The *ful-2/mir172a-2/b-2/c-1/d-3* plants produced even more axillary shoots from the axils from different rosette leaves, but also similar to *ful-2*, many axillary inflorescences initiate from the main inflorescence. Although *ful-2/mir172a-2/b-2/c-1/d-3* and *spl15-1/mir172a-2/b-3* plants behaved similarly in terms of flowering time, these plants showed striking differences in inflorescence architecture. The *ful-2/mir172a-2/b-2/c-1/d-3* plants were much shorter and bushier, whereas *spl15-1/mir172a-2/b-3* plants were taller, but still had many axillary shoots (Fig. 2.13D).

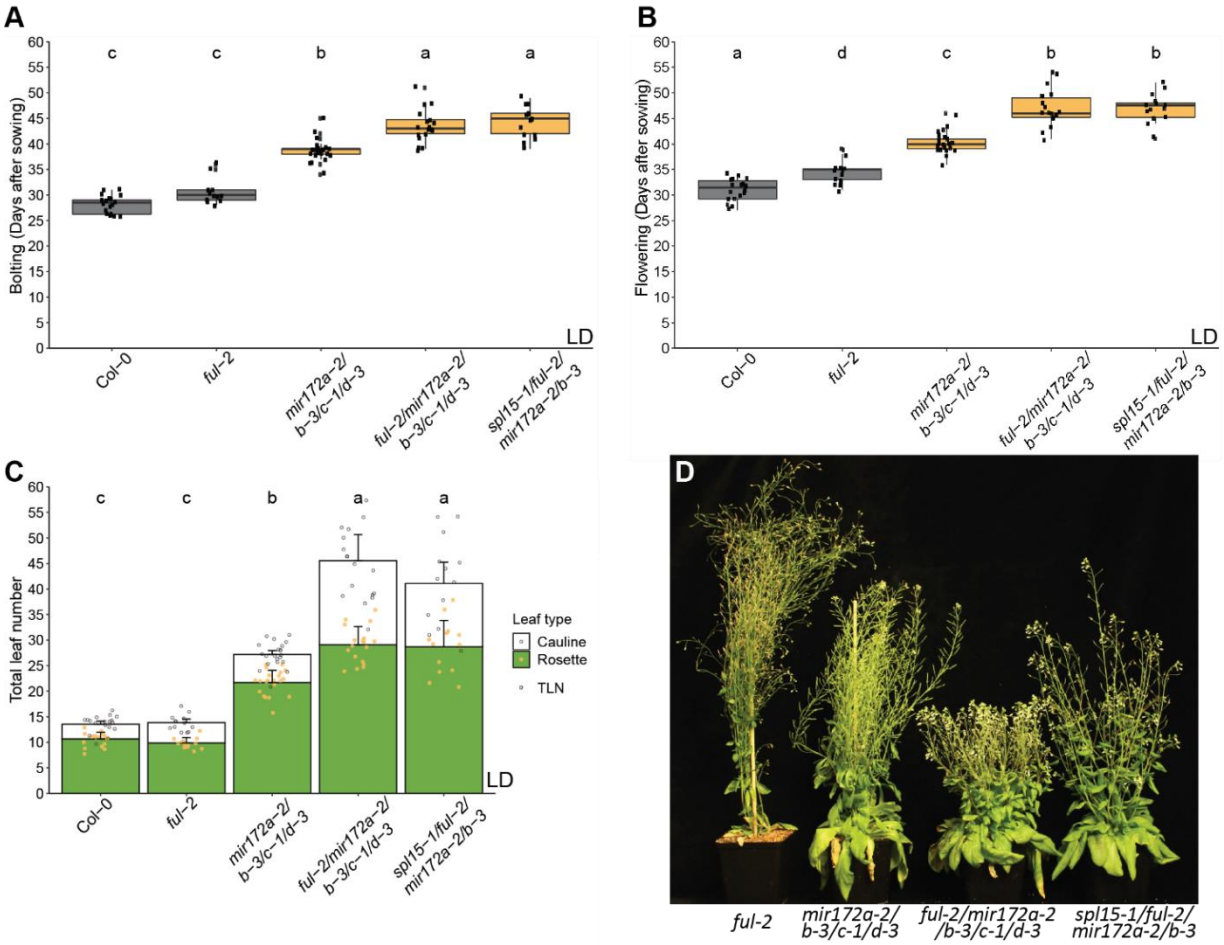

Figure 2.13. Flowering-time phenotype of higher-order mutants in LD conditions. Time to bolting (**A**), flowering time (**B**) and total leaf number (**C**; TLN) of the indicated genotypes in LD conditions (n = 13–21). (**D**) Image of representative plant phenotypes from the flowering-time assay (A–C) at 64LD. Bolting time was scored as the day on which the inflorescence extended 0.5 cm from the rosette, and flowering time was scored as the day on which the first flower opened, anywhere on the plant. Statistical differences were calculated with ANOVA followed by Tukey's HSD (honestly significant difference) test at $p < 0.01$.

Although these morphological phenotypes were not quantified in this experiment, the images clearly depict the differences in morphology between these genotypes (Fig. 2.14). In particular, *ful-2/mir172a-2/b-2/c-1/d-3* plants were morphologically very different from Col-0. Fig. 2.14A shows for instance, that they were much shorter and bushier than Col-0 and *ful-2* and were bushier than *mir172a-2/b-3/c-1/d-3* plants. Moreover, these plants continued to grow for over six months, because they continued to produce new axillary shoots (Fig. 2.14B). When *ful-2/mir172a-2/b-2/c-1/d-3* plants started to flower, axillary shoots were often produced from several inflorescences simultaneously and these shoots often repeatedly alternated between the initiation of axillary shoots and the initiation of flowers, leading to flower formation directly on the stem, with cauline leaves above them (Fig. 2.14C, D).

The flowers of this genotype often showed severe indeterminacy and initiated a flower within the carpel of the original flower, multiple times (Fig. 2.14F-H). These flowers appeared wild type and opened normally until the carpel bulged and burst open and a new flower developed (Fig. 2.14E, H). The phenotypes illustrate that in addition to having an important function in floral induction, *FUL* and *MIR172* also regulate plant morphology and meristem determinacy.

Figure 2.14. Morphological phenotypes of higher-order mutants grown in LD conditions. (**A**) Representative plant phenotypes of Col-0, *ful-2*, *mir172a-2/b-3/c-1/d-3* and *ful-2/mir172a-2/b-3/c-1/d-3* at ~55LD. (**B**) A *ful-2/mir172a-2/b-3/c-1/d-3* plant at ~4 months in LD conditions. (**C**) A top view of a *ful-2/mir172a-2/b-3/c-1/d-3* plant at ~55LD, showing the appearance of multiple inflorescences. (**D**) A top view of a *ful-2/mir172a-2/b-3/c-1/d-3* at 45LD grown in greenhouse conditions, showing the appearance of cauline leaves above flowers on the inflorescence. (**E**) Representative flowers from Col-0, *ful-2*, *mir172a-2/b-3/c-1/d-3* and *ful-2/mir172a-2/b-3/c-1/d-3* immediately after opening of the flower, showing the bulging of the carpel that only occurs in *ful-2/mir172a-2/b-3/c-1/d-3.* (**F**) Image of a *ful-2/mir172a-2/b-3/c-1/d-3* inflorescence showing the flower-in-a-flower phenotype. (**G**) Light microscopy image of a *ful-2/mir172a-2/b-3/c-1/d-3* flower showing the flower-in-a-flower phenotype in more detail. (**H**) Light microscopy image of a *ful-2/mir172a-2/b-3/c-1/d-3* flower showing the bulging of the carpel from which the flower-in-a-flower phenotype arises.

Discussion

FUL, MIR172A and *MIR172B* as targets in the SPL15 floral induction pathway

This chapter describes a genetic approach to study whether and how SPL15 induces flowering through altering a balance of the interaction among FUL, MIR172 and AP2-Ls (Fig. 2.3). I first tested the extent to which higher-order mutations of *ful-2/mir172a-2/b-3* could phenocopy the *spl15-1* flowering-time phenotype. In LDs, *spl15-1* flowers at a similar time to Col-0, but *ful-2/mir172a-2, ful-2/mir172b-3* and *ful-2/mir172a-2/b-3* all flowered later than Col-0, illustrating the importance of these genes and miRNAs for flowering in these conditions (Fig. 2.4A–C). This also suggests that in LD conditions, SPL15 is not required for the activation of *FUL, MIR172A* and *MIR172B.* In SD conditions, however, *ful-2/mir172b-3* and *ful-2mir172a-2/b-3* plants phenocopy *spl15-1* single mutants, supporting the hypothesis that in SD conditions, flowering is induced by the activation of *FUL* and *MIR172* by SPL15 (Fig. 2.4D-F). Indeed, the flowering time phenotypes and inflorescence architecture of these plants were so similar, that *FUL* and *MIR172B* and possibly *MIR172A* might be the main or only targets of SPL15 that are involved in floral induction in SD conditions. The difference in dependency on SPL15 under LD and SD conditions could be explained by the presence of other SPL transcription factors that have a more prominent role in floral induction in LD conditions (Jung *et al.*, 2016; M. Xu, Hu, Zhao, *et al.*, 2016; A. Yamaguchi *et al.*, 2009). Therefore, although the flowering-time phenotype of *spl15-1* and *ful-2/mir172b-3* and *ful-2mir172a-2/b-3* is similar, this might not only depend on the direct regulation of these genes by SPL15, but highly probably also on regulation by other transcription factors such as additional SPLs.

Moreover, the LD and SD experiments with *rSPL15* together with *ful-2, mir172a-2* and or *mir172b-3* show that even in the absence of *FUL, MIR172A* and *B*, plants that expressed *rSPL15* were still earlier bolting than the triple mutant of *ful-2mir172a-2/b-3.* However, introduction of *rSPL15* was insufficient to induce the early production of flowers in this background. The earlier-bolting phenotype that results from expression of *rSPL15* in the *ful-2/mir172a-2/b-3* background suggests that *rSPL15* might have other targets besides *FUL, MIR172A* and *MIR172B* through which it can promote the floral transition; i.e., early bolting. Because *rSPL15* is expressed from the native promoter of *SPL15*, its expression domain should fully encompass that of the native *SPL15*. However, because *rSPL15* causes *SPL15* overexpression, it is potentially expressed at times and in tissues where *SPL15* is not expressed due to its downregulation by *MIR156.* Therefore, *rSPL15* might potentially be able to regulate the expression of its direct targets earlier in development, but potentially also in tissues where they would normally not be expressed. Moreover, *rSPL15* might regulate genes that it would normally not regulate, because its binding site is highly similar,

if not identical, to the binding motifs of other SPL transcription factors (Birkenbihl *et al.*, 2005). This might in part explain the complex morphological phenotype of *rSPL15* plants, but this might also be explained by the overactivation of the direct SPL15 targets. Transcriptomic analysis of *rSPL15* might be helpful to identify its target genes during floral induction.

To fully understand the extent to which *FUL*, *MIR172A* and *B* are involved in floral induction via SPL15, it would be useful to combine *spl15-1* with the higher-order mutant *ful-2/mir172a-2/b-3/c-1/d-3* and to grow it together with *spl15-1/ful-2/mir172a-2/b-3* in SD conditions, to determine whether *spl15-1* has a synergistic effect on flowering-time behaviour under these conditions. I attempted to generate the *spl15-1/ful-2/mir172a-2/b-3/c-1/d-3* line, but did not recover the key genotype in the F_2. Moreover, the segregating plants grew mainly vegetative shoots and very few reproductive shoots, which hampered the recovery of seeds. In addition, *spl15-1* and *mir172d*-3 do not easily recombine, because they are genetically linked on chromosome 3 (*MIR172D*: Chr3.20587903-20588127 and *SPL15*: Chr3. 21444450-21445852; 856323 nucleotides apart). However, it would be interesting to at least identify plants with the *spl15-1/ful-2/mir172a-2/b-3/d-3* genotype and to study their phenotype in SD conditions.

SPL15 and the regulation of *MIR172A, B* and *D* in the SAM in SD conditions

One of the other direct targets of SPL15 might be *MIR172D,* because its mutant allele is late flowering in SD conditions (Fig. 2.6). However, when FUL::VENUS, MIR172A::VENUS, MIR172B::VENUS and MIR172D::VENUS expression was studied with confocal microscopy in the *spl15-1* background, only *FUL* was dependent upon SPL15 for wild-type expression in the meristem in SD conditions. Although *MIR172B* is a direct target of SPL15, it is unclear from the confocal data whether SPL15 is responsible for activating its expression in the SAM. It is possible that SPL15 is required for its upregulation upon floral induction, or that SPL15 regulates *MIR172B* expression in other plant tissues. *MIR172A* and *D* show similar expression patterns to *MIR172B*, and it is unclear whether SPL15 regulates them directly or indirectly in the SAM, although SPL15 does not seem required for their initial activation in the SAM. It is possible that the VENUS fusion lines of the *MIRNA* genes tested here do not fully represent the expression patterns of the primary miRNAs. Additional posttranscriptional regulation might exist, besides processing by the DICER machinery, which is lost due to the insertion of NLS::VENUS::GUS into the gene (J. Wang *et al.*, 2019). This might especially be the case when comparing the VENUS expression patterns of these *MIR172* alleles with the published *in situ* hybridization expression pattern of mature *MIR172* in SD conditions (Hyun *et al.*, 2016). *In situ* hybridization revealed no mature *MIR172* in the SAM of *spl15-1* mutants up to 9 weeks in SD

conditions. This might be due to the expression level of the miRNA or to the sensitivity of the hybridization probe. Alternatively, as mentioned above, the primary miRNAs might be regulated post-transcriptionally and be degraded in *spl15-1* but not in Col-0. This might be the reason I was able to detect the marker lines in the SAM of *spl15-1* plants, and why no mature *MIR172* was detected in the SAM of these plants via *in situ* hybridization. Maybe an SPL15-dependent stabilisation step is required for the primary miRNAs to be processed into mature *MIR172.*

Finally, miRNAs are small molecules that can move between cells; therefore, although a very restricted transcriptional pattern was observed, this pattern might not represent the functional domain of the mature miRNA (Bhogale *et al.*, 2014; A. Martin *et al.*, 2009; Skopelitis *et al.*, 2018). Moreover, the patterns of the MIR172 markers shown here do not fully recapitulate the *in situ* hybridization pattern of the mature *MIR172*, where it is present throughout the entire meristem (Hyun *et al.*, 2016). It is possible that the *MIR172A, B* and *D* marker line expression patterns in the SAM are correct, but that the mature *MIR172* only reaches the SAM when SPL15 is present. Moreover, SPL15 might regulate the expression of these three *MIR172* alleles in other tissues than the SAM, and the mature *MIR172* might be transported from these tissues into the meristem. SPL15 might be involved in the transport of *MIR172* by regulating the access to certain cells, or by developing the vasculature that leads to the meristem.

The regulation of *AP2* by SPL15

The targets of MIR172 are the *AP2-Ls*, among which AP2 has a well-established function in inhibiting flowering. I studied the protein expression of AP2::VENUS as well as its *MIR172*-resistant form rAP2::VENUS in SD conditions to determine whether expression patterns in the SAM are temporally inversely-correlated with VENUS::SPL15. Figure 2.12 showed that the expression of AP2::VENUS might overlap for approximately two weeks with that of VENUS::SPL15 in the SAM in SD conditions. This suggests that it takes two weeks for SPL15 to induce *FUL* and *MIR172* above threshold levels to downregulate AP2 in the meristem, or that the loop contains more feedback pathways between SPL15 and FUL than we currently hypothesised, leading to a slower change in the balance. Other SPL transcription factors might play a role in regulating *FUL*, potentially by inhibiting its expression, which would be relieved in the presence of sufficiently high levels of SPL15.

deally, SPL15 and AP2 could be tagged within the same plant, but this is not currently possible due to both reporter constructs carrying a VENUS fusion. Alternatively, the expression pattern of *AP2::VENUS* and *rAP2::VENUS* could be compared in *spl15-1, ful-2, spl15-1/ful-2* and perhaps even in *ful-2/mir172a-2/b-3* plants. I made these crosses, but did not have sufficient time to genotype the progeny. Moreover, perhaps *spl15-1* can still delay flowering of the *ap2-12* mutant*,* which would indicate that SPL15 regulates flowering through an additional pathway, such as one that involves other AP2-Ls. Perhaps the combination of *spl15-1* with *ap2-12* would lead to a partial rescue of the late-flowering phenotype of *spl15-1.* If so, this would mean that the late flowering of *spl15-1* is indeed caused by its inability to overcome floral repression by AP2 and would support the hypothesis that SPL15 is required to activate genes that lead to the repression of *AP2* and perhaps other *AP2-Ls,* either by transcriptional or post transcriptional downregulation. In addition, SPL15 might directly repress the transcription *AP2* and/or other *AP2-Ls*.

The effect of *MIR172* on *AP2* is clearly important for the appropriate timing of repression of *AP2,* because rAP2::VENUS remains in the meristem for much longer and these plants subsequently underwent the floral transition later than the AP2::VENUS line in SD conditions. Plants then might have to rely much more heavily on transcriptional downregulation by *FUL* and possibly other transcription factors. An important point is that these fluorescent lines are based on transgenes that might not be expressed identically to the endogenous gene. Moreover, all these lines were in the Col-0 background and therefore, all contained an additional two copies of the gene, potentially leading to overexpression of these proteins. Lastly, tagging a protein with a fluorescent protein can lead to alterations in protein folding and potentially to altered protein function.

Loss of floral meristem determinacy in higher-order combinations of *ful-2* and *mir172* mutants.

Mutants of *ful-2/mir172a-2/b-2/c-1/d-3* and *spl15-1/mir172a-2/b-3* plants bolt and flower at a similar time after sowing (Fig. 2.13). However, besides their similarities in flowering time, they differ in many aspects of plant morphology. The main inflorescence in *ful-2/mir172a-2/b-2/c-1/d-3* plants often ceased growth soon after its emergence, whereas in most *spl15-1/mir172a-2/b-3* plants, it continued growth for longer (Fig. 2.13D). Moreover, floral meristem determinacy was partially lost in *ful-2/mir172a-2/b-2/c-1/d-3*, but this never occurred in *spl15-1/mir172a-2/b-3* or *mir172a-2/b-3/c-1/d-3* plants (Fig. 2.14E–H). This floral

meristem determinacy was specific for *ful-2/mir172a-2/b-2/c-1/d-3* and *ful-2/mir172a-2/b-2/d-3* (data not shown) plants and was not observed in rAP2 plants.

AP2 normally restricts *AGAMOUS* (*AG*) expression to the inner two whorls of the flower, but also antagonises AG function in the centre of the flower (Huang *et al.*, 2017). *ag* mutants often exhibit a range of indeterminacy in the flowers, some similar to those I observed here for *ful-2/mir172a-2/b-2/c-1/d-3* and *ful-2/mir172a-2/b-2/d-3* plants (Bowman *et al.*, 1991). This phenotype is therefore probably caused by the inability to suppress *AP2* and thus, the failure to upregulate *AG* expression in the appropriate domains of the floral meristem. FUL might normally repress *AP2* activity specifically in the carpel in the central region of the flower. Based on the expression of *FUL* in the carpel valves as previously described and shown in figure 2.15, the repression of *AP2* might not only be important during the floral transition, but also during floral development (Ferrándiz *et al.*, 1999). AP2 and FUL might also be employed in a similar network to regulate floral determinacy. This is supported by the mutant morphology of flowers of *ap2-12* mutants, which clearly implicate an important role for AP2 in the flower. This function of AP2 might be restricted to specific tissues, which might explain why FUL and *MIR172* are required to inhibit *AP2* transcription in other tissues of the flower to prevent indeterminacy.

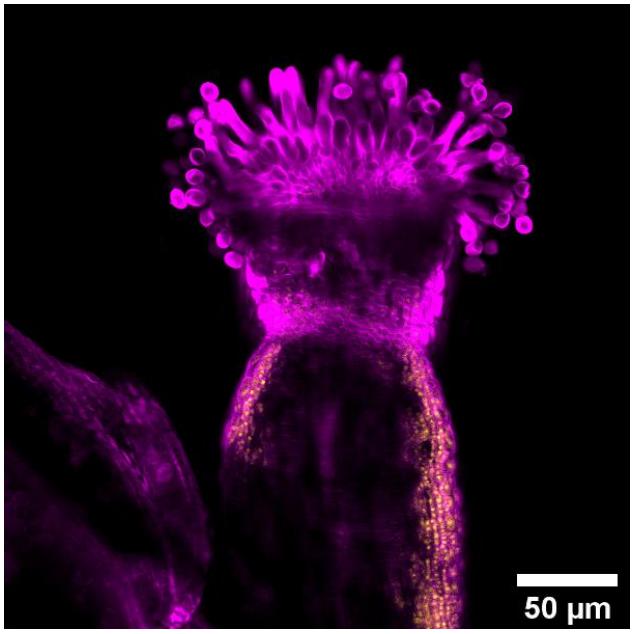

Figure 2.15. Confocal image of the carpel of *pFUL::FUL::VENUS/ful-2* line F9.1 (see Chapter 3). Fluorescence from VENUS is artificially coloured in yellow and fluorescence from the Renaissance dye is artificially coloured in magenta. The white scale bar represents 50 µm.

Chapter 3:

FRUITFULL and its functional *cis*-regulation by SQUAMOSA PROMOTER BINDING PROTEIN-LIKE transcription factors

Introduction

FRUITFULL (FUL) is a MIKC-type MADS-box transcription factor that has not only been studied for its function in floral induction and the integration of inductive signals, but also for its pleiotropic effects on plant morphology. Plants with a knock-out mutation in *FUL, ful-2*, flower slightly later under continuous light conditions and inductive long-day (LD) conditions, and flower substantially later in non-inductive short-day (SD) conditions (Fig. 3.1, Balanzà *et al.*, 2014; Ferrándiz *et al.*, 2000; Melzer *et al.*, 2008). This late flowering in SD conditions is due to a delay in flower opening, because *ful-2* plants bolt at the same time as wild-type in these conditions (Fig. 3.1D, E). Besides a role in the regulation of reproductive timing, FUL also affects inflorescence architecture: *ful-2* plants have more side shoots on the main inflorescence, and these shoots emerge from the inflorescence at a smaller angle from the stem than in wild-type plants (Fig. 3.1C, F; Bemer *et al.*, 2017). Moreover, *FUL* is involved in determinacy of the inflorescence meristem as well as meristem longevity (Balanzà *et al.*, 2018, 2019; Ferrándiz, Gu, *et al.*, 2000).

When combined with *SOC1* mutants, *soc1-3 ful-2* plants show perennial shoot characteristics such as secondary growth, increased longevity and meristem indeterminacy (Melzer *et al.*, 2008). The cauline leaves on the inflorescences of *ful-2* plants are rounder, shorter and wider than those of wild-type plants (Bemer *et al.*, 2017; Gu *et al.*, 1998; McCarthy *et al.*, 2015). Furthermore*, ful-2* plants have short and stunted siliques, and *FUL* regulates cell differentiation during the outgrowth of carpel valves (Ferrándiz, *et al.*, 2000; Gu *et al.*, 1998; McCarthy *et al.*, 2015). This role of *FUL* in fruit development has also been studied in cucumber, where different *FUL* alleles confer different fruit lengths (J. Zhao *et al.*, 2019). Lastly, FUL is important for fruit dehiscence not only in Arabidopsis, but in at least two other Brassicaceae species, *Brassica juncea* and *Brassica napus* (Ferrándiz *et al.*, 2000; Jaradat *et al.*, 2014; Østergaard *et al.*, 2006). *FUL* is directly regulated by SQUAMOSA PROMOTER BINDING PROTEIN-LIKE 15 (SPL15) and SUPPRESSOR OF OVEREXPRESSION OF CONSTANS 1 (SOC1), among other transcription factors (Hyun *et al.*, 2016; Immink *et al.*, 2012; Tao *et al.*, 2012).

In the absence of SPL15*,* flowering in SD is delayed and this is at least in part due to reduced expression of two important floral regulators: *FUL* and *MICRORNA 172B* (*MIR172B*; Fig. 2.4D-F; Hyun *et al.*, 2016). Moreover, in SPL15 mutant meristems (*spl15-1*), *FUL* transcription occurs later in development in SD

conditions and subsequently, no FUL protein can be detected in *spl15-1* plants at stages where FUL is present in the wild-type (Fig 2.8B, 4.7C, 4.11A; Hyun *et al.*, 2016). Similar to SPL15, SOC1 also directly targets *FUL* and *MIR172B* (Balanzà *et al.*, 2014; Hyun *et al.*, 2016) and plays an integrative role in flowering. SOC1 is a MIKC MADS-box transcription factors and similar to SPL15, SOC1 receives input from the age-related and GA pathways as well as from the vernalization pathway, among others (reviewed in Lee & Lee, 2010). *soc1-3* mutants flower later in LD and SD conditions and *soc1-3/ful-2* double mutants flower later than either single mutant, which further demonstrates the importance of SOC1 and FUL as floral regulators (Melzer *et al.*, 2008). Hyun *et al.*, (2016) reported that SPL15 and SOC1 cooperate to transcriptionally activate at least two of their shared targets: *FUL* and *MIR172B*.

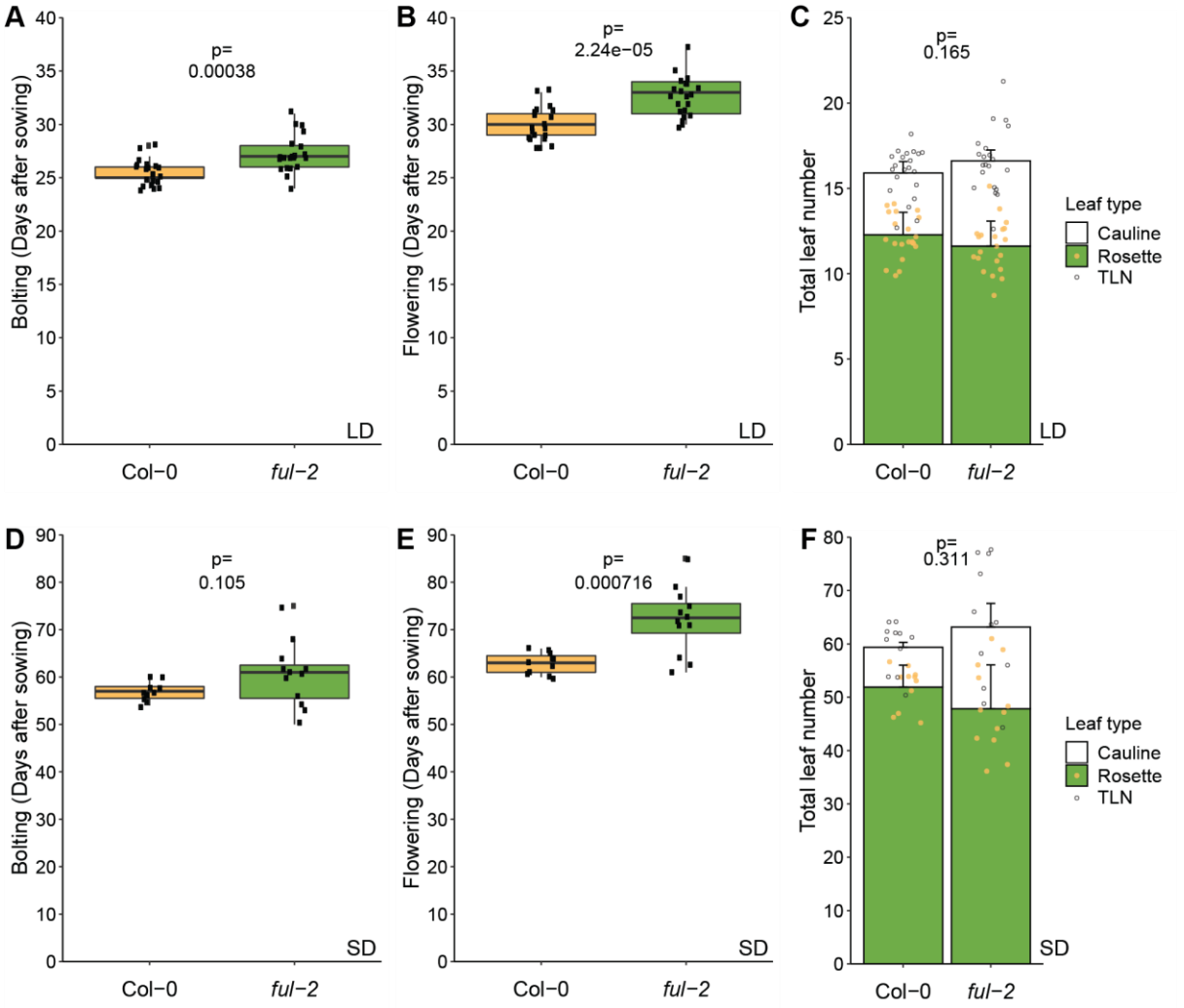

Figure 3.1. Flowering time of Col-0 and *ful-2* in LD and SD conditions. Time to bolting (**A**), flowering time (**B**) total leaf number (**C**; TLN) of Col-0 and *ful-2* in LD conditions (n = 21, *p* was calculated using the student's *t*-test). Time to bolting (**D**), flowering time (**E**) and TLN (**F**) of Col-0 and *ful-2* in SD conditions (n = 11-12, *p* was calculated using the student's *t*-test). Bolting time was score as the day on which the inflorescence extended 0.5 cm out of the rosette and flowering time was scored as the day on which the first flower opened anywhere on the plant.

SPL15 and SOC1 were proposed to be components of the same transcriptional complex that activates *FUL* and *MIR172B*. However, the proteins also have distinct roles in the transcriptional activation of these genes. SOC1 is responsible for an active chromatin state at the target loci, whereas SPL15 is involved in recruiting RNA-polymerase II (Hyun *et al.*, 2016).

Although SOC1, SPL15 and FUL are all involved in flowering-time regulation in Arabidopsis, the developmental function of binding of SOC1 and SPL15 to the *FUL* promoter is unclear.
To regulate target genes, transcription factors bind specific regions in their target gene promoters. This binding can be detected using *in-vivo* chromatin immunoprecipitation (ChIP)-PCR and ChIP-sequencing, *in-vitro* yeast-1-hybrid (Y1H) studies, electrophoretic mobility shift assay (EMSA) or a combination of these techniques (Hellman & Fried, 2007; Kaufmann, Muiño, *et al.*, 2010; Reece-Hoyes & Marian Walhout, 2012) However, the binding of a transcription factor to DNA does not necessarily mean that the interaction is functionally relevant *in planta*. These techniques do not reveal which exact binding motif within the target gene promoter is bound and this can only be determined definitively by mutagenizing putative binding motifs.

SPL15 is an SBP transcription factor that binds to the GTAC motif and SOC1 is a MADS-box transcription factor that binds to the CArG box motif, but it is still unclear which motifs in the promoter region of *FUL* are bound by SOC1 and SPL15 (Birkenbihl *et al.*, 2005; J. Lee *et al.*, 2008; C. Liu *et al.*, 2008).
In this chapter, I will discuss how I have studied the role of *FUL* in plant development in Arabidopsis, and specifically, how SPL transcription factors affect *FUL* expression via *cis*-regulatory regions in the *FUL* promoter and how SOC1 regulates *FUL.* I used *in vitro* site-directed mutagenesis of the *FUL* promoter to study the effects on *FUL* expression, FUL protein localisation, plant morphology and flowering time.

Conservation of FRUITFULL and *cis*-elements within the *FRUITFULL* promoter among the *Brassicaceae*

The *FUL* coding sequence is highly conserved among many different *Brassicaceae* species and some species have multiple copies of *FUL* in their genome.

I first examined the conservation of FUL within the *Brassicaceae*. The AtFUL coding sequence was used to identify FUL orthologues in 22 different species and found that orthologues of FUL were present in all of these species, and that some species possessed more than one copy of FUL (Fig. 3.2; performed by Dr. Edouard Severing). Furthermore, the phylogenetic tree shows that the divergence of *FUL* orthologues is consistent with the genealogy of the Brassicaceae (X. Guo *et al.*, 2017; Hohmann *et al.*, 2015; Kiefer *et al.*, 2019; Mandáková *et al.*, 2017; Nikolov *et al.*, 2019).

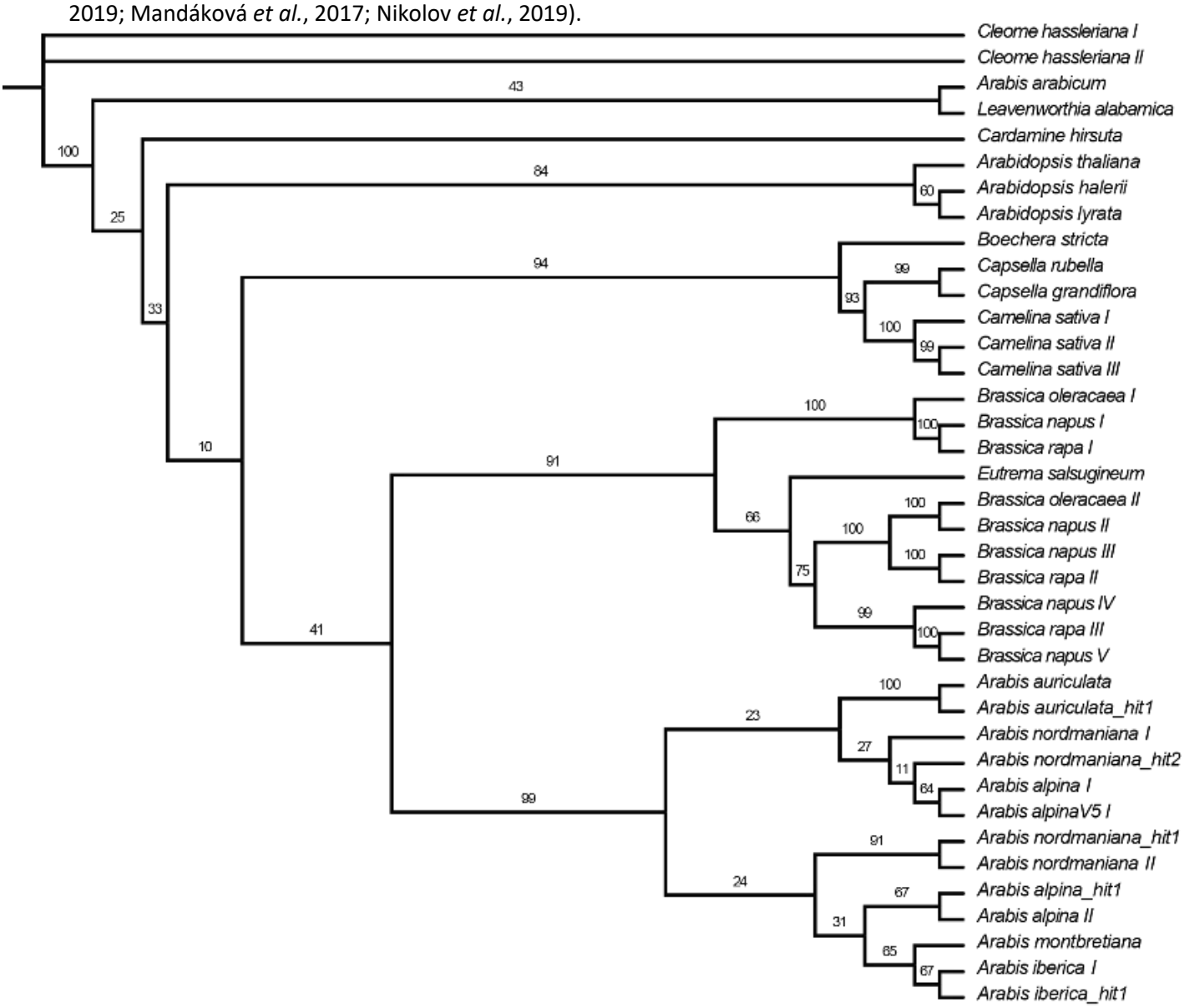

Figure 3.2. Phylogenetic tree based on similarities among coding sequences of *FUL* orthologues of 22 Brassicaceae species. Values at tree arms are bootstrap values for the next junction, *i.e.* the number of times out of 100 tree reconstructions that these species clustered together. Orthologue identification and tree construction were performed by Dr. Edouard Severing.

The *FRUITFULL*-coding sequence is highly conserved among different *Brassicaceae* members and the MADS-, Intervening- and K-domain are conserved at the amino-acid level.

To identify conserved regions within the regulatory regions of *FUL*, 14 species were selected that are representative for the Brassicaceae: *Arabidopsis thaliana, Arabidopsis halleri, Arabidopsis lyrata, Capsella rubella, Cardamine hirsuta, Eutrema salsugineum, Arabis auriculata, Arabis alpina, Arabis iberica, Arabis montbretiana, Aethionema arabicum, Leavenworthia alabamica*, and *Cleome hassleriana,* where the latter was used as an outgroup. First, the FUL protein sequences were compared, which showed that the FUL protein is highly conserved among the selected species (Fig. 3.3). The DNA-binding MADS (M) domain is conserved among all the species. Both the Intervening (I) domain and the Keratin-like (K) domain, which are required for interactions with other MADS-box proteins, show few or no differences among the species, whereas the C-terminal domain shows some divergence (Fig. 3.3; Puranik *et al.*, 2014; Purugganan *et al.*, 1995; Van Dijk *et al.*, 2010). The C-terminal domain of MADS-box proteins is thought to be necessary for higher-order protein complex formation (Puranik *et al.*, 2014; Van Dijk *et al.*, 2010). The divergence of this domain in FUL from different species might indicate that the interaction complexes that include FUL have diverged in different species.

The *FRUITFULL* promoter contains highly conserved blocks and these blocks correspond to DNAse I-hypersensitive regions in Arabidopsis.

The whole genomic regions of the *FUL* orthologs, including complete up- and downstream regions, were pairwise aligned to *AtFUL* using mVISTA, to assess the importance of potential regulatory regions (Frazer *et al.*, 2004; Mayor *et al.*, 2000). Besides exons and UTRs, the first intron is also highly conserved among

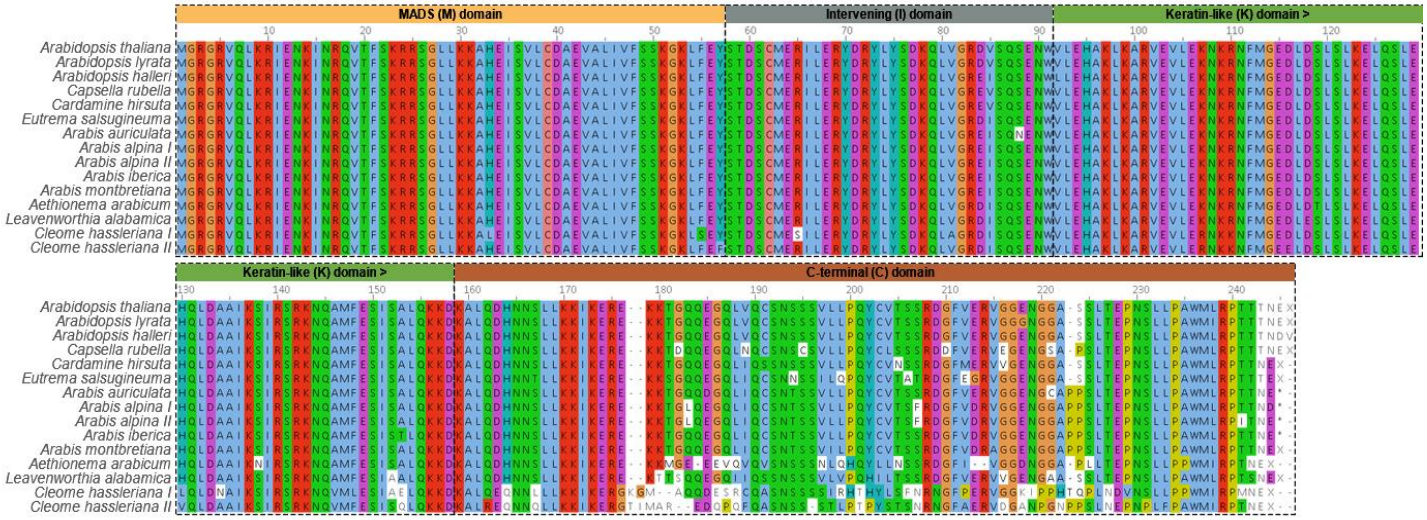

Figure 3.3. Clustal Omega multiple sequence alignment of FUL protein orthologues in 14 species. Different amino acids are marked in a different colour. Annotated are the MADS (M) domain in yellow, the Intervening (I) domain in grey, the Keratin-like (K) domain in green and the C-terminal (C) domain in brown.

the different *Brassicaceae* species, but is less conserved in *Aethionema, Leavenworthia* and the outgroup species *Cleome hassleriana* (Fig. 3.4). However, when the first intronic region was used for motif discovery using MEME, no enrichment of binding motifs for either SPL (GTAC motifs) or MADS-box transcription factors (CArG boxes) was found (Bailey & Elkan, 1994). The promoter clearly shows conserved blocks that are present throughout almost the entire set of species, and some even exist in the outgroup species *Cleome hassleriana.* When the conserved regions of the *FUL* promoter were subjected to motif discovery

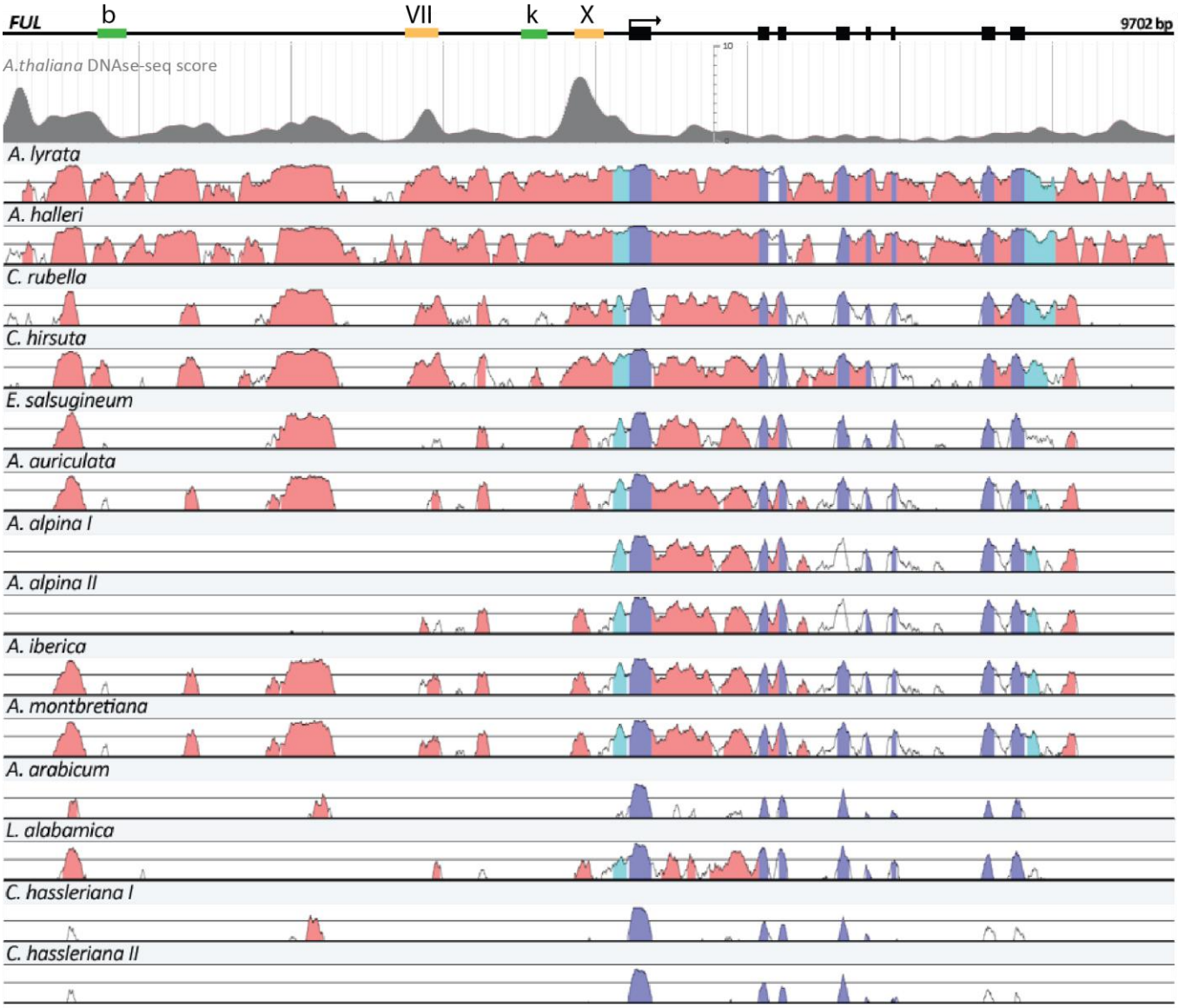

Figure 3.4. mVISTA alignments of the whole genic region of *FUL* from 14 *Brassicaceae* species and DNAse I hypersensitive sites in the Arabidopsis *FUL* genic region. Top: a graphical representation of the *FUL* locus in *Arabidopsis thaliana*. Annotated are the binding regions for SOC1 (green) and SPL15 (yellow) as determined by ChIP-qPCR (Hyun *et al.*, 2016). Below: grey patterns represent DNAse hypersensitive sites (DHS) as determined by DNAse-seq in the flower of *Arabidopsis thaliana* (Boyle et al., 2008; T. Zhang et al., 2016). The higher the score, the more accessible the DNA was at this location. Bottom: mVISTA alignments of the *FUL* whole genic region from 14 species, pairwise aligned to *FUL* in *Arabidopsis thaliana.* Annotated are: *A.thaliana* exons in purple and *A. thaliana* 3′ and 5′ UTRs in turquoise. The plots show conservation from 50% to 100% on the nucleotide level, with the central horizontal line indicating 70% conservation. Any nucleotide conservation above 70% is coloured in pink.

by MEME, several conserved motifs were identified, but similar to the first intronic region, no enrichment of binding motifs for either SPL or MADS-box transcription factors were found (Bailey & Elkan, 1994).

Pairwise conservation within the whole genomic region of *FUL* shows a great degree of overlap with DNAse I hypersensitive sites (DHSs) in *Arabidopsis* (Fig. 3.4; top). These are regions in which the chromatin is in an open and exposed state, which allows access to DNA-interacting proteins (Boyle *et al.*, 2008; T. Zhang *et al.*, 2016). DHSs can be used to detect *cis*-regulatory elements (CREs). In particular, the most distal and proximal regions of the *FUL* promoter are conserved among species and contain DHSs. The main focus was the conservation of the promoter regions that contain the putative binding sites for SPL15 and SOC1 as previously defined by ChIP-qPCR: regions VII & X and regions b and k, respectively (Fig. 3.4; 3.6; Hyun *et al.*, 2016). The resulting mVISTA alignment does not clearly indicate that the motifs of interest are located within a conserved region of the promoter. Therefore, the aligned regions containing these motifs in *AtFUL* were extracted for all species from mVISTA and re-aligned using MAFFT (Katoh *et al.*, 2002).

The proximal region in the *FRUITFULL* promoter that is bound by SPL15 contains a highly conserved tandem GTAC motif.

Comparisons at the sequence level with MAFFT indicated that the GTAC motifs in amplicon X are highly conserved in all Brassicaceae species analysed (Fig. 3.5; Katoh *et al.*, 2002). From Fig. 3.4 it is also clear that the motifs in amplicon X are located within a highly conserved region in the centre of a DHS site. The two GTAC motifs in amplicon VII (Fig. S3.1) were not spatially conserved on the sequence level, but the regions that aligned best to that containing amplicon VII in *A. thaliana* contained at least one GTAC motif in all species.

The distal region in the *FRUITFULL* promoter that is bound by SOC1 contains a highly conserved CArG-box motif.

The CArG box in the most distal region, region b (Fig. 3.5), was also well conserved among the species analysed, although it was not present in the *A. alpina* promoter (Fig. 3.5). The CArG boxes in region k in *A. thaliana* were not found in the regions aligning to the *AtFUL* promoter region in the other Brassicaceae species in the dataset (Fig. S3.2). At least one highly conserved binding motif for SPL15 and for SOC1 is present, which suggests that these motifs are evolutionarily important for spatio-temporal transcriptional regulation of *FUL*.

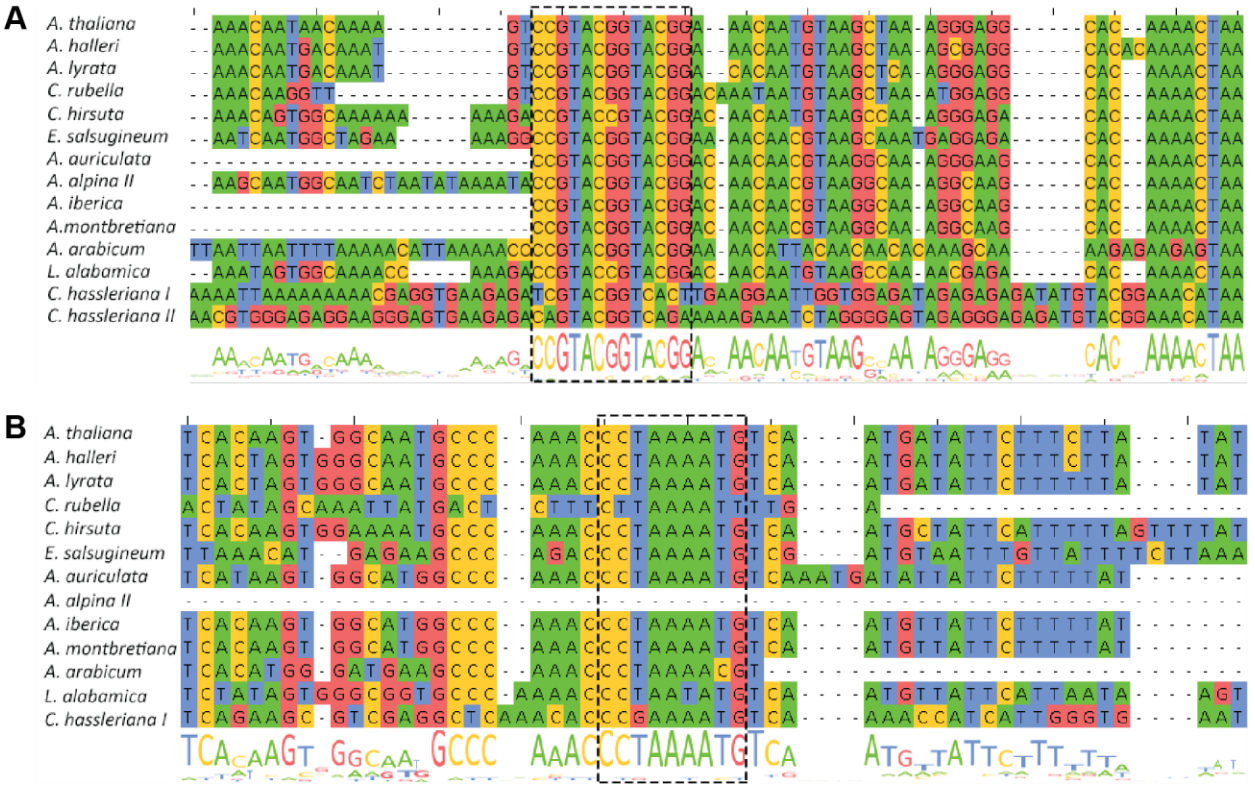

Figure 3.5. Nucleotide alignments of highly conserved motifs in the *FUL* promoter. (**A**) Alignment of region X in the proximal *FUL* promoter containing a highly conserved GTAC tandem motif and putative SPL-binding site. The consensus sequence is displayed below the alignments. Outlined is the conserved GTAC motif in this region. (**B**) Alignment of region b in the proximal *FUL* promoter containing highly CArG-box motif and putative SOC1 binding site. The consensus sequence is displayed below the alignments. Outlined is the conserved CarG-box in this region.

Studying the function of *cis*-regulatory elements in the *FRUITFULL* promoter

To study the effects of SPL15 and SOC1 binding to the *FUL* promoter, *in vitro* site-directed mutagenesis of the *FUL* promoter was performed. The putative binding sites of SPL15 (*mGTAC*) and SOC1 (*mCArG*) in the *FUL* promoter, as identified by ChIP-qPCR (top Fig. 3.4; Fig. 3.6), were mutagenized in the existing *pFUL::FUL::9AVENUS* construct, and these modified constructs were transformed into the *ful-2* mutant background (Hyun *et al.*, 2016). The exact binding sites for SOC1 and SPL15 in the *FUL* promoter are still unknown, and for both transcription factors, binding was demonstrated to more than one region in the *FUL* promoter using ChIP-qPCR (Hyun *et al.*, 2016). I therefore decided to mutate all putative binding sites to ensure that most effects of abrogating SPL15 and SOC1 binding to the *FUL* promoter would be detected (Fig. 3.6). Four constructs were generated: 1) *pFUL::FUL::9AVENUS* as a wild-type control; 2) *pFUL-mGTAC::FUL::9AVENUS*, with all putative SPL15-binding motifs mutated; 3) *pFUL-mCArG:: FUL::9AVENUS*, with all putative SOC1-binding motifs mutated; 4) *pFUL-mCArGmGTAC::FUL::9AVENUS*, with all putative binding sites for SPL15 and SOC1 mutated (Fig. 3.6).

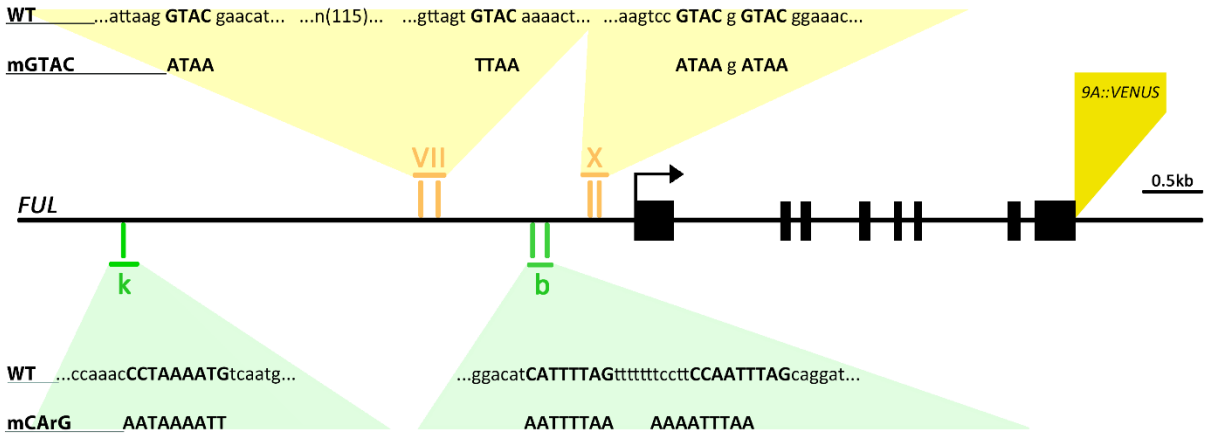

Figure 3.6. Graphic representation of the *FUL* genic region and wild-type and mutant clones generated to study the relevance of motifs in the *FUL* promoter. Schematic representation of the *FUL* genic region, with the black blocks representing the exons. VII is a region of 227 bp containing two GTAC motifs and X is a region of 153 bp containing two GTAC motifs in tandem; both regions were positively bound by SPL15 in ChIP-qPCR experiments (Hyun *et al*., 2016). Region k is a region of 157 bp containing one CArG box and b is a region of 167 bp containing two CArG boxes; both regions were positively bound by SOC1 in ChIP-qPCR experiments (Hyun *et al*., 2016). Four different constructs were generated, all of which included the whole 5′ intergenic region and the whole 3' intergenic region and *VENUS* was fused immediately before the *FUL* stop codon. The wild-type clone contained the wild-type promoter, the mGTAC clone contained four mutagenized motifs as represented in this figure below the wild-type clone. The mCArG clone contained three mutagenized motifs as represented in the figure below the schematic representation of the *FUL* locus. The mCArGmGTAC clone contains both the mutagenized motifs of the mGTAC clone as well as the mutagenized motifs of the mCArG clone.

Mutagenesis of putative SPL15-binding motifs in the *FUL* promoter abrogates SPL transcription factor binding *in vivo*.

To test whether mutagenesis of the putative SPL15 binding sites resulted in loss of binding to the *FUL* promoter, a synthetic biology assay was used. This assay uses mammalian cells (Human embryonic kidney cells) and the activity of SECRETED ALKALINE PHOSPHATASE (SEAP) as a proxy for binding events. The assays were conducted by Dr. Jennifer Andres at the Institute of Synthetic Biology at the Heinrich Heine University in Düsseldorf. SPL15 and SPL9 were both used for these assays, because the core GTAC motif is likely to be bound by any SPL transcription factor that contains the DNA-binding SBP domain and SPL9 has been shown to bind to the same region in the *FUL* promoter (Hyun *et al.*, 2016; J. W. Wang *et al.*, 2009). Furthermore, two reports show that region X is also bound by SPL3, SPL4 and possibly also SPL5 (J. W. Wang *et al.*, 2009; Xie *et al.*, 2020). Firstly, the separate promoter regions VII and X with or without (wild-type) the mutated GTAC motifs were fused upstream to the open reading frame of the reporter SEAP (Fig. 3.7A). To test these promoter fragments for binding by SPL9 and SPL15, the coding sequence of these two proteins was expressed from a constitutively active promoter and fused to the activation domain VP16 to

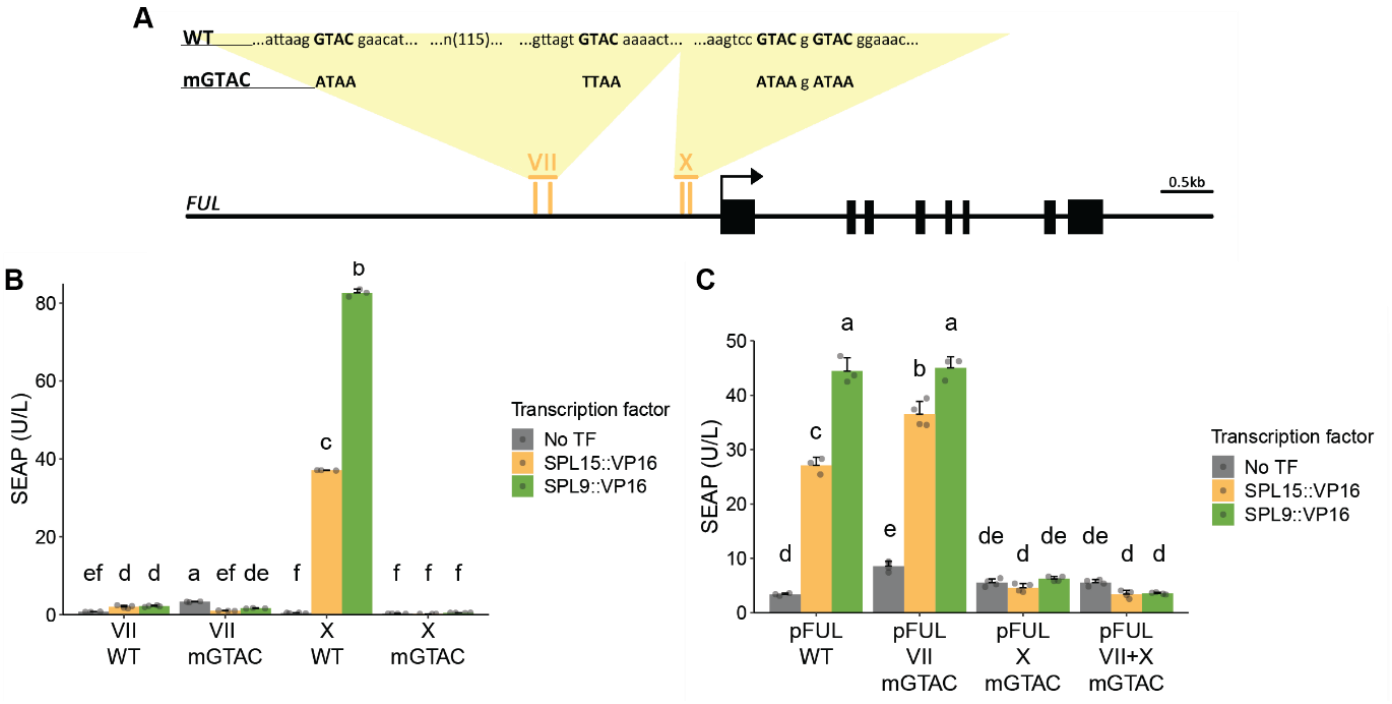

Figure 3.7. Trans-activation assay of wild-type and *mGTAC FUL* promoters by SPL9 and SPL15 in heterologous mammalian cells. (**A**) Schematic representation of the *FUL* locus. Annotated are the constructs used in this assay: WT as the wild-type *FUL* locus and mGTAC, the *FUL* locus with mutated putative SPL15 binding sites. VII is a region of 227 bp containing two GTAC motifs and X is a region of 153 bp containing two GTAC motifs in tandem. (**B**) Secreted alkaline phosphatase measurements in units per litre after binding assays with SPL9::VP16 and SPL15::VP16 to the separate regions VII and X in wild-type and mGTAC mutant versions. (**C**) Secreted alkaline phosphatase measurements in units per litre after binding assays with SPL9::VP16 and SPL15::VP16 to complete *FUL* promoter (*pFUL*) in wild-type, in a mutant version with only the GTAC motifs in region VII mutated, in a mutant version with only the GTAC motifs in region X mutated and in the original mutant version with both the GTAC motifs in region VII as well as those in region X mutated. ANOVA and Tukey's HSD (honestly significant difference) test were used to assess statistical differences ($p < 0.01$).

bind. Previous results indicated that SPL9 and SPL15 alone cannot activate transcription, and therefore, SPL9 and SPL15 were fused to the VP16 activation domain to test whether they could bind to the *FUL* promoter. The results showed that SPL9-VP16 and SPL15-VP16 both bound to region X, but not to region VII (Fig. 3.7B). This confirmed the ChIP-qPCR finding that SPL15 binds to region X, but did not confirm its interaction with region VII. It is possible that the binding of SPL15 to region VII requires accessory proteins that are absent in the mammalian cells. When the conserved GTAC motifs in region X were mutated, no transcriptional activation was detected, indicating SPL9 and SPL15 could no longer bind to this region of the *mGTAC-FUL* promoter (Fig. 3.7B). The complete *FUL* wild-type (WT) promoter, the complete promoter with only region X mutated, with only region VII mutated, or with both regions VII and X mutated, were tested for binding by SPL9 and SPL15 in a second assay.

This assay again showed a positive interaction between the SPLs and the promoter, as long as region X was intact, but binding was lost as soon as the conserved tandem GTAC motif in region X was mutated (Fig. 3.7C). Again, no difference was observed between binding to the WT promoter and binding to the promoter in which the GTAC motifs in region VII were mutated (Fig. 3.7C). These results show that binding of SPL9 and SPL15 to the GTAC motifs in region X is lost in this orthogonal system when this motif is mutated. These assays confirm that at least the mutated region X in the promoter constructs can no longer be bound by SPLs and provides evidence that these mutations might also reduce SPL binding to *FUL in planta*.

The *pFUL::FUL::VENUS* wild-type and *pFUL-mGTAC::FUL::VENUS* mutant constructs can complement ful-2 morphological phenotypes.

Homozygous lines for the wild-type construct *pFUL::FUL::9AVENUS/ful-2* (F-lines) and mutant construct *pFUL-mGTAC::FUL::9AVENUS/ful-2* (S-lines) were selected in the T_3 generation and tested for complementation of the *ful-2* morphological phenotype as well as for the basal expression level of *FUL*. All independent transformants of the wild-type or *mGTAC* mutant constructs complemented the silique phenotype of *ful-2* mutants (Fig. 3.8A, B). Next, silique length was measured from image data of 35-day-old LD-grown plants (Fig. 3.8E). These data show that variation in silique length is present among all independent transformants for either construct, but that all lines complemented the stunted silique phenotype of *ful-2* plants. Furthermore, all lines visually complemented the cauline leaf phenotype, and were therefore not quantified (Fig. 3.8C, D). These results indicate that all transformants of both wild-type and mutant promoter constructs rescued the morphological phenotype of *ful-2*. Lastly, to select transformants with a basal expression of *FUL* similar to Col-0, tissue from flowers at anthesis was harvested

from 30LD-grown plants for *FUL* expression analysis. Since all independent transformants complemented the silique phenotype, *FUL* expression in the silique and young flower should not be affected by the mutation of motifs in the *FUL* promoter. These data show that some variation in *FUL* expression exists among independent transformants of *mGTAC* mutant and wild-type constructs (Fig. 3.8F). The *mGTAC*-mutant line S11.7 showed very high *FUL* expression. This was expected because a terminal flower phenotype was observed in approximately 30% of these plants, similar to *FUL* overexpression lines (Balanzà *et al.*, 2014; Ferrándiz, Liljegren, *et al.*, 2000). Overall, *FUL* expression in most lines is similar to that in Col-0.

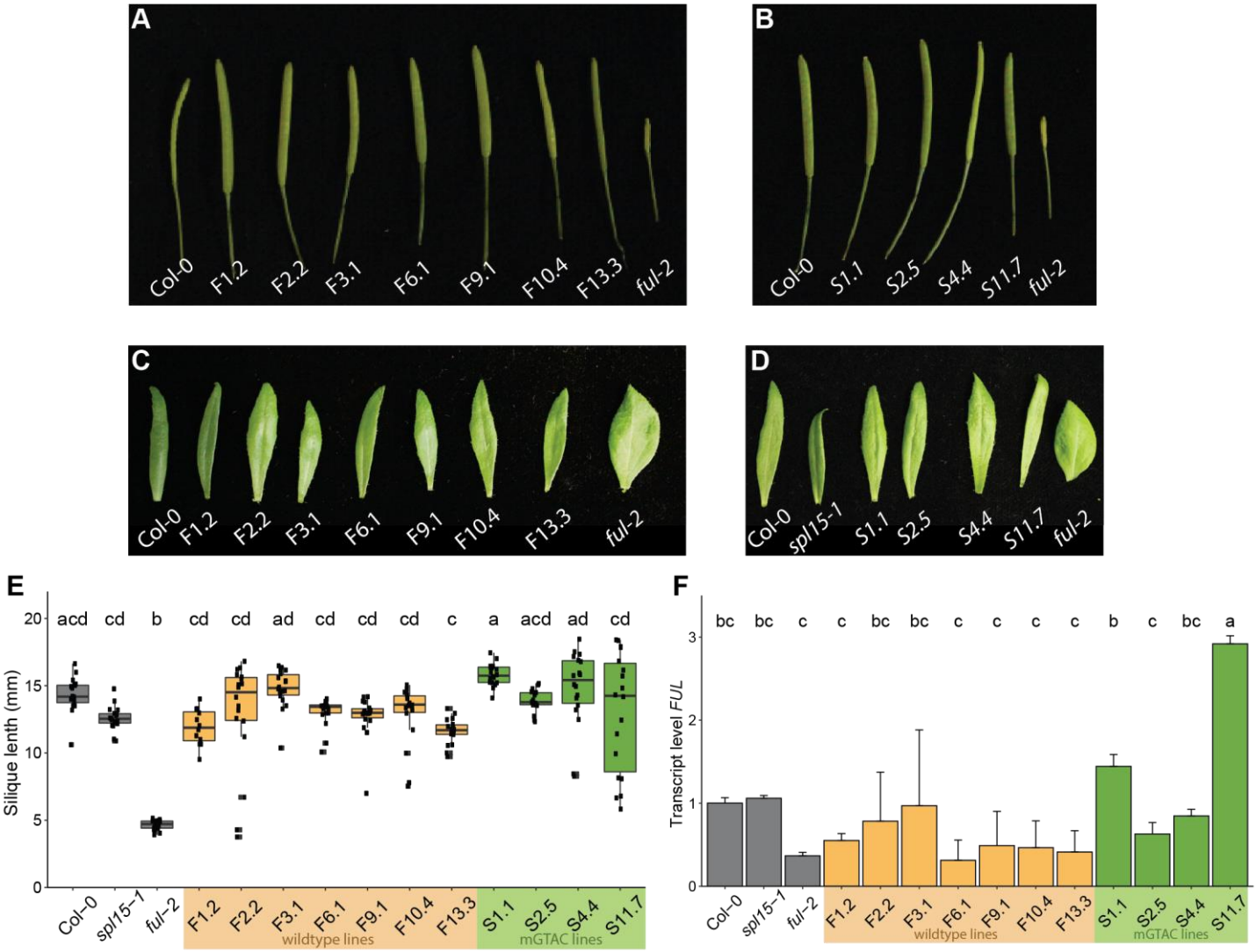

Figure 3.8. Complementation of the *ful-2* phenotype by the *FUL* wild-type gene and the *FUL* gene with mutated GTAC promoter motifs. (**A, B**) Representative siliques and (**C, D**) representative cauline leaves of independent transformants of *pFUL::FUL::9AVENUS/ful-2* (F-lines; A,C) and *pFUL-mGTAC::FUL::9AVENUS/ful-2* (S-lines; B,D) and controls Col-0 and *ful-2*. (**E**) Silique length in mm of siliques 4-10 on the main stem of three plants of independent transformants of *pFUL::FUL::9AVENUS/ful-2* (F-lines) and *pFUL-mGTAC::FUL::9AVENUS/ful-2* (S-lines) and controls Col-0, *spl15-1* and *ful-2* grown in LD for 35 days. (**F**) *FUL* expression level in flowers at anthesis from independent transformants of *pFUL::FUL::9AVENUS/ful-2* (F-lines) and *pFUL-mGTAC::FUL::9AVENUS/ful-2* (S-lines) and controls Col-0, *spl15-1* and *ful-2* at 30LD. The variation shown is derived from two independent biological replicates. Statistical differences were calculated with ANOVA followed by Tukey's HSD (honestly significant difference) test at $p < 0.01$.

Introduction of *pFUL-mGTAC::FUL::VENUS* into *ful*-2 causes early flowering in LD conditions, but has no effect in SD conditions.

The same homozygous independent transformant lines of the wild-type construct *pFUL::FUL::9AVENUS/ful-2* (F-lines) and mutant construct *pFUL-mGTAC::FUL::9AVENUS/ful-2* (S-lines) were tested for their flowering time in LD and SD conditions to assess the variation among independent transformants and the effects of promoter mutagenesis on flowering time. Both conditions were tested once with T_3 plants and once with T_4 plants, but there were no differences between the experiments with different generations. All independent transformants were tested and consistently, all four *mGTAC* mutant lines were significantly earlier bolting and flowering than Col-0 and all wild-type complementation lines and had a lower total leaf number (TLN) in LD conditions (Fig. 3.9A-D). Although differences in TLN were observed among the wild-type complementation lines and Col-0, all lines flowered at the same time as Col-0 in terms of days to flower (Fig. 3.9C).

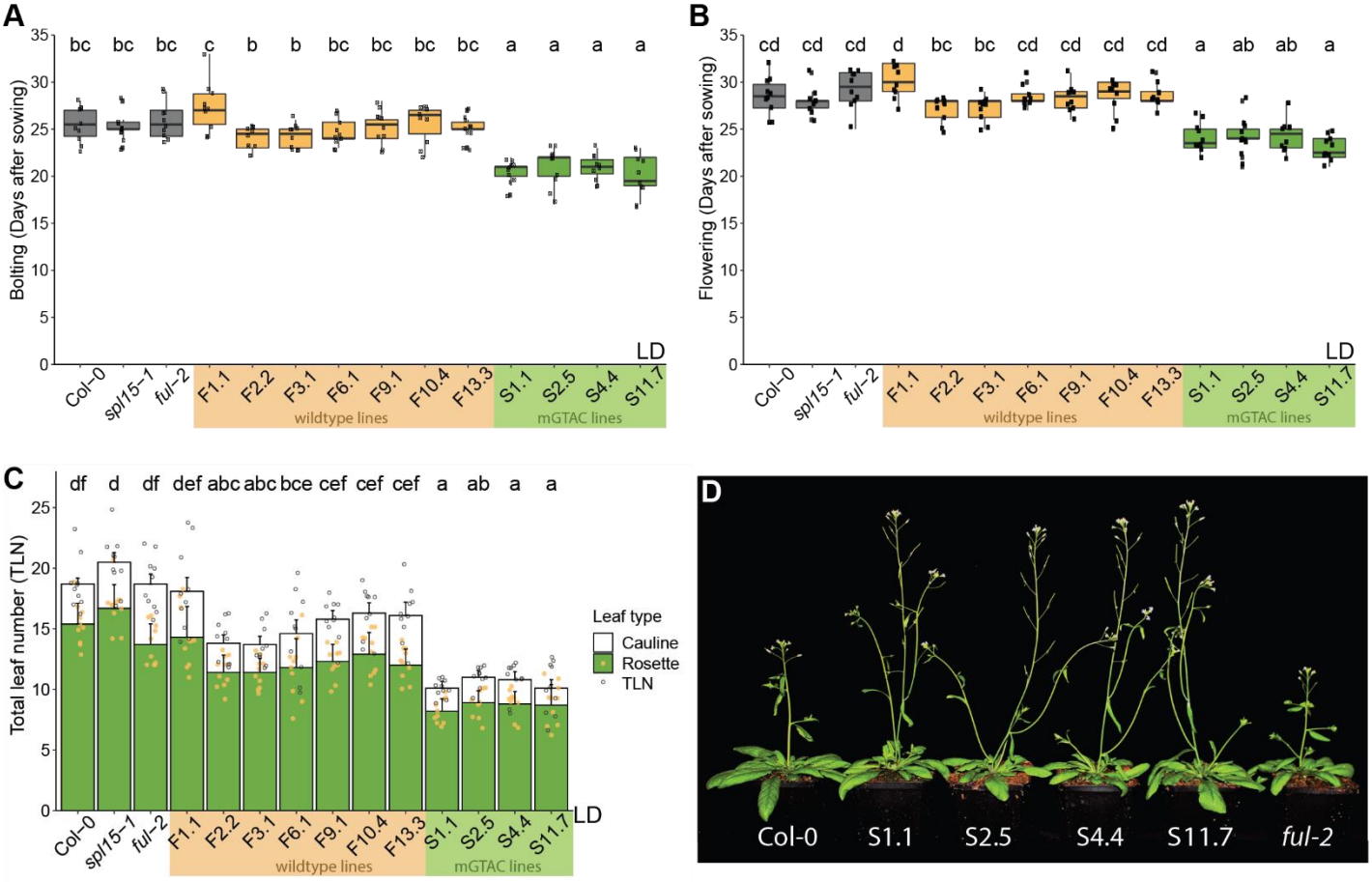

Figure 3.9. LD flowering time of independent transformants expressing *FUL* wild-type complementation constructs or *FUL mGTAC* promoter mutant constructs. Time to bolting (**A**), flowering time (**B**) and total leaf number (**C**; TLN) of independent transformants *of pFUL::FUL::9AVENUS/ful-2* (F-lines) and *pFUL-mGTAC::FUL::9AVENUS/ful-2* (S-lines), Col-0, *spl15-1* and *ful-2* in LD conditions (n = 10). Bolting time was scored as the day on which the inflorescence extended 0.5 cm out of the rosette and flowering time was scored as the day on which the first flower opened, anywhere on the plant. Statistical differences were calculated with ANOVA followed by Tukey's HSD (honestly significant difference) test at $p < 0.01$. (**D**) Representative plants of Col-0, *ful-2* and the independent transformants of *pFUL-mGTAC::FUL::9AVENUS/ful-2* (S-lines) at 39LD.

In SDs, flowering time was also scored in the T_3 (Fig. 3.10A–C) and T_4 (Fig. 3.10D–F) generation, but in these conditions, no clear mutant phenotype for any of the lines, in any of the parameters was apparent, because all lines showed relatively high variation in flowering time (Fig 3.10).

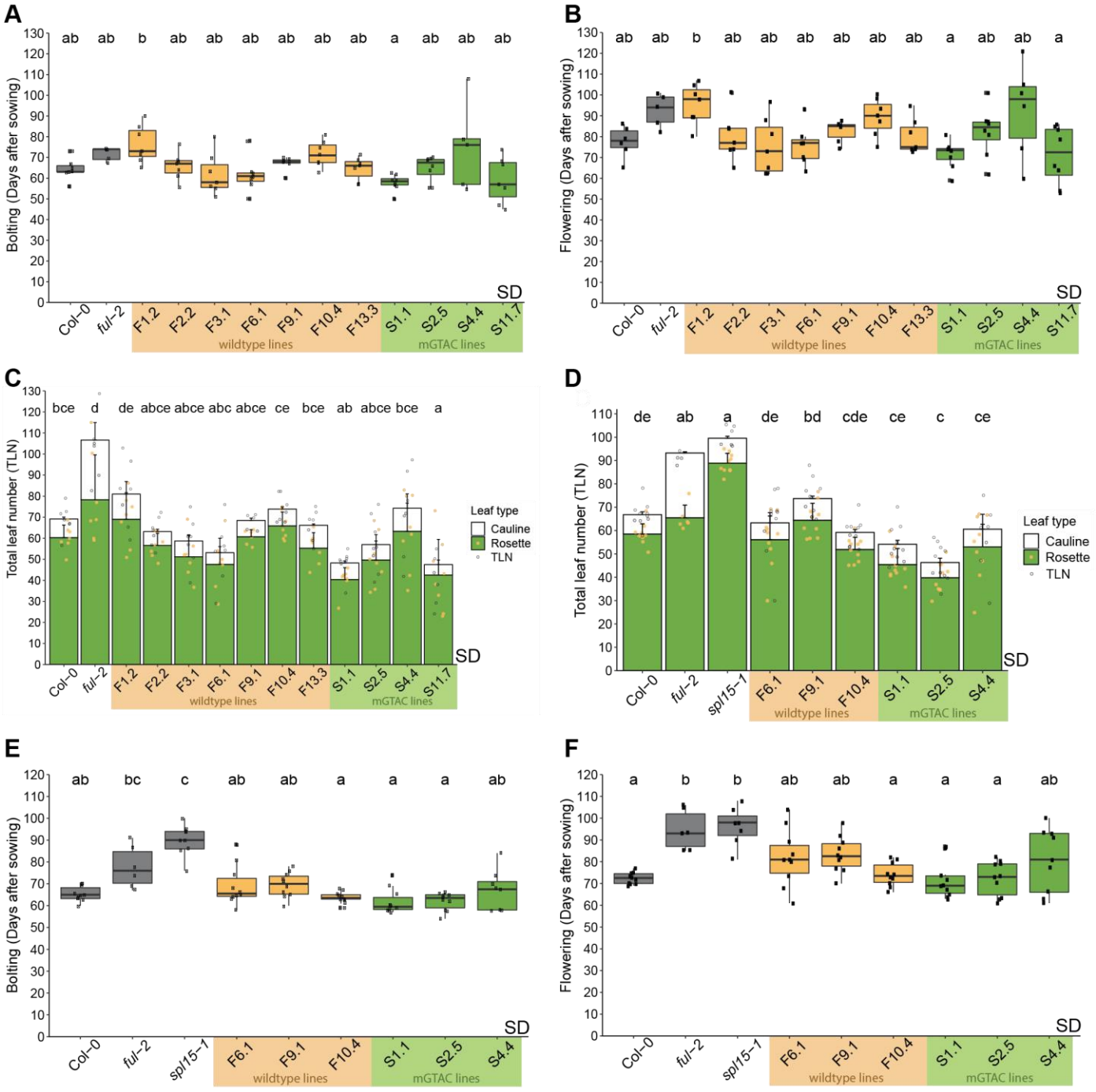

Figure 3.10. SD Flowering time of independent transformants expressing *FUL* wild-type complementation constructs or *FUL mGTAC* mutant constructs. Time to bolting (**A**), flowering time (**B**) and total leaf number (**C**; TLN) of independent transformants of *pFUL::FUL::9AVENUS/ful-2* (F-lines) and *pFUL-mGTAC::FUL::9AVENUS/ful-2* (S-lines) with Col-0 and *ful-2* in SD conditions (n = 5–7). Total leaf number (**D**; TLN), time to bolting (**E**) and flowering time (**F**) of selected independent transformants of *pFUL::FUL::9AVENUS/ful-2* (F-lines) and *pFUL-mGTAC::FUL::9AVENUS/ful-2* (S-lines), Col-0, *spl15-1* and *ful-2* in SD conditions (n = 7–8). Bolting time was scored as the day on which the inflorescence extended 0.5 cm from the rosette, and flowering time was scored as the day on which the first flower opened, anywhere on the plant. Statistical differences were calculated with ANOVA followed by Tukey's HSD (honestly significant difference) test at $p < 0.01$.

***FUL* is expressed earlier and at higher levels in apices of *pFUL-mGTAC::FUL::VENUS* than in those of *pFUL-mGTAC::FUL::VENUS* plants in both LD and SD conditions.**

To investigate whether the flowering-time phenotypes in LD and SD conditions are caused by differential expression of *FUL* in the apex, we sampled meristem-enriched tissue of selected wild-type and mutant lines over a time course in LD and SD conditions for qRT-PCR analysis. Most sampling as well as all RNA-isolations and qRT-PCR analyses were performed by Laura Trimborn. The data show that especially in LD conditions, *FUL* is expressed earlier and at much higher levels in *mGTAC* mutant lines S1.1 and S2.5 than in Col-0 and the wild-type line F9.1 throughout the time course (Fig. 3.11A). The same was observed in SD conditions for the *mGTAC* mutant lines, and initial *FUL* expression in the *mGTAC* mutant lines was approximately 32-fold higher than that in Col-0 and the wild-type line F9.1 (Fig. 3.11B, 3wSD) At later time points, *FUL* expression was >80 fold higher (Fig. 3.11B). The earlier and higher expression of *FUL* in *mGTAC* lines in LD conditions might be causal for the early flowering phenotype observed for these lines in LD conditions (Figs. 3.9, 3.11A).

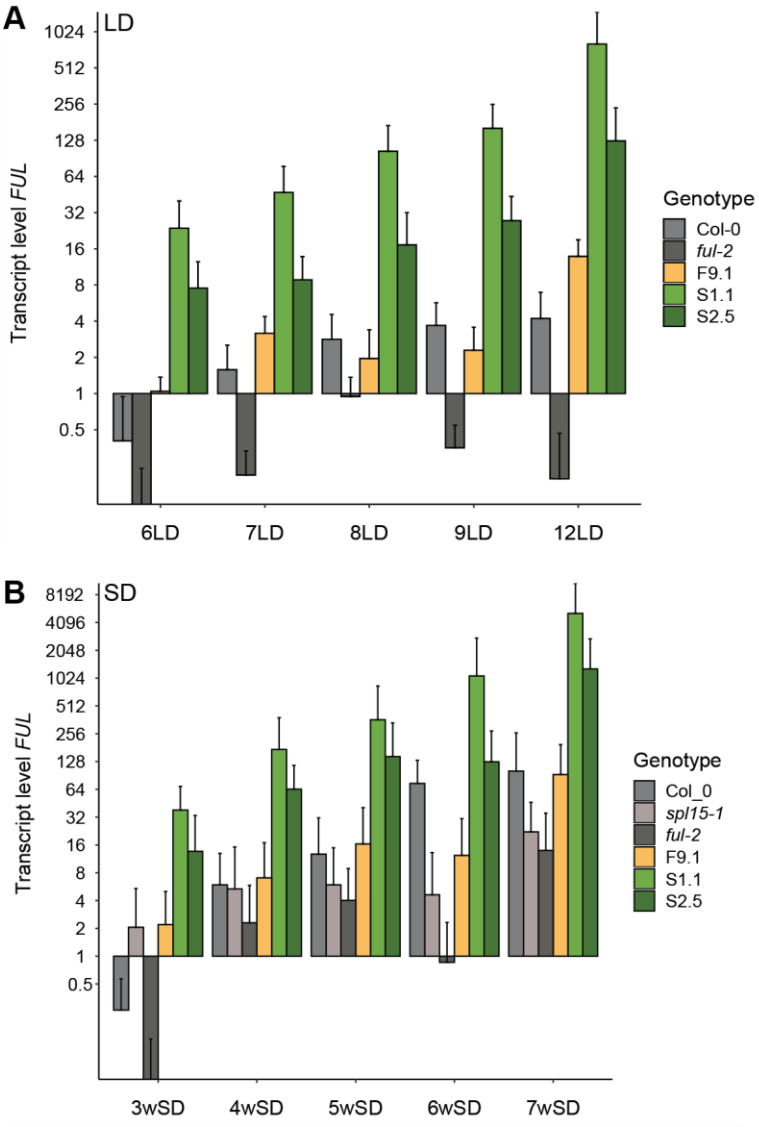

Figure 3.11. LD and SD qRT-PCR time courses of *FUL* expression in different genotypes. (**A**) Transcript level of *FUL* in LD over time in Col-0, *ful-2, pFUL::FUL::9AVENUS/ful-2* (F9.1) and *pFUL-mGTAC::FUL::9AVENUS/ful-2* (S1.1 and S2.5). (**B**) Transcript level of *FUL* in SD over time in Col-0, *ful-2, spl15-1, pFUL::FUL::9AVENUS/ful-2* (F9.1) and *pFUL-mGTAC::FUL::9AVENUS/ful-2* (S1.1 and S2.5). Total RNA was extracted from meristem-enriched material of at least 10 plants per genotype in LD and SD. For all samples, *FUL* transcript level was normalised to the expression of *PP2A* and all genotypes at all timepoints were normalised to the *FUL* transcript level of F9.1 at 6LD or 3wSD in LD and SD, respectively. Both experiments show the results of two independent biological replicates.

FUL::VENUS is visible earlier in the shoot apical meristems of *pFUL-mGTAC::FUL::VENUS* than in those of *pFUL::FUL::VENUS* plants in both LD and SD conditions.

To study whether the differential expression of *FUL* in LD and SD corresponds to differential localisation and/or timing of FUL protein expression in wild-type *FUL::FUL::9AVENUS/ful-2* (F-lines) and mutant

pFUL-mGTAC::FUL::9AVENUS/ful-2 (S-lines) lines, we examined dissected shoot apical meristems (SAMs) along a time course using confocal microscopy. Dissection and confocal microscopy were all performed in collaboration with Laura Trimborn. The results show that in plants expressing the wild-type construct, FUL became weakly visible from 9LD at the top of the meristem and became highly expressed when the SAM started to bolt and produce flowers (15- and 18LD). In the *mGTAC* mutant lines, FUL was clearly visible from 9LD throughout the whole SAM as well as abaxially in the leaves, where expression remained throughout the time course (Fig. 3.12). This expression might be causative for the early-flowering phenotype of *mGTAC* mutant plants in LD conditions, because FUL is present in these plants in the SAM in a much broader domain, and at a much higher level than in the wild-type control plants.

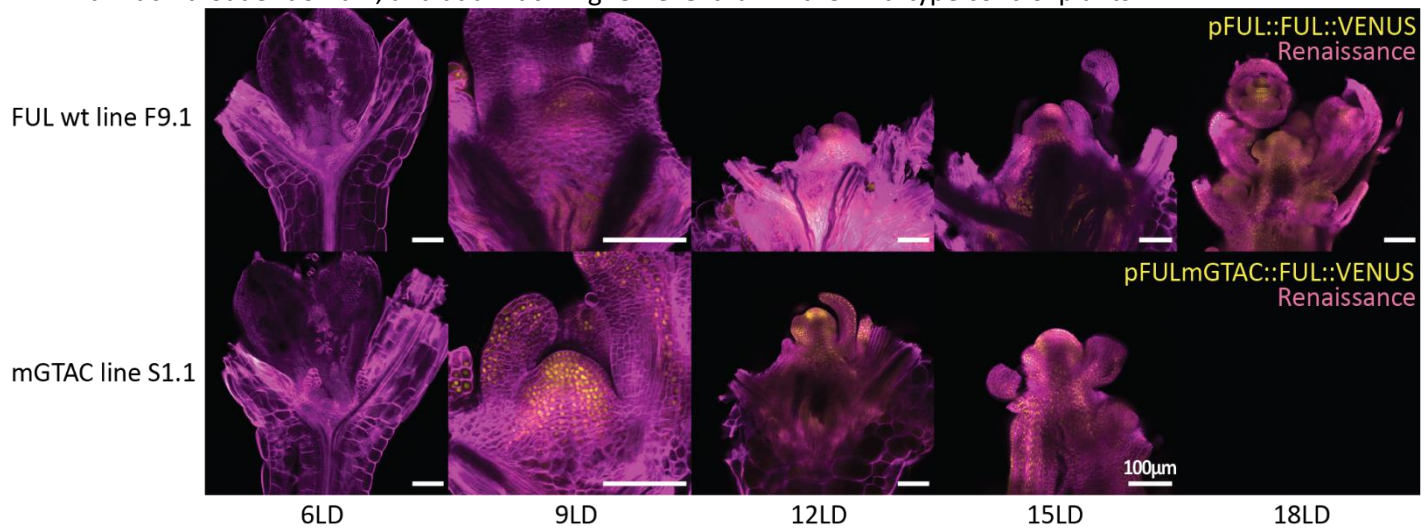

Figure 3.13. Confocal scanning microscopy time course of shoot apical meristems in LD conditions expressing *FUL* from its native promoter tagged with VENUS or from the mGTAC mutagenised promoter tagged with VENUS. Confocal laser scanning micrographs of shoot apices of *pFUL::FUL::9AVENUS/ful-2* (F9.1; top) and *pFUL-mGTAC::FUL::9AVENUS/ful-2* (S1.1; bottom) at indicated time points in LD conditions. VENUS fluorescence is artificially coloured in yellow and fluorescence from the Renaissance dye is artificially coloured in magenta. White scale bars represent 100 µm.

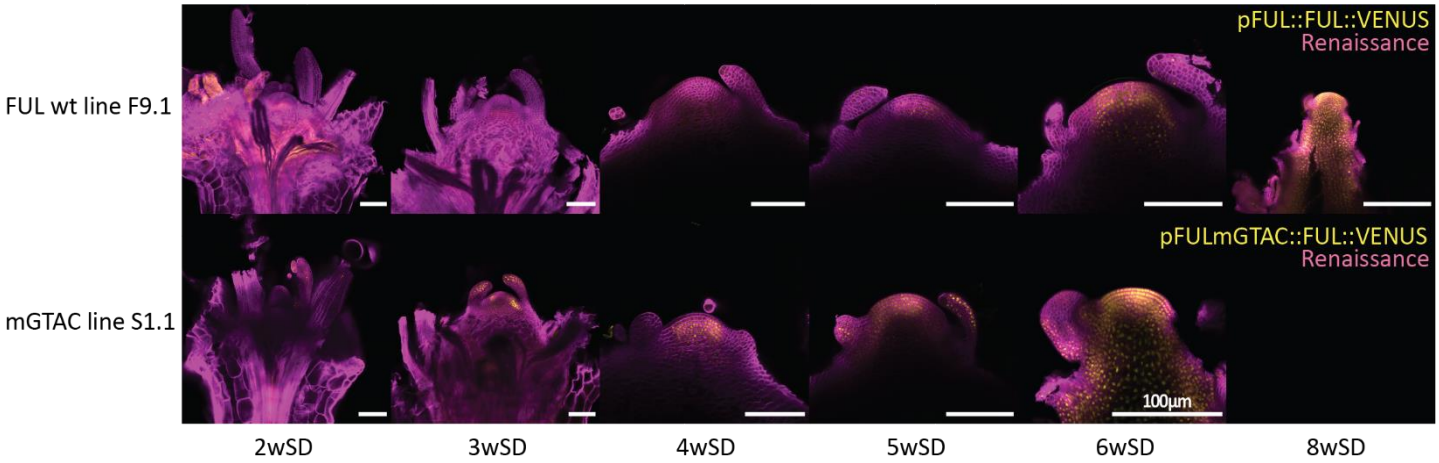

Figure 3.12. Confocal scanning microscopy time course of shoot apical meristems in SD conditions expressing *FUL* from its native promoter tagged with VENUS or from the mGTAC mutagenised promoter tagged with VENUS. Confocal laser scanning micrographs of shoot apices of *pFUL::FUL::9AVENUS/ful-2* (F9.1; top) and *pFUL-mGTAC::FUL::9AVENUS/ful-2* (S1.1; bottom) at indicated time points in SD conditions. VENUS fluorescence is artificially coloured in yellow and fluorescence from the Renaissance dye is artificially coloured in magenta. White scale bars represent 100 µm.

In SD conditions *mGTAC* mutant lines clearly expressed FUL protein in the SAM from 3wSD, which is around 2 weeks earlier than in wild-type lines (Fig. 3.13), but this was not consistent with the flowering-time phenotype of these plants in SD conditions. It is possible that in SD conditions, early and higher expression of *FUL* mRNA and FUL protein alone is not sufficient for premature floral induction.

FT and TSF expression are not different from wild-type in *mGTAC* mutant lines.

To test whether the early flowering of *pFUL-mGTAC::FUL::9AVENUS/ful-2* plants was caused by early induction of *FLOWERING LOCUS T* (*FT*) and/or *TWINSISTER OF FT* (*TSF*), qRT-PCR was used to determine the expression of these two genes. FT and TSF are essential for floral induction in LD conditions; together with FLOWERING LOCUS D (FD) they transcriptionally activate many different downstream floral regulators such as *FUL* (Abe *et al.*, 2005; Collani *et al.*, 2019; Teper-Bamnolker & Samach, 2005; Wigge *et al.*, 2005). I therefore reasoned that they might be involved in the LD flowering-time phenotype observed when the SPL binding sites in the *FUL* promoter are mutated. The expression of *FT* and *TSF* was analysed in 10-day-old LD-grown seedlings harvested at *zeitgeber* time 16, which is a common way to measure the expression of these genes (Fernández *et al.*, 2016; Hayama *et al.*, 2017).

The expression of *FT* and *TSF* was not higher in mutant GTAC lines compared to in Col-0 or the wild-type control line F9.1; the expression of *FT* was even lower in the mutant *mGTAC* lines (Fig. 3.14). *TSF* expression remained constant in all the lines included in this assay.

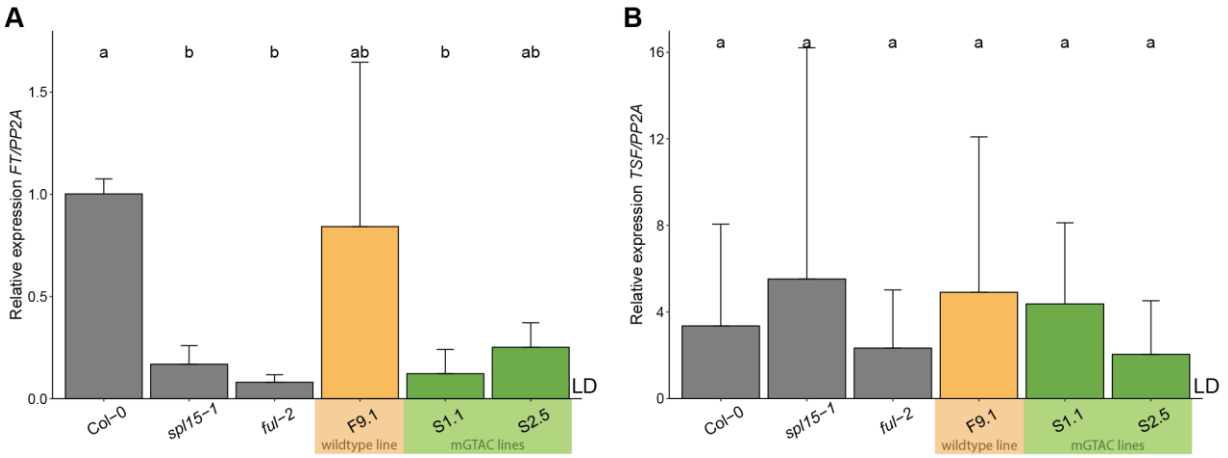

Figure 3.14. *FT* and *TSF* expression in 10-day-old LD-grown seedlings of different genotypes. A. Transcript level of *FT* at 10 LD in Col-0, *spl15-1*, *ful-2*, *pFUL::FUL::9AVENUS/ful-2* (F9.1) and *pFUL-mGTAC::FUL::9AVENUS/ful-2* (S1.1 and S2.5). **B:** Transcript level of *TSF* at 10 LD in Col-0, *spl15-1*, *ful-2*, *pFUL::FUL::9AVENUS/ful-2* (F9.1) and *pFUL-mGTAC::FUL::9AVENUS/ful-2* (S1.1 and S2.5). Total RNA was extracted from whole seedlings from at least eight plants per genotype. For all samples, transcript levels were normalised to the expression of *PP2A* and all genotypes were normalised to *FT or TSF* transcript level in Col-0. Both experiments show the results of two independent biological replicates.

Mutation of the putative SOC1-binding sites in the *FRUITFULL* promoter does not influence flowering time, but mutating putative binding sites for SOC1 and SPL15 leads to earlier flowering in LD and SD conditions.

To study the effects of mutagenesis of the putative SOC1-binding motifs in the *FUL* promoter on flowering time, I analysed the flowering time phenotype of all independent transformants of T_4 lines from the *pFUL-mCArG::FUL::VENUS/ful-2* (C-lines) and *pFUL-mCArG-mGTAC::FUL::VENUS/ful-2* (CS-lines) in LD and SD conditions. These experiments were conducted in the greenhouse between February and May, in controlled conditions of temperature and daylength (21°C, LD = 8 h dark/16 h light, supplemented with artificial light, SD = 16 h dark/8 h light), but not of light intensity. These results show that in LD conditions, all *pFUL-mCArG::FUL::VENUS/ful-2* lines flowered at a similar time to the wild-type control line F9.1, and

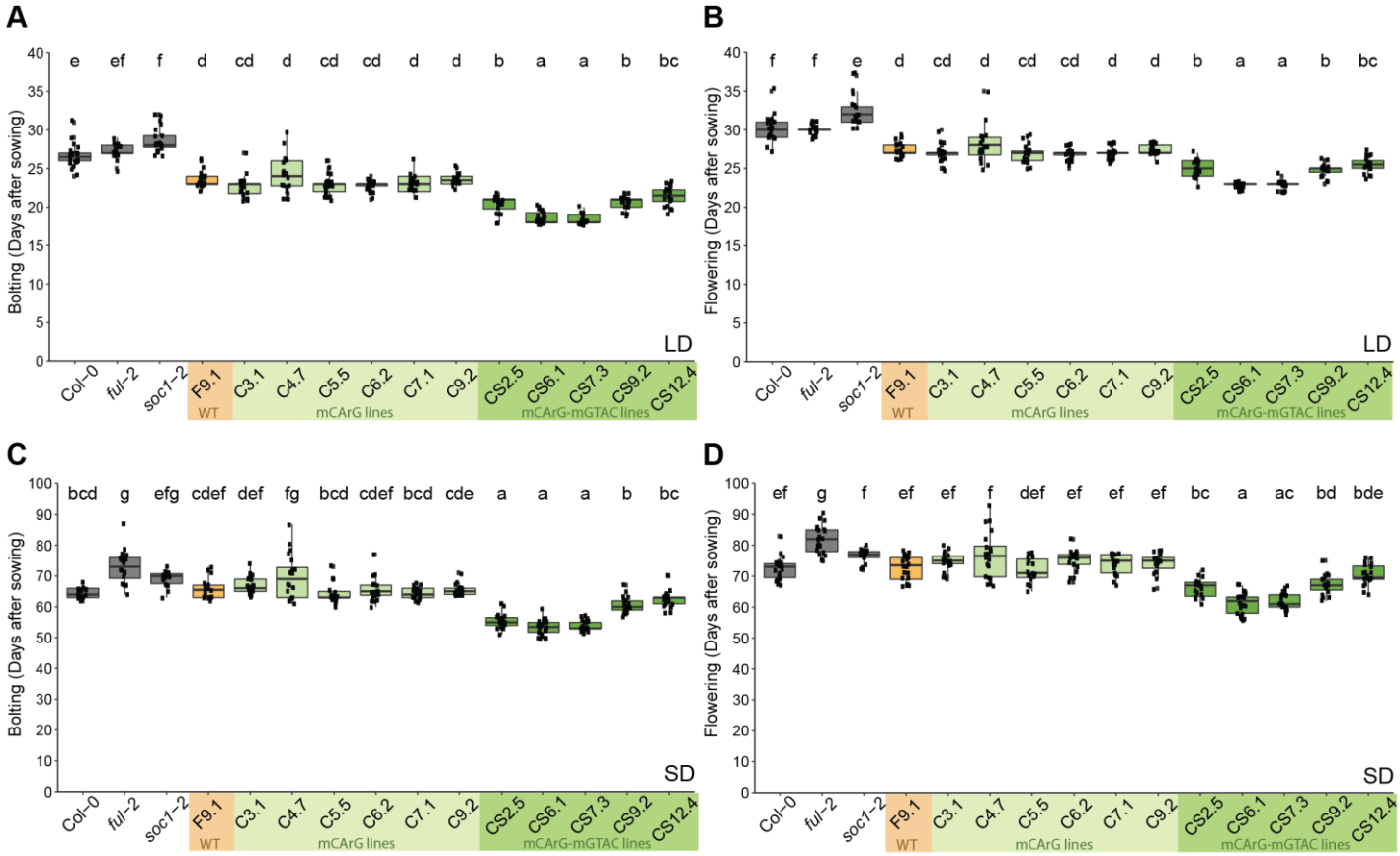

Figure 3.15. LD and SD flowering-time data of *FUL* wild-type complementation line F9.1 and independent transformants of *FUL mCArG*, and *FULmCArG/mGTAC* mutant constructs. Time to bolting (**A**) and flowering time (**B**) of independent transformants of *pFUL::FUL::9AVENUS/ful-2* (F9.1), *pFUL-mCArG::FUL::9AVENUS/ful-2* (C-lines) and *pFUL-mCArGmGTAC::FUL::9AVENUS/ful-2* (CS-lines) with Col-0, *soc1-2* and *ful-2* in LD conditions (n = 20). Time to bolting (**C**) and flowering time (**D**) of independent transformants of *pFUL::FUL::9AVENUS/ful-2* (F9.1), *pFUL-mCArG::FUL::9AVENUS/ful-2* (C-lines) and *pFUL-mCArGmGTAC::FUL::9AVENUS/ful-2* (CS-lines) with Col-0, *soc1-2* and *ful-2* in SD conditions (n = 20). Bolting time was score as the day on which the inflorescence extended 0.5 cm from the rosette, and flowering time was scored as the day on which the first flower opened, anywhere on the plant. Statistical differences were calculated with ANOVA followed by Tukey's HSD (honestly significant difference) test at $p < 0.01$. Plants were grown in greenhouse conditions with controlled temperature (21°C) and daylength, and were supplemented with artificial light to extend the days to the right daylength.

all these lines flowered slightly earlier than Col-0 (Fig. 3.15A, B). In these conditions all these lines slightly over-complemented the *ful-2* phenotype. Consistent with the early-flowering phenotype of *mGTAC::FUL::9AVENUS*/*ful-2* in LD conditions, *pFUL-mCArG-mGTAC::FUL::VENUS*/*ful-2* lines containing the same *mGTAC* mutations as *pFUL-mGTAC::FUL::VENUS* lines combined with mutagenized SOC1 binding sites flowered earlier than Col-0 and the control line F9.1. The additional CArG mutations did not seem to affect the early-flowering phenotype of the *pFUL-GTAC::FUL::VENUS*/*ful-2* in LD conditions, although definitive control lines were absent in this experiment. In SD conditions, the flowering time results were similar to those in LD conditions, where the *pFUL-mCArG-mGTAC::FUL::VENUS*/*ful-2* lines also flowered earlier than the *pFUL-mCArG::FUL::VENUS*/*ful-2* and the wild-type control line F9.1 (Fig. 2.15C, D). In these conditions, the control line F9.1 and *pFUL-mCArG::FUL::VENUS*/*ful-2* lines did not over complement the *ful-2* flowering time phenotype as these plants all flowered at a similar time as Col-0. These results are different from the results of experiments in fully controlled conditions, where no clear altered flowering phenotype of *pFUL-GTAC::FUL::VENUS*/*ful-2* lines was observed (Fig. 3.9). Therefore, the additional mutation of the putative SOC1-binding sites potentially does affect the flowering behaviour of these plants in SD conditions. To confirm this, all different *FUL* promoter lines would have to be grown alongside each other in fully controlled LD and SD conditions.

Discussion

Conservation of *FUL* and its promoter

This chapter describes mutagenesis of the *FUL* promoter to study the effects of SPL transcription factor binding to the *FUL* promoter. I found that *FUL* is highly conserved among *Brassicaceae* species and that many species contain more than one copy of *FUL* in their genome. It is unknown whether FUL functionally diverged in species with more than one copy, and it would be interesting to study the extent to which these different orthologues and their promoters can complement *ful-2* mutant plants of *A. thaliana.* Three out of the four domains of MIKC MADS-box transcription factors are well conserved in *FUL* orthologues, and only the C-terminal domain shows divergence among different species. This is a common finding for the conservation of MADS-box transcription factors (Pařenicová *et al.*, 2003; Purugganan *et al.*, 1995). The C-terminal domain of many MADS-box transcription factors is involved in the formation of higher-order protein complexes (Lai *et al.*, 2019). Therefore, if *FUL* has slightly different functions in different species, these might be caused by differences in the C-terminal domain.

The *FUL* promoter contains one highly conserved tandem GTAC motif close to the transcriptional start site. This site is present in almost all of the species analysed in this thesis and is located within an open chromatin region, facilitating its accessibility to transcription factors and other DNA-binding proteins. This DHS site was present in leaf and flower material, suggesting that this region is accessible in most shoot tissues during plant development (T. Zhang *et al.*, 2016). For the regulation of *FUL*, this could mean different things: on the one hand, the pleiotropic phenotype of *ful-2* plants shows that FUL is required in different tissues at different time points. On the other hand, this might also mean that FUL is specifically *not* required at other time points in other tissues and is subject to transcriptional inhibition. It is already known that many transcription factors, including SPL15, positively regulate *FUL* expression. To date, of all AP2-Ls, only APETALA2 (AP2) is known to bind to the *FUL* promoter, and probably inhibits its expression, because *ap2* mutants have higher *FUL* transcript levels (Yant *et al.*, 2010). The *FUL* promoter thus interacts with many different transcription factors, and similar to AP2, other transcription factors might also bind to the *FUL* promoter in this proximal DHS region and inhibit *FUL* expression. Although I focussed on *FUL* promoter conservation among only a selection of *Brassicaceae* species, it would be interesting to analyse the divergence of *FUL* promoters within a single species that has multiple copies of *FUL*. This could then be used to test whether FUL paralogs have also acquired different functions within one species.

GTAC motifs in the *FUL* promoter and their function in *FUL* regulation

The highly conserved motif in region X of the *FUL* promoter was bound by SPL9 and SPL15 in a heterologous binding assay and when this tandem motif was mutated, the binding of these transcription factors was lost. However, the other two putative SPL15 binding sites in promoter region VII were not bound by SPL9 or SPL15 in this assay and subsequent mutagenesis of these sites did not affect the binding of these two transcription factors. According to ChIP-qPCR, this site was positively bound by SPL15, although possibly to a lesser extent than the conserved proximal binding site (Hyun *et al.*, 2016). This could mean that the binding of SPL15 and potentially other SPLs to region VII in the *FUL* promoter depends on additional proteins. These proteins might be plant-specific and therefore explain the absence of binding by SPL9 and SPL15 to region VII in the heterologous binding assay.

FUL expressed from a wild-type promoter complemented all mutant phenotypes of *ful-2* (Fig. 3.9). Expression of *FUL* from the *mGTAC* promoter also complemented the morphological phenotypes of *ful-2,* however, this construct induced early flowering in LD conditions, but did not affect flowering time in SD conditions (Fig. 3.9, 3.10). This earlier flowering in LD conditions correlated with earlier and higher expression of *FUL* in these mutant lines. A similar earlier and higher expression of *FUL* was observed *mGTAC* plants in SD conditions, however, these plants did not flower significantly earlier in these conditions. In LD conditions, there might be other SPL transcription factors that use the same binding site as SPL15 to repress the expression of *FUL* during vegetative development. It is possible that in SD conditions, FUL requires another co-factor to activate flowering, and this co-factor might only be present later during development. This co-factor could be SPL15 itself. Alternatively, FUL might not induce flowering much earlier in SD conditions due to insufficiently high GA levels, leading to continued inhibition by DELLA proteins and thus inhibition of flowering.

The confocal microscopy time courses in LD and SD conditions clearly showed that the earlier and higher expression of *FUL* in *mGTAC* plants also resulted in broader FUL protein expression in the meristem, suggesting that this is causal for the early flowering phenotype in LD conditions. Because early flowering was specific to LD conditions, *FT* and *TSF* were likely candidates to be involved in this earlier flowering, although neither of these genes was expressed more highly in *mGTAC* plants. Therefore, FUL can probably induce this early flowering in *mGTAC* plants in LD conditions without the need for FT or TSF. If FT and TSF are not the two LD-specific factors that cause the early flowering time in LD conditions, then perhaps FD is involved, and FUL could activate *FD* expression earlier than in Col-0. Overexpression of FD indeed leads to early flowering in LD conditions, but this also occurs mildly in SD conditions (Wigge *et al.*, 2005). To determine whether the earlier flowering of *mGTAC* lines is caused by early or higher expression of *FD,*

FT/TSF, SOC1 or SPL15, the *mGTAC* mutant lines could be crossed to the mutant backgrounds of these genes. Scoring the resulting crosses for their flowering time phenotypes in LD conditions and whether or not they suppress the early flowering of *mGTAC* plants can shed light on which genes are involved in this early flowering time phenotype. In addition, the expression of these genes could be tested in the wild-type and *mGTAC* lines to determine if they are indeed higher expressed in *mGTAC* plants.

Alternative hypotheses for the phenotypes of *pFUL-mGTAC::FUL::VENUS/ful-2* plants

The early-flowering phenotype of plants with a mutated *FUL* promoter could be attributed to the inability of inhibitory SPL proteins to bind to this mutated site. However, because AP2 is a strong floral inhibitor and binds close to the conserved GTAC motif in region X of the *FUL* promoter the early flowering phenotype is possibly caused by the failure of AP2 to bind to *FUL* (Dinh *et al.*, 2012; Yant *et al.*, 2010). AP2 was identified by ChIP-sequencing to bind to the *FUL* promoter, and its putative binding site is located close to the conserved region X in the *FUL* promoter (Supplemental figure S3.3). As was described in Dinh *et al.,* 2012, AP2 has the highest binding affinity with the TTTGTT motif, a motif present within the same ChIP-seq peak in the *FUL* promoter, 277 nucleotides away from the conserved GTAC motif. *ap2-12* mutants flower much earlier than Col-0 in LD conditions, similar to *mGTAC* promoter mutants. This hypothesis would suggest that AP2 would interact with an SPL protein that can bind the conserved GTAC motif in region X of the *FUL* promoter to promote AP2 binding and inhibit *FUL* transcription. Upon mutagenesis of that specific motif, the SPL protein can no longer bind, and thus, AP2 can no longer inhibit *FUL* transcription, leading to earlier and potentially increased expression of *FUL*, and subsequently earlier flowering in LD conditions.

Another hypothesis is that the mutagenesis of the putative SPL15-binding sites in the *FUL* promoter leads to a gain of function for a different transcription factor. This transcription factor might have gained the ability to bind to the *FUL* promoter and activate *FUL* transcription earlier in development, leading to earlier flowering. Currently there is no evidence to support this, nor do I have a hypothesis for which binding site might have been created, but this remains a possibility. A yeast one-hybrid (Y1H) experiment with the wild-type *FUL* promoter and the mutant *FUL* promoter against a cDNA library could help deciphering whether there is a transcription factor that can bind to the mutant *FUL* promoter, but not to the wild-type *FUL* promoter. Alternatively, Y1H can also help identifying which SPLs can bind to the wild-type *FUL* promoter and which of these lose their ability to bind to the *FUL* promoter once the *mGTAC* sites are mutated.

SOC1 and CArG boxes in the *FUL* promoter

Unexpectedly, mutagenesis of the putative SOC1-binding sites in the *FUL* promoter did not lead to a flowering-time phenotype. The hypothesis was that if the floral activator SOC1 can no longer bind to the *FUL* promoter, plants would be later flowering in LD and SD conditions. Perhaps SOC1 binds to a different CArG-box in the *FUL* promoter to regulate *FUL* expression and therefore, no clear altered flowering phenotype was observed. Alternatively, mutagenesis of the putative SOC1-binding sites was not tested for abrogating SOC1 binding, so perhaps SOC1 and potentially other MADS-box transcription factors could still bind to these motifs even after mutagenesis. Additional mutagenesis of the putative SPL15-binding sites, *pFUL-mCArG-mGTAC::FUL::VENUS/ful-2* indeed caused earlier flowering of these plants, but it is unclear whether these plants were earlier or later flowering than *pFUL-mGTAC::FUL::VENUS/ful-2* plants.

A model was published by Hyun *et al.* (2016), where SOC1 and SPL15 require one another for proper transcriptional regulation and SPL15 was proposed to be dependent on SOC1 for the transcriptional activation of *FUL*. If mutagenesis of the putative binding sites of SOC1 in the *FUL* promoter leads to inability of SOC1 to bind to these sites, then I would have expected these plants to be later flowering in SD conditions. If SPL15 was partially dependent on SOC1 to transcriptionally activate *FUL*, in the absence of SOC1, SPL15 might not have been able to timely activate *FUL* transcription and thus, later flowering would have occurred. These plants might not have been as late as *spl15-1* or *soc1-2* plants, but perhaps slightly later Col-0 in SD conditions. Fig. 3.15C and D illustrate that *pFUL-mCArG::FUL::VENUS/ful-2* plants have no mutant flowering phenotype in SD conditions. This could mean that the dependency of SPL15 on SOC1 for the transcriptional regulation of *FUL* might not be important for flowering, but this interaction could be important for other developmental aspects. Alternatively, as the *FUL* promoter contains more CArG boxes than the ones that were mutated in the *mCArG* lines, perhaps SOC1 was able to bind any of these other motifs (Hyun *et al.*, 2016).

Lastly, the conserved CArG box in the *FUL* promoter that is bound by SOC1 is not present in *A. alpina*. This could mean that the SOC1 orthologue in *A. alpina* regulates *FUL* via a different CArG box. It could also mean that in *A. alpina,* SOC1 is not involved in regulating *FUL*. *soc1-3/ful-2* double mutants show secondary growth and have a woody phenotype (Melzer *et al.*, 2008). Perhaps *A. alpina* shows similar secondary growth, in which case the regulation of *FUL* by SOC1 might indeed not be needed. These ideas remain hypotheses and thorough study of *FUL* and *SOC1* in *A. alpina* is required to understand better the function of these genes in this species.

Supplementary figures

Fig. S3.1. Nucleotide alignments of non-conserved GTAC motifs in the distal *FUL* promoter. Top: Alignment of most distal GTAC motif in region VII of the *FUL* promoter (Fig. 3.6). **Bottom: :** Alignment of second GTAC motif in region VII of the *FUL* promoter (Fig. 3.6). The Consensus sequence is displayed below the alignments. Marked in blue are the GTAC motifs in these regions.

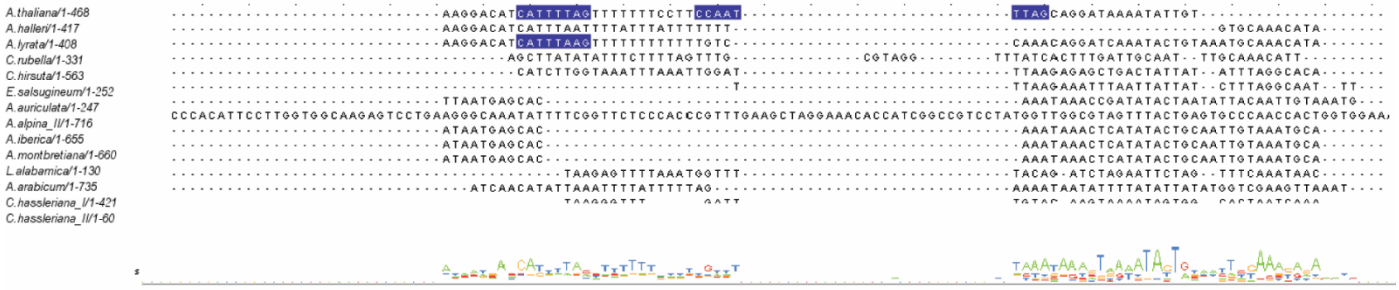

Fig. S3.2. Nucleotide alignments of non-conserved CarG-box motifs in the proximal *FUL* promoter. Alignment of region b In the *FUL* promoter containing the CarG-box motifs in A. thaliana (Fig. 3.6). The consensus sequence is displayed below the alignments. Marked in blue are the CarG-box motifs in this region.

TTCCCATATCTCTCTCTCTTCAAAATCTCAAGAACAAGAGAGAGAAACGACAACCCT-
GAAATGACCAAAGTATCTCTCTCTCTCTTTCTTTCTTATGTCTCTCTGGGTATCTTTTGTG
TTGATGAATGTGATAATAGCTATTTTATTTTTTTTTATTTTTTCTTTTATGGACTTTGTTG
GGTTTCGCGTGAGTCTACAGTGACGTAAGTGATGTGGTATAAATACGGTATGTGACGTGAA
TACATAGACGATGATATTTGTGGAAAAAAAAGAAAGAAAAAAAAAACACAAAAGCTACATA
CGAGTGGAAGAAGAGACCAGAGTGGAGATAAAGTTTTAAGGGCTGTTTGGGAAATAAACCA
TTTGATGTGTTGTCGAGTCCTCATTGGCTACTTTTTTACTGTGCTTGTAACTCGTTCGTTAG
TTTTGTGCCTCCCTTTAGCTTACATTGTTTCCGTACCGTACGG

Fig. S3.3. Sequence below AP2 ChIP-sequencing peak in the *FUL* promoter. Annotated are the highest affinity binding site for AP2 in green and the conserved putative SPL15-binding site in region X of the *FUL* promoter in red (Dinh et al., 2012).

Chapter 4:

Identification of novel SPL15-dependent pathways by RNA-seq

Introduction

As described in chapter 2 (Fig. 2.1), *squamosa promoter binding protein-like 15* (*spl15*) mutant plants flower much later than Col-0 plants in SD conditions, but show a weak late-flowering or no phenotype under LD conditions, depending on the experiment. Conversely, overexpression under its native promoter of a form of *SPL15* that is resistant to mir156-mediated transcriptional and translational control (expression of *rSPL15*; *pSPL15::VENUS::rSPL15*), leads to earlier flowering than Col-0 in LD and SD conditions (Fig. 4.1 and 2.5). SPL15 is thus required for timely flowering in SD conditions, and sufficient to induce flowering in LD. In chapter 2, I showed that *FRUITFULL* (*FUL*) and *MICRORNA172B* (*MIR172B*) are important for floral induction through SPL15 (Fig. 2.4). However, higher-order combinations of mutants in these two genes combined with *rSPL15* still bolted earlier than wild-type in LD and SD conditions (Fig. 2.5), suggesting that *FUL* and *MIR172B* are not the only genes regulated by SPL15 that contribute to floral induction.

This chapter describes multiple approaches to identify other putative targets of SPL15, that are important for floral induction.

Firstly, to identify genes that are expressed differentially in *rSPL15* plants compared to Col-0, I performed an RNA-sequencing (RNA-seq) experiment in LD conditions. Secondly, I set up the complementary experiment to compare the transcriptome of *spl15-1* with Col-0 in SD conditions, where native SPL15 exerts it function in regulating flowering time. Lastly, I constructed transgenic lines carrying *SPL15:SPL15-GR* to induce SPL15 activity chemically, and to analyse candidate target genes of SPL15 for their response to induction of SPL15.

For each transcriptome experiment, I used three approaches to analyse the data: I first analysed mRNAs of transcription factors involved in flowering-time regulation, to confirm that I captured the appropriate developmental stages, whether well-known floral integrators were differentially expressed in either *rSPL15* or *spl15-1* in comparison to Col-0. Secondly, I analysed the overlap between differentially expressed genes (DEGs) and those that have a role in flowering, to determine what proportion of DEGs have a function in flowering and which genes these are. Thirdly, I identified genes that are co-expressed with the SPL15 target *FUL* to avoid bias towards genes involved in flowering-time regulation and to identify candidate genes that are regulated by SPL15. Combining these two RNA-seq experiments and assessing their overlap is a powerful approach to identify putative novel candidate target genes of SPL15, which was

the aim of the final part of the transcriptome analysis. In that section, I also discuss the function of some of the DEGs in more detail.

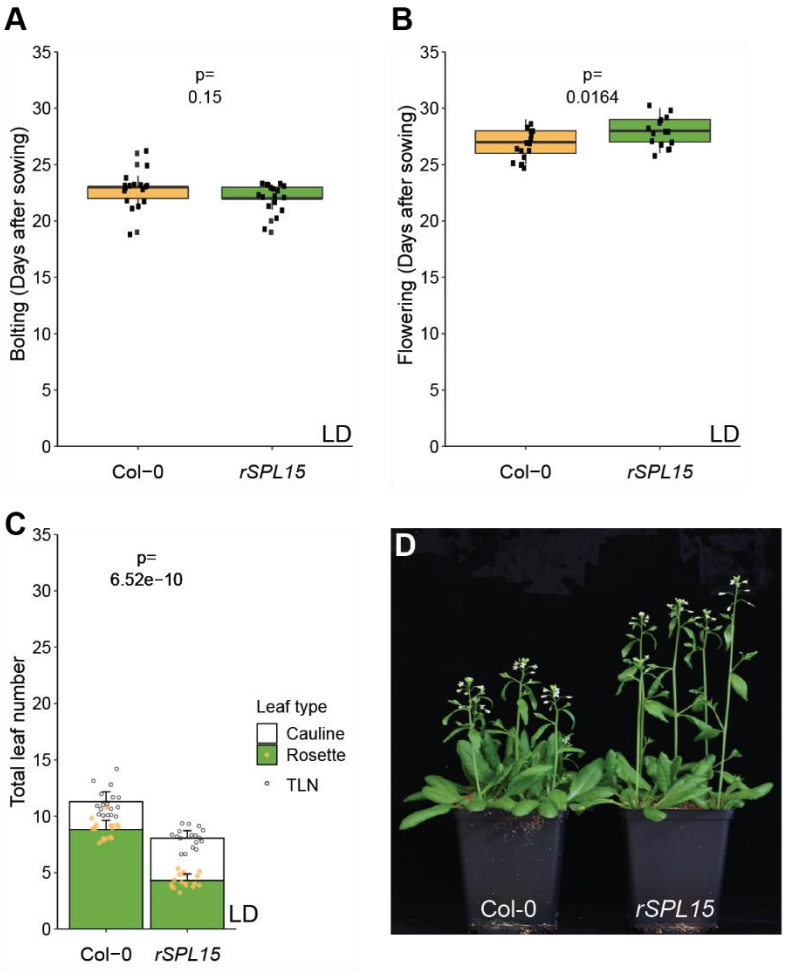

Figure 4.1. Flowering time of Col-0 and rSPL15 in LD conditions. Time to bolting **(A**), flowering time **(B)** and total leaf number **(C; TLN)** of Col-0 and pSPL15::VENUS::rSPL15 in LD conditions (n = 17, *p* was calculated using student's *t*-test). Bolting time was scored as the day on which the inflorescence extended 0.5 cm from the rosette and flowering time was scored as the day on which the first flower opened, anywhere on the plant. Error bars represent the standard deviation. (**D**) Picture of Col-0 and rSPL15 plants at 28LD.

RNA-sequencing time course of Col-0 and *rSPL15* in long-day conditions

rSPL15 flowers earlier than Col-0 in LD conditions.

I chose LD conditions in which to perform the transcriptome analysis of *rSPL15* compared to Col-0, because the *rSPL15* phenotype is visible in these conditions (Fig. 4.1). The *rSPL15* plants were not always significantly earlier bolting and flowering, but a trend towards earlier flowering was always visible and the total leaf number (TLN) was always significantly lower in *rSPL15* plants than for Col-0. *rSPL15* inflorescences were always taller than Col-0 upon opening of the first flower, even although these genotypes often bolted at the same time (Fig 4.1D). This result suggests that *rSPL15* has a positive role in the elongation of the inflorescence stem, as I also mentioned in chapter 2.

Shoot apical meristems of *rSPL15* plants dome earlier than those of Col-0 and *rSPL15* plants and show earlier and higher expression of *FUL* under LD conditions.

The transcriptome analysis was performed using shoot apical meristem (SAM)-enriched material from which most leaf material was removed with forceps by visual inspection (See methods). Harvesting for total RNA was performed simultaneously with harvesting for confocal microscopy to fully characterize the material. The confocal micrographs clearly showed early doming, the production of axillary SAMs and in some samples floral primordia in *rSPL15* plants at 12LD, whereas Col-0 plants at the same time point showed doming, but no axillary SAMs or floral primordia (Fig. 4.2B). In Col-0, no expression of *pSPL15::VENUS::SPL15* was observed at 3-, 6-, 9- or 12LD in two independent experiments (Fig. S4.1). The wild-type signal was only detectable from 15LD onwards. In the confocal images of *rSPL15,* the *rSPL15* SAMs were approximately three days more advanced in terms of floral transition than Col-0 (Fig. 4.2B). Because *rSPL15* is already present in the meristem at 6LD, the transcriptome time course included 3LD, 6LD, 9LD and 12LD (Fig. 4.2B). The 3LD time point was included because the time course should ideally start with a time point at which *rSPL15* and Col-0 plants are identical, such that even the earliest changes in expression caused by *rSPL15* would be captured in the analysis. qRT-PCR showed that *FUL* mRNA is expressed at higher levels and earlier in *rSPL15* plants than in Col-0 plants throughout the time-course. In-line with the confocal images, these qRT-PCR results indicate that considering *FUL* expression, *rSPL15* was plants had advanced developmentally about three days more than Col-0.

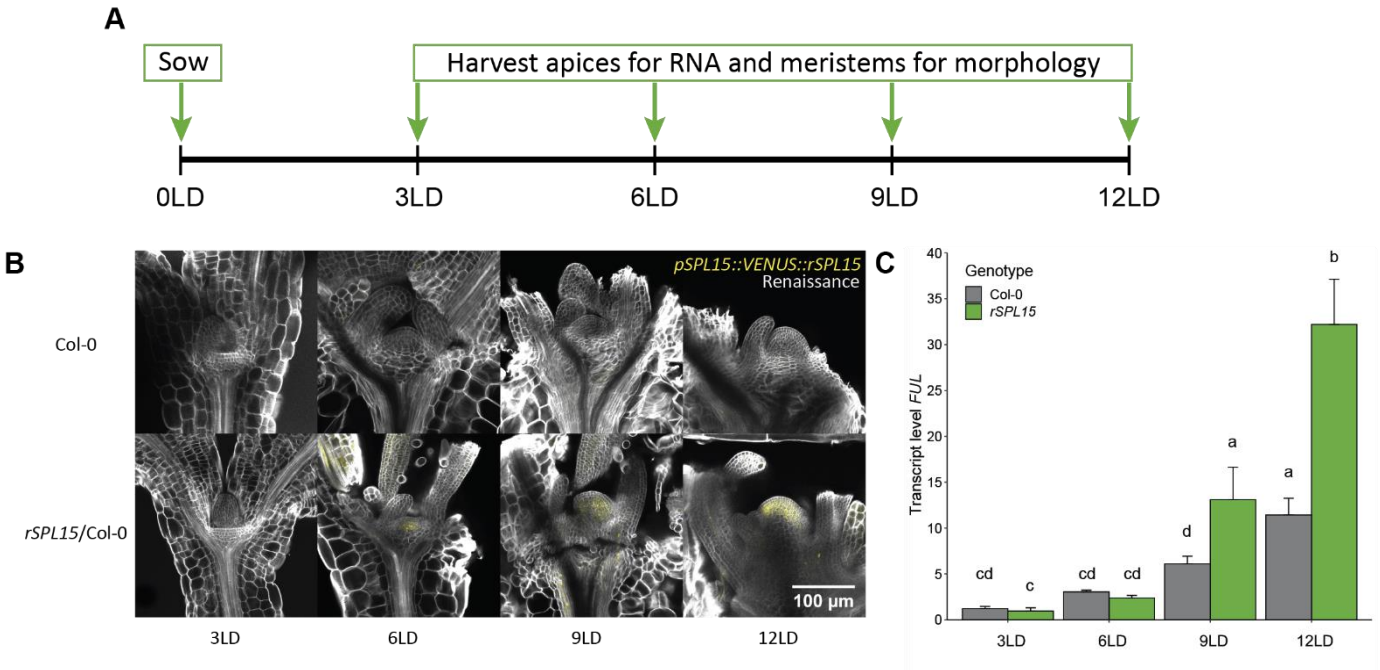

Figure 4.2. The set-up and characterisation of the LD RNA-seq experiment with Col-0 and *rSPL15*. (**A**) Schematic representation of the RNA-seq experiment indicating the time of sowing and each harvesting time point for RNA as well as the harvesting time points for confocal microscopy. (**B**) Confocal laser scanning micrographs of shoot apices of Col-0 and *pSPL15::VENUS::rSPL15* at the indicated time points in LD conditions. Fluorescence from VENUS is artificially coloured in yellow and fluorescence from the Renaissance dye is artificially coloured in white. The white scale bar represents 100 µm. (**C**) The *FUL* expression level in meristem-enriched material from Col-0 and *rSPL15* at the indicated time points; an aliquot of this material was used for RNA-seq. The variation shown was derived from three independent biological replicates, error bars indicate standard deviation. Statistical differences were calculated using ANOVA followed by Tukey's HSD (honestly significant difference) test at $p < 0.01$. The confocal analysis (B) as well as part of the harvesting for RNA-seq, the RNA isolation and QRT-PCR of *FUL* (C) were performed by MSc student Miguel Wente during his internship.

The transcriptomes of *rSPL15* and Col-0 plants differed from 6 days after sowing and onwards in LD conditions.

The transcriptomes of *rSPL15* and Col-0 plants under LD conditions showed a clear separation between 3LD and the other time points in a principal component analysis (PCA; Fig. 4.3A). Because the 3LD time point had such a large effect on the PCA, another PCA was performed excluding this time point (Fig. 4.3B). The second PCA showed that in addition to separation over time, there was also a separation between the genotypes, which was clear between *rSPL15* and Col-0 at 6LD, and smaller at 9LD and 12LD (Fig. 4.3B). In total 798, 3,543, 608 and 392 genes were differentially expressed between *rSPL15* and Col-0 at 3LD, 6LD,

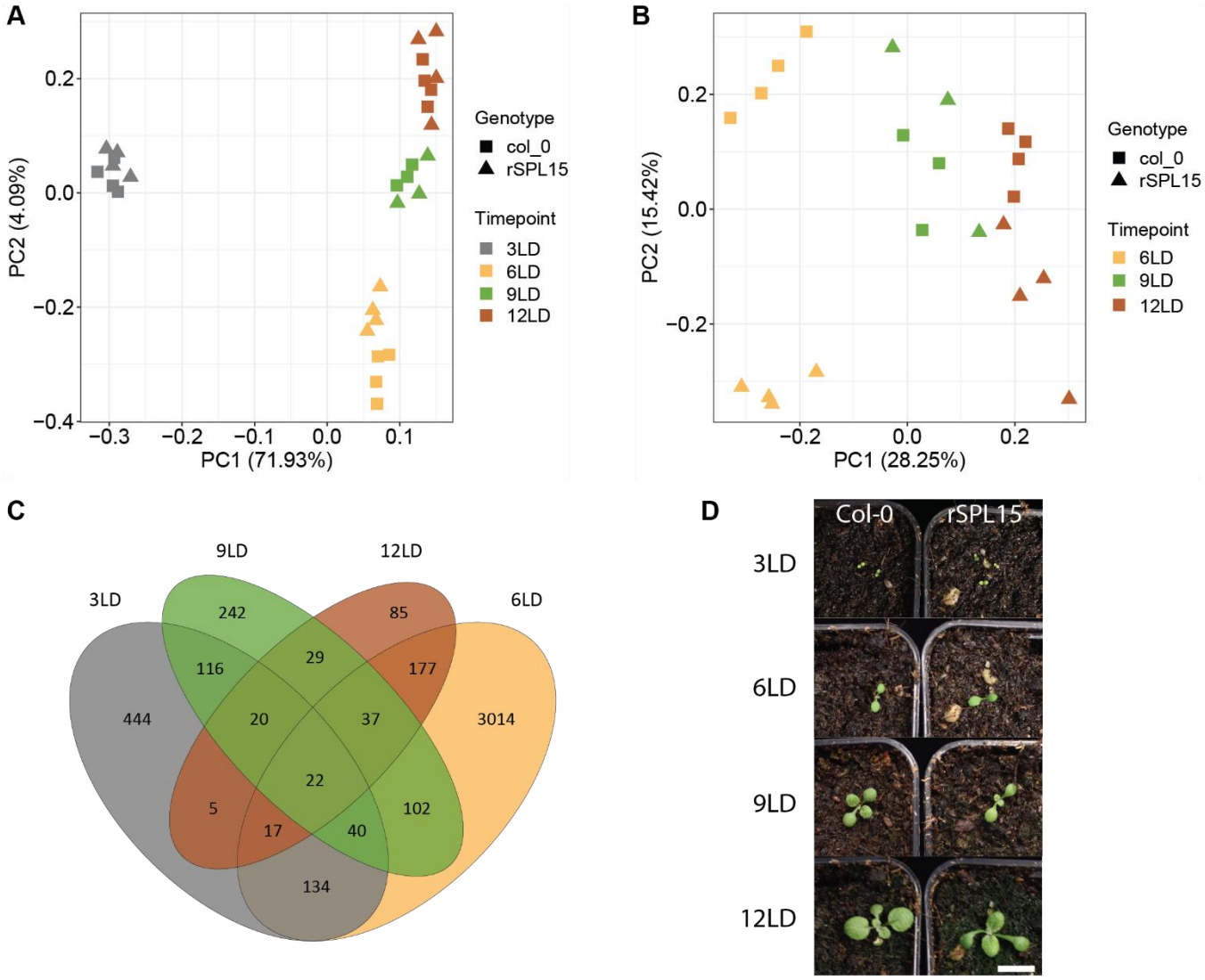

Figure 4.3. Representation of the RNA-seq experiment data for meristem-enriched tissue from Col-0 and *rSPL15* in LD conditions. (**A**) Principal component analysis (PCA) of regularised log_2-transformed read counts per gene for both genotypes at all time points. (**B**) PCA of regularised log_2-transformed read counts per gene for both genotypes at time points 6-, 9- and 12LD. **C:** Venn-diagram showing all differentially expressed genes (DEGs) between Col-0 and *rSPL15* at each time point and whether these DEGs occur at other time points. DEGs were selected for an adjusted *p*-value < 0.05. (**D**) Images of Col-0 and *rSPL15* seedlings in LD conditions at the indicated time points, corresponding to the harvesting time points of the RNA-seq experiment. The white scale bar represents 10 mm.

9LD and 12LD, respectively (Fig. 4.3C; appendix 1 (upon request); *p*. adj.< 0.05). The overlap of the differentially expressed genes between the time points showed that many genes were differentially expressed at multiple timepoints and that 22 genes were differentially expressed at all timepoints.

The large number of DEGs at 3LD was unexpected because as no expression of rSPL15-VENUS was detected in the SAM at this time and I hypothesised that the two transcriptomes would be similar. Moreover, no clear morphological differences were found between the SAMs of Col-0 and *rSPL15* plants, and no *FUL* expression was detected in either genotype at this time point, suggesting the plants and their transcriptomes would be quite similar (Fig. 4.2B, C). However, *rSPL15* showed a cotyledon phenotype with cotyledons being narrower and without a clearly distinguishable petiole, which is reminiscent of other SPL-overexpression lines (Fig. 4.3D Barrera-Rojas *et al.*, 2020; Guo *et al.*, 2017; Kim *et al.*, 2012; Xu *et al.*, 2016). In addition, *rSPL15* plants were slower in the development of their first true leaves, similar to plants with suppressed miR156 activity (MIM156; Fig. 4.3D; Franco-Zorrilla *et al.*, 2007; Wu *et al.*, 2009; Xu *et al.*, 2016). These developmental differences between Col-0 and *rSPL15* might be responsible for the large number of DEGs at 3LD and possibly also at 6LD. Because there was no enrichment in flowering time-related genes in the DEGs at 3LD, only 6LD, 9LD and 12LD were used for subsequent analyses (Fig. S4.2).

The *rSPL15* transcriptome shows precocious expression of genes encoding transcription factors that regulate floral induction.

To determine whether and which genes involved in floral induction were precociously expressed in *rSPL15* plants compared to Col-0 plants, the expression of genes encoding 97 transcription factors involved in floral induction was cross-referenced with the identified *rSPL15* DEGs (Kinoshita & Richter, 2020). Figure 4.4 shows a heatmap of the expression of these transcription factors with the Z-score of their expression. This score indicates how different a gene is expressed across the different timepoints and genotypes. The heatmap shows that *SPL15* mRNA is more highly expressed in *rSPL15* relative to Col-0. Furthermore, the data show the advancement of floral induction in *rSPL15* plants at the transcriptomic level. In particular, the lower half of Figure 4.4 shows that the expression of many transcription factors is already upregulated in *rSPL15* at 12LD, but are not yet upregulated in Col-0 plants. The lower half of the figure shows well-described floral integrators such as *SUPPRESSOR OF OVEREXPRESSION OF CONSTANS 1* (*SOC1*)*, FUL, LEAFY* (*LFY*) and the floral primordium-specific gene *APETALA1* (*AP1*). The expression of AP1 is a marker for the production of floral primordia, and its expression denotes that *rSPL15* has completed floral induction, while its expression is still absent in Col-0 plants throughout the time course (Fig. 4.4; Liu *et al.*, 2007).

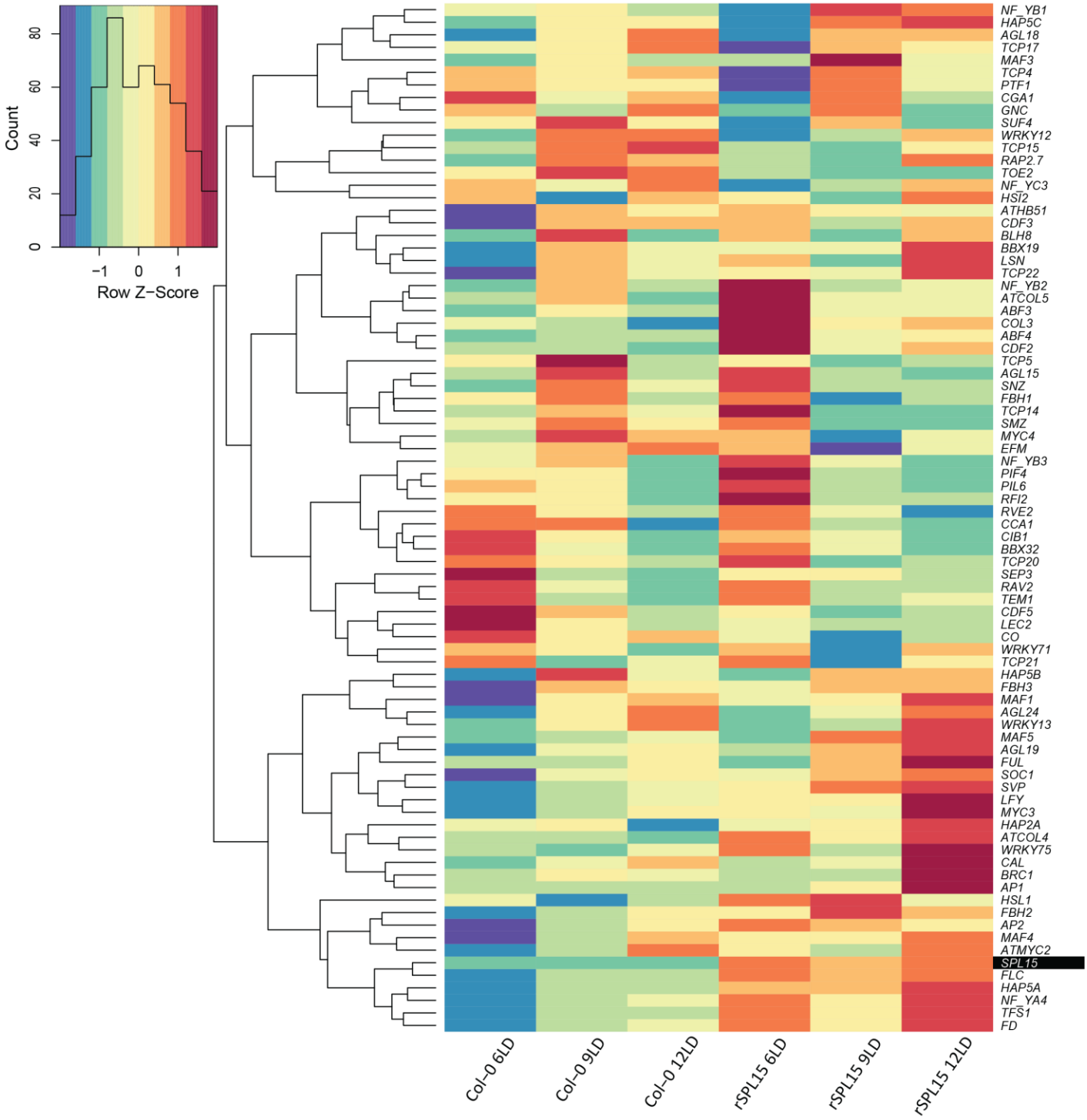

Figure 4.4. Heatmap of the expression of genes encoding transcription factors involved in the regulation of flowering. Heatmap showing the expression of genes encoding transcription factors involved in flowering-time regulation over time in Col-0 and the *rSPL15* line in the RNA-seq experiment. Genes listed here have been taken from Kinoshita & Richter (2020). All *SPL* genes except *SPL15* were excluded (the expression of all SPLs in this transcriptome time course is presented in chapter 5). Gene expression was derived from $\log_2$-transformed FPKM values normalised over the whole data set, which were transformed into the Z-score for each gene.

Out of the 4,040 differentially expressed genes between Col-0 and *rSPL15* at 6, 9 and 12LD, 59 have a function in flowering-time regulation.

In total, 4,040 genes were differentially expressed between Col-0 and *rSPL15* at 6, 9 and 12LD (*p*. adj.< 0.05). Among these genes, 3,543 were differentially expressed at 6LD only. It is unlikely that all of these genes are related to the function of SPL15 in flowering, and some might be related to roles for SPL15 in other developmental processes such as embryo or leaf development (Fig. 4.3D). I therefore cross-referenced all DEGs at time points 6, 9 and 12LD with a published list of 302 genes involved in the floral transition to see what proportion of DEGs have a function in flowering-time regulation (Kinoshita & Richter, 2020). 59 (1.5%) DEGs were described to have a genetically determined function in flowering-time regulation (Figure 4.5; Table 4.1). Included are those encoding SPL15 and two other SPL transcription factors that were upregulated in *rSPL15*, *SPL4* and *SPL2* (Table 4.1). Furthermore, genes encoding five out of the six *APETALA2-LIKE* (*AP2-L*) transcription factors were present in this list, although they were mostly upregulated at 6LD (*SMZ, SNZ* and *AP2*) and downregulated at later timepoints in *rSPL15* (*SMZ* and *TOE2*; Table 4.1; Table S4.1). *TOE3* however, was consistently upregulated in *rSPL15* at 6- and 9LD.

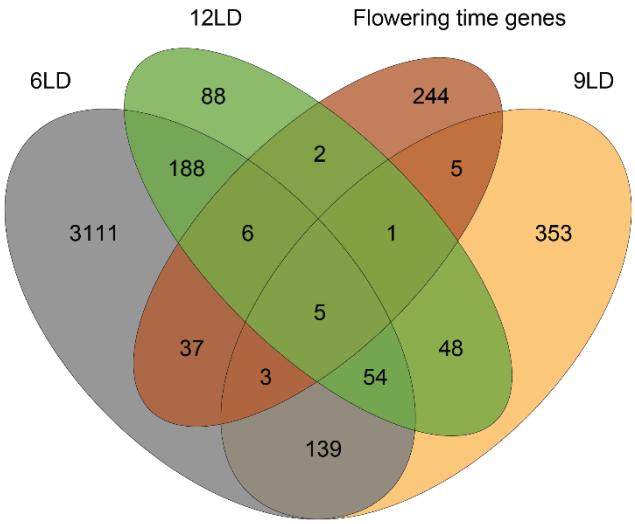

Figure 4.5. Venn diagram showing the overlap of differentially expressed genes (DEGs) between Col-0 and *rSPL15* at 6, 9 and 12LD with genes involved in flowering-time regulation.

Table 4.1. Differentially expressed genes involved in flowering time regulation. All DEGs (*p*adj<0.05) between Col-0 and *rSPL15* at time point 6LD, 9LD and/or 12LD which are also related to flowering time regulation. Stdev= standard deviation.

AGI-code	Gene symbol	Gene name / description	DE (Log_2 Fold Change ± stdev)		
			6LD	9LD	12LD
AT1G04400	*CRY2*	*CRYPTOCHROME 2*	0.34 ± 0.09	-	-
AT1G19330	*AT1G19330*		0.53 ± 0.17	-	-
AT1G24260	*SEP3*	*SEPALLATA3*	-1.92 ± 0.39	-	-
AT1G25540	*PFT1*	*PHYTOCHROME AND FLOWERING TIME 1*	-0.26 ± 0.10	-	-
AT1G32640	*MYC2*	*BHLH DNA-binding family protein*	1.12 ± 0.39	-	-
AT1G51140	*FBH3*	*FLOWERING BHLH 3*	0.59 ± 0.14	-	-
AT1G53090	*SPA4*	*SPA1-RELATED 4*	0.42 ± 0.14	-	-
AT1G53160	*SPL4*	*SQUAMOSA PROMOTER BINDING PROTEIN-LIKE 4*	-	1.93 ± 0.57	1.35 ± 0.30
AT1G69570	*AT1G69570*	*Dof-type zinc finger DNA-binding family protein*	-1.48 ± 0.44	-	-
AT1G69690	*TCP15*	*TEOSINTE BRANCHED1/CYCLOIDEA/PCF 15*	-	-0.59 ± 0.18	
AT1G78580	*TPS1*	*TREHALOSE-6-PHOSPHATE SYNTHASE*	0.30 ± 0.09	-	-
AT1G79460	*GA2*	*GA REQUIRING 2*	0.49 ± 0.15	-	-
AT2G22540	*SVP*	*SHORT VEGETATIVE PHASE*	0.40 ± 0.09	-	0.37 ± 0.09
AT2G24790	*COL3*	*CONSTANS-like 3*	0.20 ± 0.08	-	-
AT2G39250	*SNZ*	*SCHNARCHZAPFEN*	0.66 ± 0.14	-	-
AT2G41370	*BOP2*	*BLADE ON PETIOLE2*	0.97 ± 0.16	-	-
AT2G42280	*FBH4*	*FLOWERING BHLH 4*	-0.70 ± 0.16	-	-
AT2G43010	*PIF4*	*PHYTOCHROME INTERACTING FACTOR 4*	0.45 ± 0.12	-	-
AT2G44745	*WRKY12*	*WRKY DNA-binding protein 12*	-	-1.69 ± 0.48	-
AT2G45660	*AGL20*	*SOC1, AGAMOUS LIKE 20*	1.86 ± 0.28	1.03 ± 0.26	0.87 ± 0.14
AT3G04240	*SEC*	*SECRET AGENT*	0.21 ± 0.07	-	-
AT3G04910	*WNK1*	*WITH NO LYSINE (K) KINASE 1*	0.51 ± 0.12	-	-
AT3G10390	*FD*	*FLOWERING LOCUS D*	-0.33 ± 0.10	-	-
AT3G15030	*TCP4*	*TCP family transcription factor 4*	-1.09 ± 0.12	-	-
AT3G15354	*SPA3*	*SPA1-RELATED 3*	0.26 ± 0.09	-	-
AT3G16470	*JR1*	*JASMONATE RESPONSIVE 1*	0.90 ± 0.15	-0.57 ± 0.18	-
AT3G19290	*ABF4*	*ABRE BINDING FACTOR 4*	0.38 ± 0.10	-	-
AT3G47500	*CDF3*	*CYCLING DOF FACTOR 3*	0.35 ± 0.10	-	-
AT3G54990	*SMZ*	*SCHLAFMUTZE*	0.58 ± 0.20	-1.12 ± 0.27	-
AT3G57920	*SPL15*	*SQUAMOSA PROMOTER BINDING PROTEIN-LIKE 15*	4.50 ± 0.20	3.26 ± 0.20	3.36 ± 0.16
AT3G59060	*PIL6*	*PHYTOCHROME INTERACTING FACTOR 3-LIKE 6*	0.41 ± 0.09	-	-
AT3G63010	*GID1B*	*GA INSENSITIVE DWARF1B*	0.71 ± 0.22	-	-
AT4G08920	*CRY1*	*CRYPTOCHROME 1*	0.27 ± 0.07	-	-
AT4G17880	*MYC4*	*bHLH DNA-binding family protein*	-	-0.60 ± 0.18	-
AT4G26150	*CGA1*	*CYTOKININ-RESPONSIVE GATA FACTOR 1*	-1.06 ± 0.23	-	-
AT4G31877	*MIR156C*	*MICRORNA156C*	1.24 ± 0.37	-	-
AT4G34000	*ABF3*	*ABSCISIC ACID RESPONSIVE ELEMENTS-BINDING FACTOR 3*	0.90 ± 0.11	-	-
AT4G34400	*TFS1*	*TARGET OF SVP AND FLC 1*	3.51 ± 0.32	1.65 ± 0.33	2.68 ± 0.23
AT4G34530	*CIB1*	*CRYPTOCHROME-INTERACTING BASIC-HELI--LOOP-HELIX 1*	-0.62 ± 0.22	-	-
AT4G35900	*FD*	*FLOWERING LOCUS D*	1.86 ± 0.25	-	1.02 ± 0.19
AT4G36920	*AP2*	*APETALA 2*	0.50 ± 0.15	-	-
AT4G39100	*SHL1*	*SHORT LIFE*	0.33 ± 0.11	-	-
AT5G02030	*RPL*	*REPLUMLESS*	0.60 ± 0.17	-	0.42 ± 0.12
AT5G03840	*TFL1*	*TERMINAL FLOWER 1*	2.00 ± 0.55	-	2.10 ± 0.48
AT5G10140	*FLC*	*FLOWERING LOCUS C*	1.65 ± 0.20	0.79 ± 0.24	1.00 ± 0.21
AT5G24860	*FPF1*	*FLOWERING PROMOTING FACTOR 1*	-	-	4.89 ± 1.13
AT5G39660	*CDF2*	*CYCLING DOF FACTOR 2*	0.88 ± 0.13	-	-
AT5G41190	*AT5G41190*		-0.37 ± 0.07	-	-
AT5G43270	*SPL2*	*SQUAMOSA PROMOTER BINDING PROTEIN-LIKE 2*	0.36 ± 0.13	-	-
AT5G46760	*MYC3*	*bHLH DNA-binding family protein*	0.33 ± 0.10	-	-
AT5G47640	*NF-YB2*	*NUCLEAR FACTOR Y, SUBUNIT B2*	0.69 ± 0.19	-	-
AT5G51810	*GA20OX2*	*GIBBERELLIN 20 OXIDASE 2*	-	-1.62 ± 0.48	-
AT5G57660	*COL5*	*CONSTANS-like 5*	0.46 ± 0.12	-	-
AT5G60120	*TOE2*	*TARGET OF EARLY ACTIVATION TAGGED (EAT) 2*	-0.37 ± 0.13	-1.09 ± 0.15	-0.77 ± 0.11
AT5G60910	*FUL*	*AGAMOUS-like 8, FRUITFULL*	-	-	1.75 ± 0.37
AT5G61850	*LFY*	*LEAFY*	1.35 ± 0.42	-	1.56 ± 0.32
AT5G62165	*AGL42*	*AGAMOUS-like 42*	3.62 ± 1.23	-	2.69 ± 0.38
AT5G62430	*CDF1*	*CYCLING DOF FACTOR 1*	-	-0.83 ± 0.23	-
AT5G67180	*TOE3*	*TARGET OF EARLY ACTIVATION TAGGED (EAT) 3*	1.22 ± 0.31	1.59 ± 0.40	-

76 genes are positively or negatively co-expressed with *FUL* in Col-0 and *rSPL15* under LD conditions

Because *FUL* is directly bound by SPL15, and its expression is dependent on SPL15, I aimed to identify genes that are co-expressed with *FUL* in the transcriptome data set as these are candidates for additional SPL15 targets (Fig. 2.8B; Fig. 3.7; Hyun *et al.*, 2016). I analysed genes that were either positively or negatively co-expressed with *FUL,* as candidates for genes that are activated or repressed by SPL15. *FUL* is expressed upon floral induction in LD conditions, and the transcriptome dataset revealed that *FUL* is expressed earlier in *rSPL15* than in Col-0 (Fig. 4.5A). In *rSPL15*, *FUL* is already expressed more highly than Col-0 at 9LD, whereas it becomes expressed at a similar level to that in Col-0 only at 12LD.

Co-expression was analysed by calculating the Pearson correlation coefficient between $\log_2$ transformed normalised FPKM (Fragments Per Kilobase Million) values from all genes with those of *FUL* over 6, 9 and 12LD. In this data set, genes were considered to be correlating with *FUL* above a coefficient of 0.8. Out of the 76 genes that were positively or negatively co-expressed with *FUL*, 37 genes were expressed in a similar pattern as *FUL* and 39 genes expressed in opposite pattern to *FUL* (*i.e.* these genes were downregulated as *FUL* expression increased). Out of these 76 genes, only three have a described role in flowering-time regualtion: *FUL*, *SQUAMOSA PROMOTER BINDING PROTEIN-LIKE 4* (SPL4) and *AGAMOUS-LIKE 42 (AGL42;* Fig. S4.3; Cardon *et al.*, 1999; Dorca-Fornell *et al.*, 2011; Kinoshita & Richter, 2020; Wang *et al.*, 2009). Furthermore, among these 76 genes that were co-expressed with *FUL,* 32 were differentially expressed at 6LD, 9LD and/or 12LD, and these included nine genes belonging to the histone protein superfamily (Fig. S4.4, Table 4.2, Table S4.2).

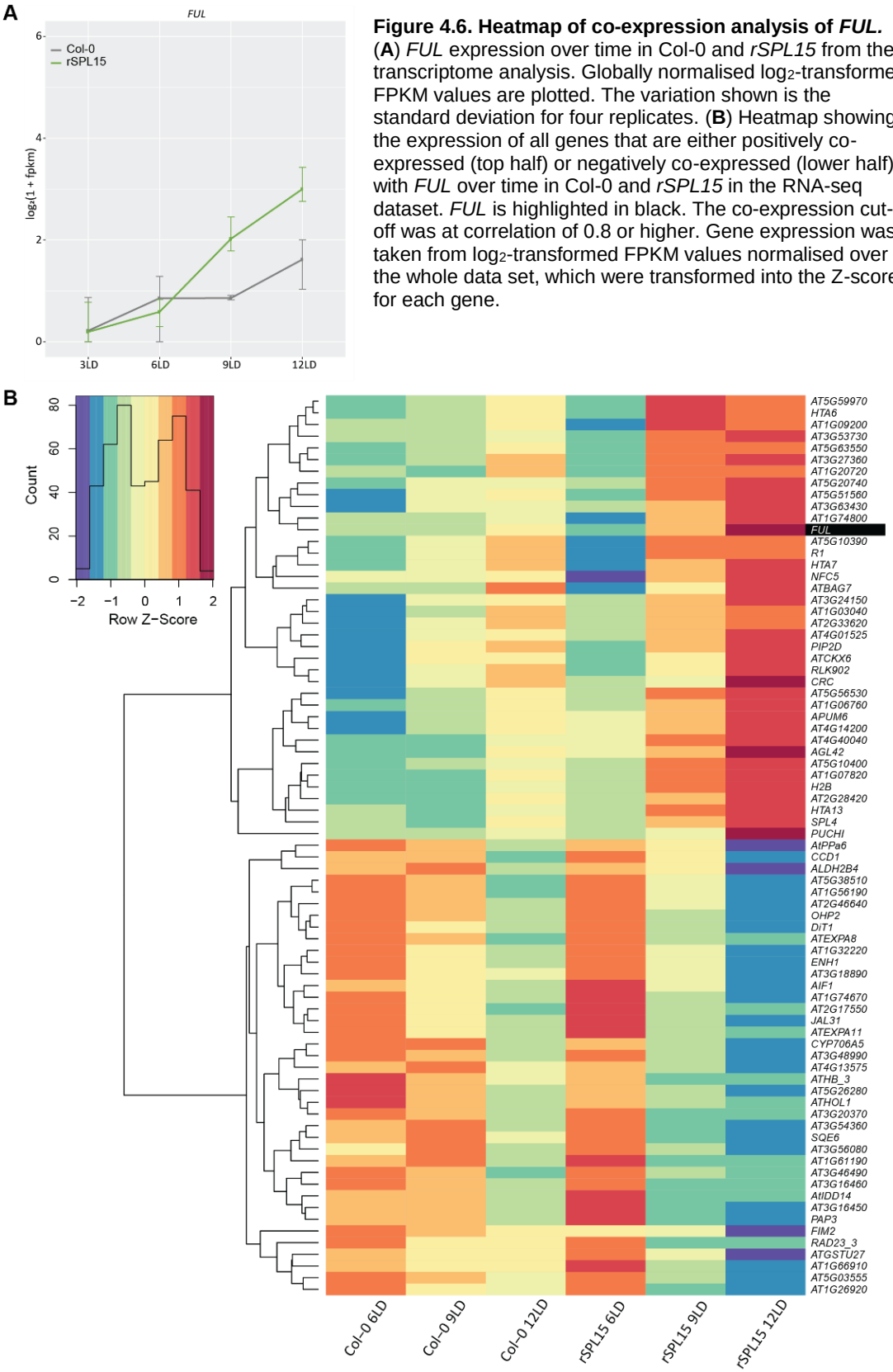

Figure 4.6. Heatmap of co-expression analysis of *FUL*. (**A**) *FUL* expression over time in Col-0 and *rSPL15* from the transcriptome analysis. Globally normalised log_2-transformed FPKM values are plotted. The variation shown is the standard deviation for four replicates. (**B**) Heatmap showing the expression of all genes that are either positively co-expressed (top half) or negatively co-expressed (lower half) with *FUL* over time in Col-0 and *rSPL15* in the RNA-seq dataset. *FUL* is highlighted in black. The co-expression cut-off was at correlation of 0.8 or higher. Gene expression was taken from log_2-transformed FPKM values normalised over the whole data set, which were transformed into the Z-score for each gene.

Table 4.2. Differentially expresed genes that are co-expressed with *FUL*. A list of all DEGs (*p*adj<0.05) that were differenftially expressed (DE) between Col-0 and *rSPL15* at time points 6-, 9- and/or 12LD and that were positively or negatively co-expressed with *FUL*. Genes marked with (●) are related to flowering-time regulation. Stdev = standard deviation.

AGI-code	Gene symbol	Gene name / description	DE (Log_2 Fold Change ± stdev)		
			6LD	9LD	12LD
AT1G06760	*AT1G06760*	*Winged-helix DNA-binding transcription factor family protein*	-	-	0.28 ± 0.07
AT1G07820	*AT1G07820*	*Histone superfamily protein*	-	0.33 ± 0.10	-
AT1G09200	*AT1G09200*	*Histone superfamily protein*	-	0.37 ± 0.10	-
AT1G14700	*PAP3*	*PURPLE ACID PHOSPHATASE 3*	0.39 ± 0.15	-0.84 ± 0.19	-
AT1G53160	*SPL4*●	*SQUAMOSA PROMOTER BINDING PROTEIN-LIKE 4*	-	1.93 ± 0.57	1.35 ± 0.30
AT1G68130	*IDD14*	*INDETERMINATE (ID)-DOMAIN 14*	0.44 ± 0.14	-	-
AT2G33620	*AT2G33620*	*AT hook motif DNA-binding family protein*	0.39 ± 0.07	-	0.30 ± 0.08
AT2G40610	*EXPA8*	*EXPANSIN A8*	-	-1.06 ± 0.29	-
AT2G43910	*HOL1*	*HARMLESS TO OZONE LAYER 1*	-	-0.41 ± 0.12	-
AT3G16450	*JAL33*	*JACALIN-RELATED LECTIN 33*	-	-1.43 ± 0.18	-
AT3G16460	*JAL34*	*JACALIN-RELATED LECTIN 34*	-	-1.15 ± 0.20	-0.44 ± 0.12
AT3G20370	*AT3G20370*	*TRAF-like family protein*	-	-1.68 ± 0.20	-
AT3G20670	*HTA13*	*HISTONE H2A 13*	-	0.59 ± 0.12	0.33 ± 0.09
AT3G46490	*AT3G46490*	*2-oxoglutarate (2OG) and Fe(II)-dependent oxygenase superfamily protein*	-	-1.28 ± 0.15	-
AT3G48990	*AAE3*	*ACYL-ACTIVATING ENZYME 3*	-	-	-0.40 ± 0.11
AT3G53730	*AT3G53730*	*Histone superfamily protein*	-	0.40 ± 0.10	-
AT3G56080	*AT3G56080*	*S-adenosyl-L-methionine-dependent methyltransferases superfamily protein*	-	-1.23 ± 0.26	-
AT3G63440	*CKX6*	*CYTOKININ OXIDASE/DEHYDROGENASE 6*	-	-	0.87 ± 0.18
AT4G01525	*SADHU5-1*	*SADHU NON-CODING RETROTRANSPOSON 5-1*	1.13 ± 0.31	0.93 ± 0.21	1.73 ± 0.14
AT4G12310	*CYP706A5*	*Cytochrome P450, family 706, subfamily A, polypeptide 5*	-	-0.63 ± 0.18	-
AT4G13575	*AT4G13575*		-	-0.88 ± 0.26	-0.70 ± 0.21
AT4G40040	*AT4G40040*	*Histone superfamily protein*	-	-	0.25 ± 0.07
AT5G10400	*AT5G10400*	*Histone superfamily protein*	-	-	0.32 ± 0.09
AT5G15150	*HB-3*	*HOMEOBOX 3*	-	-1.16 ± 0.31	-
AT5G20740	*AT5G20740*	*Plant invertase/pectin methylesterase inhibitor superfamily protein*	-	-	0.56 ± 0.10
AT5G22880	*HTB2*	*HISTONE B2*	-	0.49 ± 0.14	0.45 ± 0.13
AT5G24160	*SQE6*	*SQUALENE MONOXYGENASE 6*	-	-1.76 ± 0.43	-
AT5G26280	*AT5G26280*	*TRAF-like family protein*	-1.34 ± 0.20	-2.60 ± 0.26	-1.63 ± 0.29
AT5G35700	*FIM5*	*FIMBRIN5*	-	-	-0.45 ± 0.11
AT5G59870	*HTA6*	*HISTONE H2A 6*	-	0.40 ± 0.10	-
AT5G59970	*AT5G59970*	*Histone superfamily protein*	-	0.44 ± 0.11	-
AT5G60910	*FUL*●	*FRUITFULL*	-	-	1.75 ± 0.37
AT5G62165	*AGL42*●	*AGAMOUS-like 42*	-	-	2.69 ± 0.38

RNA-sequencing time course of Col-0 and *spl15-1* in short-day conditions

Flowering response of spl15-1 mutants and Col-0 diverge between four and six weeks after sowing under SD conditions.

SPL15 is required for timely flowering under SD conditions Chapter 2; Hyun *et al.*, 2016). To identify the gene expression differences between Col-0 and *spl15-1* during the floral transition under SD conditions, I harvested dissected meristems of Col-0 and *spl15-1* plants at 4, 5 and 6 weeks after sowing in SD conditions (4wSD, 5wSD and 6wSD respectively; 3 independent replicates each, Fig. 4.7A; see methods). I confirmed all genotypes used in this experiment by genotyping all plants after three weeks in SD conditions (Fig. 4.7A). As SPL15 is expressed in the SAM and is proposed to function there to induce flowering, I enriched the material for meristematic tissue by dissecting all SAMs under the stereo-microscope, leaving just two or three small leaf primordia (Fig. 4.7B). In addition, for each replicate, two or three dissected SAMs per harvesting time point were used for confocal microscopy analysis, to be able to correlate the transcriptional changes with morphological changes in the SAM.

These confocal images showed the same pattern for each independent biological replicate, and the SAMs of Col-0 plants were indistinguishable from those of *spl15-1* at 4wSD. The size of *spl15-1* SAMs only changed slightly over the rest of the time course. In contrast, Col-0 SAMs domed at 5wSD and produced axillary meristems and in some cases even floral primordia at 6wSD (Fig. 4.7D). Because *FUL* is a direct target of SPL15, it was used as a positive control for the transcriptome analysis. QRT-PCR on cDNA from RNA that was used for sequencing showed that there was no difference in *FUL* transcript levels between Col-0 and *spl15-1* plants at 4wSD (Fig. 4.7C). In contrast, *FUL* expression in Col-0 plants increased significantly from 5wSD onwards, whereas the expression of *FUL* in *spl15-1* mutant plants remained constant over time.

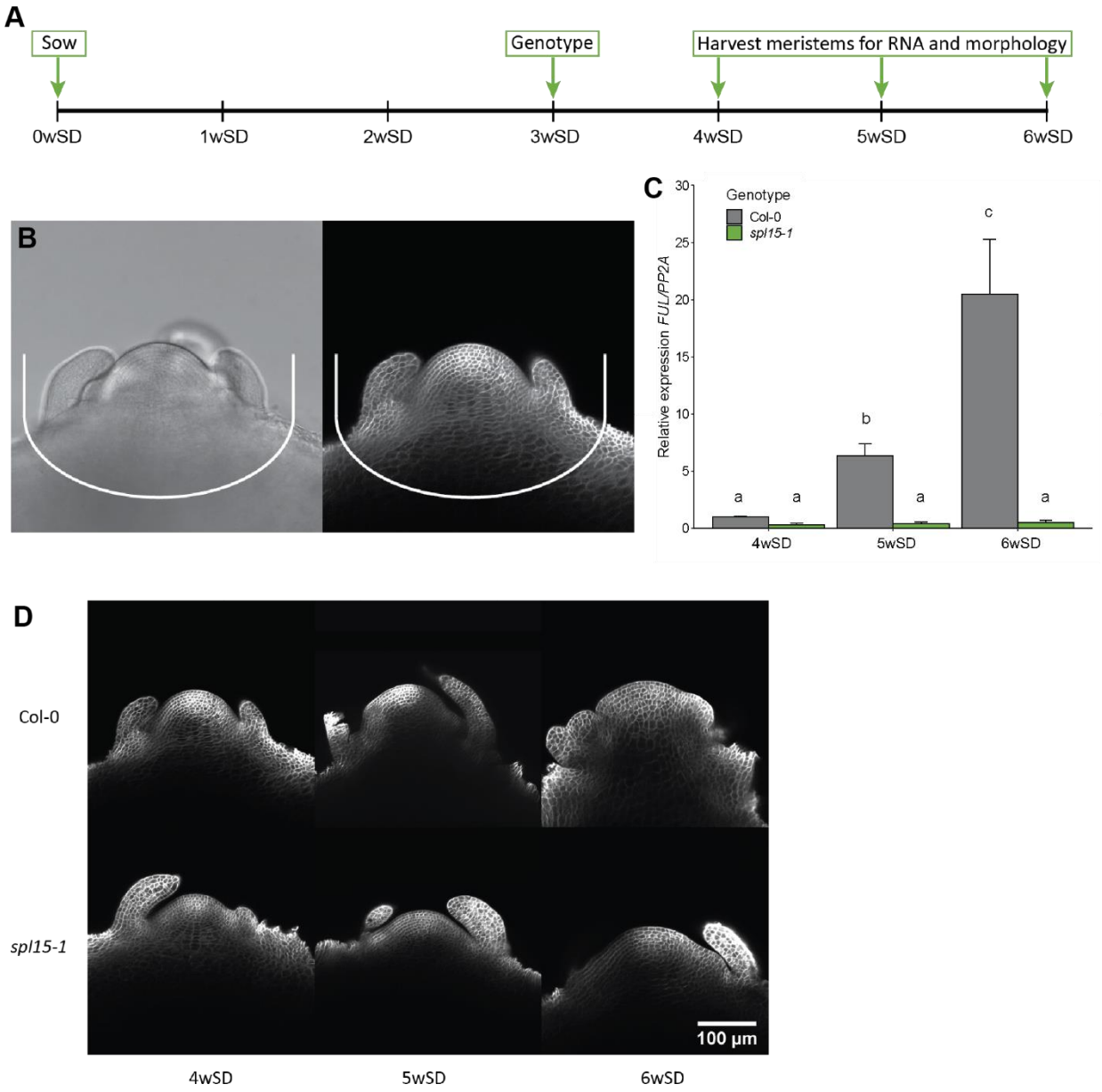

Figure 4.7. Experimental set-up and characterisation of the SD RNA-seq experiment with Col-0 and *spl15-1*. (**A**) Schematic representation of the RNA-seq experiment, indicating the time of sowing, the time of genotyping and each harvesting time point for RNA as well as the harvesting time points for confocal microscopy. (**B**) Confocal laser scanning micrograph of a shoot apex of Col-0 at 4wSD indicating the dissected tissue used for RNA isolation with a white line. On the left is the brightfield image and on the right is a confocal micrograph of the same apex, in which fluorescence from the Renaissance dye is artificially coloured in white. (**C**) The level of *FUL* expression in dissected shoot apices from Col-0 and *spl15-1* at the indicated time points; an aliquot of this material was used for RNA-seq. The variation shown was derived from three independent biological replicates; error bars indicate the standard deviation. Statistical differences were calculated with ANOVA followed by Tukey's HSD (honestly significant difference) test at $p < 0.01$. (**D**) Confocal laser scanning micrographs of shoot apices of Col-0 and *spl15-1* at the indicated time points in SD conditions. These time points are identical to those at which material was harvested for RNA isolation. Fluorescence from the Renaissance dye is artificially coloured in white. The white scale bar represents 100 µm. One representative image of six similar samples is shown for each genotype and time point.

The transcriptome of Col-0 plants starts to differ from that of *spl15-1* plants after four weeks in SD conditions.

The transcriptomes of Col-0 and *spl15-1* SAMs were analyzed by PCA, which separated the samples according to the age of the plants (Fig. 4.8A). Furthermore, the second component of the PCA separated the samples by genotype, with relatively small differences already visible at 4wSD, but clearer differences were observed at 5- and 6wSD. Although the Col-0 samples reflected large morphological changes that occurred in the meristem at 5- and 6wSDs, these samples were more similar to each other more than to any of the *spl15-1* samples. In this transcriptome analysis, 11, 402 and 481 genes were differentially expressed between Col-0 and *spl15-1* at 4-, 5-, and 6wSD, respectively (Fig. 4.8B; appendix 2 (upon request); *p*. adj.< 0.05). The largest overlap in DEGs was found between 5wSD and 6wSD, consistent with the large changes in the SAMs of Col-0 and the absence of these changes in *spl15-1* SAMs (Fig 2.7D).

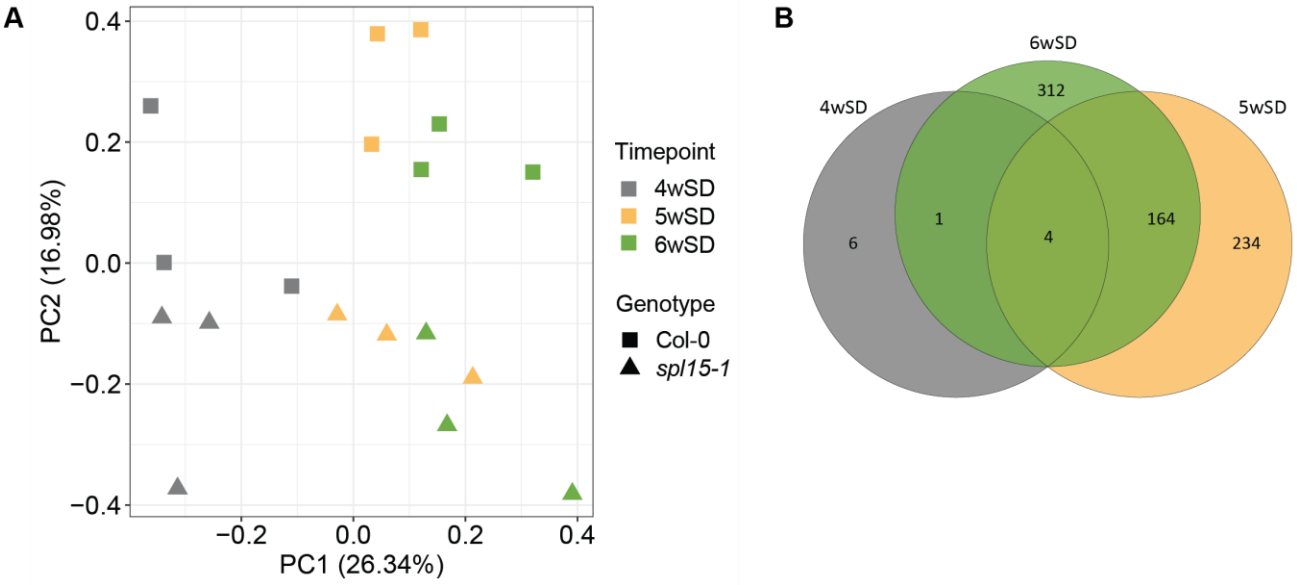

Figure 4.8. Representation of RNA-seq data for dissected apices of Col-0 and *spl15-1* in SD conditions. (**A**) Principal component analysis (PCA) of regularised log_2-transformed read counts per gene of both genotypes at all time points. (**B**) Venn diagram of all differentially expressed genes (DEGs) between Col-0 and *spl15-1* at the indicated time points and whether these DEGs occur in other time points. The DEGs were selected on the basis of an adjusted *p*-value < 0.05.

Both dissection methods of the SAM enrich for meristematic tissue

To discern whether SAM-dissection for RNA-seq (see Methods) indeed quantitatively enriched for meristematic tissue, the expression of SAM-specific genes in Col-0 at time point 9LD from the *rSPL15* transcriptome analysis was compared with their expression in Col-0 at time point 5wSD from the *spl15-1* SD transcriptome analysis. These two time points were chosen because the SAMs at these time points were at the doming stage, and therefore most comparable. The transcriptome data for these time two points were normalised and re-analysed, to be able to compare the samples from different RNA-seq experiments. Figure 4.13 shows that three SAM-specific genes: *WUSCHEL* (*WUS*), *KNOTTED-LIKE from ARABIDOPSIS THALIANA 1* (KNAT1) and *SHOOT MERISTEMLESS* (*STM*) were all expressed in both transcriptomes, although *WUS* was expressed weakly in Col-0 at 9LD (Fig. 4.9; Lincoln *et al.*, 1994; Long *et al.*, 1996; Ori *et al.*, 2000; Schoof *et al.*, 2000). Moreover, these meristem specific genes were more highly expressed in the dissected SAMs from the SD transcriptome analysis than in the meristem-enriched material from the LD transcriptome analysis, suggesting that the relative abundance of meristematic tissue in the SD material was higher. This can be explained by the difference in dissection method, but also by the the fact that the SD SAMs are larger than the LD SAMs.

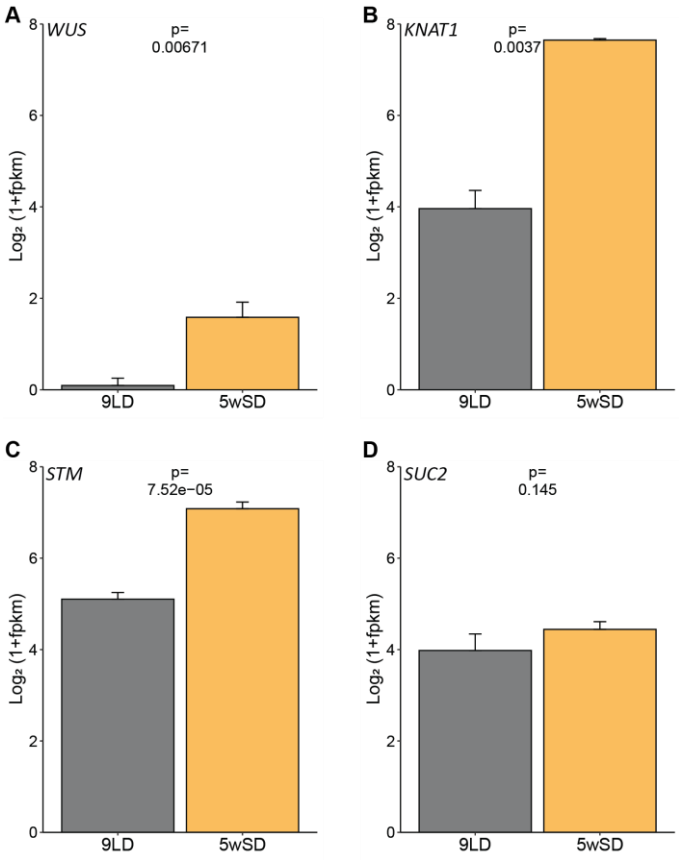

Figure 4.9. Expression of *WUS* (**A**), *KNAT1* (**B**), *STM* (**C**) and *SUC2* (**D**) over time in Col-0 from the LD (9LD) and SD (5wSD) transcriptome analyses. Plotted are globally normalised log_2-transformed FPKM values. The variation shown is the standard deviation for three independent biologial replicates.

The expression of *SUCROSE PROTON SYMPORTER 2* (*SUC2*), a vasculature-specific gene, was expressed at similar levels in Col-0 in LD and SD conditions, suggesting that microscopic dissection of SAMs in the SD transcriptome analysis enriched for more meristematic tissue (Fig. 4.9D; Truernit & Sauer, 1995). However, this cannot be definitively concluded, as neither dissection methods excluded vasculature tissue and the material was clearly different. Thus, both dissection methods enriched the RNA-seq material for meristematic tissue, although there are also clear differences between the methods.

Genes encoding transcription factors that regulate flowering time are misregulated in *spl15-1* compared to Col-0 in SD conditions

In SD-conditions, Col-0 plants do start to flower after five weeks, whereas *spl15-1*plants do not. To investigate whether this is due to misexpression of genes encoding transcription factors involved in floral induction, I compared the expression dynamics of these genes in Col-0 with their expression in *spl15-1* over time in SD conditions (Kinoshita & Richter, 2020). The expression dynamics showed that the expression well-established floral induction transcription factors such as *SOC1, FUL* and *FLOWERING LOCUS D* (*FD*) increased over time in Col-0, but hardly changed over time in *spl15-1* plants (Fig. 4.10). This indicates that floral induction occurs in Col-0 from 5wSD, but not in *spl15-1*. This is in line with the SAM morphology of these genotypes. By contrast, the mRNAs of well-described repressors of flowering, such as *AP2, SMZ, TOE2* and *AGAMOUS-LIKE 15* (*AGL15*), were transcriptionally downregulated mainly from 4- to 5wSD in Col-0, but notably, also in *spl15-1* (Fig. 4.10). The decrease in expression of these floral repressors in Col-0 and *spl15-1,* suggests that SPL15 is not required for the downregulation of these floral repressor genes in the SAM, but might influence the rate of downregulation. Taken together, the changes in expression of transcription factors involved in flowering time was more pronounced in Col-0 than in *spl15-1.*

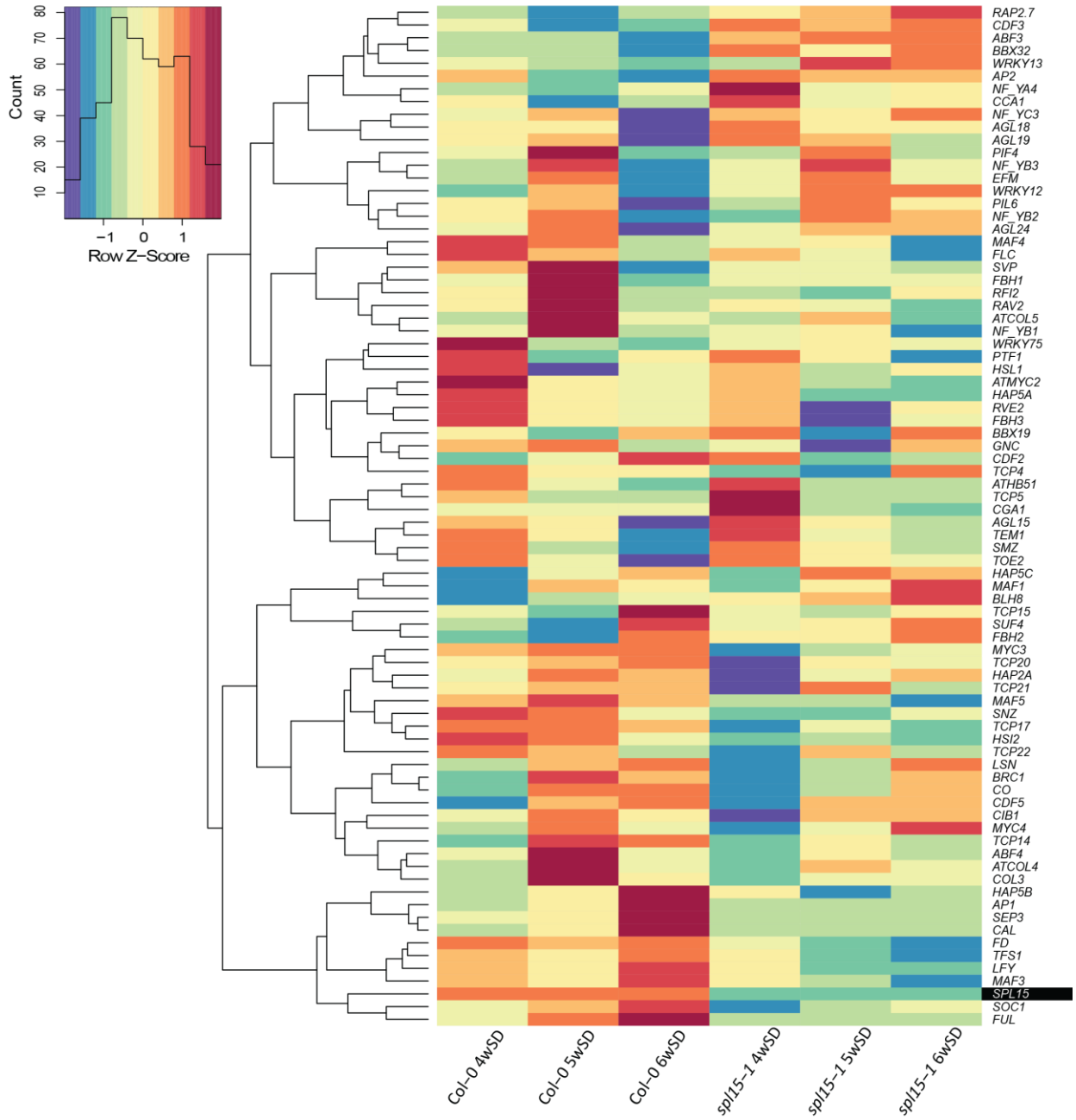

Figure 4.10. Heatmap for the expression of genes encoding transcription factors involved in the regulation of flowering time. Heatmap showing the expression of genes encoding transcription factors involved in flowering-time regulation over time in Col-0 and *spl15-1* in the RNA-seq experiment. Genes listed here have been taken from Kinoshita & Richter (2020) and exclude all *SPL*s except *SPL15* (the expression of all *SPL*s in this transcriptome time course are presented later in this section). Gene expression was taken from $\log_2$-transformed FPKM values normalised over the whole data set, which were scaled per gene into the Z-score.

31 genes out of the 721 differentially expressed genes between Col-0 and *spl15-1* at 4-, 5- and 6wSD function in flowering-time regulation.

A total of 721 genes were differentially expressed between Col-0 and *spl15-1* at 4-, 5- and 6wSD (*p*. adj.< 0.05). To analyse which proportion of these DEGs were involved in flowering-time regulation, I compared them to the published list of genes involved in flowering-time regulation (Kinoshita & Richter, 2020). This analysis showed that a function in flowering regulation has been described for 31 out of the 721 DEGs (4.3%; Fig. 4.11A). These 31 genes included four additional SPL transcription factors besides *SPL15*: *SPL3, SPL4, SPL5* and *SPL9* (Table 4.3). Figure 4.11B shows the expression dynamics of all *SPLs* over time in Col-0 and *spl15-1* in SD conditions. All SPLs showed differences in expression over time, although the differences between Col-0 and *spl15-1* were not always significant (Table 4.3). The expression of most of these *SPL* genes increased over time in Col-0, whereas others remained stable over time in both genotypes. In *spl15-1,* expression of most *SPLs* did not increase, or change much over time, although additional analysis between the time points in *spl15-1* would be necessary to conclude if these differences are significant or not (Fig. 4.11A, Table 4.3).

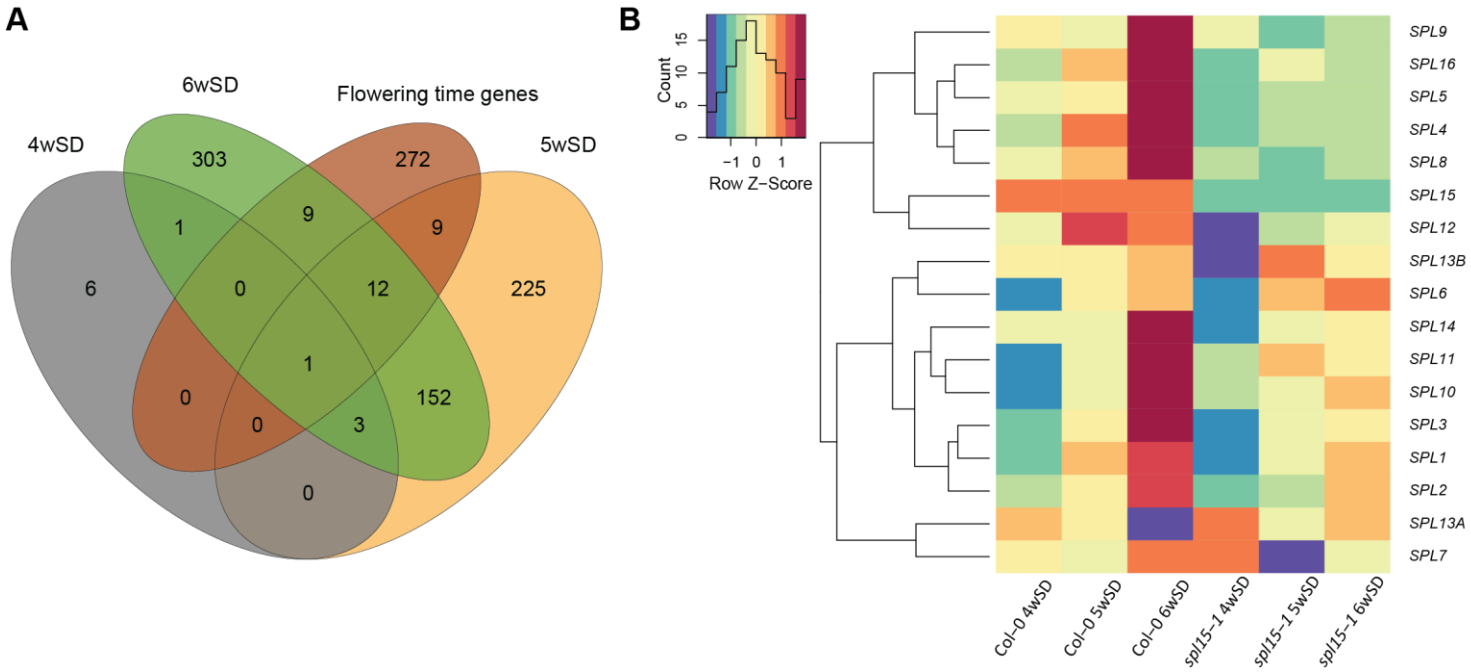

Figure 4.11. Differentially expressed genes between Col-0 and *spl15-1* and *SPL* gene expression over time in Col-0 and *spl15-1* in SD conditions. (**A**) Venn diagram showing the overlap between differentially expressed genes (DEGs) between Col-0 and *spl15-1* at 4-, 5- and 6wSD with genes involved in flowering-time regulation. (**B**) Heatmap showing the expression of genes encoding SPL transcription factors over time in Col-0 and *spl15-1* in the RNA-seq experiment. Gene expression was taken from log_2-transformed FPKM values normalised over the whole data set, which were transformed into the Z-score for each gene.

The expression of core transcription factors that integrate floral induction signals were significantly differently expressed between Col-0 and *spl15-1*, *e.g. SOC1, FUL, FD* and *LFY* (Table 4.3). Moreover, five genes involved in the regulation of plant circadian rhythm were also differentially expressed between Col-0 and *spl15-1*: *ELF4*, *LHY*, *PRR3*, *PRR5* and *TOC1* (Table 4.3; Table S4.3; Hayama *et al.*, 2017; Oakenfull & Davis, 2017; Para *et al.*, 2007). However, closer examination of their expression profiles over time showed that all these genes, except *CO*, were only expressed slightly higher in Col-0 than in *spl15-1*, and their expression did not change over time (Fig S4.5).

Table 4.3. Differentially expressed genes involved in flowering-time regulation. A list of all DEGs (*p*adj<0.05) between Col-0 and *spl15-1* at time points 4-, 5- and/or 6wSD, which were also related to flowering-time regulation. Stdev= standard deviation.

AGI-code	Gene symbol	Gene name / description	DE (Log_2 Fold Change ± stdev)		
			4wSD	5wSD	6wSD
AT1G01060	*LHY*	*LATE ELONGATED HYPOCOTYL*	-	0.97 ± 0.27	-
AT1G15550	*GA3OX1*	*GIBBERELLIN 3-OXIDASE 1*	-	0.69 ± 0.15	0.66 ± 0.13
AT1G26310	*CAL*	*CAULIFLOWER*	-	-	-5.70 ± 1.54
AT1G53160	*SPL4*	*SQUAMOSA PROMOTER BINDING PROTEIN-LIKE 4*	-	-5.36 ± 0.86	-6.18 ± 0.37
AT1G69120	*AP1*	*APETALA1*	-	-	-8.89 ± 1.24
AT1G78580	*TPS1*	*TREHALOSE-6-PHOSPHATE SYNTHASE*	-	-	0.45 ± 0.10
AT2G21660	*GRP7*	*GLYCINE-RICH RNA-BINDING PROTEIN 7*	-	-0.74 ± 0.11	-
AT2G33810	*SPL3*	*SQUAMOSA PROMOTER BINDING PROTEIN-LIKE 3*	-	-	-1.67 ± 0.23
AT2G40080	*ELF4*	*EARLY FLOWERING 4*	-	-	-1.11 ± 0.32
AT2G41370	*BOP2*	*BLADE ON PETIOLE2*	-	-0.58 ± 0.18	-
AT2G42200	*SPL9*	*SQUAMOSA PROMOTER BINDING PROTEIN-LIKE 9*	-	-	-0.61 ± 0.13
AT2G45660	*SOC1*	*AGAMOUS-LIKE 20, SUPPRESSOR OF OVEREXPRESSION OF*	-	-1.13 ± 0.30	-1.55 ± 0.25
AT2G46340	*SPA1*	*SUPPRESSOR OF PHYA-105 1*	-	0.44 ± 0.12	0.54 ± 0.14
AT3G03450	*RGL2*	*RGA-LIKE 2*	-	0.79 ± 0.23	-
AT3G15270	*SPL5*	*SQUAMOSA PROMOTER BINDING PROTEIN-LIKE 5*	-	-	-3.05 ± 0.52
AT3G15354	*SPA3*	*SPA1-RELATED 3*	-	0.97 ± 0.21	1.09 ± 0.22
AT3G18550	*BRC1*	*BRANCHED 1*	-	-2.15 ± 0.42	-
AT3G20810	*JMJD5*	*JUMONJI DOMAIN CONTAINING 5*	-	-1.77 ± 0.21	-1.41 ± 0.34
AT3G47500	*CDF3*	*CYCLING DOF FACTOR 3*	-	0.76 ± 0.16	0.72 ± 0.21
AT3G57920	*SPL15*	*SQUAMOSA PROMOTER BINDING PROTEIN-LIKE 15*	-5.05 ± 0.30	-4.53 ± 0.29	-5.12 ± 0.32
AT4G34400	*TFS1*	*TARGET OF FLC AND SVP 1*	-	-0.54 ± 0.11	-1.00 ± 0.14
AT4G35900	*FD*	*FLOWERING LOCUS D*	-	-0.56 ± 0.15	-0.77 ± 0.18
AT5G03840	*TFL1*	*TERMINAL FLOWER 1*	-	-1.39 ± 0.22	-
AT5G15840	*CO*	*CONSTANS*	-	-1.25 ± 0.27	-
AT5G24470	*PRR5*	*PSEUDO-RESPONSE REGULATOR 5*	-	-	-0.69 ± 0.16
AT5G60100	*PRR3*	*PSEUDO-RESPONSE REGULATOR 3*	-	-0.46 ± 0.14	-
AT5G60910	*FUL*	*AGAMOUS-LIKE 8, FRUITFULL*	-	-4.87 ± 0.75	-6.06 ± 0.55
AT5G61380	*TOC1*	*TIMING OF CAB EXPRESSION 1*	-	-0.41 ± 0.09	-
AT5G61850	*LFY*	*LEAFY*	-	-1.20 ± 0.26	-1.97 ± 0.23
AT5G62165	*AGL42*	*AGAMOUS-LIKE 42*	-	-1.32 ± 0.21	-1.13 ± 0.17
AT5G67180	*TOE3*	*TARGET OF EARLY ACTIVATION TAGGED (EAT) 3*	-	-	-1.53 ± 0.35

76 genes are co-expressed with *FUL* in Col-0 and *spl15-1* in SD conditions.

To obtain a better understanding of the genes that depend on SPL15 for their expression, I performed a co-expression analysis of genes that were expressed similarly to the direct-SPL15 target *FUL.* In this transcriptome analysis in SD conditions, *FUL* was expressed after 4wSD and its expression increased over time in Col-0 (Fig. 4.12A). *FUL* expression was similar at 4wSD between Col-0 and *spl15-1,* but at 5- and 6wSD, *FUL* was significantly higher expressed in Col-0 than in *spl15-1* (Table 4.3). Consistent with the qPCR results and the confocal microscopy images of FUL::VENUS, no expression of *FUL* was observed in *spl15-1* plants in this time course (Fig 4.7C; Fig. 2.8B). The co-expression was performed as described for the LD transcriptome analysis in the beginning of this chapter, and showed that 76 genes were positively or negatively co-expressed with *FUL* with a correlation of 0.85 or higher (Fig. 4.12B; Pearson Correlation). The majority of these genes were positively co-expressed with *FUL* and showed an increasing expression pattern over time in Col-0, but a stably low expression in *spl15-1*(Fig. 4.12B).

To analyse whether these co-expressed genes were also differentially expressed between Col-0 and *spl15-1*, I compared them with the DEGs at 4-, 5- and 6wSD. This showed that 60 of these co-expressed genes were also differentially expressed at one or more of the time points in the time course (Fig. S4.7; Table 4.4; Table S4.4). Eight out of these 60 DEGs that were co-expressed with *FUL*, have been described to regulate flowering time (Fig. S4.6). Closer examination of the positively co-expressed DEGs showed that *SPL4, SPL5* and *SPL8* were present in this list, as were the floral integrator *SOC1* and the *AP2-L* gene *TOE3*. In particular, *TOE3*, which belongs to a family of floral repressors, showed an increase in expression over time in SD conditions (Fig. 4.12B; Aukerman & Sakai, 2003; Zhang *et al.*, 2015). This expression pattern is in sharp contrast to that of most of the other *AP2-Ls* in this data set, since these *AP2-Ls* reduce in expression over time (Fig. 4.10). TOE3 appears to function later in floral development; similarly to *AP2,* TOE3 restricts *AGAMOUS* expression in the flower, which could explain its expression pattern (Huang *et al.*, 2017; Jung *et al.*, 2014). Taken together, many genes are co-expressed with *FUL* in an *SPL15*-dependent manner and are differentially expressed between Col-0 and *spl15-1,* suggesting that SPL15 indeed regulates many different genes at the SAM in SD conditions.

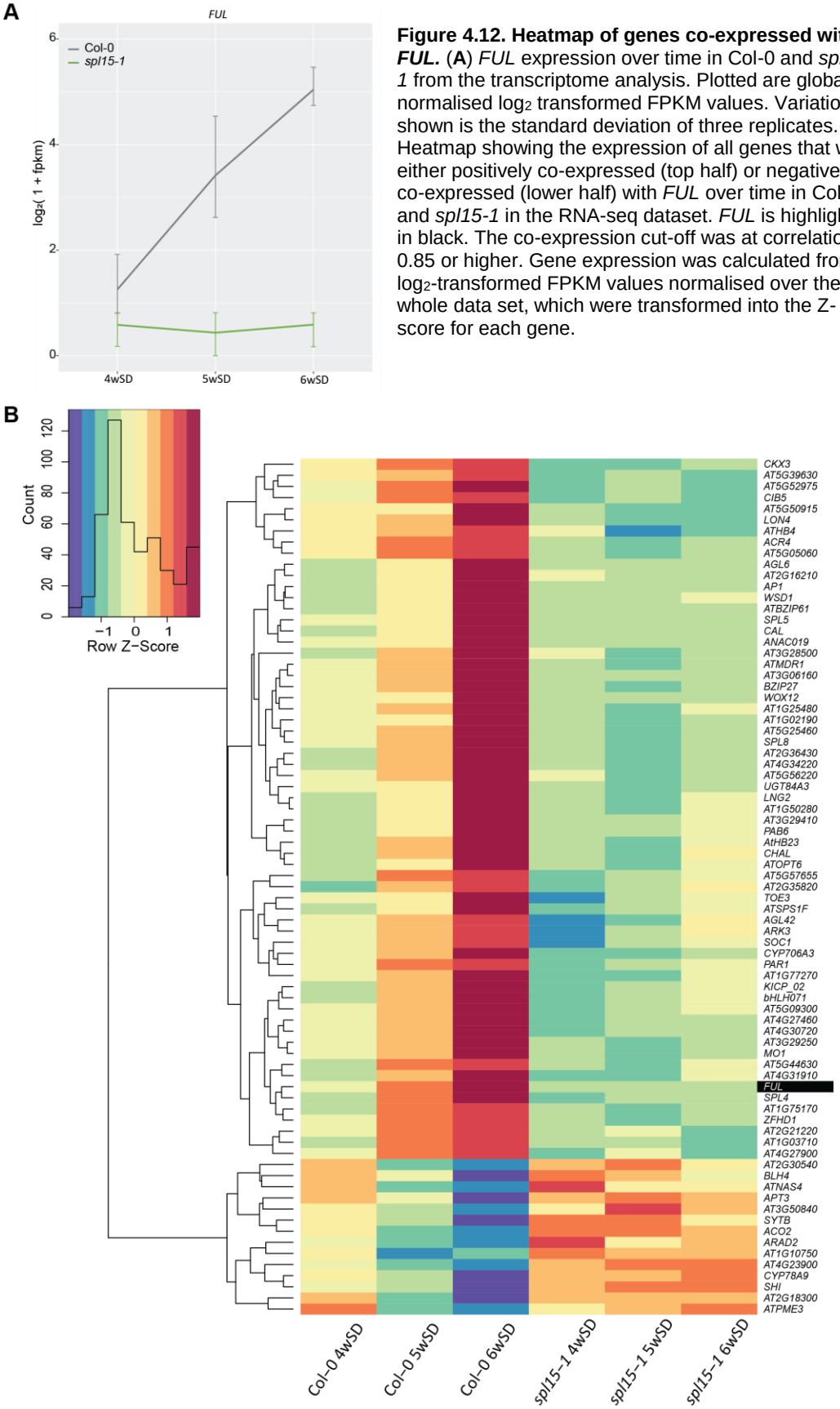

Figure 4.12. Heatmap of genes co-expressed with *FUL*. (**A**) *FUL* expression over time in Col-0 and *spl15-1* from the transcriptome analysis. Plotted are globally normalised log_2 transformed FPKM values. Variation shown is the standard deviation of three replicates. (**B**) Heatmap showing the expression of all genes that were either positively co-expressed (top half) or negatively co-expressed (lower half) with *FUL* over time in Col-0 and *spl15-1* in the RNA-seq dataset. *FUL* is highlighted in black. The co-expression cut-off was at correlation of 0.85 or higher. Gene expression was calculated from log_2-transformed FPKM values normalised over the whole data set, which were transformed into the Z-score for each gene.

Table 4.4 DEGs that are co-expressed with *FUL*. Table displaying all DEGs (*p*adj<0.05) that were differenftially expressed (DE) between Col-0 and *spl15-1* at time point 4-, 5- and/or 6wSD, and were positively or negatively co-expressed with *FUL*. Genes marked with (●) are also involved in flowering-time regulation. Stdev=standard deviation.

AGI-code	Gene symbol	Gene name / description	DE (Log_2 Fold Change ± stdev)		
			4wSD	5wSD	6wSD
AT1G02065	*SPL8*	*SQUAMOSA PROMOTER BINDING PROTEIN-LIKE 8*	-	-1.37 ± 0.28	-1.92 ± 0.22
AT1G02190	*AT1G02190*	*FATTY ACID HYDROXYLASE SUPERFAMILY*	-	-2.47 ± 0.63	-2.58 ± 0.45
AT1G03710	*AT1G03710*	*CYSTATIN/MONELLIN SUPERFAMILY PROTEIN*	-	-1.17 ± 0.35	-1.68 ± 0.38
AT1G12430	*ARK3*	*ARMADILLO REPEAT KINESIN 3*	-	-	-0.40 ± 0.11
AT1G25480	*AT1G25480*	*ALUMINIUM ACTIVATED MALATE TRANSPORTER FAMILY PROTEIN*	-	-	-0.97 ± 0.29
AT1G26260	*CIB5*	*CRYPTOCHROME-INTERACTING BASIC-HELIX-LOOP-HELIX 5*	-	-0.57 ± 0.16	-0.66 ± 0.18
AT1G26310	*CAL*●	*CAULIFLOWER*	-	-	-5.70 ± 1.54
AT1G26960	*AtHB23*	*HOMEOBOX PROTEIN 23*	-	-1.52 ± 0.34	-1.76 ± 0.30
AT1G50280	*AT1G50280*	*PHOTOTROPIC-RESPONSIVE NPH3 FAMILY PROTEIN*	-	-	-1.76 ± 0.44
AT1G53160	*SPL4*●	*SQUAMOSA PROMOTER BINDING PROTEIN-LIKE 4*	-	-5.36 ± 0.86	-6.18 ± 0.37
AT1G56430	*NAS4*	*NICOTIANAMINE SYNTHASE 4*	-	0.94 ± 0.22	1.40 ± 0.18
AT1G69040	*ACR4*	*ACT DOMAIN REPEAT 4*	-	-0.71 ± 0.16	-0.75 ± 0.17
AT1G69120	*AP1*●	*APETALA1*	-	-	-8.89 ± 1.24
AT1G69600	*ZFHD1*	*ZINC FINGER HOMEODOMAIN 1*	-	-0.80 ± 0.19	-0.91 ± 0.21
AT1G75170	*AT1G75170*	*SEC14P-LIKE PHOSPHATIDYLINOSITOL TRANSFER FAMILY PROTEIN*	-	-0.97 ± 0.20	-1.03 ± 0.18
AT2G16210	*AT2G16210*	*TRANSCRIPTIONAL FACTOR B3 FAMILY PROTEIN*	-	-	-4.65 ± 1.01
AT2G17770	*BZIP27*	*BASIC REGION/LEUCINE ZIPPER MOTIF 27*	-	-	-1.37 ± 0.28
AT2G21220	*AT2G21220*	*SAUR-LIKE AUXIN-RESPONSIVE PROTEIN FAMILY*	-	-	-2.68 ± 0.72
AT2G23760	*BLH4*	*BEL1-LIKE HOMEODOMAIN 4*	-	-	1.01 ± 0.22
AT2G30370	*CHAL*	*CHALLAH*	-	-	-1.04 ± 0.30
AT2G30540	*AT2G30540*	*THIOREDOXIN SUPERFAMILY PROTEIN*	-	1.01 ± 0.29	-
AT2G35820	*AT2G35820*	*UREIDOGLYCOLATE HYDROLASES*	-	-1.27 ± 0.36	-1.40 ± 0.39
AT2G44910	*HB4*	*HOMEOBOX-LEUCINE ZIPPER PROTEIN 4*	-	-0.78 ± 0.18	-0.84 ± 0.19
AT2G45650	*AGL6*	*AGAMOUS-LIKE 6*	-	-	-6.24 ± 1.46
AT2G45660	*SOC1*●	*SUPPRESSOR OF OVEREXPRESSION OF CONSTANS 1*	-	-1.13 ± 0.30	-1.55 ± 0.25
AT3G02170	*LNG2*	*LONGIFOLIA2*	-	-1.08 ± 0.25	-1.84 ± 0.42
AT3G05790	*LON4*	*LON PROTEASE 4*	-	-	-1.97 ± 0.49
AT3G06160	*AT3G06160*	*AP2/B3-LIKE TRANSCRIPTIONAL FACTOR FAMILY PROTEIN*	-	-	-1.09 ± 0.25
AT3G14310	*PME3*	*PECTIN METHYLESTERASE 3*	-	-	0.31 ± 0.10
AT3G15270	*SPL5*●	*SQUAMOSA PROMOTER BINDING PROTEIN-LIKE 5*	-	-	-3.05 ± 0.52
AT3G28500	*AT3G28500*	*60S ACIDIC RIBOSOMAL PROTEIN FAMILY*	-	-1.43 ± 0.34	-2.64 ± 0.27
AT3G28860	*ABCB19*	*ATP-BINDING CASSETTE B19*	-	-0.61 ± 0.13	-1.02 ± 0.12
AT3G29250	*SDR4*	*SHORT-CHAIN DEHYDROGENASE REDUCTASE 4*	-	-	-2.05 ± 0.59
AT3G50840	*AT3G50840*	*PHOTOTROPIC-RESPONSIVE NPH3 FAMILY PROTEIN*	-	0.87 ± 0.25	-
AT3G58120	*BZIP61*	*BASIC-LEUCINE ZIPPER (BZIP) TRANSCRIPTION FACTOR FAMILY PROTEIN*	-	-	-2.71 ± 0.44
AT3G61880	*CYP78A9*	*CYTOCHROME P450 78A9*	-	0.80 ± 0.23	1.87 ± 0.33
AT4G15490	*UGT84A3*	*UDP-GLYCOSYLTRANSFERASE SUPERFAMILY PROTEIN*	-	-	-2.47 ± 0.54
AT4G22570	*APT3*	*ADENINE PHOSPHORIBOSYL TRANSFERASE 3*	-	-	0.91 ± 0.18
AT4G23900	*AT4G23900*	*NUCLEOSIDE DIPHOSPHATE KINASE FAMILY PROTEIN*	-	0.90 ± 0.27	1.12 ± 0.28
AT4G26970	*ACO2*	*ACONITASE 2*	-	0.31 ± 0.09	0.36 ± 0.10
AT4G27460	*CBSX5*	*CBS DOMAIN CONTAINING PROTEIN 5*	-	-	-2.96 ± 0.90
AT4G27730	*OPT6*	*OLIGOPEPTIDE TRANSPORTER 1*	-	-0.92 ± 0.27	-1.15 ± 0.25
AT4G27900	*AT4G27900*	*CCT MOTIF FAMILY PROTEIN*	-	-	-0.76 ± 0.18
AT4G31910	*BAT1*	*BR-RELATED ACYLTRANSFERASE1*	-	-2.66 ± 0.44	-2.38 ± 0.33
AT4G34220	*AT4G34220*	*LEUCINE-RICH REPEAT PROTEIN KINASE FAMILY PROTEIN*	-	-	-0.78 ± 0.16
AT5G09300	*AT5G09300*	*THIAMIN DIPHOSPHATE-BINDING FOLD (THDP-BINDING) SUPERFAMILY*	-	-	-1.72 ± 0.32
AT5G20280	*SPS1F*	*SUCROSE PHOSPHATE SYNTHASE 1F*	-	-	-0.81 ± 0.17
AT5G25460	*DGR2*	*DUF642 L-GALL RESPONSIVE GENE 2*	-	-	-1.33 ± 0.24
AT5G37300	*WSD1*	*O-ACYLTRANSFERASE (WSD1-LIKE) FAMILY PROTEIN*	-	-	-4.07 ± 0.97
AT5G44620	*CYP706A3*	*CYTOCHROME P450, FAMILY 706, SUBFAMILY A, POLYPEPTIDE 3*	-0.69 ± 0.15	-1.29 ± 0.33	-1.59 ± 0.14
AT5G44630	*AT5G44630*	*TERPENOID CYCLASES/PROTEIN PRENYLTRANSFERASES SUPERFAMILY PROTEIN*	-	-2.96 ± 0.48	-2.46 ± 0.32
AT5G46690	*bHLH071*	*BETA HLH PROTEIN 71*	-	-	-2.06 ± 0.58
AT5G50915	*AT5G50915*	*BASIC HELIX-LOOP-HELIX (BHLH) DNA-BINDING SUPERFAMILY PROTEIN*	-	-	-2.45 ± 0.43
AT5G56220	*AT5G56220*	*P-LOOP CONTAINING NUCLEOSIDE TRIPHOSPHATE HYDROLASES SUPERFAMILY*	-	-0.65 ± 0.15	-0.81 ± 0.15
AT5G56970	*CKX3*	*CYTOKININ OXIDASE 3*	-	-1.45 ± 0.40	-1.59 ± 0.37
AT5G57655	*AT5G57655*	*XYLOSE ISOMERASE FAMILY PROTEIN*	-	-0.64 ± 0.12	-0.69 ± 0.14
AT5G60910	*FUL*●	*AGAMOUS-LIKE 8, FRUITFULL*	-	-4.87 ± 0.75	-6.06 ± 0.55
AT5G62165	*AGL42*●	*AGAMOUS-LIKE 42*	-	-1.32 ± 0.21	-1.13 ± 0.17
AT5G66350	*SHI*	*SHORT INTERNODES*	-	0.41 ± 0.11	0.77 ± 0.14
AT5G67180	*TOE3*●	*TARGET OF EARLY ACTIVATION TAGGED (EAT) 3*	-	-	-1.53 ± 0.35

Expression of *SPL4*, *AGL42* and *FUL* increases over time in Col-0, but not in *spl15-1* in SD conditions.

To confirm the differences in expression for some of the DEGs with a role in the floral transition, MSc student Tim Neefjes performed an qRT-PCR time course in SD conditions to analyse the expression of *SPL15*, *SPL4, AGL42, SOC1* and *FUL.* In this experiment, apices from Col-0 and *spl15-1* at 4-, 5-, 6- and 7wSD were used for qRT-PCR analysis (See methods). The relative expression of *SPL15* in Col-0 did not clearly change over time, and no expression was found in *spl15-1,* which was similar to the expression pattern of *SPL15* in the transcriptome experiment (Fig. S4.8). *SPL4, AGL42* and *FUL* showed an expression pattern that was highly similar to that observed in the RNA-seq analysis (Fig. 4.13). The expression of *SPL4* and *FUL* increased over time in Col-0, and this did not occur in *spl15-1* (Figs. 4.13A, B, G and 4.12A). *AGL42* expression increased over time in both Col-0 and *spl15-1,* but in *spl15-1* this increase was less steep than in Col-0 (Fig. 4.13C, D). The latter also suggests that *AGL42* expression is only partly dependent on SPL15. In the qRT-PCR analysis the differences between the genotypes occurred later in time, which might be due to differences in tissue sampling or to the greater accuracy of the quantification of RNA-seq data. This might also be the reason that the expression of *SOC1* increased over time in both genotypes and both analyses, but significant differences between Col-0 and *spl15-1* were only observed in the transcriptome analysis (Fig. 4.13.E, F).

These results indicate that the changes observed in the RNA-seq are reproducible, and moreover, that *SPL4, FUL* and *AGL42* expression patterns in Col-0 in SD conditions indeed depends on SPL15.

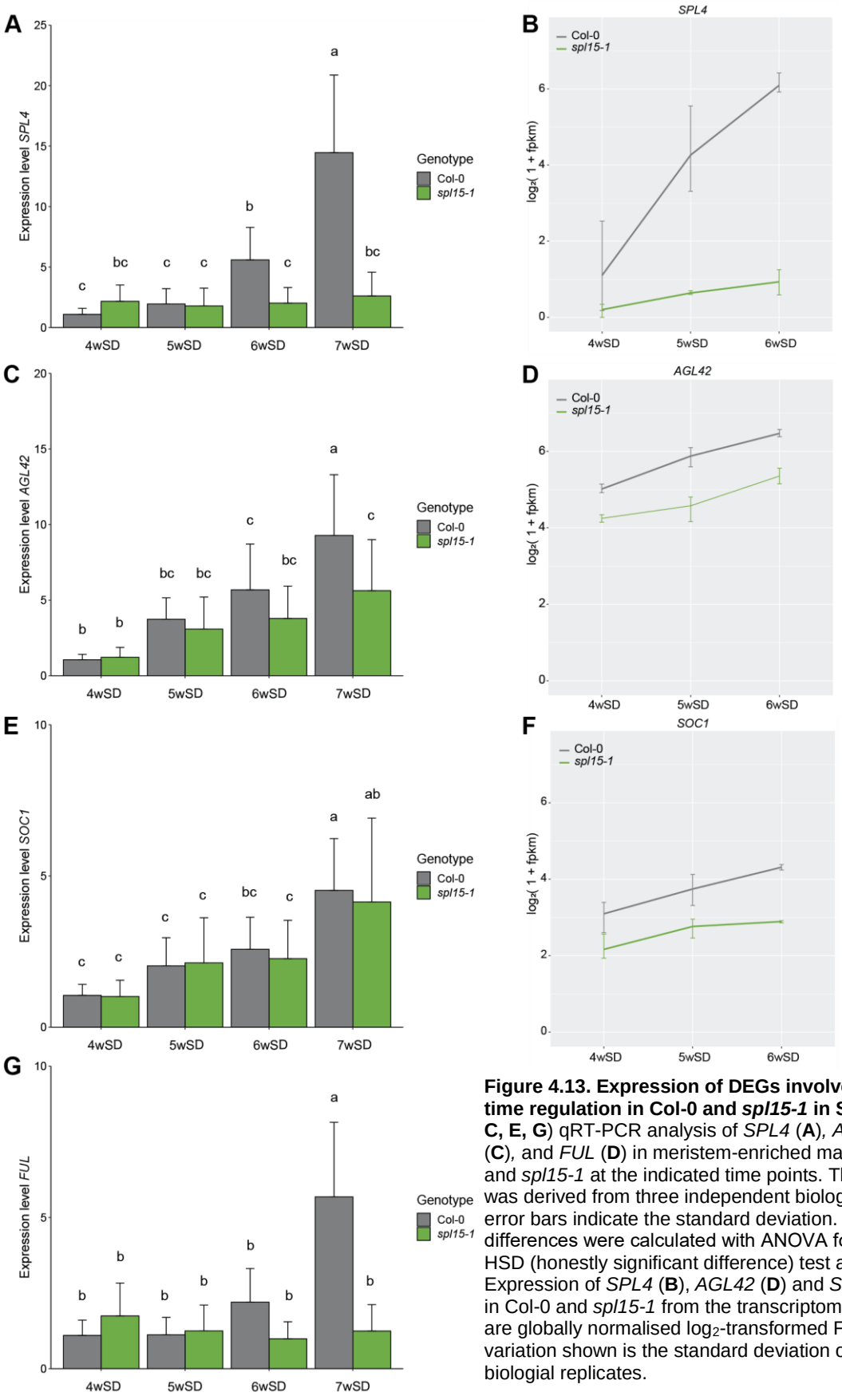

Figure 4.13. Expression of DEGs involved in flowering-time regulation in Col-0 and *spl15-1* in SD conditions. (**A, C, E, G**) qRT-PCR analysis of *SPL4* (**A**), *AGL42* (**B**), *SOC1* (**C**), and *FUL* (**D**) in meristem-enriched material from Col-0 and *spl15-1* at the indicated time points. The variation shown was derived from three independent biological replicates; error bars indicate the standard deviation. Statistical differences were calculated with ANOVA followed by Tukey's HSD (honestly significant difference) test at $p < 0.01$. (**B, D, F**) Expression of *SPL4* (**B**), *AGL42* (**D**) and *SOC1* (**F**) over time in Col-0 and *spl15-1* from the transcriptome analysis. Plotted are globally normalised log_2-transformed FPKM values. The variation shown is the standard deviation of three independent biologial replicates.

The spl8-1 mutation does not affect flowering-time in SD conditions.

The DEGs between Col-0 and *spl15-1* that were positively co-expressed with *FUL* in SD conditions included *SPL8*. *SPL8* has been characterised for its role in *Arabidopsis* fertility because it is involved in gynoecium patterning and pollen-sac development in the flower (Unte *et al.*, 2003; Xing *et al.*, 2010, 2013). It is expressed in the inflorescence, but its expression has not previously been shown in the *SAM.* The SD transcriptome analysis showed that *SPL8* was not only expressed at 4wSD, when no flowers are present, but its expression also increased over time in Col-0 (Fig. 4.14A). To test whether *spl8-1* mutant plants have an altered flowering-time phenotype, they were grown in SD conditions along with Col-0 as control. However, no differences were observed between Col-0 and *spl8-1* in terms of time to bolting, flowering time or TLN in this experiment (Fig. 4.14B–D). This suggests that *SPL8* expression in the SAM prior to flowering does not contribute to flowering time, or its function may be highly redundant with other SPLs and therefore is not visible in *spl8-1* single mutants.

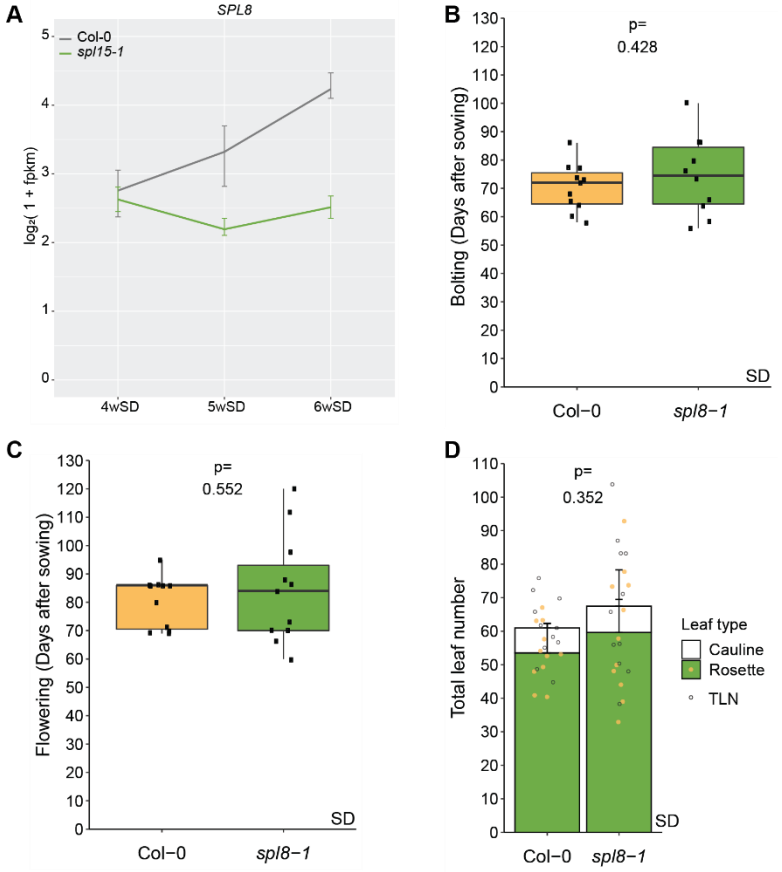

Figure 4.14. Expression *SPL8* and Flowering time phenotype of Col-0 and *spl8-1* in SD conditions. Time to bolting (**B**), flowering time (**C**) and total leaf number (**D;** TLN) of Col-0 and *spl8-1* in SD conditions (n = 11; *p* was calculated using the student's *t*-test). Time to bolting was scored as the day on which the inflorescence extended 0.5 cm from the rosette and flowering time was scored as the day on which the first flower opened, anywhere on the plant. This experiment was performed by MSc student Tim Neefjes, during his thesis internship.

Candidate target genes of SPL15

14 differentially expressed genes and four genes that are positively co-expressed with *FUL* overlap between the LD- and SD transcriptome analyses

To identify putative target genes of SPL15 with higher confidence, I chose very stringent selection criteria. I compared all DEGs at 6-, 9- and 12LD with those at 5- and 6wSD and analysed which DEGs overlap between the two datasets. The results show that only nine genes were differentially expressed at all timepoints in both LD and SD datasets (Fig. 4.15A; including *SPL15*). Five additional genes were differentially expressed at 9- and 12LD as well as at 5- and 6wSD. These 14 overlapping DEGs are listed in Table 4.5 and include multiple genes with a role in flowering-time regulation (Table S4.5 for details). In addition, I compared all genes that were co-expressed with *FUL* between the two datasets and found an overlap of just four genes (Fig. 4.15B; Table 4.6; S4.5). Below, I described the function of these candidate genes in more detail and discussed whether they could play a role in SPL15-mediated floral induction.

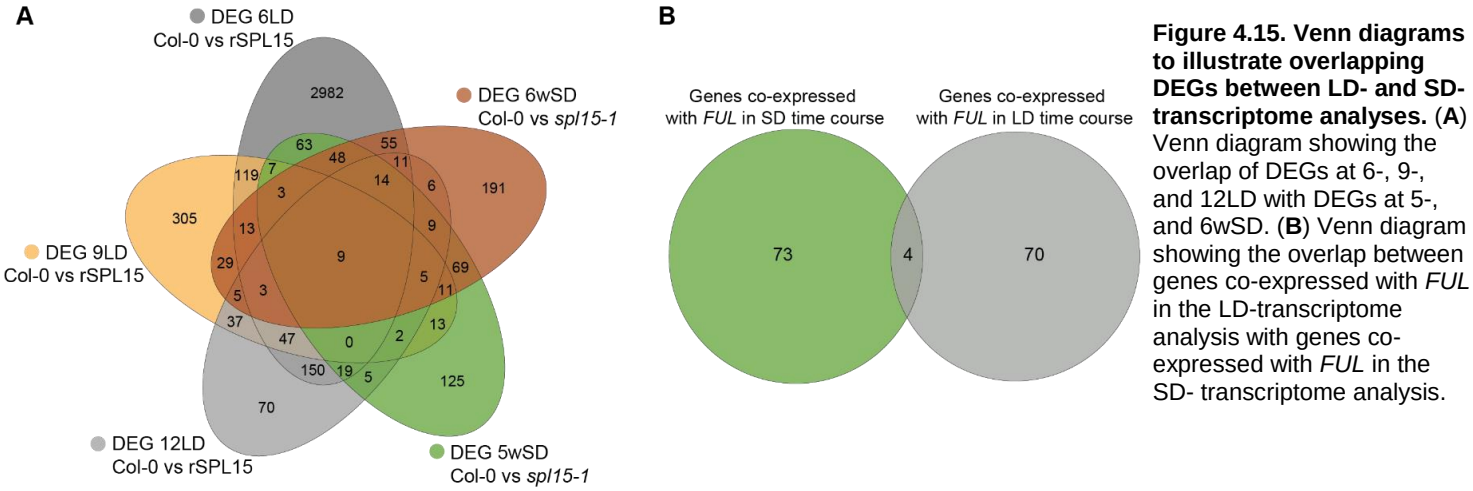

Figure 4.15. Venn diagrams to illustrate overlapping DEGs between LD- and SD-transcriptome analyses. (**A**) Venn diagram showing the overlap of DEGs at 6-, 9-, and 12LD with DEGs at 5-, and 6wSD. (**B**) Venn diagram showing the overlap between genes co-expressed with *FUL* in the LD-transcriptome analysis with genes co-expressed with *FUL* in the SD- transcriptome analysis.

Table 4.5. A list of the overlapping DEGs in the LD and SD transcriptome analyses. Indicated are time points at which these genes were differentially expressed in both transcriptomes. Details on expression can be found in Table S4.5.

AGI-code	Gene symbol	Gene name / description	DEG at time points	
			LD transcriptome	SD transcriptome
AT1G53160	*SPL4*	*SQUAMOSA PROMOTER BINDING PROTEIN-LIKE 4*	9LD and 12LD	5wSD and 6wSD
AT1G69040	*ACR4*	*ACT DOMAIN REPEAT 4*	9LD and 12LD	5wSD and 6wSD
AT2G25900	*ATTZF1*	*Zinc finger C-x8-C-x5-C-x3-H type family protein*	6LD, 9LD and 12LD	5wSD and 6wSD
AT2G45660	*SOC1*	*AGAMOUS-LIKE 20, SUPPRESSOR OF OVEREXPRESSION OF CONSTANS 1*	6LD, 9LD and 12LD	5wSD and 6wSD
AT3G57920	*SPL15*	*SQUAMOSA PROMOTER BINDING PROTEIN-LIKE 15*	6LD, 9LD and 12LD	5wSD and 6wSD
AT4G13495	*AT4G13495*	*Other RNA*	6LD, 9LD and 12LD	5wSD and 6wSD
AT4G30250	*AT4G30250*	*P-loop containing nucleoside triphosphate hydrolases superfamily protein*	9LD and 12LD	5wSD and 6wSD
AT4G34400	*TFS1*	*TARGET OF FLC AND SVP 1*	6LD, 9LD and 12LD	5wSD and 6wSD
AT4G37800	*XTH7*	*XYLOGLUCAN ENDOTRANSGLUCOSYLASE/HYDROLASE 7*	9LD and 12LD	5wSD and 6wSD
AT5G20700	*AT5G20700*	*Protein of unknown function (DUF581)*	9LD and 12LD	5wSD and 6wSD
AT5G28640	*AN3*	*ANGUSTIFOLIA 3*	6LD, 9LD and 12LD	5wSD and 6wSD
AT5G44620	*CYP706A3*	*Cytochrome P450, family 706, subfamily A, polypeptide 3*	6LD, 9LD and 12LD	5wSD and 6wSD
AT5G54160	*OMT1*	*O-METHYLTRANSFERASE 1*	6LD, 9LD and 12LD	5wSD and 6wSD
AT5G57655	*AT5G57655*	*Xylose isomerase family protein*	6LD, 9LD and 12LD	5wSD and 6wSD

Table 4.6. A list of the genes overlapping between *FUL* co-expressed genes in LD and SD transcriptome analyses. Details on expression can be found in Table S4.5.

AGI-code	Gene symbol	Gene name / description	DEG at time points	
			LD transcriptome	SD transcriptome
AT1G02190	*AT1G02190*	*Fatty acid hydroxylase superfamily*	12LD	5wSD and 6wSD
AT5G56970	*CKX3*	*CYTOKININ OXIDASE 3*	6LD	5wSD and 6wSD
AT5G60910	*FUL*	*AGAMOUS-like 8, FRUITFULL*	12LD	5wSD and 6wSD
AT5G62165	*AGL42*	*AGAMOUS-like 42*	6LD and 12LD	5wSD and 6wSD

SQUAMOSA PROMOTER BINDING PROTEIN-LIKE 4

The SPL4 transcription factor belongs to the SPL family, the same family to which SPL15 belongs. Within the phylogeny of this family, SPL4 clusters together with SPL3 and SPL5 and these are the three smallest SPL transcription factors in *Arabidopsis* (G. Cardon *et al.*, 1999; A. Y. Guo *et al.*, 2008; Preston & Hileman, 2013). SPL4 is involved in diverse developmental functions, among which flowering time regulation is one of the most prominent. *SPL4* is expressed in the shoot apex during floral transition (Fig. 4.12A-B; Fig. 4.16A ; Cardon *et al.*, 1999; Schmid *et al.*, 2003; Xu *et al.*, 2016). *SPL4* and *SPL5* share high sequence similarity, however, *SPL5* is expressed in a slightly different domain in the SAM, suggesting a non-redundant function of *SPL5* in the SAM (G. Cardon *et al.*, 1999).

In the LD-transcriptome dataset, *SPL5* expression did not differ between Col-0 and *rSPL15,* and in the SD-transcriptome dataset, *SPL5* was differentially expressed between Col-0 and *spl15-1*, but these differences only occurred at 6wSD, whereas *SPL4* was differentially expressed at 5- and 6wSD (Fig. 4.16B-C). *SPL4* expression is increased in plants where AP2-Ls *TOE1, TOE2* and *SMZ* have been mutated or in plants that overexpress *MIR172*, suggesting these *AP2-Ls* repress *SPL4* expression before the floral transition (Jung *et al.*, 2011). I therefore examined an AP2 chromatin immunoprecipitation-sequencing (ChIP-seq) experiment, and identified *SPL4* among the genes that were bound and transcriptionally regulated by AP2 (Yant *et al.*, 2010). Besides AP2, SOC1 also directly binds to the *SPL4* promoter and activates *SPL4* expression in LD conditions (Jung *et al.*, 2012). Furthermore, *SPL4* expression is lower in *ft-10* mutants and even lower in *soc1-2/ft-10* mutants, indicating that *SPL4* expression is also stimulated by the FT-pathway independently of SOC1. This FT-dependent *SPL4* upregulation might be mediated via FD, a transcription factor and interaction partner of FT, which was shown to bind the *SPL4* promoter in electrophoretic mobility shift assays (EMSAs (Jung *et al.*, 2016). However, *SPL4* was not differentially expressed in Col-0 compared to *fd-3*, nor was it directly bound by FD in ChIP-seq (Jung *et al.*, 2012; Romera-Branchat *et al.*, 2020). SPL4 has been suggested to function as a co-factor, because it directly binds to FD and enhances the activity of FD as a transcription factor (Jung *et al.*, 2016). When overexpressed, *SPL4* causes earlier

flowering, and this can be partially suppressed by introgression of the *ft-10* mutation, indicating that *SPL4* affects floral induction through and FT-dependent and an FT-independent pathway (Jung *et al.*, 2016). Moreover, overexpression of *SPL4* induces premature expression of *LFY* and *FUL* in LD and SD conditions, suggesting that SPL4 regulates the expression of these two genes (Yamaguchi *et al.*, 2009). Consistent with this, SPL4 directly binds to the *FUL* promoter at the same conserved region where SPL15 and SPL9 can bind (Fig. 3.7; Hyun *et al.*, 2016; Xie *et al.*, 2020). Moreover, transient assays also demonstrated binding of SPL4 to the *LFY* and *AP1* promoters (Xie *et al.*, 2020). Lastly, *SPL4* expression was lower in higher-order *spl* mutants that included *spl15-1,* suggesting that *SPL4* expression is partially dependent on other SPLs (M. Xu, Hu, Zhao, *et al.*, 2016). Therefore, *SPL4* is a likely candidate to be directly regulated by SPL15, because it is involved in floral induction, but also binds to the *FUL* promoter.

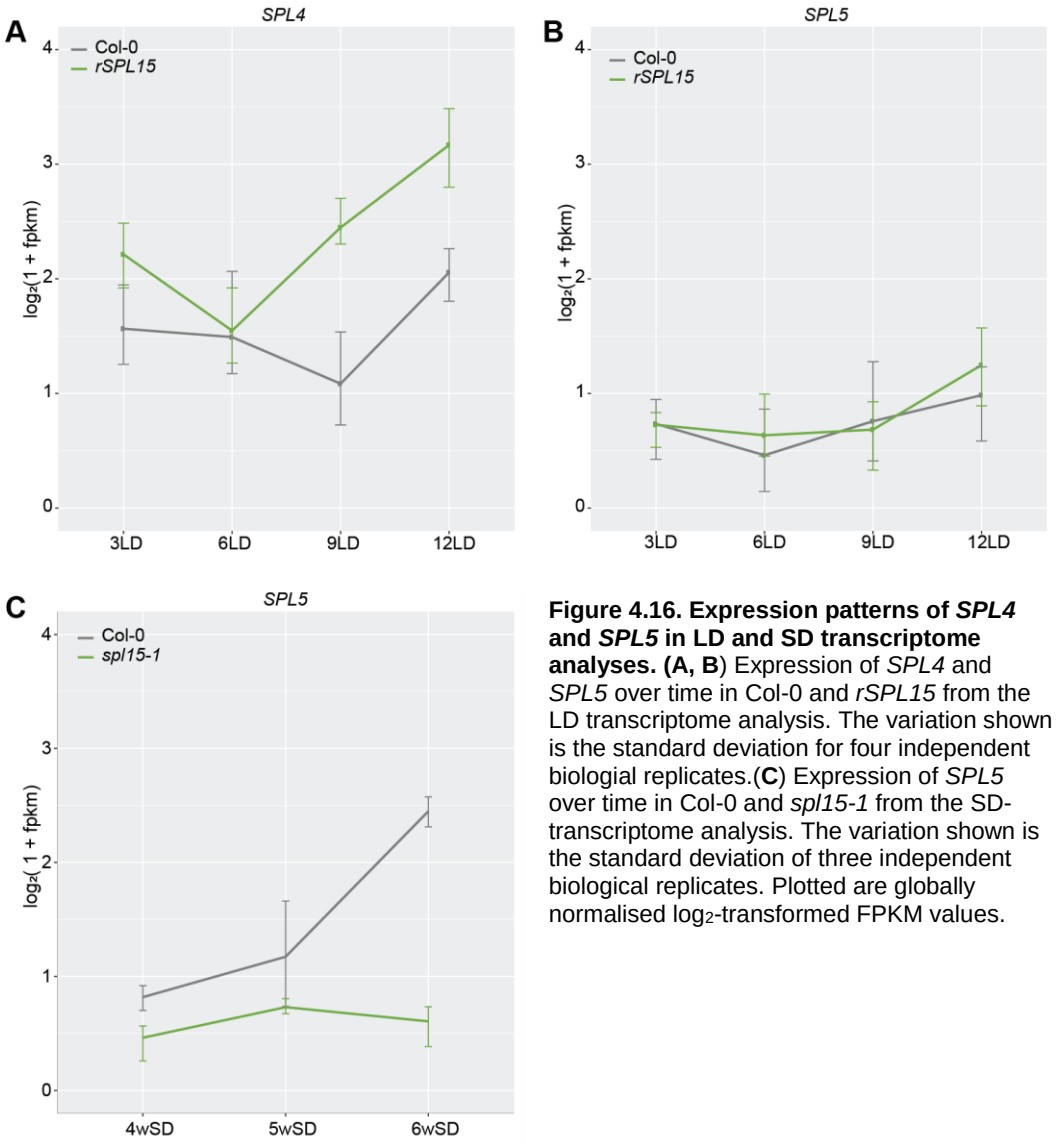

Figure 4.16. Expression patterns of *SPL4* and *SPL5* in LD and SD transcriptome analyses. (A, B) Expression of *SPL4* and *SPL5* over time in Col-0 and *rSPL15* from the LD transcriptome analysis. The variation shown is the standard deviation for four independent biologial replicates.(**C**) Expression of *SPL5* over time in Col-0 and *spl15-1* from the SD-transcriptome analysis. The variation shown is the standard deviation of three independent biological replicates. Plotted are globally normalised log_2-transformed FPKM values.

In SD conditions, SPL15 might regulate *SPL4* during the floral transition and SPL4 might fulfil some of the same functions as SPL15 in these conditions. However, *spl4* single mutants have not been characterised for their role in floral induction in SD conditions, and therefore it remains unclear whether *SPL4* contributes non-redundantly to flowering in these conditions.

ACT DOMAIN REPEAT 4 (ACR4)

The ACR4 protein contains several ACT domain repeats. These domains were originally identified in bacteria to bind amino acids and to harbour enzymatic function related to amino-acid metabolism. In plants, however, proteins containing these domains do not contain an enzymatic domain, and their precise function remains unknown (Hsieh & Goodman, 2002). *ACR4* is specifically expressed in reproductive tissues and is upregulated in response to cytokinins (CK), suggesting that this protein has a function in CK-dependent processes (Brenner & Schmülling, 2015; Hsieh & Goodman, 2002). Because CK is involved in regualting meristem size, it is conceivable that ACR4 is involved in the developmental changes that occur in the SAM during floral transition (Skylar & Wu, 2011). In the two transcriptome analyses conducted here, *ACR4* expression remained stable over time in LD and SD conditions, was more highly expressed in *rSPL15* than in Col-0 (LD) and more lowly expressed in *spl15-1* than in Col-0, suggesting an SPL15-dependent role in development (SD; Fig. S4.9). However, a specific function for *ACR4* has not yet been described, nor is it known whether *ACR4* contributes to SAM development or flowering time.

A. THALIANA TANDEM ZINC FINGER PROTEIN 1 (AtTZF1)

The TZF1 protein is a protein containing to small zinc finger structures that were shown to bind to RNA and stimulate RNA degradation (Qu *et al.*, 2014). *TZF1* expression is higher in *rSPL15* plants in LD conditions, and lower in *spl15-1* plants in SD conditions than in Col-0, suggesting a stimulating role in the floral transition (Fig. S4.10). However, overexpression of *TZF1* leads to pleiotropic growth defects and delayed flowering. These effects can be partially rescued by gibberellin (GA) application, suggesting that ZTF1 may be a negative regulator of GA-signalling or *vice versa* (Lin *et al.*, 2011). GA-signalling is stimulates the floral transition, but it is unclear whether *TZF1* has a function in GA-dependent floral induction or in the developmental changes in the SAM during floral transition.

AT4G13495 – non-coding RNA

AT4G13495 is annotated as a region of non-coding RNA; however, in the TAIR10 annotation, two primary *MIRNAs* appear to be encoded by this region. These two putative primary *MIRNAs*, *MIR850* and *MIR5026*, have only been inferred to exist and to be loaded onto the *MIRNA* processing machinery. The expression of *MIR850* is affected by nitrogen starvation and *MIR5026* might be important in male germline

development, however there is no further evidence of them being biologically functional. (Arribas-Hernández *et al.*, 2016; Borges *et al.*, 2011; G. Liang *et al.*, 2012). In the two transcriptome analyses, *AT4G13495* mRNA expression was lower in *spl15-1* than Col-0 under SD conditions, and more highly than Col-0 in *rSPL15* under LD conditions (Fig. S4.11).

AT4G30250 – P-loop-containing nucleoside triphosphate hydrolase superfamily protein

This is a protein of unknown function, but its sequence shares similarities with bacterial GTPases, that are important for ribosome assembly. A related protein in *Arabidopsis*, NITRIC OXIDE ASSOCIATED 1, belongs to the same family as *AT4G30250* and is involved in salicylic acid signalling pathways (Sun *et al.*, 2010; X. Zhao *et al.*, 2015). Potentially, *AT4G30250* has a similar role in hormone signalling in the SAM that might contribute to the floral transition. In the LD transcriptome analysis, *AT4G30250* was expressed at a lower level in *rSPL15* than in Col-0, and conversely, was more highly expressed in *spl15-1* than in Col-0 in SD conditions(Fig. S4.12).

TARGET OF FLC AND SVP 1 (TFS1)

TFS1 (REM17) is a B3-type transcription factor that is part of the reproductive meristem (REM) family of B3-type transcription factors (Romanel *et al.*, 2009). *TFS1* is a direct target of the floral repressors FLOWERING LOCUS C (FLC) and SHORT VEGETATIVE PHASE (SVP) and of the floral integrator SOC1 (Richter *et al.*, 2019). *tfs1-1* mutants are slightly later flowering than wild-type in LD conditions and the effect is more pronounced in sensitised backgrounds. In contrast, *tfs1* mutants are much later flowering in SD

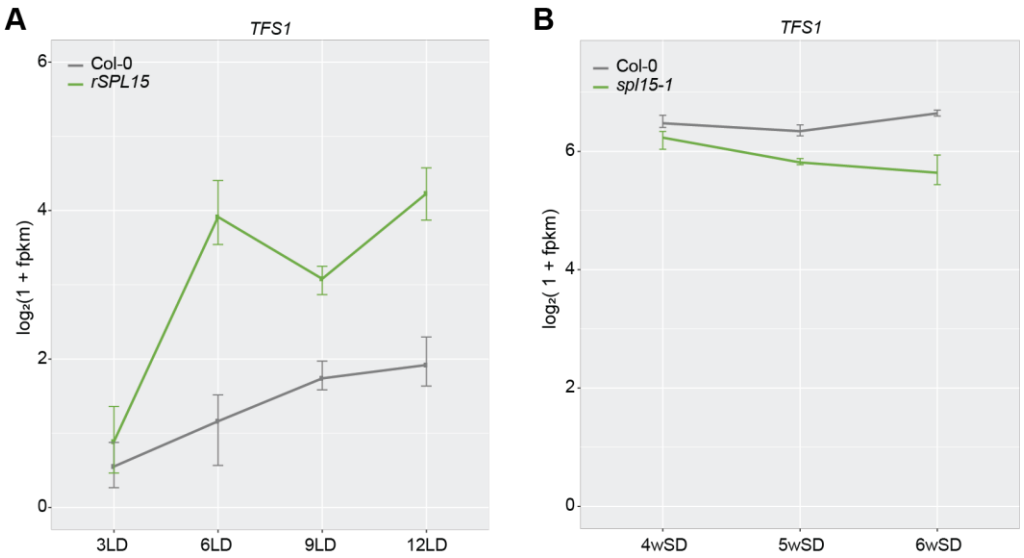

Figure 4.17. Expression patterns of *TSF1* in LD and SD transcriptome analyses. (**A**) Expression of *TSF1* over time in Col-0 and *rSPL15* from the LD- transcriptome analysis. The variation shown is the standard deviation for four independent biologial replicates. (**B**) Expression of *TSF1* over time in Col-0 and *spl15-1* from the SD- transcriptome analysis. The variation shown is the standard deviation for three independent biological replicates. Plotted are globally normalised log_2-transformed FPKM values.

conditions, a flowering phenotype similar to that of *spl15-1*. *TFS1* expression is upregulated in the SAM during floral transition and this is partially dependent on SOC1. Moreover, *TFS1* expression is higher in *rSPL9* plants, where rSPL9 was shown to directly bind to the promoter and downstream region of *TFS1.* Notably, *TFS1* expression is lower in plants that overexpress *MIR156B,* suggesting that its expression is regulated by SPLs. Moreover, *TFS1* expression in the SAM occurs later and at lower levels in *spl15-1* and *spl9-1* mutants than in wild-type (Richter *et al.*, 2019). Consistently, *TFS1* mRNA was more highly expressed in *rSPL15* than in Col-0, and was expressed at a lower level in *spl15-1* than in Col-0 in the transcriptome analyses described in this chapter (Fig. 4.17). This suggests that SPL15 can bind to the *TFS1* promoter, potentially at the same sites as SPL9. Taken together, SPL15 is involved in the upregulation of *TFS1* expression during the floral transition, and similar to *SPL15*, *TFS1* is expressed in the SAM, making *TFS1* is a likely target gene contributing to SPL15-mediated floral induction.

XYLOGLUCAN ENDOTRANSGLUCOSYLASE/HYDROLASE 7 (XTH7)

XTH7 belongs to a large family of xyloglucan endotransglucosylases. XTH enzymes stimulate cell expansion via the rapid detachment and attachment of xyloglucan molecules, an important component of plant cell walls (Rose *et al.*, 2002). *XTH7* is a direct target of BRASSINOZOLE-RESISTANT1 (BZR1), a brassinosteroid (BR) signalling transcription factor (K. Liu *et al.*, 2018). BRs stimulate plant growth and development and are specifically involved in cell elongation (Nolan *et al.*, 2020). It is therefore conceivable that BRs stimulate SAM doming as well as elongation of the rib region and inflorescence stem during the floral transition. However, in the LD transcriptome, *XTH7* mRNA was expressed at a lower level in *rSPL15* than in Col-0 plants and at a higher level in *spl15-1* than in Col-0 in SD conditions, suggesting that SPL15 represses *XTH7* expression (Fig. S4.13). The expression of *XTH7* is lower under conditions in which flowering occurs, suggesting that less cell elongation would take place, or that cell extension would occur in a different direction during the floral trantision. Understanding the role of *XTH7* during floral transition will require a higher resolution description of its spatio-temporal pattern of expression in the SAM. Perhaps *XTH7* is down regulated in specific cell-types or layers, while being upregulated in others, thereby allowing a directional expansion leading to doming or rib meristem extension.

AT5G20700 protein with DOMAINS of UNKNOWN FUNCTION 581

AT5G20700 encodes a zinc-finger protein with a plant-specific DUF581 domain (K & Laxmi, 2014). These proteins are differentially expressed during plant development and interact with SNF1-RELATED PROTEIN KINASE 1 (SnRK1; Nietzsche *et al.*, 2014). The SnRK1 complex is important for modulating plant sugar metabolism during growth and development, and thereby also regulates the floral transition (Baena-González *et al.*, 2007; Wurzinger *et al.*, 2018). Although no specific function has been described for

AT5G20700, it is possible that it is involved in sugar-signalling, and thereby regulates floral induction in the SAM. In my transcriptome datasets, this gene was expressed at a lower level in *rSPL15* in LD conditions and at a higher level in *spl15-1* mutants in SD conditions compared to Col-0 (Fig. S4.14).

ANGUSTIFOLIA 3 (AN3)

AN3 has roles in cell proliferation and leaf outgrowth and functions as a cofactor for GROWTH-REGULATING FACTOR (GRF) transcription factors, which regulate organ growth (Kim & Tsukaya, 2015). AN3 promotes cell proliferation and *an3-4* mutants produce much smaller leaves than Col-0 (Kawade *et al.*, 2013). In addition, *an3* mutants have smaller petals and higher-order mutants of *an3* and its related family members lead to defects in floral morphology (Lee *et al.*, 2009; Lee *et al.*, 2014; Liu *et al.*, 2019). In the transcriptome datasets, *AN3* was more highly expressed in *rSPL15* than in Col-0 in LD conditions, and more lowly expressed in *spl15-1* than in Col-0 in SD conditions (Fig. 4.18). Therefore, AN3 might stimulate the growth of different tissues and organs by interacting with GRFs.

AN3 is also expressed in the root apical meristem where it plays a role in stem cell population organisation (Ercoli *et al.*, 2018). To date, a clear function for AN3 in the SAM has not been described, although it might be expressed there and might be involved in controlling stem-cell maintenance in the SAM (Rodriguez *et al.*, 2010). AN3 might also play a role in meristem doming, where cell proliferation is important, but perhaps also during the later stages of the floral transition, when the rib region proliferates and extends to give rise to the inflorescence stem (Kinoshita & Vaysierres *et al.,* in preparation).

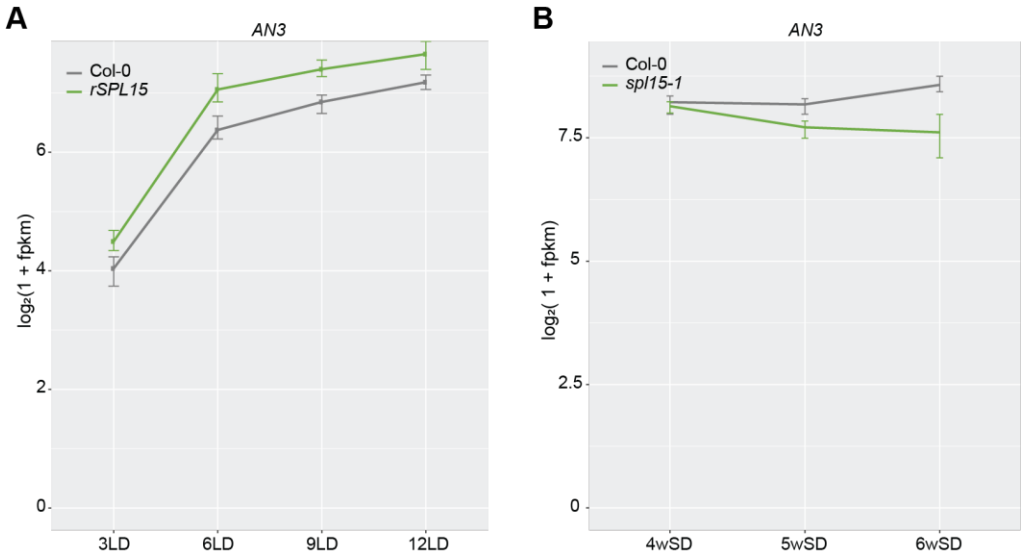

Figure 4.18. Expression patterns of *AN3* in LD and SD transcriptome analyses. (**A**) Expression of *AN3* over time in Col-0 and *rSPL15* from the LD transcriptome analysis. The variation shown is the standard deviation for four independent biologial replicates.(**B**) Expression of *AN3* over time in Col-0 and *spl15-1* from the SD transcriptome analysis. The variation shown is the standard deviation for three independent biological replicates. Plotted are globally normalised log_2-transformed FPKM values.

CYP706A3

CYP706A3 is one of the many cytochrome P450 proteins in *Arabidopsis*. These proteins belong to one of the largest families in A*rabidopsis,* which encode for enzymes that are active in a plethora of biosynthesis pathways (Bak *et al.*, 2011). The subfamily CYP706 consists of seven members, and the only report on the function of CYP707A3 concerns production of volatile-compounds in the flower (Boachon *et al.*, 2019). In the RNA-seq datasets, this gene was expressed more highly in *rSPL15* than Col-0 in LD conditions, and less highly in *spl15-1* than in Col-0 in SD conditions (Fig. S4.15). However, it is unclear whether expression of *CYP706A3* is involved in floral induction or SPL15-mediated developmental pathways.

O-METHYL TRANSFERASE 1 (OMT1)

OMT1 is an enzyme involved in lignin biosynthesis and its mutation leads to alterations in lignin, but do not affect plant length or stem diameter (Goujon *et al.*, 2003; Moinuddin *et al.*, 2010). Lignin is an important component of the cell wall; therefore, OMT1 might regulate cell-wall integrity. It is unclear whether OMT1 is important for cell-wall integrity in Col-0 during floral transition, because the only phenotypes that have been described for *omt1* knockout mutants involve differences in lignin composition. Differences in the expression of *OMT1* between Col-0 and *spl15-1* in SD conditions were small, and *OMT1* was expressed slightly more highly in *spl15-1* than in Col-0 (Fig. S4.16B). In LD conditions, *OMT1* was expressed at a slightly lower level in *rSPL15* plants than in Col-0, suggesting SPL15 downregulates *OMT1* (Fig. S4.16A).

AT5G57655

AT5G57655 is a xylose isomerase family protein. Xylose is a component of xyloglucans, which are part of the plant cell wall. This gene encoding this protein might be involved cell-wall synthesis or loosening. However, no detailed reports exist for this gene and its function in cell wall integrity, and therefore, the function it might have in the SAM or during floral transition is unclear. *AT5G57655* mRNA level was higher in *rSPL15* than in Col-0 under LD conditions, and lower in *spl15-1* than in Col-0 under SD conditions (Fig S4.17).

AT1G02190, ECERIFERUM1-LIKE1 (CER1-L1)

CER1-L1 is one of the genes that was consistently positively co-expressed with *FUL* in the transcriptome analyses. Its mRNA level increased in Col-0 SAMs in SD conditions, but remained stable in *spl15-1* SAMs (Fig. S4.18B). In LD conditions, *CER1-L1* was expressed more highly in *rSPL15* plants than in Col-0 plants, and its expression increased over time (Fig. S4.18A). *CER1-L1* was also differentially expressed between meristems in which floral organ identity MADS-domain transcription factor AGAMOUS (AG) was activated

and where AG was not activated (Gómez-Mena *et al.*, 2005). CER1-L1 is an enzyme that stimulates cuticle wax production (Pascal *et al.*, 2019). The cuticle is important for the protection of the outer cell layers of plants, yet it is unclear whether CER1-L1 function is specific to the SAM or important during the floral transition.

CYTOKININ OXIDASE 3 (CKX3)

CKX3 was also positively co-expressed with *FUL* in both RNA-seq experiments. The CKX3 enzyme catalyses the degradation of CK and is expressed in the SAM in the WUS-expressing domain (Bartrina *et al.*, 2011). The same report showed that the *ckx3/ckx5* double mutant has a larger inflorescence meristem with more flowers and more but smaller cells in the L1 layer of the SAM. *ckx3* single mutants also showed a slight increase in the number of flowers on the inflorescence stem, indicating redundancy between different CKX enzymes. In the LD transcriptome, *CKX3* was expressed more highly in *rSPL15* than in Col-0 and at a lower level in SD conditions in *spl15-1* plants than in Col-0, suggesting SPL15 stimulates *CKX3* expression in the SAM (Fig. 4.19A). These data support a correlation between *CKX3* expression and floral transition downstream of SPL15 and suggest that CKX3 is important for the increase in SAM size during the floral transition. *CKX3* expression increased earlier in plants where flowering was induced earlier (*rSPL15*) and remained stable over time in SAMs of plants where floral transition was not induced (*spl15-1;* Fig. 4.19). Together with its co-expression with *FUL* in both transcriptome datasets, *CKX3* is a plausible candidate to be directly targeted by SPL15 and to have a role in the SAM during floral induction.

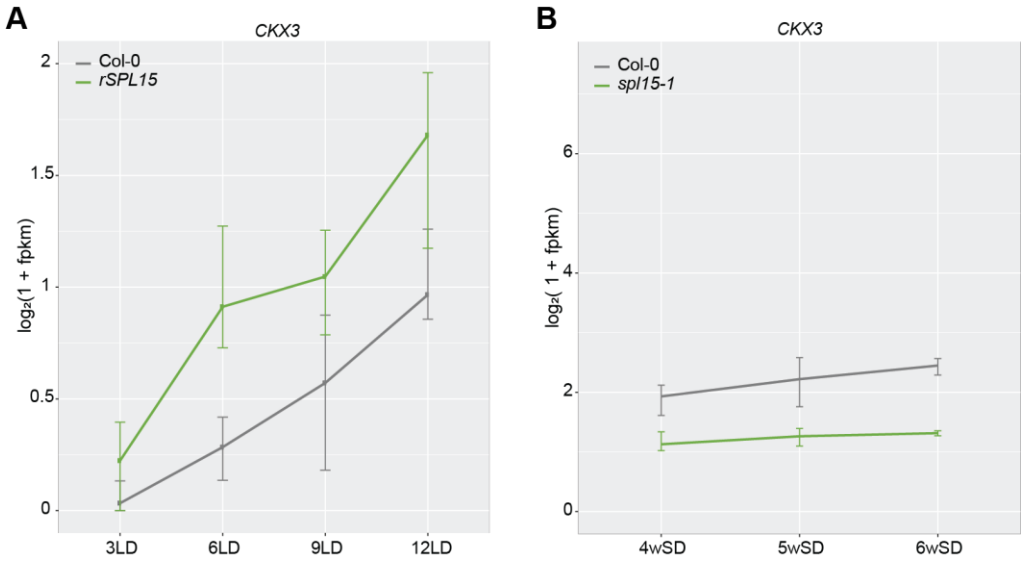

Figure 4.19. Expression patterns of *CKX3* in the LD and SD transcriptome analyses. (**A**) Expression of *CKX3* over time in Col-0 and *rSPL15* from the LD- transcriptome analysis. The variation shown is the standard deviation of four independent biologial replicates. (**B**) Expression of *CKX3* over time in Col-0 and *spl15-1* from the SD- transcriptome analysis. The variation shown is the standard deviation of three independent biological replicates. Plotted are globally normalised $\log_2$-transformed FPKM values.

AGAMOUS-LIKE 42 (AGL42)

ALG42 was positively co-expressed with *FUL* in LD and SD conditions and its temporal expression pattern was influenced by SPL15 (Fig. 4.12C-D; 4.20). Although it was not differentially expressed at all time points in both datasets, it was expressed more highly in *rSPL15* than in Col-0 at 6- and 12LD and was expressed at a lower level in *spl15-1* than in Col-0 at 5- and 6wSD (Table 4.4 and 4.2). AGL42 is a MIKC MADS-domain transcription factor, similar to FUL and SOC1 and is highly related to SOC1 (Pařenicová *et al.*, 2003). It is expressed in the SAM before and during the floral transition, similar to *SOC1* (M. K. Chen *et al.*, 2011; Dorca-Fornell *et al.*, 2011). Additionally, *agl42* mutants did not exhibit an altered flowering-time phenotype in LD conditions, but produced more rosette leaves than Col-0 in SD conditions (M. K. Chen *et al.*, 2011; Dorca-Fornell *et al.*, 2011). Overexpression of *AGL42* leads to earlier flowering in LD conditions, further illustrating its role in the floral transition (M. K. Chen *et al.*, 2011). SOC1 binds directly to the *AGL42* promoter, and *AGL42* expression is upregulated in *soc1* mutants, suggesting that SOC1 represses *AGL42*. Taken together, *AGL42* expression is directly or indirectly regulated by SPL15 and *agl42* mutants show a flowering-time phenotype related to that of *spl15-1* mutants; flowering later under SD conditions. This makes *AGL42* a good candidate to be directly regulated by SPL15. Moreover, SOC1 and SPL15 might cooperate in the regulation of *AGL42* expression, as described for *FUL* regulation (Hyun *et al.*, 2016).

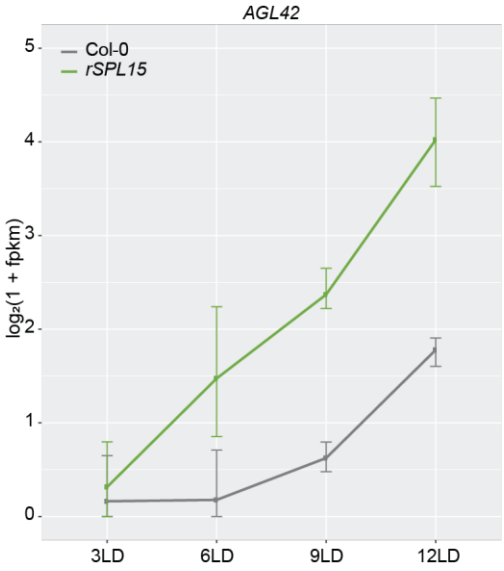

Figure 4.20. Expression pattern of *AGL42* in the LD transcriptome analysis. Expression of *AGL42* over time in Col-0 and *rSPL15* from the LD transcriptome analysis. The variation shown is the standard deviation for four independent biologial replicates. Plotted are globally normalised log_2-transformed FPKM values.

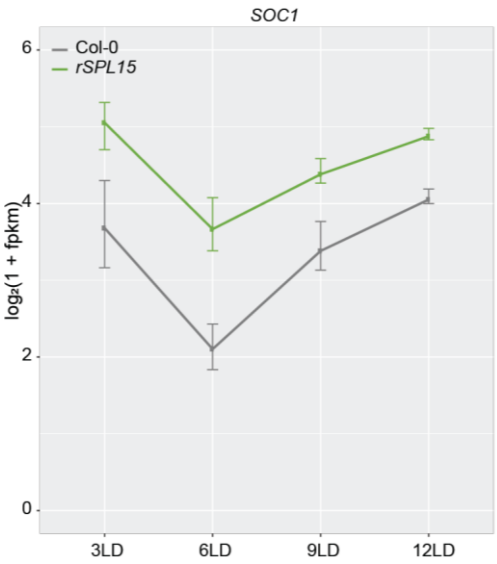

Figure 4.21. Expression pattern of *SOC1* in LD transcriptome analyses. Expression of *SOC1* over time in Col-0 and *rSPL15* from the LD- transcriptome analysis. The variation shown is the standard deviation for four independent biologial replicates. Plotted are globally normalised log_2-transformed FPKM values.

SUPPRESSOR OF OVEREXPRESSION OF CONSTANS 1 and FRUITFULL

SOC1 and FUL encode MADS-domain transcription factors that play important roles in integrating floral induction signals (Introduction; chapters 2 and 3). SOC1 cooperates with SPL15 in the activation of transcription of *FUL* and *MIR172B* and possibly other genes (Hyun *et al.*, 2016). It is therefore conceivable that SPL15 activates *SOC1* expression, as part of a feed-forward loop. In LD and SD conditions, *SOC1* is expressed either more highly in *rSPL15* than in Col-0, or less

highly in *spl15-1* than in Col-0 based on the RNA-seq data (Fig. 4.12F; 4.21). However, in the qRT-PCR analysis designed to confirm the RNA-seq results, *SOC1* was expressed similarly in both genotypes under SD conditions. The initial expression of *SOC1* does not dependent on SPL15, but SPL15 might be involved in timely upregulation of *SOC1* expression during floral transition. *FUL* mRNA is expressed at a lower level and later in Col-0 plants in comparison to in *rSPL15* plants under LD conditions, and is dependent on SPL15 for its timely expression in SD conditions (Fig. 4.6A; 4.11A).

spl15-1 further delays flowering of the *soc1-2/ful-2* double mutant under LD conditions

To analyse the importance of *SOC1, FUL* and *SPL15* for flowering, I generated the *soc1-2/spl15-1* double mutant and the *soc1-2/ful-2/spl15-1* triple mutant and analysed their flowering time in LD and SD conditions. MSc student Miguel Wente scored and evaluated the LD experiment. The results show that out of all single mutants, only *soc1-2* bolted significantly later than Col-0 in LD conditions. However, the double mutant combinations *soc1-2/ful-2, soc1-2/spl15-1* and *spl15-1/ful-2* all bolted and flowered significantly later than Col-0 (Fig 4.22A–C). In addition, *spl15-1/ful-2* bolted and flowered as late as *soc1-2*, with a similar TLN, suggesting that SOC1, FUL and SPL15 genes function in the same pathway. However, the triple mutant

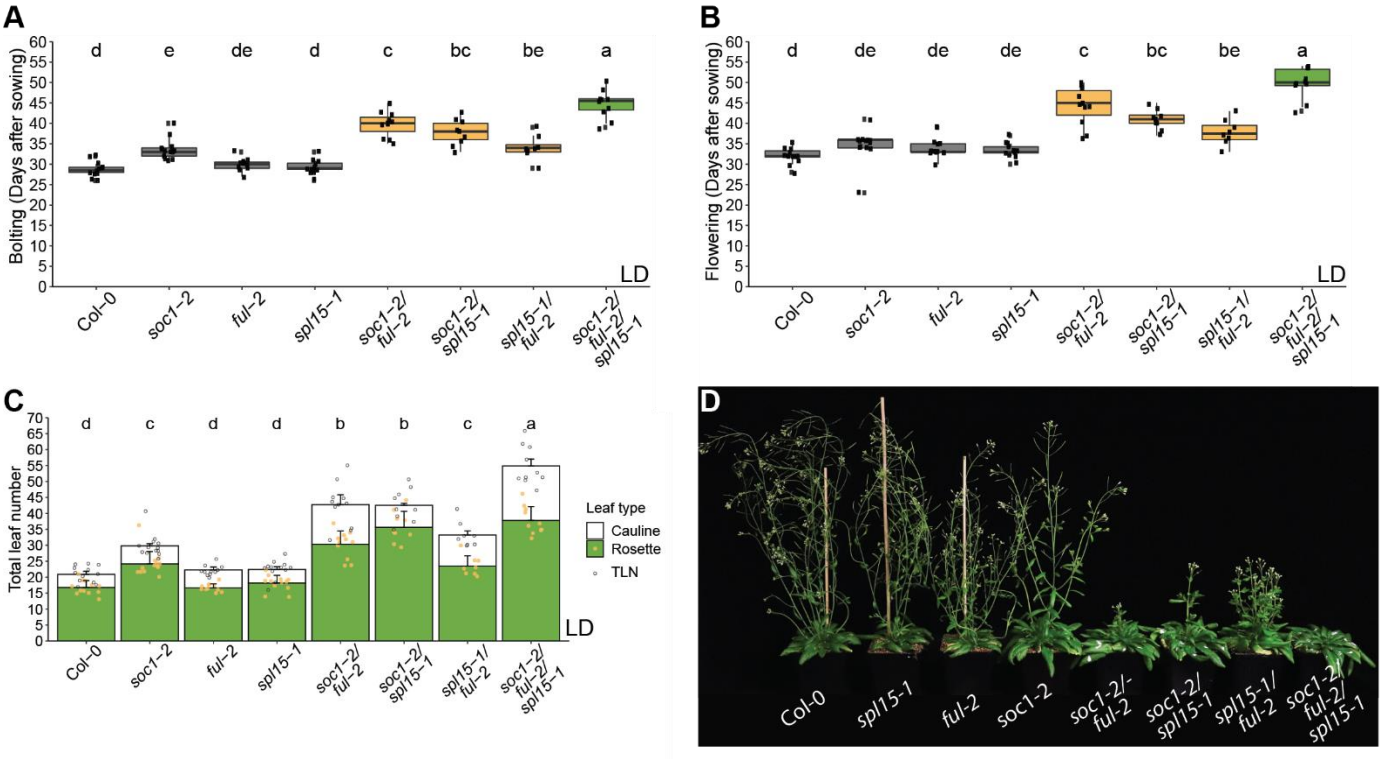

Figure 4.22. Flowering-time phenotypes of Col-0, *spl15-1, ful-2, soc1-2, soc1-2/ful-2, soc1-2/spl15-1, spl15-1/ful-2* and *soc1-2/ful-2.spl15-1* in LD conditions. Time to bolting (**A**), flowering time (**B**) and total leaf number (**C**; TLN) of the indicated genotypes in LD conditions (n = 12). Time to bolting was scored as the day on which the inflorescence extended 0.5 cm from the rosette, and flowering time was scored as the day on which the first flower opened, anywhere on the plant. Statistical differences were calculated with ANOVA followed by Tukey's HSD (honestly significant difference) test at $p < 0.01$. (**D**) Picture of representative plants per genotype at 44LD. This experiment was performed by MSc student Miguel Wente during his internship.

soc1-2/ful-2/spl15-1 bolted and flowered significantly later than all other genotypes. This indicates that SOC1, FUL and SPL15 regulate floral induction partially independently in LD conditions, even though these genes have overlapping roles. Moreover, *ful-2* single mutants are known for their increase cauline leaf number in SD-conditions (chapter 2, 3). In LD-conditions, this phenotype is not so apparent. Notably, in the *ful-2/spl15-1* and *ful-2/soc1-2* double mutants and in the *soc1-2/ful-2/spl15-1* triple mutant there was a significant increase in the number of cauline leaves on the plants (4.22C, $p < 0.01$). This suggests that additional mutation of *SOC1* and/or *SPL15* in the *ful-2* background can enhance this phenotype. Besides their roles in floral induction, SOC1, FUL and SPL15 also contribute to plant architecture. Although *soc1-2/spl15-1* plants were phenotypically similar to Col-0 in terms of architecture, the *soc1-2/ful-2* and *spl15-1/ful-2* double mutants showed a very bushy phenotype with more axillary shoots branches arising from the rosette (Fig. 4.22D). In the *soc1-2/ful-2/spl15-1* triple mutant, this phenotype was slightly enhanced and the plants were very bushy with very short inflorescences (data not shown).

soc1-2/ful-2/spl15-1 triple mutants flower at the same time as *soc1-2/ful*, *soc1-2/spl15-1* and *spl15-1/ful-2* double mutants in SD conditions.

To assess the contribution of SOC1, FUL and SPL15 to flowering in SD conditions, the same single, double and triple mutants were used in a flowering time experiment in SD conditions (Fig. 4.23). In contrast to LD conditions , all single mutants showed a delay in flowering time, with *spl15-1* and *soc1*-2 plants flowering latest. Time to bolting of these plants was scored, yet as most double and triple mutants flowered from axillary rosette shoots and not from the main shoot, this could not be scored for all plants (Fig. 23C).

The double mutants all flowered at the same time as the triple mutant, and were all later flowering than Col-0 and all single mutants. This indicates that in SD conditions, SPL15, SOC1 and FUL control floral induction and function both coordinately and redundantly. Furthermore, when two of these genes are no longer functional, the third one can no longer induce flowering. This supports the data that SOC1 and SPL15 cooperate to activate their targets in these conditions (Hyun *et al.*, 2016). This might represent a more general module for cooperation between MADS-domain transcription factors and SPLs. Moreover, in the case of floral induction, SPL15 might be able to interact with SOC1 and FUL to induce flowering in SD conditions.

In LD conditions, the situation is different, since floral induction is not dependent on SPL15, instead, flowering proceeds through the FT/TSF/FD pathway (Abe *et al.*, 2005; Corbesier *et al.*, 2007; Jaeger & Wigge, 2007). *SOC1* and *FUL* integrate signals from this pathway, suggesting that in *soc1/ful* mutants in LD conditions flowering is induced through SPL15. This explains why in LD conditions, the triple mutant is even

later flowering than either one of the double mutants. In SD conditions, *FT* and *TFS* do not play a role, and they do not act on *FUL* and *SOC1.* This might be the reason why additional mutation of *SPL15* in the *soc1-2/ful-2* mutant background in SD conditions can no longer enhance the delay in flowering.

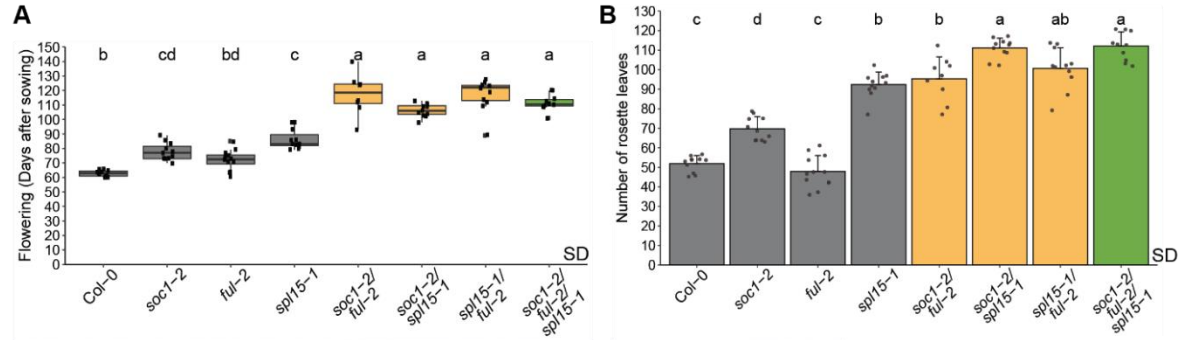

Figure 4.23. Flowering-time phenotypes of Col-0, *spl15-1*, *ful-2*, *soc1-2*, *soc1-2/ful-2*, *soc1-2/spl15-1*, *spl15-1/ful-2* and *soc1-2/ful-2.spl15-1* under SD conditions. Flowering time (**A**) and rosette leaf number (**B**) of the indicated genotypes under SD conditions (n = 11-12). Time to bolting is not shown as most double and triple mutants did not flower from the main shoot. Flowering time was scored as the day on which the first flower opened, anywhere on the plant. Statistical differences were calculated with ANOVA followed by Tukey's HSD (honestly significant difference) test at $p < 0.01$. (**C**) Picture of representative plants per genotype at 112SD.

Induction of SPL15 activity

To identify the direct gene targets of a transcription factor, inducible lines can be used. Upon induction, the transcription factor will be activated and start regulating its targets, and comparison between the expression of putative targets in induced plants and non-induced plants can be informative about the genes regulated by the transcription factor (Brand *et al.*, 2006; Craft *et al.*, 2005; Simon *et al.*, 1996). Use of translational fusions of the transcription factor to steroid responsive domains allows additional treatment with cycloheximide to be used, an inhibitor of translation, to select only for direct targets that are activated independently of translation (Roig-Villanova *et al.*, 2006). Induction of SPL15 using such a system might thus assist in identifying SPL15 target genes as well as confirming its putative direct targets. To this end, Dexamethasone (DEX)-inducible constructs of SPL15 fused to the hormone-binding domain of the Rat Glucocorticoid Receptor (GR) and expressed from the *SPL15* regulatory sequences were constructed and introduced into the *spl15-1* mutant background. Fusion to GR sequesters the SPL15::GR fusion protein in the cytoplasm, rendering it unable to enter the nucleus until DEX is provided (N. Yamaguchi *et al.*, 2015).

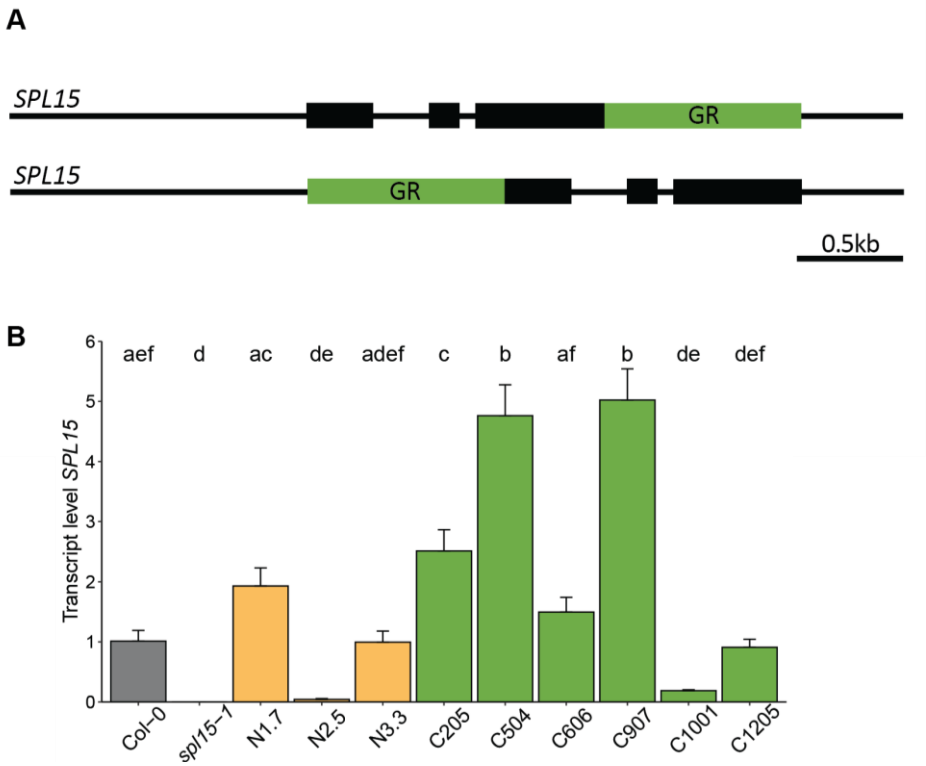

Figure 4.24. Graphical representation of constructs cloned and SPL15 expression in every independent line. (**A**) Schematic representation of the two constructs that were cloned and used to transform *spl15-1* plants. The clones included the entire upstream and downstream regions. Green represents the GR::HA or HA::GR fusion protein; all black boxes represent the native exons of *SPL15.* GR was inserted either C-terminally (top) or N-terminally (bottom). (**B**) *SPL15* transcript level in Col-0, *spl15-1*, N-terminal GR fusion lines N1.7, N2.5 and N3.3, as well as C-terminal fusion lines C205, C504, C606, C907, C1001 and C1205. Data are presented for a single biological replicate. The variation shown is the standard deviation for three technical replicates. Statistical differences were calculated with ANOVA followed by Tukey's HSD (honestly significant difference) test at $p < 0.01$.

The existing *pSPL15::VENUS9A::SPL15* clone was used as a template to create two constructs: *pSPL15::HA::GR::SPL15* (labelled 'N' for amino-terminal fusion) and *pSPL15::SPL15::GR::HA* (labelled 'C' for carboxy-terminal fusion; Fig. 4.24A; Hyun *et al.*, 2016). To test the expression of SPL15 fused to GR in homozygous independent transformants of both N- and C-terminal fusion constructs, I performed qRT-PCR on meristem-enriched tissue of plants grown in SD conditions for five weeks. I compared the mRNA level of *SPL15* in Col-0 and *spl15-1* at this timepoint and found that there was variation in *SPL15* expression among the transgenic lines (Fig. 4.24B). The N-terminal fusion lines N1.7, and N3.3 and C-terminal fusion lines C606 and C1205 all exhibited a level of *SPL15* expression level similar to that in Col-0.

Two out of six inducible lines respond by earlier flowering after dexamethasone application under SD conditions.

I performed a trial induction experiment in SD-conditions with independent homozygous T_3 lines for the N- and C-terminal fusion constructs of SPL15 to GR and tested their functionality. Because the constructs were all introduced into the *spl15-1* mutant background, a functional line should flower at the same time as the *spl15-1* mutant when treated with a mock solution and should flower at a similar time to Col-0 when treated with DEX solution. In this experiment, plants were treated by applying droplets of mock or DEX solution directly onto the meristem once-weekly from 3wSDs onwards.

The mock solution consisted of 0.01% EtOH and 0.015% Silwet in dH_20 and the DEX solution consisted of 10 µM dexamethasone, 0.01% EtOH and 0.015% Silwet in dH_20. Col-0 and *spl15-1* plants were included as controls for the treatments and the *pAP1::AP1::GR*/*ap1/cal* line that was inducible for AP1 was used as a control for the DEX treatment (Ó'Maoiléidigh *et al.*, 2013). *pAP1::AP1::GR*/*ap1/cal* plants flower earlier than Col-0 when treated with DEX. The results show that for the three independent lines containing *pSPL15::HA::GR::SPL15*, treatment with DEX or mock did not affect flowering time as all these plants flowered at the same time as Col-0. Genotyping of the lines confirmed their *spl15-1* mutant background, suggesting the GR::SPL15 fusion protein is constitutively active, or perhaps GR is cleaved, so that these lines cannot be used to induce SPL15 activity.

Out of the six independent lines containing *pSPL15::SPL15::GR::HA*, only lines C606, C907 and C1205 responded to DEX treatment by flowering significantly earlier than mock-treated plants (Fig. 4.25A-C). Out of these three lines, line 606 only flowered earlier with respect to rosette leaf number (Fig. 4.25C). Moreover, the mock-treated plants of line C606 flowered significantly earlier than *spl15-1* mutants, suggesting that SPL15::GR . In contrast, lines C907 and C1205 were both earlier flowering than mock-treated plants when treated with DEX, and when treated with mock solution, these plants flowered at the

same time as *spl15-1* (Fig. 4.25A-C). I therefore selected lines C907 and C1205 as the best candidates for further analysis. Line C1205 expressed *SPL15* at a near wild-type level and responded well to DEX induction. Nevertheless, line C907 was analysed in parallel with C1205 during further induction experiments.

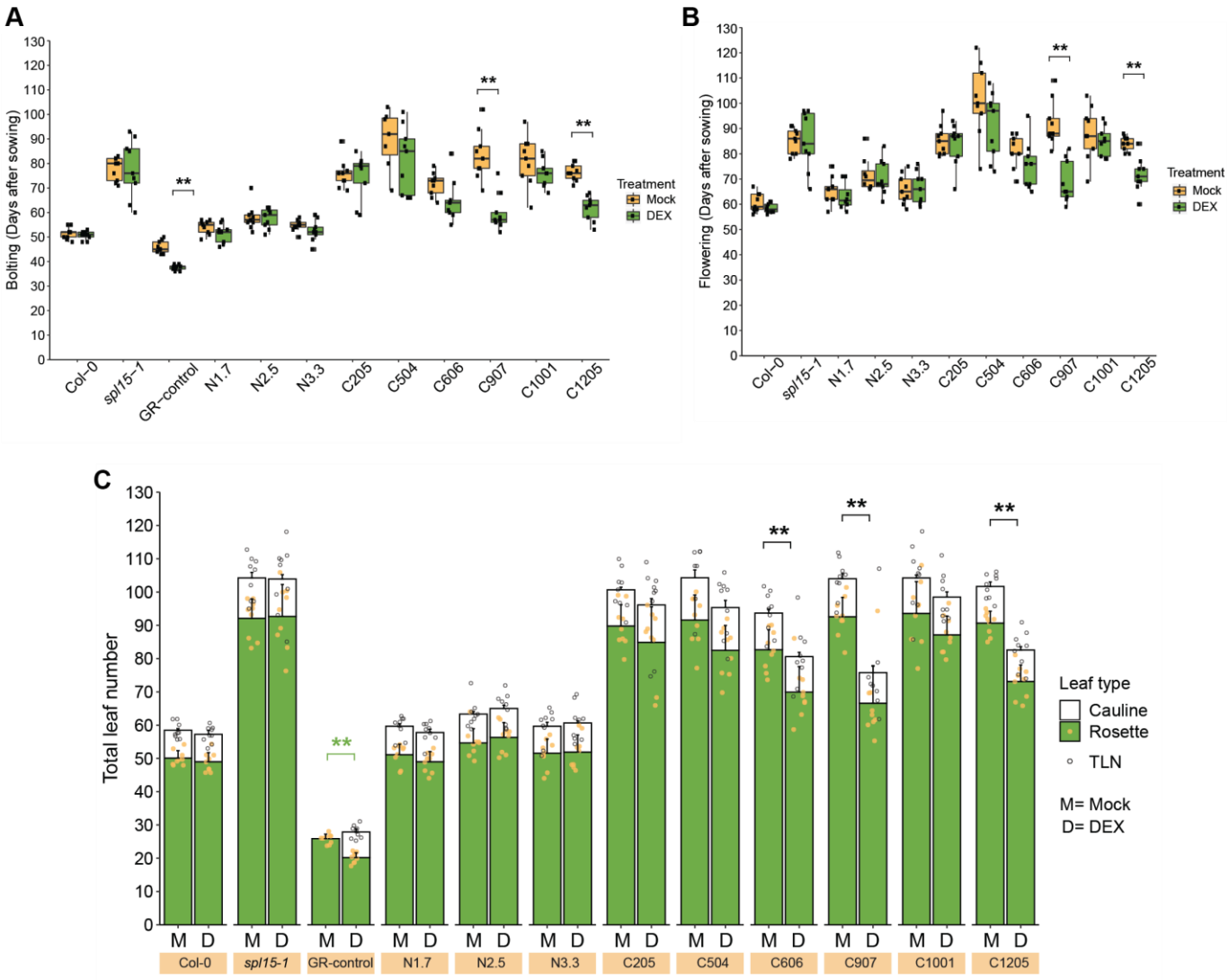

Figure 4.25. Flowering time of Col-0, *spl15-1*, GR control AP1::GR/*ap1/cal* and independent transformants of GR::SPL15 (N-lines) and SPL15::GR (C-lines) after repeated DEX induction in SD conditions. Time to bolting (**A**), flowering time (**B**) and total leaf number (**C**; TLN) of the indicated genotypes in SD conditions (n = 9). Plants were treated weekly with dexamethasone (DEX, D) or mock (M) solution. Bolting time was scored as the day on which the inflorescence extended 0.5 cm from the rosette, and flowering time was scored as the day on which the first flower opened, anywhere on the plant. Statistical differences were calculated between mock and DEX treated plants of the same genotype using the student's *t*-test at $p < 0.01$. For the GR control line AP1::GR/*ap1*/*cal*, the student's *t*-test was performed for the number of rosette leaves and not TLN, because the mock-treated plants did not have any cauline leaves.

The inducible SPL15 line C1205 responded to repeated dexamethasone treatment by doming and flowering earlier than mock-treated plants, but flowering was delayed by two weeks compared with that of Col-0 under SD conditions.

To further optimise SPL15 induction in SD conditions, MSc student Tim Neefjes and I designed multiple induction experiments. We first tested whether a single application with DEX to the centre of the rosette was sufficient to induce flowering in DEX-treated plants, but not in mock treated plants. However, regardless of the age at which plants were treated (4-, 5-, 6- or 7-week-old SD-grown plants), the inducible lines C907 and C1205 did not respond to DEX treatment by flowering earlier than the mock-treated plants. We next decided to test consecutive treatments and treated plants with DEX or mock every 2-3 days for two or three times at different ages (4-, 5-, 6- or 7-week-old SD-grown plants). These treatments also did not lead to differences in flowering time in C907 or C1205, nor were any differences observed in the expression of SPL15 target genes *FUL* and *SPL4.*

T. Neefjes then performed a time-course experiment in which he tested consecutive treatments with DEX or mock, treating the plants every three days from 3wSD onwards. He tested the expression of *FUL* and *SPL4* with qRT-PCR on a weekly basis, but did not observe consistent differences between DEX- and mock-treated plants. In addition to performing qRT-PCR, he also harvested apices weekly for confocal microscopy to study the effects of DEX and mock treatments on SAM morphology. Confocal imaging showed that the SAMs of Col-0 began to dome after 5wSD and produced floral primordia from 7wSD onwards, irrespective of the treatment (Fig. 4.26, left). By contrast, *spl15-1* mutant plants remained vegetative throughout the time course, and started to dome after 8wSD (Fig. 4.26, centre).

The SAMs of the SPL15::GR inducible line C1205 began to dome after 7wSD and produced axillary meristems at 8wSD when treated with DEX, but behaved like *spl15-1* when treated with mock solution (Fig. 4.26, right). This demonstrated that C1205 plants responded to the repeated induction of SPL15::GR activity. However, these treatmens were insufficient to induce flowering to the wild type level, as flowering was delayed by two weeks compared to Col-0.

Consistently, DEX-treated C1205 plants flowered significantly earlier than mock-treated C1205 plants (Fig. 4.27A, B). Similar to the previous flowering-time experiment after DEX or mock treatment, C1205 plants flowered at the same time as *spl15-1* when treated with mock (Fig. 4.25A, B; 4.27A, B). Notably, plants were treated every three days in the current experiment versus only once weekly in the first flowering-time experiment. However, this increase in DEX treatment frequency did not further accelerate flowering time in SPL15:GR line C1205 (Figs. 4.25, 4.27).

When T. Neefjes tested whether even more frequent DEX-application affected the plants, the young leaves of the plants senesced and most plants died after only several treatments. This illustrates that treatment of 2-3 times per week is the maximum treatment frequency with which the treated plants can cope.

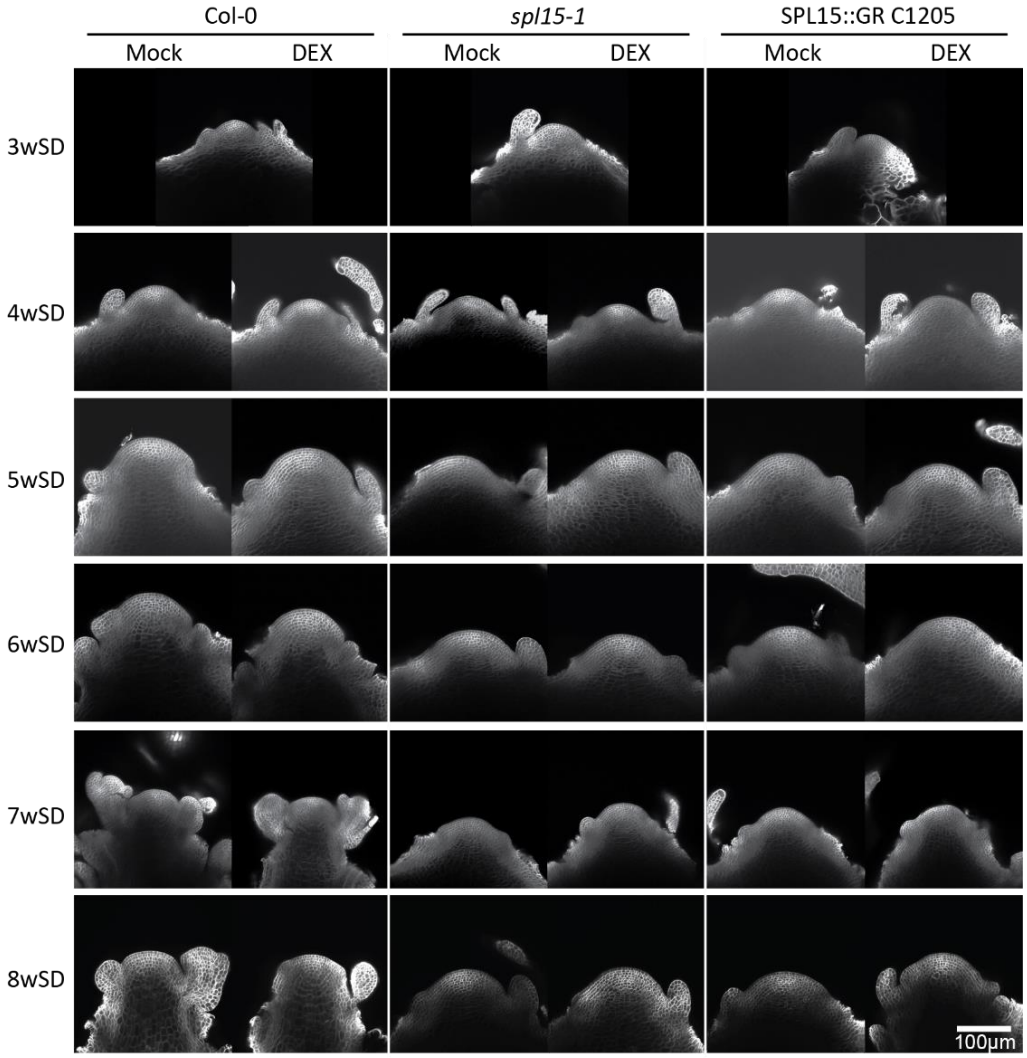

Figure 4.26. Confocal imaging of Col-0, *spl15-1* and SPL15::GR apices after treatment with mock or DEX in SD conditions along a time course. Confocal laser scanning micrographs of shoot apices of Col-0 (left two panels), *spl15-1* (centre two panels) and *pSPL15::SPL15::GR*/*spl15-1* line 1205 (right two panels) at the indicated time points after mock or dexamethasone (DEX) treatment every three days in SD conditions. Fluorescence from the Renaissance cell-wall staining dye is artificially coloured in magenta. The white scale bar represents 100 µm. Most of the harvesting for confocal imaging as well as the microscopy in this experiment was performed by MSc student Tim Neefjes, during his thesis internship.

In conclusion, frequent DEX treatment is necessary for the DEX-inducible line C1205 to respond by flowering earlier than mock-treated plants. Although differences in flowering time were observed, the response was delayed by at least two weeks. This indicates that without rapid response to the treatment, it is not possible to identify whether transcriptional changes that occur later in development are a direct result of SPL15 induction, or rather an indirect result of floral induction.

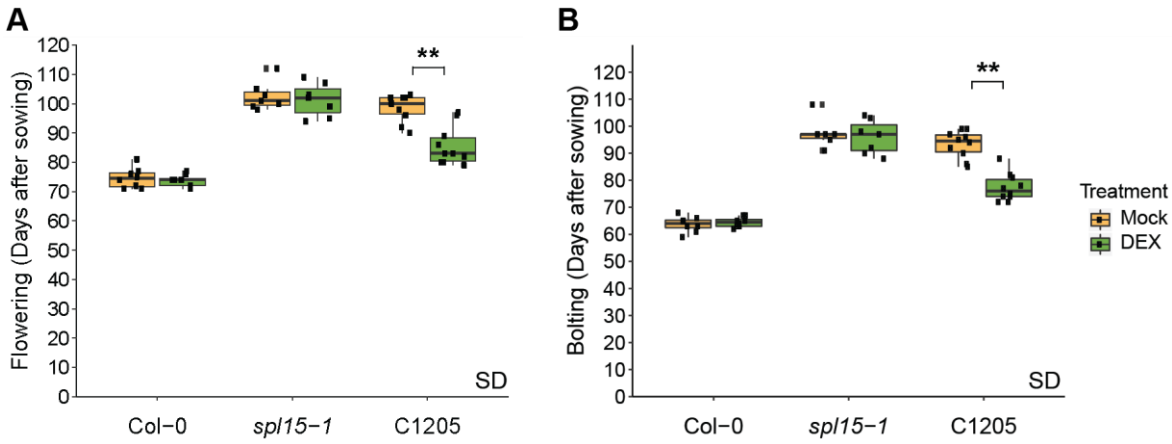

Figure 4.27. Time to bolting (**A**) and flowering time (**B**) of the indicated genotypes in SD conditions (n = 7–10). Plants were treated every three days with dexamethasone (DEX) or mock solution. Bolting time was scored as the day on which the inflorescence extended 0.5 cm from the rosette, and flowering time was scored as the day on which the first flower opened, anywhere on the plant. Statistical differences were calculated between mock- and DEX-treated plants of the same genotype using the student's *t*-test at $p < 0.01$. The experiment was performed in collaboration with MSc student Tim Neefjes.

Discussion

Floral induction through SPL15 in LD and SD conditions

In this chapter, I have presented the analysis of two RNA-seq time courses. One in LD conditions with apices of the early-flowering *rSPL15* line compare to Col-0 and the other one in SD conditions with the dissected SAMs of non-flowering *spl15-1* compared to Col-0. Both experiments show that several genes were differentially expressed at specific time points, whereas other genes remained consistently differentially expressed between the two genotypes. The accelerated floral induction and bolting time observed in the meristems of *rSPL15* plants correlated with the increased expression of genes encoding for transcription factors involved in flowering-time regulation (Fig. 4.4). Conversely, the expression of only few genes encoding these transcription factors increased in *spl15-1* SAMs in SD conditions, whereas floral induction clearly occurred in Col-0 during the time course, which is is reflected in the large changes in expression of these transcription factors (Fig. 4.10).

One of the most striking differences between the two datasets is the large number of DEGs at the two earliest time points of the LD experiment, with 798 and 3,543 DEGs at 3- and 6LD, respectively. I expected hardly any differences in the expression of flowering-time genes at 3LD, because the plants had only just germinated. I expected to observe the first differences at 6LD, which was the first time point at which *VENUS::rSPL15* can be detected in the meristem, but certainly fewer than 3,500 DEGs. The overexpression of SPL15 in these plants might lead to a gain-of-function phenotype where rSPL15 binds genes that it does not normally bind. DNA affinity-purification sequencing (DAP-seq) with PCR-amplified DNA performed with SPL15, revealed that SPL15 bound to more than 13,000 genes *in vitro* (O'Malley *et al.*, 2016). However, this method disregards secondary DNA structures and DNA methylation, which could explain the high number of binding sites.This means that the specificity of SPL15 binding to DNA is not defined by its DNA-binding SBP domain, nor by the specificity of the motifs, but rather by the accessibilty of the GTAC motifs and possibly other transription factors. This does indeed suggest that when *rSPL15* is expressed earlier, at a higher level and potentially in different domains, it might acquire the ability to bind to genes and motifs which it would not normally access. This might explain the high number of DEGs in *rSPL15* at the early two time points. Moreover *rSPL15* plants are slightly delayed in the production of the first true leaves and this is a specific phenotype for many other *SPL* overexpression lines (Fig. 4.3D; Franco-Zorrilla *et al.*, 2007; Wu *et al.*, 2009; Xu *et al.*, 2016), which suggests that this phenotype might be the result of the acquisition of increased binding ability by SPLs.

MIR156 was shown to function in the developing *Arabidopsis* embryo as well, suggesting that proper regulation of *SPLs* in the embryo is important for proper development (Armenta-Medina *et al.*, 2017; Plotnikova *et al.*, 2019). Plants with disturbed miRNA processing machinery also show severe defects in embryo development (Armenta-Medina *et al.*, 2017). It is therefore plausible that rSPL15 can regulate processes involved in embryo development which it would normally not affect as its spatio-temporal expression is restricted by miR156.

The number of DEGs observed in the SD transcriptome analysis was in line with my expections; the differences in transcription of an increasing number of genes changes as the developmental differences between Col-0 and *spl15-1* in SD conditions become prominent. Col-0 undergoes the floral transition and this includes large epigenetic rearrangements that would lead to large transcriptional changes (Kinoshita & Richter, 2020).

Candidate target genes of SPL15

The analysis of two independent transcriptome experiments under different conditions using different genotypes enabled me to derive a stringently selected list of candidate target genes of SPL15. By overlapping DEGs and by identifying genes that are co-expressed with the known direct SPL15-target *FUL* in both transcriptome experiments, a list of 18 putative SPL15 target genes was compiled. Encouragingly, several of these genes have established functions in floral induction (*i.e. SOC1, FUL, AGL42, TFS1* and *SPL4*), whereas the functions of some genes are unknown (*ATTZF1, AT4G30250, AT4G13495, AT5G20700,* and *CYP706A3)* and other genes have a role in cell division, elongation or growth (*i.e. ACR4, XTH7, AN3, OMT1, AT5G57655, CER1-L1* and *CKX3*).

To analyse whether these candidate genes are indeed direct targets of SPL15, it would be useful to use an inducible SPL15 line that fully complements the *spl15-1* mutant phenotype and has a rapid response to induction (further described below). This line could then be used for qRT-PCR studies either with or without induction, or even for RNA-seq experiments. Furthermore, the addition of translation inhibitor cycloheximide might help to determine even more specifically whether these genes are direct SPL15 targets (N. Yamaguchi *et al.*, 2015). Moreover, chromatin immunoprecipitation (ChIP)-qPCR could be employed to confirm the binding of SPL15 to these genes.

During my PhD, I tested many different immunoprecipitation approaches for SPL15, but unfortunately none was consistently succesful. I therefore think that the newly generated line: *pSPL15::3xHA::VENUS::SPL15/spl15-1* is a useful tool with which to performe ChIP of SPL15 (the line was designed by me, and was generated and transformed into *spl15-1* by Kerstin Luxa). In the *spl15-1* mutant

background, this construct is expressed at a near wild-type level and will therefore not be affected by dilution in a similar way to the original *pSPL15::VENUS::SPL15*/Col-0 line. The latter line contains two alleles of *SPL15;* the native allele and the transgene, which could lead to competition between native SPL15 and VENUS::SPL15 for binding to DNA. This possibly leads to the dilution of the number of DNA binding sites that are occupied by VENUS::SPL15, as both SPL15 and VENUS::SPL15 would bind to the locus of interest. Moreover, the HA-antibody is a highly specific and robust antibody for immunoprecipitation in plants and may be more efficient for the pull-down of 3xHA::VENUS::SPL15 than the previously used GFP antibody.

Inducible SPL15 line and the confirmation of direct targets

The inducible SPL15::GR lines I generated partially complemented the *spl15-1* mutation when treated with DEX (Fig. 4.25). However, even following multiple DEX applications, SPL15 activity was not rapidly induced in these lines, and did not lead to transcriptional changes that would induce floral transition at the same time as Col-0 (Fig. 4.26).

DEX may not effectively penetrate the SAM, or it may have been degraded rapidly before reaching the SAM. It has been reported that after root application in tobacco, the effects of DEX persisted for 48 h, whereas spraying it onto aerial parts of *Arabidopsis* plants still showed an effect on gene expression after 96 h (Aoyama & Chua, 1997; Geng & Mackey, 2011). It is possible that the application method we used of applying 1.5 µL DEX solution to the centre of the rosette, led to an even shorter activity window.

Currently, not enough is known about the efficacy of this application method of DEX to the SAM. Potentially, the strong regulation of SPL15 by *MIR156* and DELLA proteins needs to be overcome first before SPL15 can transcriptionally activate its targets. SPL15 itself might play a role in this process through negative feedback loops, and SPL15 might therefore have to be present for a long enough time to overcome these repressive effects and to begin to activate transcription of its targets. Alternatively, it is also possible that other repressive transcription factors repress some of the direct targets of SPL15, and that SPL15 first needs to outcompete these transcription factors before it can activate transcription and initiate flowering. This would again require the persistent accumulation of nuclear SPL15, which might not happen in the current SPL15::GR lines. As a consequence, SPL15::GR plants might flower later than Col-0, but earlier than mock-treated plants.

An inducible system for SPL15 is nevertheless a useful tool with which to test genes affected by SPL15, and to identify direct targets, but the lines described in this chapter do not function sufficiently well for this goal. In the future, it would be worthwhile to test different SPL15-inducible constructs. I therefore suggest

that different lines with *SPL15* driven by a different promoter be generated. One option would be to use the CaMV 35S overexpression promoter, although it would first have to be determined how well this is expressed in the SAM. Alternatively, a meristem-specific constitutively highly active promoter such as that of *STM* or *KNAT1* could be used to specifically over express SPL15 in the SAM. Similarly, the *SPL15* wild-type open reading frame could be exchanged for the *MIR156*-resistant *rSPL15* to enhance the level of SPL15 protein expression. As shown in this chapter, *rSPL15* is expressed earlier and at a higher level than *SPL15* and might therefore be more responsive to DEX treatment. It could be combined with the native *SPL15* promoter or with any of the promoter options mentioned above.

Furthermore, transcriptional two component systems could be used rather than the translational fusions here (Brand *et al.*, 2006; Siligato *et al.*, 2016). This inducible system allows the induction of a transcriptional activator such as XVE under a promoter of interest, which upon estradiol induction will bind to its recognition site on a minimal promoter driving the expression of the gene of interest (Zuo *et al.*, 2000). These systems would have the disadvantage that they are not activated post-translationally and therefore cannot be used in conjunction with cycloheximide. However, the advantage is that the induced protein is not a translational fusion with the GR domain, which might reduce protein activity, and that after induction, the mRNA of the induced gene can be followed. MSc Laura Trimborn has previously started to clone the native *SPL15* promoter combined with the *rSPL15* sequence in such a two-component vector.

Supplementary figures

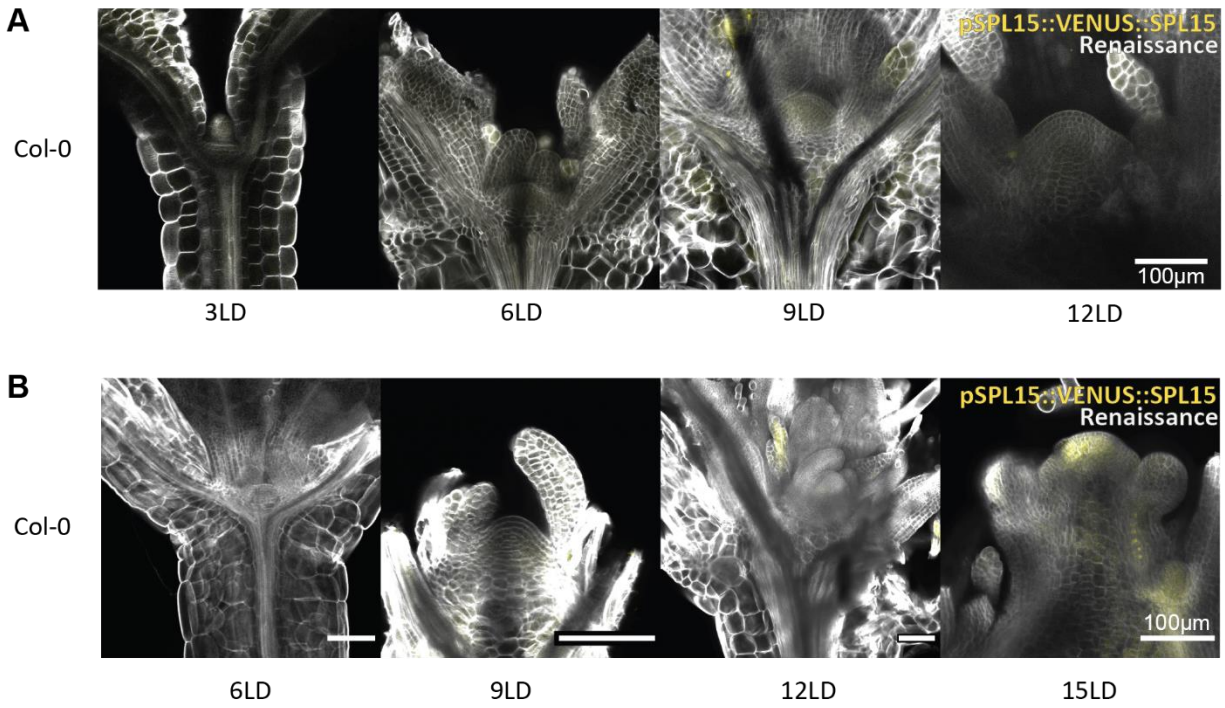

Fig. S4.1. Confocal laser scanning micrographs of shoot apices of *pSPL15::VENUS::SPL15*/Col-0 at the indicated time points in LD conditions. (**A**) Confocal images of *pSPL15::VENUS::SPL15*/Col-0 at 3-, 6-, 9- and 12LD. Material and images by MSc student Miguel Wente. (**B**) Confocal images of *pSPL15::VENUS::SPL15*/Col-0 at 6-, 9-, 12- and 15LD. Material and images by MSc Laura Trimborn. Fluorescence from VENUS is artificially coloured in yellow and fluorescence from the Renaissance dye is artificially coloured in white. The white scale bar represents 100 µm.

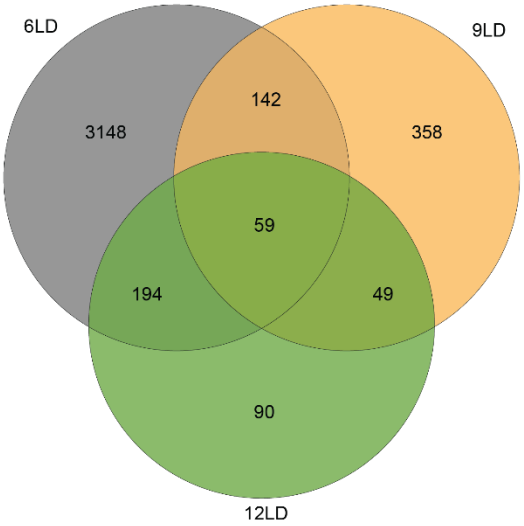

Fig. S4.2. Venn diagram showing all differentially expressed genes (DEGs) between Col-0 and *rSPL15* at 6LD, 9LD and 12LD and whether these DEGs occur at other time points. DEGs were selected for an adjusted *p*-value <0.05.

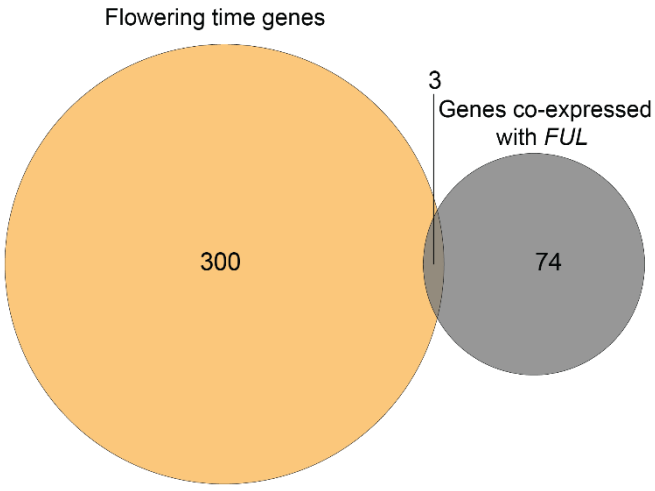

Fig. S4.3. Venn diagram showing the overlap between genes related to flowering-time regulation and genes that were positively co-expressed with *FUL* in Col-0 and *rSPL15* in LD-conditions.

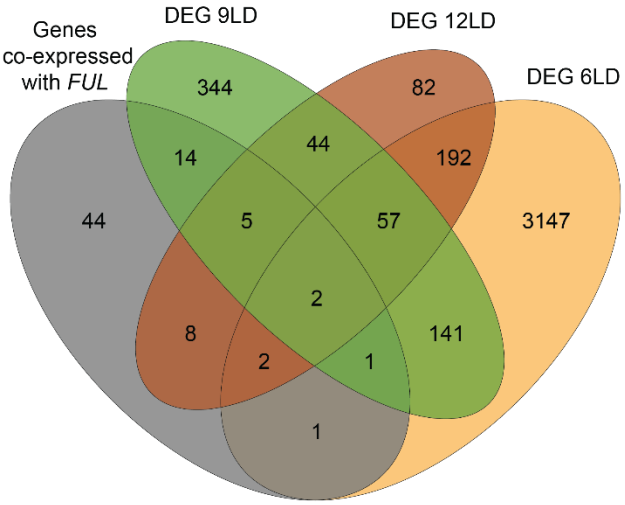

Fig. S4.4. Venn diagram showing DEGs at 6LD, 9LD and 12LD and the overlap with genes that were co-expressed with *FUL* in LD conditions.

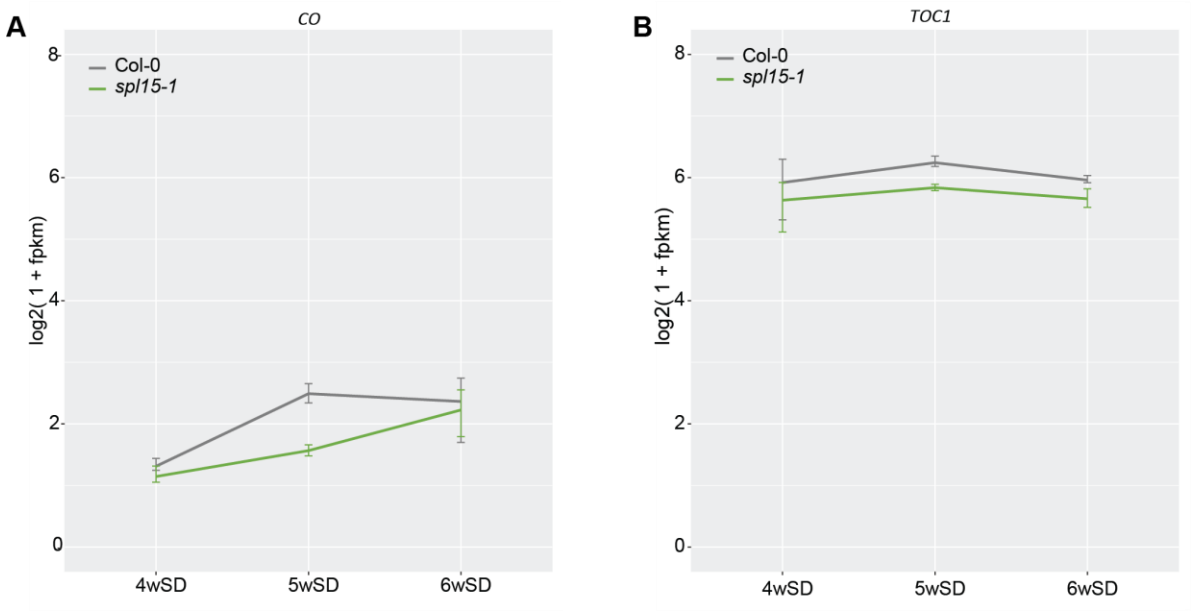

Fig. S4.5. Expression patterns of *CONSTANS* (*CO*) and *TIMING OF CAB EXPRESSION 1* (*TOC1*). *CO* (**A**) and *TOC1* (**B**) expression from the transcriptome analysis over time in Col-0 and *spl15*-1 in SD conditions. Plotted are globally normalised log_2-transformed FPKM values. The variation shown is the standard deviation for three replicates.

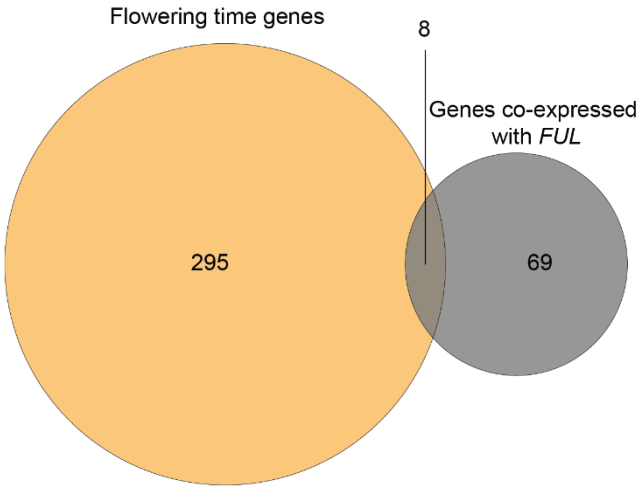

Fig. S4. Venn diagram showing the overlap between genes related to flowering-time regulation and genes that were co-expressed with *FUL* in Col-0 and *spl15-1* in SD conditions.

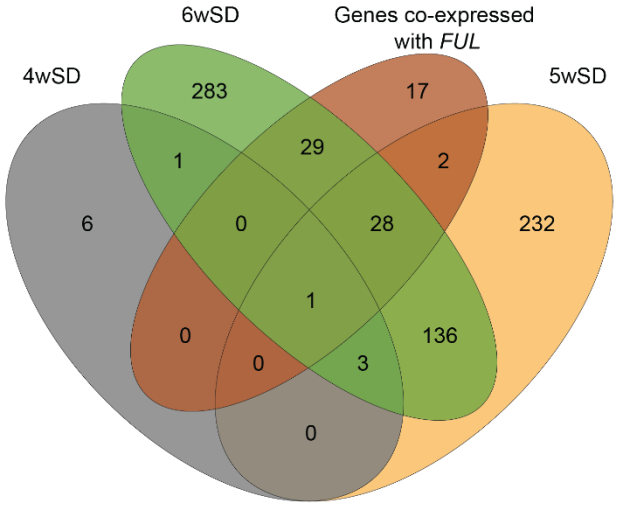

Fig. S4.6. Venn diagram showing DEGs at 4-, 5- and 6wSD and the overlap with genes that were co-expressed with *FUL* in SD conditions.

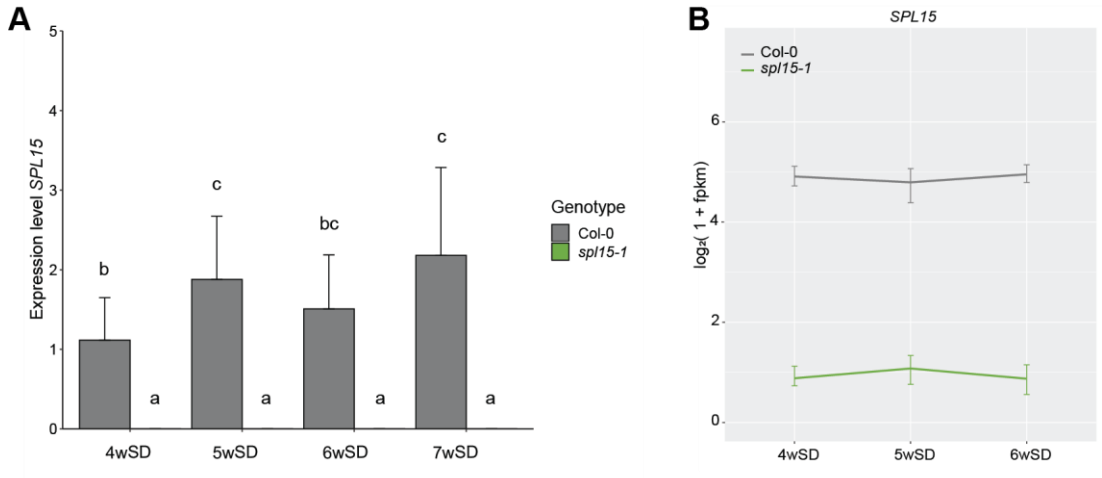

Fig. S4.7. Expression of *SPL15* in Col-0 and *spl15-1* in SD conditions. (**A**) QRT-PCR analysis of *SPL15* expression in meristem-enriched material from Col-0 and *spl15-1* at the indicated time points. The variation shown was derived from three independent biological replicates; error bars indicate the standard deviation. Statistical differences were calculated with ANOVA followed by Tukey's HSD (honestly significant difference) test at $p < 0.01$. (**B**) Expression of *SPL15* over time in Col-0 and *spl15-1* from the transcriptome analysis. Plotted are globally normalised log_2-transformed FPKM values. The variation shown is the standard deviation for three independent biological replicates.

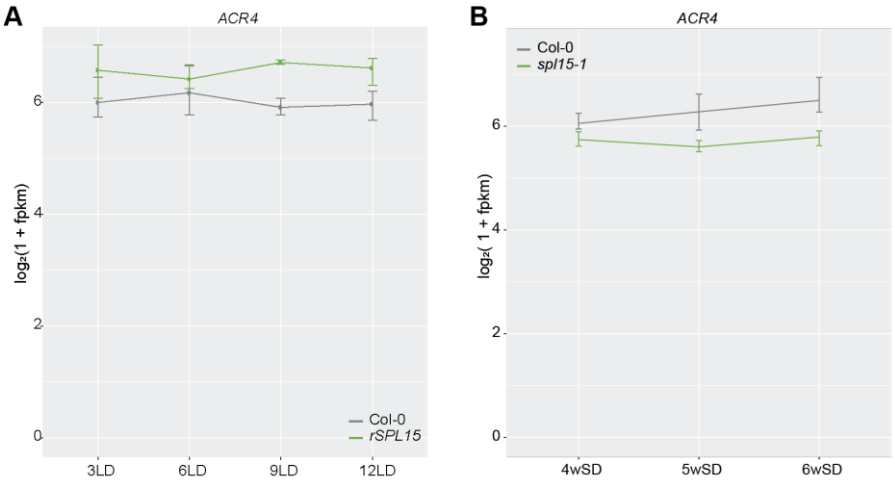

Fig. S4.8 Expression patterns of *ACR4* in the LD and SD transcriptome analyses. (**A**) Expression of *ACR4* over time in Col-0 and *rSPL15* from the LD transcriptome analysis. The variation shown is the standard deviation for four independent biological replicates. (**B**) Expression of *ACR4* over time in Col-0 and *spl15-1* from the SD transcriptome analysis. The variation shown is the standard deviation for three independent biological replicates. Plotted are globally normalised log_2-transformed FPKM values.

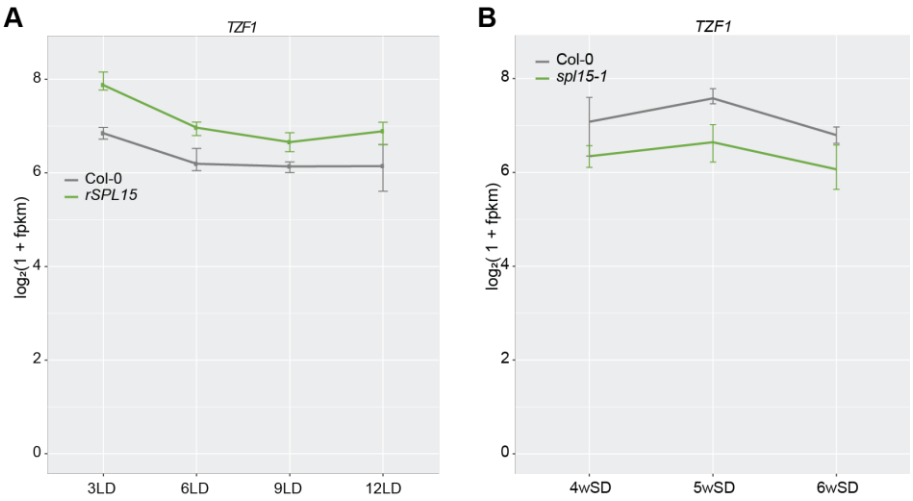

Fig. S4.9 Expression patterns of *TZF1* in the LD and SD transcriptome analyses. (**A**) Expression of *TZF1* over time in Col-0 and *rSPL15* from the LD transcriptome analysis. The variation shown is the standard deviation for four independent biologial replicates. (**B**) Expression of *TZF1* over time in Col-0 and *spl15-1* from the SD transcriptome analysis. The variation shown is the standard deviation for three independent biological replicates. Plotted are globally normalised log_2-transformed FPKM values.

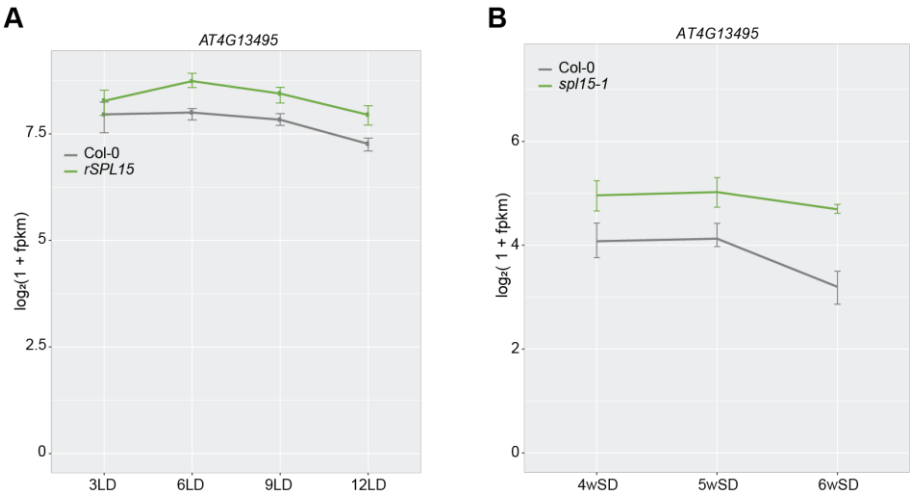

Fig. S4.10 Expression patterns of *AT4G13495* in the LD and SD transcriptome analyses. (**A**) Expression of *AT4G13495* over time in Col-0 and *rSPL15* from the LD transcriptome analysis. The variation shown is the standard deviation for four independent biologial replicates. (**B**) Expression of *AT4G13495* over time in Col-0 and *spl15-1* from the SD transcriptome analysis. The variation shown is the standard deviation for three independent biological replicates. Plotted are globally normalised log_2-transformed FPKM values.

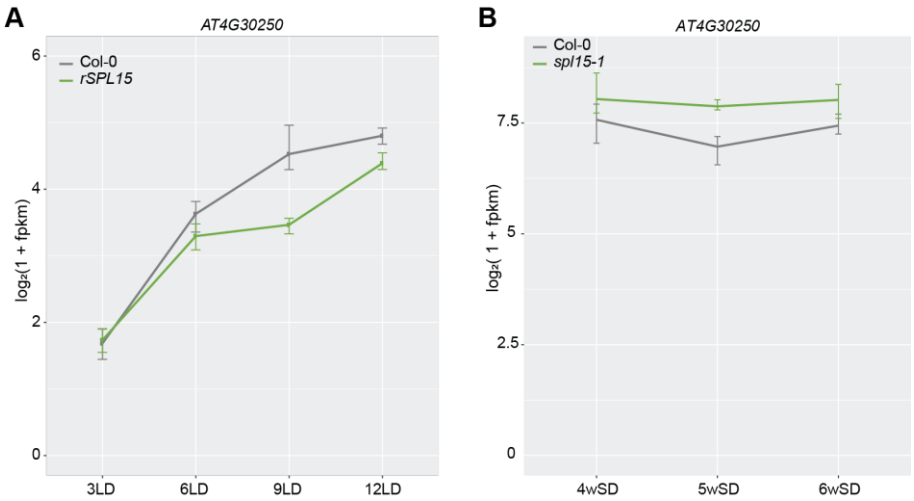

Fig. S4.11. Expression patterns of *AT4G30250* in the LD and SD transcriptome analyses. (**A**) Expression of *AT4G30250* over time in Col-0 and *rSPL15* from the LD transcriptome analysis. The variation shown is the standard deviation for four independent biologial replicates. (**B**) Expression of *AT4G30250* over time in Col-0 and *spl15-1* from the SD transcriptome analysis. The variation shown is the standard deviation for three independent biological replicates. Plotted are globally normalised log_2-transformed FPKM values.

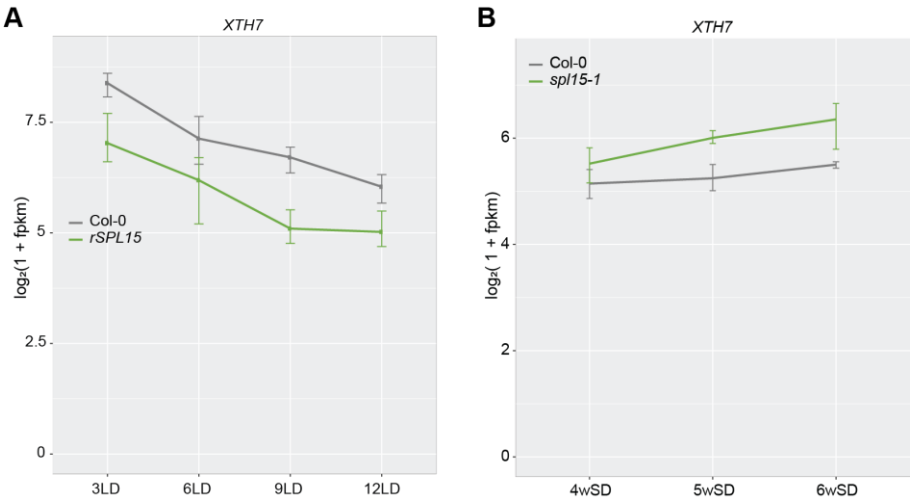

Fig. S4.12. Expression patterns of *XTH7* in the LD and SD transcriptome analyses. (**A**) Expression of *XTH7* over time in Col-0 and *rSPL15* from the LD transcriptome analysis. The variation shown is the standard deviation for four independent biologial replicates. (**B**) Expression of *XTH7* over time in Col-0 and *spl15-1* from the SD transcriptome analysis. The variation shown is the standard deviation for three independent biological replicates. Plotted are globally normalised log_2-transformed FPKM values.

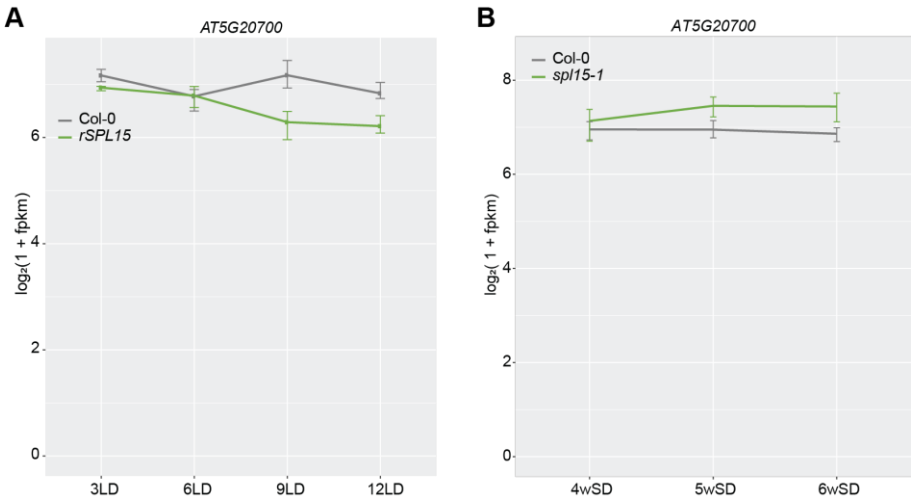

Fig. S4.13. Expression patterns of *AT5G20700* in the LD and SD transcriptome analyses. (**A**) Expression of *AT5G20700* over time in Col-0 and *rSPL15* from the LD transcriptome analysis. The variation shown is the standard deviation for four independent biologial replicates. **(B**) Expression of *AT5G20700* over time in Col-0 and *spl15-1* from the SD transcriptome analysis. The variation shown is the standard deviation for three independent biological replicates. Plotted are globally normalised log_2-transformed FPKM values.

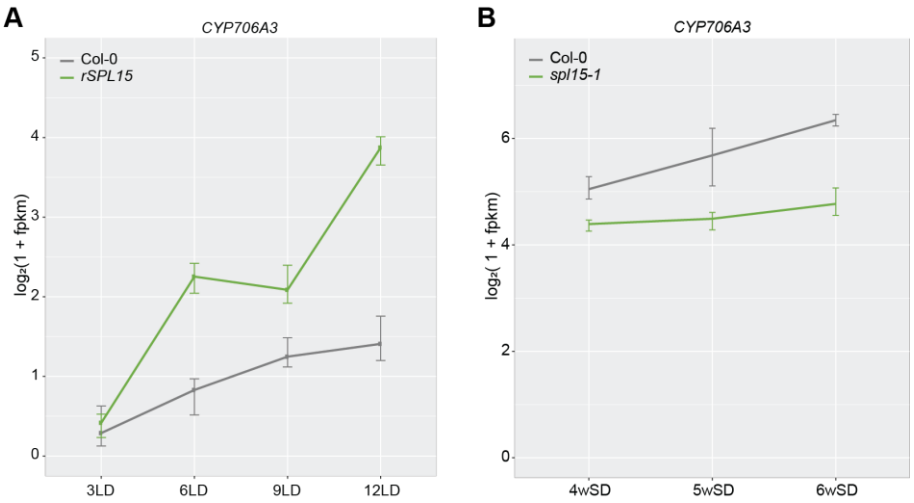

Fig. S4.14. Expression patterns of *CYP706A3* in the LD and SD transcriptome analyses. (**A**) Expression of *CYP706A3* over time in Col-0 and *rSPL15* from the LD transcriptome analysis. The variation shown is the standard deviation for four independent biologial replicates. (**B**) Expression of *CYP706A3* over time in Col-0 and *spl15-1* from the SD transcriptome analysis. The variation shown is the standard deviation for three independent biological replicates. Plotted are globally normalised log_2-transformed FPKM values.

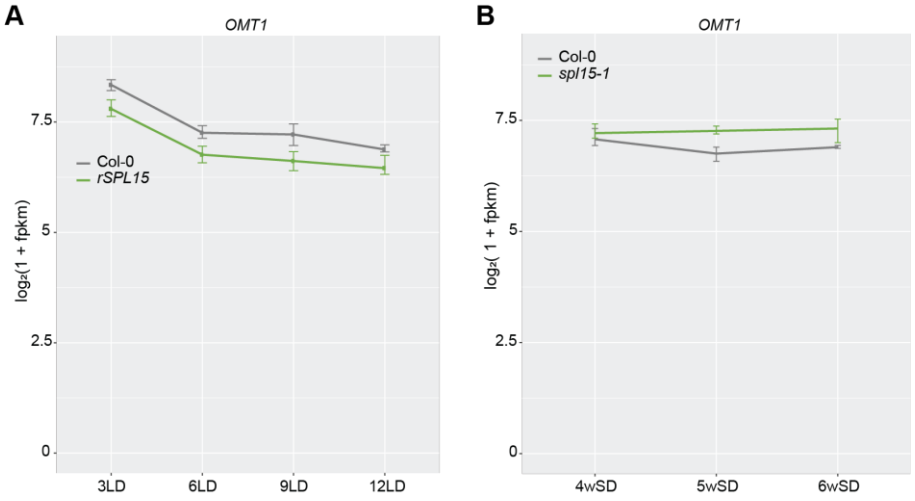

Fig. S4.15. Expression patterns of *OMT1* in the LD and SD transcriptome analyses. (**A**) Expression of *OMT1* over time in Col-0 and *rSPL15* from the LD transcriptome analysis. The variation shown is the standard deviation for four independent biologial replicates. (**B**) Expression of *OMT1* over time in Col-0 and *spl15-1* from the SD transcriptome analysis. The variation shown is the standard deviation for three independent biological replicates. Plotted are globally normalised log_2-transformed FPKM values.

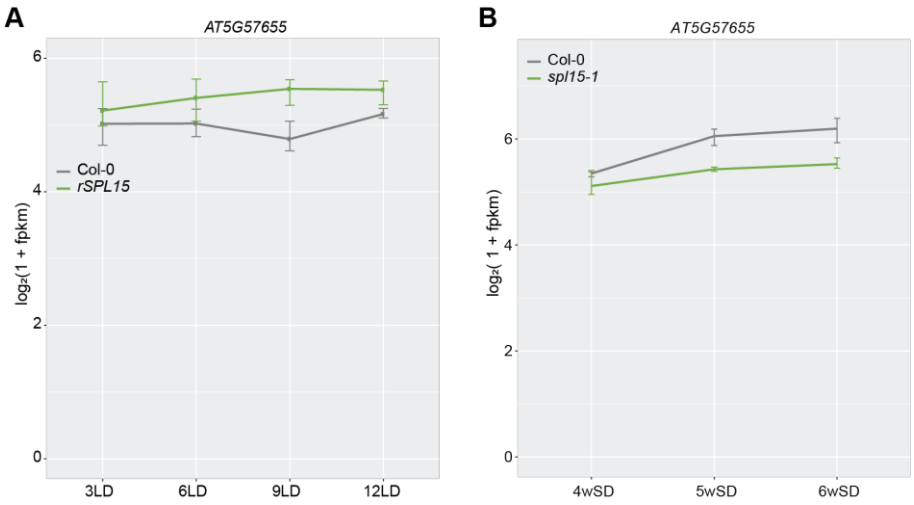

Fig. S4.16. Expression patterns of *AT5G57655* in the LD and SD transcriptome analyses. (**A**) Expression of *AT5G57655* over time in Col-0 and *rSPL15* from the LD transcriptome analysis. The variation shown is the standard deviation for four independent biologial replicates. (**B**) Expression of *AT5G57655* over time in Col-0 and *spl15-1* from the SD transcriptome analysis. The variation shown is the standard deviation for three independent biological replicates. Plotted are globally normalised log_2-transformed FPKM values.

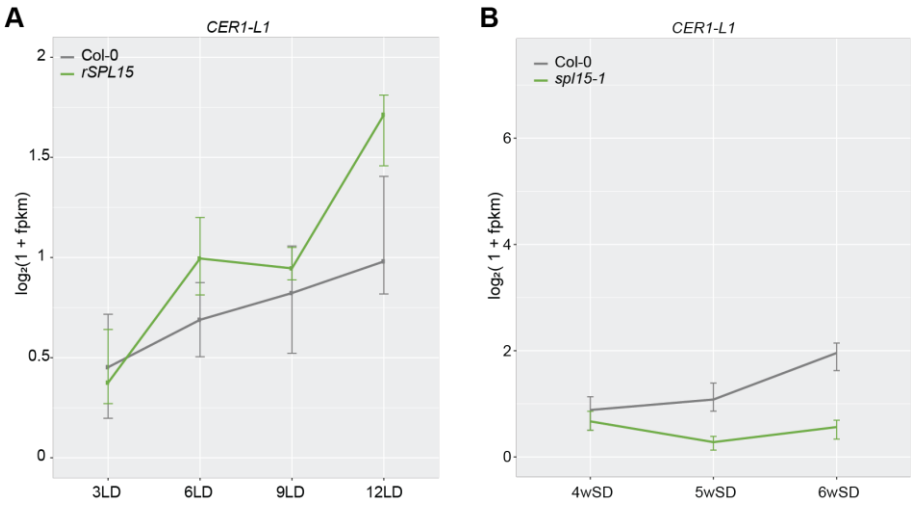

Fig. S4.17. Expression patterns of *CER1-L1* in the LD and SD transcriptome analyses. (**A**) Expression of *CER1-L1* over time in Col-0 and *rSPL15* from the LD transcriptome analysis. The variation shown is the standard deviation for four independent biologial replicates. (**B**) Expression of *CER1-L1* over time in Col-0 and *spl15-1* from the SD transcriptome analysis. The variation shown is the standard deviation for three independent biological replicates. Plotted are globally normalised log_2-transformed FPKM values.

Table S4.1. Differentially expressed genes at 6-, 9-, and/or 12LD involved in flowering-time regulation. A list of all DEGs (*p*adj < 0.05) between Col-0 and *rSPL15* at time point 6LD, 9LD and/or 12LD which are also related to flowering time regulation. BaseMean= Mean of normalised counts for all samples, log_2FoldChange= Log_2 Fold Change relative to Col-0, lfcSE= Standard error of Log_2 Fold Change, stat= Wald statistic for comparing expression in Col-0 to that of rSPL15, pvalue= *p-value* for Wald test, padj= Adjusted *p*-value using Benjamini-Hochberg correction for multiple testing (used to determine significance of expression differences), DEG at time point= Time point at which gene is statistically significantly differentially expressed (*p*adj < 0.05). Results file generated with DESeq2 software.

AGI-code	Gene symbol	TAIR computational description (Source: Araport11)	baseMean	log_2FoldChange	lfcSE	stat	pvalue	padj	DEG at time point
AT1G04400	*CRY2*	*cryptochrome 2*	*790.53*	*0.34*	*0.09*	*3.58*	*3.39E-04*	*3.50E-03*	*6LD*
AT1G19330	*AT1G19330*	*histone deacetylase complex subunit*	*120.15*	*0.53*	*0.17*	*3.14*	*1.71E-03*	*1.35E-02*	*6LD*
AT1G24260	*SEP3*	*K-box region and MADS-box transcription factor family protein*	*39.06*	*-1.92*	*0.39*	*-4.91*	*9.05E-07*	*2.13E-05*	*6LD*
AT1G25540	*PFT1*	*phytochrome and flowering time regulatory protein (PFT1)*	*307.84*	*-0.26*	*0.10*	*-2.73*	*6.40E-03*	*3.85E-02*	*6LD*
AT1G32640	*MYC2*	*Basic helix-loop-helix (bHLH) DNA-binding family protein*	*329.06*	*1.12*	*0.39*	*2.89*	*3.88E-03*	*2.59E-02*	*6LD*
AT1G51140	*FBH3*	*basic helix-loop-helix (bHLH) DNA-binding superfamily protein*	*171.52*	*0.59*	*0.14*	*4.27*	*1.96E-05*	*3.06E-04*	*6LD*
AT1G53090	*SPA4*	*SPA1-related 4*	*163.56*	*0.42*	*0.14*	*2.98*	*2.90E-03*	*2.06E-02*	*6LD*
AT1G53160	*SPL4*	*squamosa promoter binding protein-like 4*	*18.69*	*1.93*	*0.57*	*3.40*	*6.73E-04*	*2.63E-02*	*9LD*
AT1G53160	*SPL4*	*squamosa promoter binding protein-like 4*	*40.39*	*1.35*	*0.30*	*4.51*	*6.63E-06*	*1.08E-03*	*12LD*
AT1G69570	*AT1G69570*	*Dof-type zinc finger DNA-binding family protein*	*28.54*	*-1.48*	*0.44*	*-3.38*	*7.19E-04*	*6.54E-03*	*6LD*
AT1G69690	*TCP15*	*TCP family transcription factor*	*249.84*	*-0.59*	*0.18*	*-3.26*	*1.13E-03*	*3.82E-02*	*9LD*
AT1G78580	*TPS1*	*trehalose-6-phosphate synthase*	*686.88*	*0.30*	*0.09*	*3.48*	*5.01E-04*	*4.87E-03*	*6LD*
AT1G79460	*GA2*	*Terpenoid cyclases/Protein prenyltransferases superfamily protein*	*159.28*	*0.49*	*0.15*	*3.27*	*1.06E-03*	*9.08E-03*	*6LD*
AT2G22540	*SVP*	*K-box region and MADS-box transcription factor family protein*	*573.27*	*0.40*	*0.09*	*4.32*	*1.56E-05*	*2.51E-04*	*6LD*
AT2G22540	*SVP*	*K-box region and MADS-box transcription factor family protein*	*710.65*	*0.37*	*0.09*	*4.20*	*2.67E-05*	*3.40E-03*	*12LD*
AT2G24790	*COL3*	*CONSTANS-like 3*	*1102.01*	*0.20*	*0.08*	*2.63*	*8.54E-03*	*4.80E-02*	*6LD*
AT2G39250	*SNZ*	*Integrase-type DNA-binding superfamily protein*	*210.09*	*0.66*	*0.14*	*4.73*	*2.20E-06*	*4.52E-05*	*6LD*
AT2G41370	*BOP2*	*Ankyrin repeat family protein / BTB/POZ domain-containing protein*	*200.08*	*0.97*	*0.16*	*6.04*	*1.55E-09*	*7.22E-08*	*6LD*
AT2G42280	*FBH4*	*basic helix-loop-helix (bHLH) DNA-binding superfamily protein*	*99.78*	*-0.70*	*0.16*	*-4.27*	*1.94E-05*	*3.04E-04*	*6LD*
AT2G43010	*PIF4*	*phytochrome interacting factor 4*	*821.05*	*0.45*	*0.12*	*3.62*	*3.00E-04*	*3.17E-03*	*6LD*
AT2G44745	*WRKY12*	*WRKY family transcription factor*	*23.38*	*-1.69*	*0.48*	*-3.55*	*3.87E-04*	*1.71E-02*	*9LD*
AT2G45660	*AGL20*	*AGAMOUS-like 20*	*56.14*	*1.86*	*0.28*	*6.72*	*1.86E-11*	*1.33E-09*	*6LD*
AT2G45660	*AGL20*	*AGAMOUS-like 20*	*100.76*	*1.03*	*0.26*	*3.98*	*6.87E-05*	*4.38E-03*	*9LD*
AT2G45660	*AGL20*	*AGAMOUS-like 20*	*162.52*	*0.87*	*0.14*	*6.35*	*2.17E-10*	*1.17E-07*	*12LD*
AT3G04240	*SEC*	*Tetratricopeptide repeat (TPR)-like superfamily protein*	*671.46*	*0.21*	*0.07*	*3.01*	*2.63E-03*	*1.91E-02*	*6LD*
AT3G04910	*WNK1*	*with no lysine (K) kinase 1*	*858.13*	*0.51*	*0.12*	*4.25*	*2.10E-05*	*3.26E-04*	*6LD*

AT3G10390	*FLD*	*protein FLOWERING locus D-like protein*	*303.21*	*-0.33*	*0.10*	*-3.38*	*7.27E-04*	*6.60E-03*	*6LD*
AT3G15030	*TCP4*	*TCP family transcription factor 4*	*504.83*	*-1.09*	*0.12*	*-9.18*	*4.25E-20*	*1.67E-17*	*6LD*
AT3G15354	*SPA3*	*SPA1-related 3*	*495.05*	*0.26*	*0.09*	*2.77*	*5.67E-03*	*3.50E-02*	*6LD*
AT3G16470	*JR1*	*Mannose-binding lectin superfamily protein*	*1814.29*	*0.90*	*0.15*	*6.16*	*7.05E-10*	*3.57E-08*	*6LD*
AT3G16470	*JR1*	*Mannose-binding lectin superfamily protein*	*1612.52*	*-0.57*	*0.18*	*-3.16*	*1.58E-03*	*4.84E-02*	*9LD*
AT3G19290	*ABF4*	*ABRE binding factor 4*	*303.75*	*0.38*	*0.10*	*3.96*	*7.45E-05*	*9.58E-04*	*6LD*
AT3G47500	*CDF3*	*cycling DOF factor 3*	*656.61*	*0.35*	*0.10*	*3.29*	*9.88E-04*	*8.54E-03*	*6LD*
AT3G54990	*SMZ*	*Integrase-type DNA-binding superfamily protein*	*100.28*	*0.58*	*0.20*	*2.89*	*3.89E-03*	*2.59E-02*	*6LD*
AT3G54990	*SMZ*	*Integrase-type DNA-binding superfamily protein*	*78.92*	*-1.12*	*0.27*	*-4.12*	*3.81E-05*	*2.74E-03*	*9LD*
AT3G57920	*SPL15*	*squamosa promoter binding protein-like 15*	*433.02*	*4.50*	*0.20*	*21.94*	*1.01E-106*	*1.99E-102*	*6LD*
AT3G57920	*SPL15*	*squamosa promoter binding protein-like 15*	*260.50*	*3.26*	*0.20*	*16.01*	*1.02E-57*	*1.88E-53*	*9LD*
AT3G57920	*SPL15*	*squamosa promoter binding protein-like 15*	*313.87*	*3.36*	*0.16*	*20.45*	*6.44E-93*	*1.25E-88*	*12LD*
AT3G59060	*PIL6*	*phytochrome interacting factor 3-like 6*	*903.89*	*0.41*	*0.09*	*4.43*	*9.50E-06*	*1.63E-04*	*6LD*
AT3G63010	*GID1B*	*alpha/beta-Hydrolases superfamily protein*	*68.91*	*0.71*	*0.22*	*3.16*	*1.57E-03*	*1.26E-02*	*6LD*
AT4G08920	*CRY1*	*cryptochrome 1*	*1015.63*	*0.27*	*0.07*	*3.92*	*8.94E-05*	*1.12E-03*	*6LD*
AT4G17880	*MYC4*	*Basic helix-loop-helix (bHLH) DNA-binding family protein*	*218.06*	*-0.60*	*0.18*	*-3.35*	*7.98E-04*	*2.96E-02*	*9LD*
AT4G26150	*CGA1*	*cytokinin-responsive gata factor 1*	*120.08*	*-1.06*	*0.23*	*-4.54*	*5.54E-06*	*1.01E-04*	*6LD*
AT4G31877	*MIR156C*	*microRNA ath-MIR156c precursor*	*24.42*	*1.24*	*0.37*	*3.39*	*6.88E-04*	*6.33E-03*	*6LD*
AT4G34000	*ABF3*	*abscisic acid responsive elements-binding factor 3*	*335.09*	*0.90*	*0.11*	*7.91*	*2.56E-15*	*3.79E-13*	*6LD*
AT4G34400	*TFS1*	*AP2/B3-like transcriptional factor family protein*	*99.56*	*3.51*	*0.32*	*10.88*	*1.49E-27*	*1.55E-24*	*6LD*
AT4G34400	*TFS1*	*AP2/B3-like transcriptional factor family protein*	*57.14*	*1.65*	*0.33*	*5.04*	*4.65E-07*	*6.56E-05*	*9LD*
AT4G34400	*TFS1*	*AP2/B3-like transcriptional factor family protein*	*129.10*	*2.68*	*0.23*	*11.43*	*3.09E-30*	*8.55E-27*	*12LD*
AT4G34530	*CIB1*	*cryptochrome-interacting basic-helix-loop-helix 1*	*152.43*	*-0.62*	*0.22*	*-2.84*	*4.57E-03*	*2.95E-02*	*6LD*
AT4G35900	*FD*	*Basic-leucine zipper (bZIP) transcription factor family protein*	*69.12*	*1.86*	*0.25*	*7.29*	*3.14E-13*	*3.08E-11*	*6LD*
AT4G35900	*FD*	*Basic-leucine zipper (bZIP) transcription factor family protein*	*99.34*	*1.02*	*0.19*	*5.43*	*5.72E-08*	*1.91E-05*	*12LD*
AT4G36920	*AP2*	*Integrase-type DNA-binding superfamily protein*	*351.49*	*0.50*	*0.15*	*3.37*	*7.47E-04*	*6.75E-03*	*6LD*
AT4G39100	*SHL1*	*PHD finger family protein / bromo-adjacent homology (BAH) domain-containing protein*	*241.76*	*0.33*	*0.11*	*3.10*	*1.93E-03*	*1.48E-02*	*6LD*
AT5G02030	*RPL*	*POX (plant homeobox) family protein*	*220.32*	*0.60*	*0.17*	*3.60*	*3.15E-04*	*3.30E-03*	*6LD*
AT5G02030	*RPL*	*POX (plant homeobox) family protein*	*261.72*	*0.42*	*0.12*	*3.40*	*6.74E-04*	*3.76E-02*	*12LD*
AT5G03840	*TFL1*	*PEBP (phosphatidylethanolamine-binding protein) family protein*	*11.66*	*2.00*	*0.55*	*3.65*	*2.62E-04*	*2.82E-03*	*6LD*
AT5G03840	*TFL1*	*PEBP (phosphatidylethanolamine-binding protein) family protein*	*15.38*	*2.10*	*0.48*	*4.35*	*1.39E-05*	*1.98E-03*	*12LD*
AT5G10140	*FLC*	*K-box region and MADS-box transcription factor family protein*	*130.10*	*1.65*	*0.20*	*8.24*	*1.67E-16*	*3.02E-14*	*6LD*

AT5G10140	*FLC*	*K-box region and MADS-box transcription factor family protein*	*106.20*	*0.79*	*0.24*	*3.32*	*9.00E-04*	*3.21E-02*	*9LD*
AT5G10140	*FLC*	*K-box region and MADS-box transcription factor family protein*	*127.02*	*1.00*	*0.21*	*4.78*	*1.79E-06*	*3.63E-04*	*12LD*
AT5G24860	*FPF1*	*flowering promoting factor 1*	*6.69*	*4.89*	*1.13*	*4.33*	*1.52E-05*	*2.13E-03*	*12LD*
AT5G39660	*CDF2*	*cycling DOF factor 2*	*166.77*	*0.88*	*0.13*	*6.65*	*2.90E-11*	*1.96E-09*	*6LD*
AT5G41190	*AT5G41190*	*RNA-binding NOB1-like protein*	*753.79*	*-0.37*	*0.07*	*-4.97*	*6.59E-07*	*1.61E-05*	*6LD*
AT5G43270	*SPL2*	*squamosa promoter binding protein-like 2*	*226.73*	*0.36*	*0.13*	*2.78*	*5.50E-03*	*3.42E-02*	*6LD*
AT5G46760	*MYC3*	*Basic helix-loop-helix (bHLH) DNA-binding family protein*	*484.13*	*0.33*	*0.10*	*3.35*	*7.97E-04*	*7.14E-03*	*6LD*
AT5G47640	*NF-YB2*	*nuclear factor Y, subunit B2*	*207.37*	*0.69*	*0.19*	*3.73*	*1.95E-04*	*2.18E-03*	*6LD*
AT5G51810	*GA20OX2*	*gibberellin 20 oxidase 2*	*24.81*	*-1.62*	*0.48*	*-3.33*	*8.62E-04*	*3.12E-02*	*9LD*
AT5G57660	*COL5*	*CONSTANS-like 5*	*1189.19*	*0.46*	*0.12*	*3.81*	*1.39E-04*	*1.64E-03*	*6LD*
AT5G60120	*TOE2*	*target of early activation tagged (EAT) 2*	*331.05*	*-0.37*	*0.13*	*-2.86*	*4.23E-03*	*2.78E-02*	*6LD*
AT5G60120	*TOE2*	*target of early activation tagged (EAT) 2*	*357.85*	*-1.09*	*0.15*	*-7.36*	*1.79E-13*	*1.32E-10*	*9LD*
AT5G60120	*TOE2*	*target of early activation tagged (EAT) 2*	*345.01*	*-0.77*	*0.11*	*-6.82*	*9.20E-12*	*5.94E-09*	*12LD*
AT5G60910	*AGL8*	*AGAMOUS-like 8*	*28.77*	*1.75*	*0.37*	*4.68*	*2.83E-06*	*5.22E-04*	*12LD*
AT5G61850	*LFY*	*floral meristem identity control protein LEAFY (LFY)*	*16.81*	*1.35*	*0.42*	*3.18*	*1.45E-03*	*1.18E-02*	*6LD*
AT5G61850	*LFY*	*floral meristem identity control protein LEAFY (LFY)*	*34.66*	*1.56*	*0.32*	*4.86*	*1.16E-06*	*2.62E-04*	*12LD*
AT5G62165	*AGL42*	*AGAMOUS-like 42*	*4.77*	*3.62*	*1.23*	*2.94*	*3.27E-03*	*2.27E-02*	*6LD*
AT5G62165	*AGL42*	*AGAMOUS-like 42*	*37.92*	*2.69*	*0.38*	*7.11*	*1.18E-12*	*9.97E-10*	*12LD*
AT5G62430	*CDF1*	*cycling DOF factor 1*	*111.20*	*-0.83*	*0.23*	*-3.67*	*2.40E-04*	*1.20E-02*	*9LD*
AT5G67180	*TOE3*	*target of early activation tagged (EAT) 3*	*42.58*	*1.22*	*0.31*	*3.87*	*1.09E-04*	*1.34E-03*	*6LD*
AT5G67180	*TOE3*	*target of early activation tagged (EAT) 3*	*52.29*	*1.59*	*0.40*	*3.99*	*6.56E-05*	*4.27E-03*	*9LD*

Table S4.2. Differentially expresed genes that are co-expressed with *FUL* and differentially expressed at 4-, 5- and/or 6wSD. A list of all DEGs (*p*adj<0.05) that were differenftially expressed between Col-0 and *rSPL15* at time points 6-, 9- and/or 12LD and that were positively or negatively co-expressed with *FUL*. BaseMean= Mean of normalised counts for all samples, log_2FoldChange= Log_2 Fold Change relative to Col-0, lfcSE= Standard error of Log_2 Fold Change, stat= Wald statistic for comparing expression in Col-0 to that of *rSPL15*, pvalue= *p-value* for Wald test, padj= Adjusted *p*-value using Benjamini-Hochberg correction for multiple testing (used to determine significance of expression differences), DEG at time point= Time point at which gene is statistically significantly differentially expressed (*p*adj < 0.05). Results file generated with DESeq2 software.

AGI-code	Gene symbol	TAIR computational description (Source: Araport11)	baseMean	log2FoldChange	lfcSE	stat	pvalue	padj	DEG at time point
AT1G06760	*AT1G06760*	*winged-helix DNA-binding transcription factor family protein*	3478.52	0.28	0.07	4.11	3.91E-05	4.6E-03	12LD
AT1G07820	*AT1G07820*	*Histone superfamily protein*	1472.88	0.33	0.10	3.29	1.02E-03	3.5E-02	9LD
AT1G09200	*AT1G09200*	*Histone superfamily protein*	1843.51	0.37	0.10	3.61	3.02E-04	1.4E-02	9LD
AT1G14700	*PAP3*	*purple acid phosphatase 3*	327.14	0.39	0.15	2.67	7.67E-03	4.4E-02	6LD
AT1G14700	*PAP3*	*purple acid phosphatase 3*	173.64	-0.84	0.19	-4.33	1.49E-05	1.2E-03	9LD
AT1G53160	*SPL4*	*squamosa promoter binding protein-like 4*	18.69	1.93	0.57	3.40	6.73E-04	2.6E-02	9LD
AT1G53160	*SPL4*	*squamosa promoter binding protein-like 4*	40.39	1.35	0.30	4.51	6.63E-06	1.1E-03	12LD
AT1G68130	*IDD14*	*indeterminate(ID)-domain 14*	201.60	0.44	0.14	3.14	1.71E-03	1.3E-02	6LD
AT2G33620	*AT2G33620*	*AT hook motif DNA-binding family protein*	682.64	0.39	0.07	5.27	1.39E-07	4.0E-06	6LD
AT2G33620	*AT2G33620*	*AT hook motif DNA-binding family protein*	1151.68	0.30	0.08	3.70	2.17E-04	1.6E-02	12LD
AT2G40610	*EXPA8*	*expansin A8*	129.41	-1.06	0.29	-3.62	3.00E-04	1.4E-02	9LD
AT2G43910	*HOL1*	*HARMLESS TO OZONE LAYER 1*	1272.00	-0.41	0.12	-3.54	4.04E-04	1.8E-02	9LD
AT3G16450	*JAL33*	*Mannose-binding lectin superfamily protein*	455.74	-1.43	0.18	-7.74	9.59E-15	1.3E-11	9LD
AT3G16460	*JAL34*	*Mannose-binding lectin superfamily protein*	1180.13	-1.15	0.20	-5.63	1.84E-08	3.7E-06	9LD
AT3G16460	*JAL34*	*Mannose-binding lectin superfamily protein*	777.60	-0.44	0.12	-3.74	1.84E-04	1.5E-02	12LD
AT3G20370	*AT3G20370*	*TRAF-like family protein*	176.70	-1.68	0.20	-8.29	1.12E-16	2.1E-13	9LD
AT3G20670	*HTA13*	*histone H2A 13*	996.28	0.59	0.12	4.98	6.32E-07	8.3E-05	9LD
AT3G20670	*HTA13*	*histone H2A 13*	1130.55	0.33	0.09	3.66	2.55E-04	1.9E-02	12LD
AT3G46490	*AT3G46490*	*2-oxoglutarate (2OG) and Fe(II)-dependent oxygenase superfamily protein*	306.81	-1.28	0.15	-8.59	9.00E-18	2.4E-14	9LD
AT3G48990	*AAE3*	*AMP-dependent synthetase and ligase family protein*	406.95	-0.40	0.11	-3.50	4.65E-04	2.9E-02	12LD
AT3G53730	*AT3G53730*	*Histone superfamily protein*	1817.54	0.40	0.10	3.80	1.46E-04	8.1E-03	9LD
AT3G56080	*AT3G56080*	*S-adenosyl-L-methionine-dependent methyltransferases superfamily protein*	71.34	-1.23	0.26	-4.75	2.03E-06	2.2E-04	9LD
AT3G63440	*CKX6*	*cytokinin oxidase/dehydrogenase 6*	347.13	0.87	0.18	4.95	7.56E-07	1.9E-04	12LD
AT4G01525	*SADHU5-1*	*transposable_element_gene*	36.38	1.13	0.31	3.67	2.43E-04	2.6E-03	6LD

AT4G01525	*SADHU5-1*	*transposable_element_gene*	146.14	0.93	0.21	4.44	8.87E-06	7.9E-04	9LD
AT4G01525	*SADHU5-1*	*transposable_element_gene*	294.43	1.73	0.14	12.18	4.10E-34	2.0E-30	12LD
AT4G12310	*CYP706A5*	*cytochrome P450, family 706, subfamily A, polypeptide 5*	164.58	-0.63	0.18	-3.49	4.90E-04	2.1E-02	9LD
AT4G13575	*AT4G13575*	*hypothetical protein*	154.87	-0.88	0.26	-3.35	8.14E-04	3.0E-02	9LD
AT4G13575	*AT4G13575*	*hypothetical protein*	101.06	-0.70	0.21	-3.33	8.55E-04	4.5E-02	12LD
AT4G40040	*AT4G40040*	*Histone superfamily protein*	3168.96	0.25	0.07	3.76	1.68E-04	1.4E-02	12LD
AT5G10400	*AT5G10400*	*Histone superfamily protein*	1622.84	0.32	0.09	3.48	5.07E-04	3.1E-02	12LD
AT5G15150	*HB-3*	*homeobox 3*	55.99	-1.16	0.31	-3.78	1.54E-04	8.5E-03	9LD
AT5G20740	*AT5G20740*	*Plant invertase/pectin methylesterase inhibitor superfamily protein*	450.72	0.56	0.10	5.68	1.38E-08	5.3E-06	12LD
AT5G22880	*HTB2*	*histone B2*	3191.03	0.49	0.14	3.59	3.27E-04	1.5E-02	9LD
AT5G22880	*HTB2*	*histone B2*	3902.83	0.45	0.13	3.60	3.23E-04	2.2E-02	12LD
AT5G24160	*SQE6*	*squalene monooxygenase 6*	29.95	-1.76	0.43	-4.04	5.34E-05	3.6E-03	9LD
AT5G26280	*AT5G26280*	*TRAF-like family protein*	478.57	-1.34	0.20	-6.76	1.37E-11	1.0E-09	6LD
AT5G26280	*AT5G26280*	*TRAF-like family protein*	145.30	-2.60	0.26	-10.18	2.41E-24	1.5E-20	9LD
AT5G26280	*AT5G26280*	*TRAF-like family protein*	37.81	-1.63	0.29	-5.63	1.83E-08	7.0E-06	12LD
AT5G35700	*FIM5*	*fimbrin-like protein 2*	210.01	-0.45	0.11	-3.90	9.79E-05	9.3E-03	12LD
AT5G59870	*HTA6*	*histone H2A 6*	2424.44	0.40	0.10	3.84	1.25E-04	7.2E-03	9LD
AT5G59970	*AT5G59970*	*Histone superfamily protein*	900.35	0.44	0.11	3.83	1.26E-04	7.2E-03	9LD
AT5G60910	*AGL8*	*AGAMOUS-like 8*	28.77	1.75	0.37	4.68	2.83E-06	5.2E-04	12LD
AT5G62165	*AGL42*	*AGAMOUS-like 42*	37.92	2.69	0.38	7.11	1.18E-12	1.0E-09	12LD

Table S4. 3: Differentially expressed genes at 4-, 5-, and/or 6wSD involved in flowering-time regulation. A list of all DEGs (*p*adj<0.05) between Col-0 and *spl15-1* at time points 4-, 5- and/or 6wSD, which were also related to flowering-time regulation. BaseMean= Mean of normalised counts for all samples, log_2FoldChange= Log_2 Fold Change relative to Col-0, lfcSE= Standard error of Log_2 Fold Change, stat= Wald statistic for comparing expression in Col-0 to that of *spl15-1*, pvalue= *p-value* for Wald test, padj= Adjusted *p*-value using Benjamini-Hochberg correction for multiple testing (used to determine significance of expression differences), DEG at time point= Time point at which gene is statistically significantly differentially expressed (*p*adj < 0.05). Results file generated with DESeq2 software.

AGI-code	Gene symbol	TAIR computational description (Source: Araport11)	baseMean	log2FoldChange	lfcSE	stat	pvalue	padj	DEG at time point
AT1G01060	*LHY*	*Homeodomain-like superfamily protein*	78.85	0.97	0.27	3.63	2.88E-04	1.92E-02	5wSD
AT1G15550	*GA3OX1*	*gibberellin 3-oxidase 1*	1348.11	0.69	0.15	4.48	7.56E-06	1.30E-03	5wSD
AT1G15550	*GA3OX1*	*gibberellin 3-oxidase 1*	1119.02	0.66	0.13	5.00	5.72E-07	1.19E-04	6wSD
AT1G26310	*CAL*	*K-box region and MADS-box transcription factor family protein*	4.49	-5.70	1.54	-3.70	2.19E-04	1.38E-02	6wSD
AT1G53160	*SPL4*	*squamosa promoter binding protein-like 4*	93.90	-5.36	0.86	-6.26	3.82E-10	3.06E-07	5wSD
AT1G53160	*SPL4*	*squamosa promoter binding protein-like 4*	232.69	-6.18	0.37	-16.51	3.14E-61	6.20E-57	6wSD
AT1G69120	*AP1*	*K-box region and MADS-box transcription factor family protein*	40.89	-8.89	1.24	-7.19	6.35E-13	6.27E-10	6wSD
AT1G78580	*TPS1*	*trehalose-6-phosphate synthase*	4773.27	0.45	0.10	4.36	1.30E-05	1.58E-03	6wSD
AT2G21660	*GRP7*	*cold, circadian rhythm, and rna binding 2*	37396.89	-0.74	0.11	-6.55	5.79E-11	6.66E-08	5wSD
AT2G33810	*SPL3*	*squamosa promoter binding protein-like 3*	213.69	-1.67	0.23	-7.13	1.01E-12	9.48E-10	6wSD
AT2G40080	*ELF4*	*EARLY FLOWERING-like protein (DUF1313)*	89.06	-1.11	0.32	-3.52	4.26E-04	2.34E-02	6wSD
AT2G41370	*BOP2*	*Ankyrin repeat family protein / BTB/POZ domain-containing protein*	226.67	-0.58	0.18	-3.32	9.12E-04	4.47E-02	5wSD
AT2G42200	*SPL9*	*squamosa promoter binding protein-like 9*	582.63	-0.61	0.13	-4.56	5.06E-06	7.52E-04	6wSD
AT2G45660	*AGL20*	*AGAMOUS-like 20*	79.08	-1.13	0.30	-3.77	1.63E-04	1.27E-02	5wSD
AT2G45660	*AGL20*	*AGAMOUS-like 20*	85.20	-1.55	0.25	-6.22	4.95E-10	2.64E-07	6wSD
AT2G46340	*SPA1*	*SPA (suppressor of phyA-105) protein family*	608.35	0.44	0.12	3.64	2.74E-04	1.88E-02	5wSD
AT2G46340	*SPA1*	*SPA (suppressor of phyA-105) protein family*	529.44	0.54	0.14	3.86	1.14E-04	8.39E-03	6wSD
AT3G03450	*RGL2*	*RGA-like 2*	118.92	0.79	0.23	3.41	6.50E-04	3.51E-02	5wSD
AT3G15270	*SPL5*	*squamosa promoter binding protein-like 5*	25.98	-3.05	0.52	-5.91	3.50E-09	1.50E-06	6wSD
AT3G15354	*SPA3*	*SPA1-related 3*	161.69	0.97	0.21	4.66	3.20E-06	6.61E-04	5wSD
AT3G15354	*SPA3*	*SPA1-related 3*	160.08	1.09	0.22	5.01	5.52E-07	1.16E-04	6wSD

AT3G18550	*BRC1*	*TCP family transcription factor*	47.88	-2.15	0.42	-5.12	3.11E-07	1.02E-04	5wSD
AT3G20810	*JMJD5*	*2-oxoglutarate (2OG) and Fe(II)-dependent oxygenase superfamily protein*	247.45	-1.77	0.21	-8.47	2.52E-17	1.54E-13	5wSD
AT3G20810	*JMJD5*	*2-oxoglutarate (2OG) and Fe(II)-dependent oxygenase superfamily protein*	128.50	-1.41	0.34	-4.14	3.54E-05	3.39E-03	6wSD
AT3G47500	*CDF3*	*cycling DOF factor 3*	277.07	0.76	0.16	4.79	1.68E-06	3.97E-04	5wSD
AT3G47500	*CDF3*	*cycling DOF factor 3*	237.57	0.72	0.21	3.50	4.63E-04	2.51E-02	6wSD
AT3G57920	*SPL15*	*squamosa promoter binding protein-like 15*	212.36	-5.05	0.30	-16.86	8.56E-64	1.75E-59	4wSD
AT3G57920	*SPL15*	*squamosa promoter binding protein-like 15*	200.10	-4.53	0.29	-15.43	1.00E-53	1.85E-49	5wSD
AT3G57920	*SPL15*	*squamosa promoter binding protein-like 15*	172.31	-5.12	0.32	-15.98	1.65E-57	1.63E-53	6wSD
AT4G34400	*TFS1*	*AP2/B3-like transcriptional factor family protein*	936.73	-0.54	0.11	-5.08	3.68E-07	1.15E-04	5wSD
AT4G34400	*TFS1*	*AP2/B3-like transcriptional factor family protein*	818.23	-1.00	0.14	-7.10	1.24E-12	1.12E-09	6wSD
AT4G35900	*FD*	*Basic-leucine zipper (bZIP) transcription factor family protein*	550.56	-0.56	0.15	-3.65	2.65E-04	1.84E-02	5wSD
AT4G35900	*FD*	*Basic-leucine zipper (bZIP) transcription factor family protein*	482.28	-0.77	0.18	-4.22	2.40E-05	2.51E-03	6wSD
AT5G03840	*TFL1*	*PEBP (phosphatidylethanolamine-binding protein) family protein*	115.49	-1.39	0.22	-6.40	1.57E-10	1.32E-07	5wSD
AT5G15840	*CO*	*B-box type zinc finger protein with CCT domain-containing protein*	70.87	-1.25	0.27	-4.57	4.99E-06	9.46E-04	5wSD
AT5G24470	*PRR5*	*two-component response regulator-like protein*	644.28	-0.69	0.16	-4.33	1.46E-05	1.71E-03	6wSD
AT5G60100	*PRR3*	*pseudo-response regulator 3*	319.07	-0.46	0.14	-3.38	7.26E-04	3.83E-02	5wSD
AT5G60910	*AGL8*	*AGAMOUS-like 8*	38.05	-4.87	0.75	-6.50	8.21E-11	8.39E-08	5wSD
AT5G60910	*AGL8*	*AGAMOUS-like 8*	94.12	-6.06	0.55	-11.08	1.64E-28	6.48E-25	6wSD
AT5G61380	*TOC1*	*CCT motif -containing response regulator protein*	1776.55	-0.41	0.09	-4.37	1.22E-05	1.85E-03	5wSD
AT5G61850	*LFY*	*floral meristem identity control protein LEAFY (LFY)*	99.62	-1.20	0.26	-4.53	5.78E-06	1.09E-03	5wSD
AT5G61850	*LFY*	*floral meristem identity control protein LEAFY (LFY)*	118.45	-1.97	0.23	-8.47	2.38E-17	4.70E-14	6wSD
AT5G62165	*AGL42*	*AGAMOUS-like 42*	209.76	-1.32	0.21	-6.23	4.73E-10	3.62E-07	5wSD
AT5G62165	*AGL42*	*AGAMOUS-like 42*	255.07	-1.13	0.17	-6.64	3.19E-11	2.17E-08	6wSD
AT5G67180	*TOE3*	*target of early activation tagged (EAT) 3*	64.97	-1.53	0.35	-4.37	1.22E-05	1.50E-03	6wSD

Table S4. 4. DEGs that are co-expressed with *FUL* and differentially expressed at 4-, 5- and/or 6wSD. Table displaying all DEGs (*p*adj < 0.05) that were differenftially expressed (DE) between Col-0 and *spl15-1* at time point 4-, 5- and/or 6wSD, and were positively or negatively co-expressed with *FUL*. BaseMean= Mean of normalised counts for all samples, log_2FoldChange= Log_2 Fold Change relative to Col-0, lfcSE= Standard error of Log_2 Fold Change, stat= Wald statistic for comparing expression in Col-0 to that of *spl15-1*, pvalue= *p-value* for Wald test, padj= Adjusted *p*-value using Benjamini-Hochberg correction for multiple testing (used to determine significance of expression differences), DEG at time point= Time point at which gene is statistically significantly differentially expressed (*p*adj < 0.05). Results file generated with DESeq2 software.

AGI-code	Gene symbol	TAIR computational description (Source: Araport11)	baseMean	log2FoldChange	lfcSE	stat	pvalue	padj	DEG at time point
AT1G02065	*SPL8*	*squamosa promoter binding protein-like 8*	106.87	-1.37	0.28	-4.90	9.37E-07	2.5E-04	5wSD
AT1G02065	*SPL8*	*squamosa promoter binding protein-like 8*	153.82	-1.92	0.22	-8.88	6.52E-19	1.6E-15	6wSD
AT1G02190	*AT1G02190*	*Fatty acid hydroxylase superfamily*	16.95	-2.47	0.63	-3.90	9.60E-05	8.7E-03	5wSD
AT1G02190	*AT1G02190*	*Fatty acid hydroxylase superfamily*	34.26	-2.58	0.45	-5.74	9.35E-09	3.5E-06	6wSD
AT1G03710	*AT1G03710*	*Cystatin/monellin superfamily protein*	42.70	-1.17	0.35	-3.35	7.96E-04	4.0E-02	5wSD
AT1G03710	*AT1G03710*	*Cystatin/monellin superfamily protein*	36.95	-1.68	0.38	-4.40	1.08E-05	1.4E-03	6wSD
AT1G12430	*ARK3*	*armadillo repeat kinesin 3*	1153.68	-0.40	0.11	-3.75	1.80E-04	1.2E-02	6wSD
AT1G25480	*AT1G25480*	*aluminum activated malate transporter family protein*	73.29	-0.97	0.29	-3.37	7.61E-04	3.6E-02	6wSD
AT1G26260	*CIB5*	*cryptochrome-interacting basic-helix-loop-helix 5*	259.12	-0.57	0.16	-3.55	3.84E-04	2.3E-02	5wSD
AT1G26260	*CIB5*	*cryptochrome-interacting basic-helix-loop-helix 5*	215.35	-0.66	0.18	-3.71	2.10E-04	1.3E-02	6wSD
AT1G26310	*CAL*	*K-box region and MADS-box transcription factor family protein*	4.49	-5.70	1.54	-3.70	2.19E-04	1.4E-02	6wSD
AT1G26960	*AtHB23*	*homeobox protein 23*	43.91	-1.52	0.34	-4.50	6.93E-06	1.2E-03	5wSD
AT1G26960	*AtHB23*	*homeobox protein 23*	75.11	-1.76	0.30	-5.82	5.76E-09	2.4E-06	6wSD
AT1G50280	*AT1G50280*	*Phototropic-responsive NPH3 family protein*	26.08	-1.76	0.44	-3.96	7.44E-05	6.2E-03	6wSD
AT1G53160	*SPL4*	*squamosa promoter binding protein-like 4*	93.90	-5.36	0.86	-6.26	3.82E-10	3.1E-07	5wSD
AT1G53160	*SPL4*	*squamosa promoter binding protein-like 4*	232.69	-6.18	0.37	-16.51	3.14E-61	6.2E-57	6wSD
AT1G56430	*NAS4*	*nicotianamine synthase 4*	274.34	0.94	0.22	4.37	1.25E-05	1.9E-03	5wSD
AT1G56430	*NAS4*	*nicotianamine synthase 4*	194.65	1.40	0.18	7.76	8.26E-15	1.0E-11	6wSD
AT1G69040	*ACR4*	*ACT domain repeat 4*	767.91	-0.71	0.16	-4.43	9.46E-06	1.5E-03	5wSD
AT1G69040	*ACR4*	*ACT domain repeat 4*	736.35	-0.75	0.17	-4.27	1.95E-05	2.1E-03	6wSD
AT1G69120	*AP1*	*K-box region and MADS-box transcription factor family protein*	40.89	-8.89	1.24	-7.19	6.35E-13	6.3E-10	6wSD

AT1G69600	*ZFHD1*	*zinc finger homeodomain 1*	169.26	-0.80	0.19	-4.13	3.62E-05	4.1E-03	5wSD
AT1G69600	*ZFHD1*	*zinc finger homeodomain 1*	159.16	-0.91	0.21	-4.34	1.43E-05	1.7E-03	6wSD
AT1G75170	*AT1G75170*	*Sec14p-like phosphatidylinositol transfer family protein*	254.42	-0.97	0.20	-4.77	1.87E-06	4.3E-04	5wSD
AT1G75170	*AT1G75170*	*Sec14p-like phosphatidylinositol transfer family protein*	250.59	-1.03	0.18	-5.64	1.65E-08	5.7E-06	6wSD
AT2G16210	*AT2G16210*	*Transcriptional factor B3 family protein*	12.85	-4.65	1.01	-4.61	4.07E-06	6.3E-04	6wSD
AT2G17770	*BZIP27*	*basic region/leucine zipper motif 27*	91.87	-1.37	0.28	-4.91	9.31E-07	1.8E-04	6wSD
AT2G21220	*AT2G21220*	*SAUR-like auxin-responsive protein family*	12.44	-2.68	0.72	-3.72	1.96E-04	1.3E-02	6wSD
AT2G23760	*BLH4*	*BEL1-like homeodomain 4*	129.38	1.01	0.22	4.59	4.36E-06	6.6E-04	6wSD
AT2G30370	*CHAL*	*allergen-like protein*	62.27	-1.04	0.30	-3.43	5.93E-04	3.0E-02	6wSD
AT2G30540	*AT2G30540*	*Thioredoxin superfamily protein*	71.31	1.01	0.29	3.49	4.84E-04	2.8E-02	5wSD
AT2G35820	*AT2G35820*	*ureidoglycolate hydrolase*	46.16	-1.27	0.36	-3.56	3.67E-04	2.3E-02	5wSD
AT2G35820	*AT2G35820*	*ureidoglycolate hydrolase*	63.92	-1.40	0.39	-3.56	3.75E-04	2.1E-02	6wSD
AT2G44910	*HB4*	*homeobox-leucine zipper protein 4*	210.80	-0.78	0.18	-4.33	1.49E-05	2.2E-03	5wSD
AT2G44910	*HB4*	*homeobox-leucine zipper protein 4*	196.11	-0.84	0.19	-4.50	6.85E-06	9.3E-04	6wSD
AT2G45650	*AGL6*	*AGAMOUS-like 6*	6.51	-6.24	1.46	-4.29	1.83E-05	2.0E-03	6wSD
AT2G45660	*AGL20*	*AGAMOUS-like 20*	79.08	-1.13	0.30	-3.77	1.63E-04	1.3E-02	5wSD
AT2G45660	*AGL20*	*AGAMOUS-like 20*	85.20	-1.55	0.25	-6.22	4.95E-10	2.6E-07	6wSD
AT3G02170	*LNG2*	*longifolia2*	187.61	-1.08	0.25	-4.23	2.30E-05	3.0E-03	5wSD
AT3G02170	*LNG2*	*longifolia2*	336.68	-1.84	0.42	-4.34	1.42E-05	1.7E-03	6wSD
AT3G05790	*LON4*	*lon protease 4*	24.78	-1.97	0.49	-4.05	5.21E-05	4.6E-03	6wSD
AT3G06160	*AT3G06160*	*AP2/B3-like transcriptional factor family protein*	83.45	-1.09	0.25	-4.41	1.05E-05	1.4E-03	6wSD
AT3G14310	*PME3*	*pectin methylesterase 3*	5098.84	0.31	0.10	3.29	1.02E-03	4.4E-02	6wSD
AT3G15270	*SPL5*	*squamosa promoter binding protein-like 5*	25.98	-3.05	0.52	-5.91	3.50E-09	1.5E-06	6wSD
AT3G28500	*AT3G28500*	*60S acidic ribosomal protein family*	83.86	-1.43	0.34	-4.21	2.53E-05	3.2E-03	5wSD
AT3G28500	*AT3G28500*	*60S acidic ribosomal protein family*	138.63	-2.64	0.27	-9.90	3.98E-23	1.3E-19	6wSD
AT3G28860	*ABCB19*	*ATP binding cassette subfamily B19*	2101.94	-0.61	0.13	-4.51	6.63E-06	1.2E-03	5wSD
AT3G28860	*ABCB19*	*ATP binding cassette subfamily B19*	2173.31	-1.02	0.12	-8.16	3.38E-16	5.1E-13	6wSD

AT3G29250	*SDR4*	*NAD(P)-binding Rossmann-fold superfamily protein*	26.39	-2.05	0.59	-3.49	4.77E-04	2.6E-02	6wSD
AT3G50840	*AT3G50840*	*Phototropic-responsive NPH3 family protein*	87.21	0.87	0.25	3.42	6.38E-04	3.4E-02	5wSD
AT3G58120	*BZIP61*	*Basic-leucine zipper (bZIP) transcription factor family protein*	38.08	-2.71	0.44	-6.21	5.25E-10	2.7E-07	6wSD
AT3G61880	*CYP78A9*	*cytochrome p450 78a9*	98.03	0.80	0.23	3.43	6.13E-04	3.4E-02	5wSD
AT3G61880	*CYP78A9*	*cytochrome p450 78a9*	69.47	1.87	0.33	5.74	9.20E-09	3.5E-06	6wSD
AT4G15490	*UGT84A3*	*UDP-Glycosyltransferase superfamily protein*	23.11	-2.47	0.54	-4.60	4.31E-06	6.6E-04	6wSD
AT4G22570	*APT3*	*adenine phosphoribosyl transferase 3*	261.05	0.91	0.18	5.12	3.00E-07	6.7E-05	6wSD
AT4G23900	*AT4G23900*	*Nucleoside diphosphate kinase family protein*	98.31	0.90	0.27	3.38	7.35E-04	3.9E-02	5wSD
AT4G23900	*AT4G23900*	*Nucleoside diphosphate kinase family protein*	73.61	1.12	0.28	3.96	7.63E-05	6.3E-03	6wSD
AT4G26970	*ACO2*	*aconitase 2*	1998.41	0.31	0.09	3.53	4.11E-04	2.5E-02	5wSD
AT4G26970	*ACO2*	*aconitase 2*	1493.04	0.36	0.10	3.69	2.25E-04	1.4E-02	6wSD
AT4G27460	*CBSX5*	*Cystathionine beta-synthase (CBS) family protein*	8.35	-2.96	0.90	-3.28	1.05E-03	4.5E-02	6wSD
AT4G27730	*OPT6*	*oligopeptide transporter 1*	89.49	-0.92	0.27	-3.40	6.78E-04	3.6E-02	5wSD
AT4G27730	*OPT6*	*oligopeptide transporter 1*	127.45	-1.15	0.25	-4.52	6.05E-06	8.7E-04	6wSD
AT4G27900	*AT4G27900*	*CCT motif family protein*	218.32	-0.76	0.18	-4.26	2.08E-05	2.2E-03	6wSD
AT4G31910	*BAT1*	*HXXXD-type acyl-transferase family protein*	36.48	-2.66	0.44	-6.00	1.92E-09	1.2E-06	5wSD
AT4G31910	*BAT1*	*HXXXD-type acyl-transferase family protein*	60.51	-2.38	0.33	-7.22	5.32E-13	5.5E-10	6wSD
AT4G34220	*AT4G34220*	*Leucine-rich repeat protein kinase family protein*	332.63	-0.78	0.16	-4.94	7.66E-07	1.5E-04	6wSD
AT5G09300	*AT5G09300*	*Thiamin diphosphate-binding fold (THDP-binding) superfamily protein*	65.96	-1.72	0.32	-5.39	7.14E-08	2.0E-05	6wSD
AT5G20280	*SPS1F*	*sucrose phosphate synthase 1F*	274.41	-0.81	0.17	-4.62	3.79E-06	5.9E-04	6wSD
AT5G25460	*DGR2*	*transmembrane protein, putative (Protein of unknown function, DUF642)*	197.76	-1.33	0.24	-5.60	2.14E-08	7.2E-06	6wSD
AT5G37300	*WSD1*	*O-acyltransferase (WSD1-like) family protein*	11.04	-4.07	0.97	-4.18	2.91E-05	2.88E-03	6wSD
AT5G44620	*CYP706A3*	*cytochrome P450, family 706, subfamily A, polypeptide 3*	594.87	-0.69	0.15	-4.66	3.16E-06	9.25E-03	4wSD
AT5G44620	*CYP706A3*	*cytochrome P450, family 706, subfamily A, polypeptide 3*	837.41	-1.29	0.33	-3.86	1.11E-04	9.80E-03	5wSD
AT5G44620	*CYP706A3*	*cytochrome P450, family 706, subfamily A, polypeptide 3*	960.36	-1.59	0.14	-11.12	9.57E-29	4.73E-25	6wSD
AT5G44630	*AT5G44630*	*Terpenoid cyclases/Protein prenyltransferases superfamily protein*	57.43	-2.96	0.48	-6.20	5.81E-10	4.11E-07	5wSD

AT5G44630	*AT5G44630*	*Terpenoid cyclases/Protein prenyltransferases superfamily protein*	73.11	-2.46	0.32	-7.76	8.82E-15	1.0E-11	6wSD
AT5G46690	*bHLH071*	*beta HLH protein 71*	17.29	-2.06	0.58	-3.54	4.03E-04	2.3E-02	6wSD
AT5G50915	*AT5G50915*	*basic helix-loop-helix (bHLH) DNA-binding superfamily protein*	39.40	-2.45	0.43	-5.76	8.47E-09	3.3E-06	6wSD
AT5G56220	*AT5G56220*	*P-loop containing nucleoside triphosphate hydrolases superfamily protein*	487.40	-0.65	0.15	-4.31	1.61E-05	2.3E-03	5wSD
AT5G56220	*AT5G56220*	*P-loop containing nucleoside triphosphate hydrolases superfamily protein*	501.75	-0.81	0.15	-5.52	3.48E-08	1.1E-05	6wSD
AT5G56970	*CKX3*	*cytokinin oxidase 3*	39.35	-1.45	0.40	-3.63	2.83E-04	1.9E-02	5wSD
AT5G56970	*CKX3*	*cytokinin oxidase 3*	37.06	-1.59	0.37	-4.27	1.96E-05	2.1E-03	6wSD
AT5G57655	*AT5G57655*	*xylose isomerase family protein*	917.81	-0.64	0.12	-5.57	2.56E-08	1.2E-05	5wSD
AT5G57655	*AT5G57655*	*xylose isomerase family protein*	812.74	-0.69	0.14	-4.94	7.86E-07	1.6E-04	6wSD
AT5G60910	*AGL8*	*AGAMOUS-like 8*	38.05	-4.87	0.75	-6.50	8.21E-11	8.4E-08	5wSD
AT5G60910	*AGL8*	*AGAMOUS-like 8*	94.12	-6.06	0.55	-11.08	1.64E-28	6.5E-25	6wSD
AT5G62165	*AGL42*	*AGAMOUS-like 42*	209.76	-1.32	0.21	-6.23	4.73E-10	3.6E-07	5wSD
AT5G62165	*AGL42*	*AGAMOUS-like 42*	255.07	-1.13	0.17	-6.64	3.19E-11	2.2E-08	6wSD
AT5G66350	*SHI*	*Lateral root primordium (LRP) protein-like protein*	691.93	0.41	0.11	3.61	3.09E-04	2.0E-02	5wSD
AT5G66350	*SHI*	*Lateral root primordium (LRP) protein-like protein*	506.02	0.77	0.14	5.45	4.92E-08	1.5E-05	6wSD
AT5G67180	*TOE3*	*target of early activation tagged (EAT) 3*	64.97	-1.53	0.35	-4.37	1.22E-05	1.5E-03	6wSD

Table S4.5. Table listing genes overlapping between LD- and SD-transcriptome analysis and genes overlapping between *FUL* co-expressed genes in LD and SD transcriptome analyses. BaseMean= Mean of normalised counts for all samples, log_2FoldChange= Log_2 Fold Change relative to Col-0, lfcSE= Standard error of Log_2 Fold Change, stat= Wald statistic for comparing expression in Col-0 to that of rSPL15 (LD) or spl15-*1* (SD), pvalue= *p-value* for Wald test, padj= Adjusted *p*-value using Benjamini-Hochberg correction for multiple testing (used to determine significance of expression differences), DEG at time point= Time point at which gene is statistically significantly differentially expressed (*p*adj < 0.05). Results file generated with DESeq2 software. Genes marked with (●) were co-expressed with *FUL*.

AGI-code	Gene symbol	TAIR computational description (Source: Araport11)	baseMean	log_2FoldChange	lfcSE	stat	pvalue	padj	DEG at time point
AT1G02190	AT1G02190 ●	Fatty acid hydroxylase superfamily	37.62	1.20	0.31	3.88	1.06E-04	1.00E-02	12LD
AT1G02190	AT1G02190 ●	Fatty acid hydroxylase superfamily	16.95	-2.47	0.63	-3.90	9.60E-05	8.75E-03	5wSD
AT1G02190	AT1G02190 ●	Fatty acid hydroxylase superfamily	34.26	-2.58	0.45	-5.74	9.35E-09	3.49E-06	6wSD
AT1G53160	SPL4	squamosa promoter binding protein-like 4	18.69	1.93	0.57	3.40	6.73E-04	2.63E-02	9LD
AT1G53160	SPL4	squamosa promoter binding protein-like 4	40.39	1.35	0.30	4.51	6.63E-06	1.08E-03	12LD
AT1G53160	SPL4	squamosa promoter binding protein-like 4	93.90	-5.36	0.86	-6.26	3.82E-10	3.06E-07	5wSD
AT1G53160	SPL4	squamosa promoter binding protein-like 4	232.69	-6.18	0.37	-16.51	3.14E-61	6.20E-57	6wSD
AT1G69040	ACR4	ACT domain repeat 4	820.11	0.79	0.12	6.55	5.59E-11	2.11E-08	9LD
AT1G69040	ACR4	ACT domain repeat 4	891.61	0.66	0.13	4.99	6.03E-07	1.57E-04	12LD
AT1G69040	ACR4	ACT domain repeat 4	767.91	-0.71	0.16	-4.43	9.46E-06	1.50E-03	5wSD
AT1G69040	ACR4	ACT domain repeat 4	736.35	-0.75	0.17	-4.27	1.95E-05	2.10E-03	6wSD
AT2G25900	ATTZF	Zinc finger C-x8-C-x5-C-x3-H type family protein	1271.96	0.80	0.11	6.95	3.64E-12	2.98E-10	6LD
AT2G25900	ATTZF	Zinc finger C-x8-C-x5-C-x3-H type family protein	1010.94	0.52	0.13	3.85	1.20E-04	7.02E-03	9LD
AT2G25900	ATTZF	Zinc finger C-x8-C-x5-C-x3-H type family protein	1190.74	0.73	0.17	4.28	1.84E-05	2.52E-03	12LD
AT2G25900	ATTZF	Zinc finger C-x8-C-x5-C-x3-H type family protein	2014.61	-0.91	0.16	-5.55	2.79E-08	1.25E-05	5wSD
AT2G25900	ATTZF	Zinc finger C-x8-C-x5-C-x3-H type family protein	982.94	-0.69	0.19	-3.61	3.10E-04	1.81E-02	6wSD
AT2G45660	SOC1	AGAMOUS-like 20	56.14	1.86	0.28	6.72	1.86E-11	1.33E-09	6LD
AT2G45660	AGL20	AGAMOUS-like 20	100.76	1.03	0.26	3.98	6.87E-05	4.38E-03	9LD
AT2G45660	AGL20	AGAMOUS-like 20	162.52	0.87	0.14	6.35	2.17E-10	1.17E-07	12LD
AT2G45660	AGL20	AGAMOUS-like 20	79.08	-1.13	0.30	-3.77	1.63E-04	1.27E-02	5wSD
AT2G45660	AGL20	AGAMOUS-like 20	85.20	-1.55	0.25	-6.22	4.95E-10	2.64E-07	6wSD
AT3G57920	SPL15	squamosa promoter binding protein-like 15	433.02	4.50	0.20	21.94	1.01E-106	1.99E-102	6LD
AT3G57920	SPL15	squamosa promoter binding protein-like 15	260.50	3.26	0.20	16.01	1.02E-57	1.88E-53	9LD
AT3G57920	SPL15	squamosa promoter binding protein-like 15	313.87	3.36	0.16	20.45	6.44E-93	1.25E-88	12LD
AT3G57920	SPL15	squamosa promoter binding protein-like 15	200.10	-4.53	0.29	-15.43	1.00E-53	1.85E-49	5wSD
AT3G57920	SPL15	squamosa promoter binding protein-like 15	172.31	-5.12	0.32	-15.98	1.65E-57	1.63E-53	6wSD
AT4G13495	AT4G13495	other_RNA	1343.99	0.77	0.09	8.29	1.15E-16	2.20E-14	6LD
AT4G13495	AT4G13495	other_RNA	1039.15	0.60	0.13	4.60	4.17E-06	4.06E-04	9LD
AT4G13495	AT4G13495	other_RNA	780.48	0.70	0.11	6.18	6.54E-10	3.33E-07	12LD
AT4G13495	AT4G13495	other_RNA	107.52	0.93	0.25	3.73	1.88E-04	1.43E-02	5wSD

AT4G13495	AT4G13495	other_RNA	60.60	1.58	0.31	5.16	2.45E-07	5.56E-05	6wSD
AT4G30250	AT4G30250	P-loop containing nucleoside triphosphate hydrolases superfamily protein	267.91	-1.19	0.21	-5.69	1.23E-08	2.53E-06	9LD
AT4G30250	AT4G30250	P-loop containing nucleoside triphosphate hydrolases superfamily protein	407.22	-0.42	0.11	-3.96	7.37E-05	7.63E-03	12LD
AT4G30250	AT4G30250	P-loop containing nucleoside triphosphate hydrolases superfamily protein	3512.27	0.89	0.15	6.04	1.54E-09	9.74E-07	5wSD
AT4G30250	AT4G30250	P-loop containing nucleoside triphosphate hydrolases superfamily protein	3406.29	0.61	0.17	3.64	2.69E-04	1.61E-02	6wSD
AT4G34400	TFS1	AP2/B3-like transcriptional factor family protein	99.56	3.51	0.32	10.88	1.49E-27	1.55E-24	6LD
AT4G34400	TFS1	AP2/B3-like transcriptional factor family protein	57.14	1.65	0.33	5.04	4.65E-07	6.56E-05	9LD
AT4G34400	TFS1	AP2/B3-like transcriptional factor family protein	129.10	2.68	0.23	11.43	3.09E-30	8.55E-27	12LD
AT4G34400	TFS1	AP2/B3-like transcriptional factor family protein	936.73	-0.54	0.11	-5.08	3.68E-07	1.15E-04	5wSD
AT4G34400	TFS1	AP2/B3-like transcriptional factor family protein	818.23	-1.00	0.14	-7.10	1.24E-12	1.12E-09	6wSD
AT4G37800	XTH7	xyloglucan endotransglucosylase/hydrolase 7	661.31	-1.64	0.21	-7.98	1.52E-15	2.34E-12	9LD
AT4G37800	XTH7	xyloglucan endotransglucosylase/hydrolase 7	491.31	-1.02	0.17	-5.95	2.71E-09	1.19E-06	12LD
AT4G37800	XTH7	xyloglucan endotransglucosylase/hydrolase 7	569.52	0.77	0.15	5.19	2.12E-07	7.51E-05	5wSD
AT4G37800	XTH7	xyloglucan endotransglucosylase/hydrolase 7	577.24	0.92	0.19	4.79	1.63E-06	2.86E-04	6wSD
AT5G20700	AT5G20700	senescence-associated family protein, putative (DUF581)	1096.28	-0.90	0.17	-5.46	4.86E-08	8.39E-06	9LD
AT5G20700	AT5G20700	senescence-associated family protein, putative (DUF581)	972.15	-0.62	0.10	-6.09	1.13E-09	5.33E-07	12LD
AT5G20700	AT5G20700	senescence-associated family protein, putative (DUF581)	1711.79	0.51	0.13	3.88	1.04E-04	9.31E-03	5wSD
AT5G20700	AT5G20700	senescence-associated family protein, putative (DUF581)	1327.67	0.60	0.15	4.05	5.21E-05	4.62E-03	6wSD
AT5G28640	AN3	SSXT family protein	785.48	0.72	0.12	5.98	2.25E-09	1.01E-07	6LD
AT5G28640	AN3	SSXT family protein	947.49	0.53	0.14	3.96	7.51E-05	4.74E-03	9LD
AT5G28640	AN3	SSXT family protein	1221.98	0.49	0.11	4.53	5.93E-06	9.90E-04	12LD
AT5G28640	AN3	SSXT family protein	2017.01	-0.47	0.12	-3.76	1.69E-04	1.31E-02	5wSD
AT5G28640	AN3	SSXT family protein	1892.85	-0.92	0.17	-5.28	1.28E-07	3.29E-05	6wSD
AT5G44620	CYP706A3	cytochrome P450, family 706, subfamily A, polypeptide 3	49.20	2.27	0.29	7.83	4.75E-15	6.69E-13	6LD
AT5G44620	CYP706A3	cytochrome P450, family 706, subfamily A, polypeptide 3	46.29	1.22	0.37	3.33	8.63E-04	3.12E-02	9LD
AT5G44620	CYP706A3	cytochrome P450, family 706, subfamily A, polypeptide 3	160.18	3.03	0.21	14.80	1.44E-49	1.39E-45	12LD
AT5G44620	CYP706A3	cytochrome P450, family 706, subfamily A, polypeptide 3	837.41	-1.29	0.33	-3.86	1.11E-04	9.80E-03	5wSD
AT5G44620	CYP706A3	cytochrome P450, family 706, subfamily A, polypeptide 3	960.36	-1.59	0.14	-11.12	9.57E-29	4.73E-25	6wSD

AT5G54160	OMT1	O-methyltransferase 1	1641.62	-0.47	0.10	-4.65	3.31E-06	6.37E-05	6LD
AT5G54160	OMT1	O-methyltransferase 1	1443.66	-0.62	0.15	-4.18	2.88E-05	2.15E-03	9LD
AT5G54160	OMT1	O-methyltransferase 1	1260.72	-0.41	0.10	-3.96	7.60E-05	7.76E-03	12LD
AT5G54160	OMT1	O-methyltransferase 1	1794.49	0.51	0.11	4.68	2.84E-06	6.07E-04	5wSD
AT5G54160	OMT1	O-methyltransferase 1	1531.71	0.44	0.13	3.29	1.01E-03	4.37E-02	6wSD
AT5G56970	CKX3 ●	cytokinin oxidase 3	7.54	2.09	0.71	2.96	3.05E-03	2.14E-02	6LD
AT5G56970	CKX3 ●	cytokinin oxidase 3	39.35	-1.45	0.40	-3.63	2.83E-04	1.91E-02	5wSD
AT5G56970	CKX3 ●	cytokinin oxidase 3	37.06	-1.59	0.37	-4.27	1.96E-05	2.11E-03	6wSD
AT5G57655	AT5G57655	xylose isomerase family protein	550.17	0.44	0.14	3.10	1.94E-03	1.49E-02	6LD
AT5G57655	AT5G57655	xylose isomerase family protein	500.78	0.75	0.17	4.45	8.60E-06	7.80E-04	9LD
AT5G57655	AT5G57655	xylose isomerase family protein	591.36	0.38	0.10	3.77	1.65E-04	1.37E-02	12LD
AT5G57655	AT5G57655	xylose isomerase family protein	917.81	-0.64	0.12	-5.57	2.56E-08	1.18E-05	5wSD
AT5G57655	AT5G57655	xylose isomerase family protein	812.74	-0.69	0.14	-4.94	7.86E-07	1.55E-04	6wSD
AT5G60910	FUL ●	AGAMOUS-like 8	28.77	1.75	0.37	4.68	2.83E-06	5.22E-04	12LD
AT5G60910	FUL ●	AGAMOUS-like 8	38.05	-4.87	0.75	-6.50	8.21E-11	8.39E-08	5wSD
AT5G60910	FUL ●	AGAMOUS-like 8	94.12	-6.06	0.55	-11.08	1.64E-28	6.48E-25	6wSD
AT5G62165	AGL42 ●	AGAMOUS-like 42	4.77	3.62	1.23	2.94	3.27E-03	2.27E-02	6LD
AT5G62165	AGL42 ●	AGAMOUS-like 42	37.92	2.69	0.38	7.11	1.18E-12	9.97E-10	12LD
AT5G62165	AGL42 ●	AGAMOUS-like 42	209.76	-1.32	0.21	-6.23	4.73E-10	3.62E-07	5wSD
AT5G62165	AGL42 ●	AGAMOUS-like 42	255.07	-1.13	0.17	-6.64	3.19E-11	2.17E-08	6wSD

Chapter 5:

General discussion

The role of SPL15 and its putative target genes in floral induction

FUL and *MIR172B* are not the only targets of SPL15 in the floral induction pathway

In chapter 2, I set out to study the contribution of *FUL* and *MIR172B* to floral induction mediated by SPL15. These two targets are not expressed during vegetative growth and thus their products are not present to repress the *AP2-L* family of floral repressors. AP2-Ls are expressed during the vegetative phase, where they inhibit the floral transition (Fig. 5.1A). I found that under LD conditions, *FUL* and *MIR172B* are required for timely floral induction, however, their role in floral induction is independent of SPL15 (Fig. 2.4). In contrast, in SD conditions the flowering-time phenotype of *ful-2/mir172b-3* was similar to that of *spl15-1*, with only some differences in plant morphology (Fig. 2.4). Consistent with this, the early-flowering phenotype of *rSPL15* was suppressed by mutation of *FUL* and *MIR172B* in both LD and SD conditions (Fig. 2.5). This indicates that *FUL* and *MIR172B* are required for flowering under both LD and SD conditions, and they might therefore be involved in floral induction by SPL15 under SD conditions.

Notably, *rSPL15/ful-2/mir172a-2/b-3* plants bolted earlier than the *ful-2/mir172a-2/b-3* triple mutants in SD conditions, suggesting that *FUL* and *MIR172B* are not the only targets of SPL15 that are important for flowering (Fig. 2.5). One putative downstream component of SPL15-signalling is *MIR172D*. MIR172D also plays an important role in floral induction in SD conditions, as its single mutant displays a late flowering phenotype under these conditions (Fig. 2.7). To dissect the contribution of *MIR172D* to floral induction by SPL15, the quintuple mutant of *rSPL15/ful-2/mir172a-2/b-3/d* should be generated and scored for its flowering time in LD and SD conditions.

To identify other genes regulated by SPL15, I analysed the transcriptome of *rSPL15* compared with that of Col-0 in LD conditions and that of *spl15-1* compared to Col-0 in SD conditions (Chapter 4). These data showed that many genes known to be involved in flowering-time regulation were differentially expressed, as well as other genes that had not previously been identified to be differentially expressed during the floral transition. Comparison of the differentially expressed genes (DEGs) from both SD- and LD-transcriptomes and *FUL* co-expression analysis in these data sets, revealed that multiple genes related to flowering-time regulation were common to both two datasets. The most prominent genes in this analysis

were *SOC1, FUL, AGL42, TFS1* and *SPL4,* which have all been described previously to function in the floral transition. These putative SPL15 target genes aid the generation of new hypotheses concerning regulation of the floral transition by SPL15.

FUL, SOC1, AGL42, TFS1 and SPL4 are putative targets of SPL15 during the floral transition

FUL, SOC1, AGL42, TFS1 and *SPL4* are all genes with a described function in flowering regulation (G. H. Cardon *et al.*, 1997; M. K. Chen *et al.*, 2011; Dorca-Fornell *et al.*, 2011; Jung *et al.*, 2016; H. Lee *et al.*, 2000; J. H. Lee *et al.*, 2006; Richter *et al.*, 2019). *FUL, SOC1* and *AGL42* were previously proposed to be direct SPL targets through comparative transcriptome analyses of plants with disrupted miRNA processing machinery and plants that overexpress *MIR156* (Wang *et al.*, 2009). *FUL* is a confirmed direct target of SPL15 as it was previously shown that SPL15 bound directly to its promoter and that its expression is dependent on SPL15 under SD conditions (Fig. 2.8B; Hyun *et al.*, 2016). In addition, *AGL42, SOC1* and *TFS1* were directly bound by rSPL9 in ChIP-qPCR experiments (Richter *et al.*, 2019; J. W. Wang *et al.*, 2009). The close phylogenetic relationship between SPL9 and SPL15 suggests that *AGL42, SOC1* and *TFS1* could also be direct targets of SPL15. In addition, SOC1 functions in cooperation with SPL15 in transcriptional activation of *FUL* and *MIR172B*, suggesting dependency on one another (Hyun *et al.*, 2016). However, SOC1 is not exclusively required for SPL15 to induce flowering in SD, because *soc1-2* mutants flower earlier than *spl15-1* mutants in terms of rosette leaf number, and the double mutant flowered later than either single mutant (Fig. 4.23). Thus, SOC1 and SPL15 may have common, but also distinct functions during the floral transition under SD conditions. The early-flowering phenotype of plants expressing *rSPL15* is suppressed in the *soc1-2/ful*-2 mutant background under SD conditions. This suggests that *FUL* and *SOC1* are indeed critical for floral induction by SPL15 in these conditions, and supports the hypothesis that these genes are direct targets of SPL15 (Hyun *et al.*, 2016).

Another putative target of SPL15 is *SPL4*, which is also involved in floral induction and is closely related to *SPL3* and *SPL5*. In plants that overexpress *SPL3, 4* or 5 in LD conditions, *FUL* and *AP1* expression is higher. Conversely, *FUL* and *AP1* are expressed lower in the *spl3/4/5* triple and knock-down mutants, suggesting a redundant function of SPL3/4/5 (Jung *et al.*, 2016; Xie *et al.*, 2020; M. Xu, Hu, Zhao, *et al.*, 2016; A. Yamaguchi *et al.*, 2009). In *soc1* mutants, *SPL3/4/5* are expressed at a lower level, whereas overexpression of SOC1 leads to the increased expression of these *SPLs* in LD conditions. This indicates that SOC1 is involved in *SPL3/4/5* transcriptional upregulation (Jung *et al.*, 2012). Moreover, their expression in the

SAM follows quickly after that of *SOC1* in the SAM, which does not occur in *soc1-2* mutants (Porri *et al.*, 2012; Torti *et al.*, 2012). These data suggest that *SPL4* might be a target of both SOC1 and SPL15.

On the basis of what is described above, as well as the expression dynamics of *SPL15, SOC1, FUL, AGL42* and *SPL4* in chapter 4 and their specific role in floral induction, I hypothesise that *SOC1* and *AGL42* are early, or `first wave´ targets of SPL15 (Chapter 4; Fig. 5.1). Once these two are expressed, their products could activate other target genes involved in floral induction, some of which might be activated via cooperation with SPL15 (described further below). *SOC1* and *AGL42* were among the earliest differentially expressed genes in both my LD and SD transcriptome analyses (Table 4.1, 4.3; Figs. 4.13, 4.20 and 4.21).

The expression dynamics of *FUL* and *SPL4* were similar in both transcriptome analyses, but differed slightly from those of *SOC1* and *AGL42. FUL* and *SPL4* were differentially expressed at later timepoints than *SOC1* and *AGL42*. Moreover, their expression increased greatly as floral induction was initiated (Table 4.1, 4.3; Figs. 2.8, 4.6, 4.12, 4.13, 4.16). Although the difference in expression of *FUL* occurs later, SPL15 was shown previously to bind directly to this gene, indicating that direct targets are not necessarily the first ones to change in expression after SPL15 becomes active (Hyun *et al.*, 2016). *FUL* and *SPL4* are therefore induced directly and/or indirectly by SPL15 slightly later than *SOC1* and *AGL42* during the `second wave´ of gene induction downstream of SPL15.

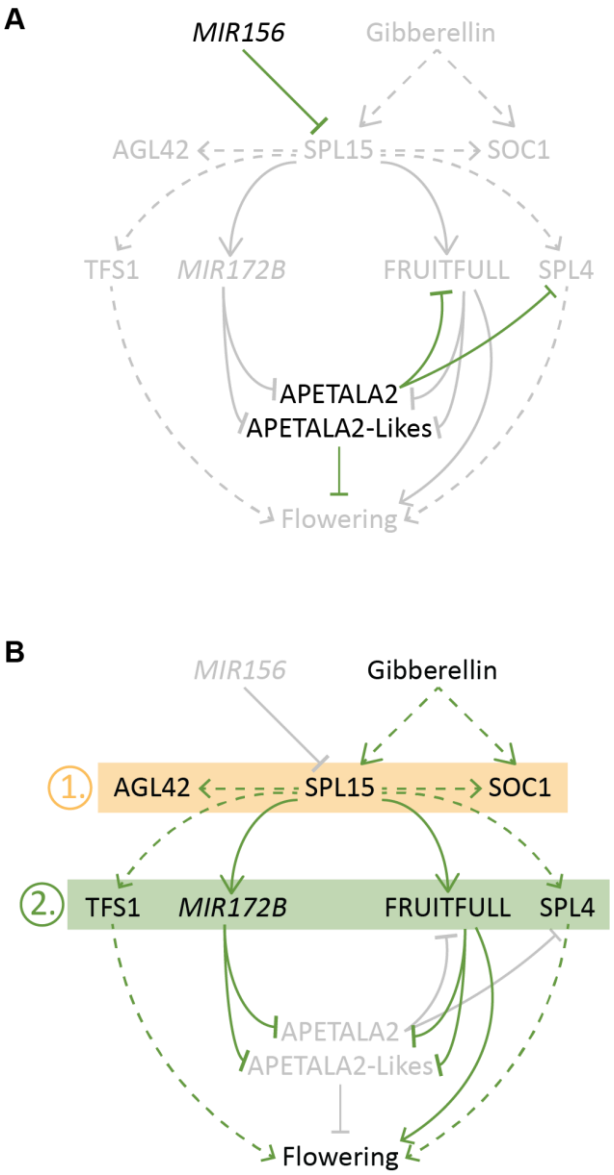

Figure 5. 1.: Proposed interactions among SPL15 and its candidate target genes involved in floral induction in SD conditions. A: Simplified model of gene interactions during vegetative growth. **B:** Simplified model for interactions during the floral transition mediated by SPL15. Marked in orange are the proposed 'first wave' target genes of SPL15 are marked in orange are and marked in green are the proposed 'second wave' target genes of SPL15 during the floral transition are marked in green. This simplified model does not display the changing dynamics between AP2-Ls and MIR172B and FUL occurring during the floral transition.

The expression of *TFS1* differed between the LD and SD transcriptomes. Under LD conditions, it was induced early in *rSPL15* in a pattern similar to that of *AGL42,* whereas in SD conditions, it was expressed similarly to *FUL* and *SPL4*, but the expression differences compared to wild-type are much smaller (Tables 4.2, 4.3; Figs. 4.19/4.20). Because *TFS1* is proposed to function in floral primordia (Richter *et al.*, 2019), it is likely to be expressed similarly to *FUL* and *SPL4,* and thus, slightly later than *SOC1* and *AGL42.* Moreover, SPL15 has a clear function in controlling flowering under SD conditions, in which *TFS1* is expressed in a similar pattern to that of *FUL* and *SPL4*. To test if SPL15 indeed directly regulates putative genes such as *SOC1, SPL4*, *AGL42* and *TFS1*, an inducible SPL15 line as well as ChIP-qPCR should be used, as I proposed in chapter 4.

Reverse-genetic analysis will be necessary to further analyse the roles of these putative target genes in floral induction downstream of SPL15. Therefore, I made crosses between *rSPL15* and *spl4* mutants (generated by Dr. Youbong Hyun) and between *rSPL15* and *tfs1-1*, to determine to what extent these mutations suppress the early-flowering phenotype of *rSPL15* (Richter *et al.*, 2019). In addition, I have crossed the same *spl4* and *tfs1-1* mutants to *spl15-1* to determine whether they further enhance the late-flowering phenotype of *spl15-1* in SD conditions. The *agl42* mutant should also be crossed to *spl15-1* and *rSPL15* to assess the effect of this mutation on the flowering-time of *spl15-1* in SD conditions and on that of *rSPL15* in LD conditions (Dorca-Fornell *et al.*, 2011). I also crossed *spl15-1* to the cell-cycle marker line pCDKB2;1::CDKB2;1::VENUS to study potential differences in cell division within the SAM between Col-0 and *spl15-1* (I generated the CDKB2;1::VENUS line previously; unpublished material).
Additionally, the expression of these candidate target genes can be studied using fluorescent marker lines. To this end, to study whether the expression of these putative target genes is dependent on SPL15, I crossed *rSPL15* and *spl15-1* with plants carrying SOC1::GFP (Immink *et al.*, 2012). I also crossed *TFS1::VENUS* with *spl15-1* and *soc1-2/spl15-1/ful-2* to generate the respective mutant and higher-order mutant transgenic lines. The existing *SPL4::VENUS* construct should also be transformed into plants and be crossed with *spl15-1* to answer the same questions.

Cooperative regulation of target genes by MADS-domain and SPL transcription factors.

The proposed cooperative transcriptional activation between SPL15 and the MADS-domain transcription factor SOC1 may have more general significance (Hyun *et al.*, 2016). Other MADS-domain transcription factors related to SOC1, such as AGL42, may also cooperate with SPL15 in transcriptional activation of targets (Pařenicová *et al.*, 2003). *agl42* mutants show delayed flowering compared with Col-0 in SD conditions (Dorca-Fornell *et al.*, 2011). Similarly, FUL, another MADS-domain transcription factor, might

fulfil a similar cooperative function in transcriptional activation by SPL15. Although SOC1 and FUL might be involved in transcriptional activation in cooperation with SPL15, both are likely to have additional roles in floral induction in SD conditions. Double mutants between *spl15-1* and either *soc1-2* or *ful-2* flower later than *spl15-1* single mutants in these conditions, and similarly, *soc1-2/ful-2* mutants also flower as late as the other double mutants (Fig. 4.23). Notably, the triple mutant *soc1-2/ful-2/spl15-1* flowered as late as all three double mutant combinations, indicating that these genes function in the same pathway, consistent with *FUL* expression being reduced in *spl15-1* mutants (Hyun *et al.*, 2016; this thesis). In the absence of two of these three proteins, flowering is severely delayed in SD conditions, and loss of the third protein has no additional effect as it cannot promote flowering in the absence of the other two.

If this cooperative module between MADS-domain and SPL transcription factors indeed has more general significance in the regulation of floral induction, it is possible that a similar module exists among SOC1, FUL and AGL42 and other SPLs, particularly SPL9, which is so closely related to SPL15. SPL9 also binds to the *FUL* promoter at the same conserved binding region as SPL15 (Fig. 3.7; Wang *et al.*, 2009). Although mutation of *SPL9* in the *spl15-1* mutant background did not further enhance the flowering -time phenotype of *spl15-1*, cooperativity between SPL9 and SOC1 might also occur and be important in other tissues or growth conditions (Hyun *et al.*, 2016). *SPL9* and *SPL15* are expressed in different regions of the SAM, with *SPL9* expressed on the flanks and *SPL15* in the centre, which is presumably relevant for their individual functions (Hyun *et al.*, 2016). SPL9 binds to SOC1 and regulates the transcription of *TFS1* in cooperation with SOC1, analogously to the regulation of *FUL* by SOC1 and SPL15 (Richter *et al.*, 2019). This cooperative regulation of *TFS1* was proposed to be important in floral primordia, based on the expression domains of *SPL9* and *TFS1.* Combinatorial effects of other SPLs with transcription factors of other families have also been implicated in flowering time control (Jung *et al.*, 2016).

A report on the effect of *SPL3, 4* and *5* on floral induction showed that overexpression of *SPL3* caused early flowering, and this phenotype was partially suppressed in a *soc1-2* mutant background, suggesting that floral induction by *SPL3* overexpression is at least partially dependent on SOC1 (Jung *et al.*, 2012). Because these proteins share some direct targets, they might cooperatively regulate some of these targets, similar to SPL15 and SPL9 with SOC1 (Hyun *et al.*, 2016; Richter *et al.*, 2019).

SPL15 interacts with MED18, a component of the mediator complex that is required for recruitment of the RNA Polymerase II machinery and this interaction occurs at the *FUL* locus (Hyun *et al.*, 2016). A similar cooperative module was demonstrated between SPL10 and MED25, another component of the mediator

complex that plays an important role in floral induction (Iñigo *et al.*, 2012; Yao *et al.*, 2019). This interaction occurs at the *FUL* locus*,* where *MIR156*-resistant *rSPL10* binds to the conserved SPL-binding motif in the *FUL* promoter (Yao *et al.*, 2019). Potentially, *rSPL10* also interacts with a MADS-domain transcription factor to form open chromatin and form an active RNA transcription complex, similar to when SPL15 and SOC1 bind to the *FUL* promoter (Hyun *et al.*, 2016). Altogether, these reports further extend the co-operative interactions between SPL an MADS box transcription factors.

This cooperative model between SPLs and MADS-domain proteins is adopted in Fig. 5.1B to explain sequential gene activation by SPL15. In this scheme, SPL15 activates *SOC1* and *AGL42* (marked in orange), and then cooperates with SOC1 and AGL42 proteins to activate a `second wave´ of SPL15 targets (marked in green). To test this general cooperative module hypothesis, larger-scale protein interaction studies could be performed. For example, Yeast-2-Hybrid (Y2H) assay could be used to test whether SOC1, AGL42 and FUL can interact with other SPLs. Interactions detected in yeast could then be tested *in planta* by co-immunoprecipitation (Co-IP) in meristem-enriched tissue to assess if they occur in biologically relevant contexts. In addition bimolecular fluorescence complementation (BiFC) could be used to test if the SPL15 interacts with the suggested MADS-domain proteins *in planta* and even in the SAM (Abe *et al.*, 2019).
Similarly, these experiments could be performed in a staged series of meristem samples to relate the formation of these complexes to the developmental transition. ChIP-qPCR on the *FUL* promoter could also be employed to study whether the MADS-domain and SPL transcription factors depend on each other for binding to the promoter, and for the recruitment of the RNA-polymerase II machinery (Hyun *et al.*, 2016; Richter *et al.*, 2019).

A targeted approach could test whether SPL3 can interact with SOC1 in Y2H and Co-IP *in planta* and to test whether this interaction also occurs at the *FUL* locus with ChIP-qPCR. Furthermore, this would show whether the interaction is required to recruit the transcriptional machinery and to transcriptionally activate *FUL* during the floral transition under LD conditions where SPL15 is not critical for the floral transition.

A putative role for SPL15 in cell division and growth

The group of candidate genes involved in cell division, elongation or growth (*ACR4, XTH7, AN3, OMT1, AT5G57655, CER1-L1* and *CKX3*) is particularly relevant, because these genes might play a role in the morphological development of the SAM or the elongation of the rib region that occurs during inflorescence

growth. Based on the expression dynamics of these genes in the SD transcriptome analysis, most of these genes would belong to the proposed group of `second wave' of SPL15 target genes (Chapter 4; Table 4.3, 4.4, Fig. 5.1B). The morphological changes at the SAM that occur during floral involve coordinated increases in cell division and size (Kinoshita & Vaysierres *et al.,* in preparation; Kwiatkowska, 2008). However, it remains unknown how floral integrators such as SOC1 and FUL are linked to these changes.

Studying the DEGs from my two transcriptome analyses with a role in cell division and that are expressed in the SAM might help to understand this. SPL15 might play a role in cell division in the rib meristem, because *spl15*-1 mutants do not always show elongation of the primary shoot and reversely, *rSPL15* shows shoot elongation before floral buds are visible (Further described below). Moreover, plants carrying an EMS-induced mutation in the *MIR156* target site of SPL15 (*msc-D*) have an increased cell number and decreased cell size in the leaves (Usami *et al.*, 2009). This mutant is comparable to *rSPL15*, although weaker, and suggests a role for SPL15 in the regulation of cell proliferation. Furthermore, certain mutants with similar cell proliferation defects in the leaves as those described for *msc-D* plants show changes in the vegetative phase transition (Usami *et al.*, 2009). In addition, the *fugu1* mutant, a cell-proliferation mutant with smaller cells in the leaves, showed delayed flowering (Ferjani *et al.*, 2007). Therefore, genes described to have general roles in cell proliferation can influence transitions in the meristem, where SPL15 might be one of the floral integrators that regulates these genes thereby affecting the floral transition.

I propose to study mutants such as *an3, ckx3* and *fugu1* and analyse their flowering time phenotype, cell proliferation patterns and morphological changes in the SAM during the floral transition using confocal microscopy on cleared-tissue with stained cell walls, combined with meristem analysis using MorphoGraphX (de Reuille *et al.*, 2015; Kurihara *et al.*, 2015; T. J. Musielak *et al.*, 2015). These approaches could help to determine whether *an3, ckx3* and *fugu1* display morphological phenotypes in the SAM, including cell proliferation and meristem growth dynamics, specifically during the floral transition. Moreover, the transcriptomes of published and available flowering-time mutants could be examined to address whether these candidate genes with a role in cell division, elongation and growth are differentially expressed in these mutants. This could help to determine whether these genes are involved in the floral transition in the SAM, in addition to being putative targets of SPL15.

The role of SPL15 in regulating SAM development and apical dominance

Related to a role for SPL15 in cell proliferation and growth, and as described in chapter 2, higher-order mutations in genes encoding repressors of *AP2-L* gene expression lead to changes in plant morphology after the floral transition. The quintuple mutant *ful-2/mir172a-2/b-2/c-1/d-3,* the quadruple mutant *mir172a-2/b-3/c-1/d-3* and the triple mutant *spl15-1/mir172a-2/b-3* all showed partial loss of apical dominance. These genotypes displayed outgrowth of side shoots from the rosette that started to emerge shortly after or even before bolting of the main inflorescence (Fig. 2.13D; 2.14A). This led to a bushier plant architecture, where the extent to which this occurred differed among genotypes.

For example, approximately 10% of *spl15-1* single mutants showed emergence of a secondary shoot from the rosette before the emergence of the primary inflorescence (Fig. 5.2). The primary SAM remained active in the plants, and in most cases, it was reactivated one or two weeks after the secondary shoots emerged from the rosette. Moreover, I described inflorescence phenotypes for *rSPL15* grown in SD conditions, which suggested that rSPL15 is involved in regulating elongation of the inflorescence stem, as well as in the floral transition (Fig. 2.5; 2.6). However, its main role does not involve the production or opening of flowers. These data suggests that SPL15 normally stimulates apical dominance, perhaps by regulating auxin or cytokinin fluxes (Bertheloot *et al.*, 2020; Kebrom, 2017). *SPL15* expression likely responds to auxin, as SPL15::GUS expression from the native promoter increased rapidly in the root after treatment with auxin, supporting a role for SPL15 in auxin signalling (Schwarz, 2006). Alternatively, in wild-type plants SPL15 might promote elongation of the primary inflorescence stem but not of axillary shoots, so that in *spl15* mutants axillary shoots grow out normally, but appear before the primary shoot as its elongation is delayed.

Figure 5.2. *spl15-1* plant grown in SD conditions showing the emergence of secondary shoots from the rosette before the appearance of the primary shoot.

rSPL15 regulates rosette leaf number before bolting, potentially by reducing the plastochron (leaf emergence rate). Furthermore, *rSPL15* plants grown in LD and SD conditions produced fewer rosette leaves than Col-0, although they flowered at a similar time. Consistently, *spl9-1*/*spl15-1* mutants have previously been described for an increased plastochron compared to Col-0 (Wang *et al.*, 2008). The role of

rSPL15 in shoot elongation might also contribute to lower rosette leaf number, as earlier internode elongation could reduce rosette leaf number and increase the number of cauline leaves on the stem (Fig. 2.5). However, this implies that the cauline leaves on *rSPL15* plants resemble rosette leaves instead of cauline leaves, which in terms of morphology appears not to be the case (Fig. 2.6).

Lastly, delayed production of flowers after bolting in *rSPL15* plants might cause a large increase in the number of nodes forming cauline leaves and lead to tall inflorescence shoots before flowers appear (Fig. 2.6C-D).

To test these possibilities, it would be useful to perform a confocal microscope time-course of cell wall-stained SAMs from *rSPL15* and Col-0 plants grown in SD conditions. In Col-0, initial elongation of the main inflorescence appears to always coincide with the production of floral organs, such that the floral buds are already visible before the main inflorescence elongates. However, in *rSPL15* plants the coincidence between floral bud formation and bolting seems partially lost, where the main inflorescence elongates before floral organs are visible. It is unclear whether reproductive organs are present on the microscopic scale during elongation of the main inflorescence in *rSPL15* plants. Collectively, these results combined with the cell proliferation candidate-target genes of SPL15 mentioned above, suggests that *rSPL15* might not be sufficient to activate the full floral transition at the SAM, but rather activates extension of the rib meristem prematurely, prior to the floral transition. Therefore, elongation of the main stem might be a prerequisite for the production of flowers in Col-0 plants.

The regulation of *AP2-Ls* by SPL15

I initially proposed that SPL15 could also directly repress *AP2-Ls* in SD conditions, as well as indirectly downregulating their expression by activating *FUL* and *MIR172B*. However, several lines of evidence suggest that this is not the case for most *AP2-Ls*. Firstly, in the dissected SAM samples of the SD transcriptome analyses in chapter 4, no consistent correlation between the expression of *AP2-Ls* and SPL15 activity was observed (Fig 4.10). One would have expected that the expression of all *AP2-Ls* goes down in the SAM if that is where they are functioning in floral repression. However, although all *AP2-Ls* have been implicated in the repression of flowering, *AP2-Ls* might not all function in the SAM and might therefore not all be subjected to SPL15-mediated repression at the SAM (Yant *et al.*, 2010). Genes that would be directly repressed by SPL15, might have an opposite expression pattern to *SPL15* and would only be downregulated in the presence of SPL15.

In SD-conditions, the expression of *SMZ* and *TOE2* goes down in both Col-0 and *spl15-1*, indicating their downregulation occurs independently of SPL15 (Fig. 4.10). The expression of *SNZ* and *TOE1* did not significantly change over time in neither Col-0 nor *spl15-1* SAMs, suggesting they might not be critical for the repression of the floral transition in the SAM.

TOE3 was the only *AP2-L* differentially expressed between Col-0 and *spl15-1* in the SD transcriptome analysis (Table 4.3). *TOE3* was positively co-expressed with *FUL*; *i.e.* its expression increased over time (Fig. 4.12). Notably, *TOE3* expression differed from that of the other *AP2-Ls*, in both datasets. This suggests that TOE3 plays a role that is unrelated to floral induction. Such a role has been described for TOE3 in floral patterning and restricting *AGAMOUS* expression, suggesting that higher expression of TOE3 might be specific to the floral primordia (Jung *et al.*, 2014).

Expression of *AP2, TOE1* and *SNZ* did not significantly differ between Col-0 and *spl15-1* plants at any time point in SD conditions, although *AP2* expression seemed slightly higher in *spl15-1* plants over all time points (Fig. 4.10; *p*adj < 0.05). In addition, confocal analysis of SAMs from plants expressing *VENUS::SPL15* or *AP2::VENUS* in a SD time course showed that these two proteins are co-expressed in the SAM for at least two weeks (Fig. 2.12). Direct repression of *AP2* by SPL15 would have likely led to a much more rapid downregulation of *AP2::VENUS* in the SAM. However, this delay in AP2::VENUS downregulation could also be dependent on the stability of the AP2 protein, and might therefore not be visible rapidly, even though its transcription would be going down.

As *AP2, TOE1* and *SNZ,* mRNA expression does not clearly differ between Col-0 and *spl15-1* in SD conditions, SPL15 might not directly downregulate them in the SAM. Alternatively, SPL15 might regulate *AP2, TOE1* and *SNZ* directly and indirectly via FUL and miR172B in which case the differences between direct and indirect regulation might not be clear on the level of mRNA.

In the LD transcriptome analysis *SMZ* was downregulated in Col-0 and *rSPL15* and its expression was significantly lower in *rSPL15* at 9LD. *TOE2* showed a similar pattern, but was significantly lower expressed in *rSPL15* than in Col-0 at 6-, 9-, and 12LD. The expression of *TOE1* did not differ between these two genotypes and *SNZ* and *AP2* were significantly higher expressed in *rSPL15* at 6LD, suggesting that SPL15 is not involved in their downregulation.

Altogether, as the expression patterns of *AP2-L*s differ between LD and SD conditions, the role of *AP2-Ls* in floral induction might be different between LD and SD conditions. Although the expression pattern of some of the *AP2-Ls* goes down over time in LD or SD conditions, it is unclear whether this is by direct repression of SPL15 or even if it is dependent on SPL15. ChIP-qPCR of SPL15 on the loci of these genes in SD conditions will help in determining whether the *AP2-Ls* are directly targeted by SPL15. Moreover, induction of SPL15 activity can be used to find out if the expression of these *AP2-Ls* also changes when SPL15 were to bind to their promoters.

During the stringent selection of candidate SPL15 target genes, and the overlapping of the LD and SD transcriptomes, none of the *AP2-Ls* were identified. Ideally, the expression of the *AP2-Ls* in both transcriptome datasets should be compared with that of the *MIR172* alleles. However, primary MIRNA transcripts were not present in sufficient numbers for analysis in either of the datasets, suggesting that these transcripts are either processed extremely rapidly through the MIRNA-processing machinery to be detected, or that their turn-over is more rapid than that of mRNAs (Chang *et al.*, 2015; Lepe-Soltero *et al.*, 2017). Collectively, these data suggest that the *AP2-Ls* are not directly repressed by SPL15, but indirectly through activation of *FUL* and *MIR172B* and possibly other factors.

The regulation of *FUL* by SPLs

FUL is a direct target of SPL15 and its expression is dependent on SPL15 in SD conditions.

In chapter 2, I showed that *FUL* is important for floral induction by SPL15 in SD conditions (Fig. 2.4; 2.5). Confocal microscopy analyses showed that the initial expression of *FUL* is dependent on SPL15, but flowering-time data also showed that *FUL* is eventually expressed even in the absence of SPL15 (Fig. 2.8; 4.19). In chapter 3, I therefore studied the effect of preventing SPL15 binding to the *FUL* promoter using promoter mutagenesis. I found that mutation of the SPL15 binding sites does not prevent *FUL* expression in SD conditions, suggesting that SPL15 can also indirectly induce *FUL* expression. Unexpectedly, I also observed that mutagenesis of the SPL15-binding sites leads to earlier flowering in LD conditions. The SPL-binding sites in the *FUL* promoter can be bound by, SPL15 and SPL9, as shown in Figure 3.7, but also by SPL3, 4, 5 and 10 (Hyun *et al.*, 2016; Wang *et al.*, 2009; Xie *et al.*, 2020; Yamaguchi *et al.*, 2009; Yao *et al.*, 2019). The earlier flowering phenotype of plants with mutations in the SPL-binding sites in the *FUL* promoter might therefore be caused by loss of binding of other SPLs that act as transcriptional repressors of *FUL*.

The structure of the conserved GTAC motif in the FUL promoter

Region X of the *FUL* promoter contains the core GTAC SPL binding sequence within a highly conserved tandem GTAC motif (Figs. 3.4-3.6; Birkenbihl *et al.*, 2005; Lu *et al.*, 2013; Y. Wang *et al.*, 2009). Combined with several reports showing that other SPLs also bind to this region, suggests a conserved role of SPLs in the regulation of *FUL.* The conserved tandem GTAC motif in the *FUL* promoter suggest that SPLs can bind these motifs as homo-/hetero-dimer or possibly even as a homo-/hetero-tetramer.

A well-described example of how transcription factors regulate genes and confer specificity is that of auxin response factors (ARFs). Some ARFs can form heterodimers, but it was unclear how they bind DNA. Boer *et al.* showed that their binding specificity is determined by the spacing of their binding motifs (Boer *et al.*, 2014). This might not be similar for SPLs, but SPL heterodimers recognising differently spaced GTAC motifs could explain how such a simple 4 bp (GTAC-) motif is specifically recognised by different SPLs. In addition, it would illustrate how the phenotypes of *spl* mutants can be so different.

The DNA-binding domains of all SPLs are highly similar in sequence and structure, but it is unknown whether any protein interaction domains exist that could facilitate dimerization and heterodimerization (K. Yamasaki *et al.*, 2004). *In vitro* binding assays, yeast-two-hybrid assays, or transient expression assays

in planta could be conducted to test whether SPLs can heterodimerise with other SPLs. Alternatively, IP or proximity-labelling using TurboID combined with liquid chromatography to tandem mass spectrometry (LC-MS/MS) could be used to identify SPL15 binding partners *in vivo* during the floral transition in Arabidopsis (Y. Zhang *et al.*, 2019). SPL9, SPL10 and SPL15 have been shown to interact with other proteins such as DELLA, SOC1 and MEDIATOR proteins (Hyun *et al.*, 2016; Richter *et al.*, 2019; N. Yamaguchi *et al.*, 2014; Yao *et al.*, 2019). However, whether SPL15 binds other floral regulators, such as the SPL-target genes AGL42 and FUL, remains unknown. The above-mentioned techniques can be used to identify these interactions to further support the hypothesis of a rather general cooperative module between SPLs and MADS-domain transcription factors.

Candidate SPLs that may bind to the GTAC motifs in the *FUL* promoter to repress transcription

The data in chapter 3 illustrates that *FUL* is regulated by SPL transcription factors, and proposes that the same GTAC motif in the *FUL* promoter is used by SPLs that activate and repress *FUL* transcription. In LD conditions, *ful-2* plants complemented with the *mGTAC FUL* promoter construct already undergo floral transition, even before SPL15 protein is expressed in the meristem. This led me to hypothesis that the GTAC sites in the *FUL* promoter that are bound by SPL15 are also bound by other SPL transcription factors, and that these SPLs inhibit *FUL* expression under LD conditions during the early stages of vegetative development. Because this occurs so early during vegetative development, when miR156 is highly expressed, these repressive SPL transcription factors are likely not targets for miR156-directed posttranscriptional inhibition (G. Wu *et al.*, 2009; G. Wu & Poethig, 2006).

Of the 17 SPL transcription factors in the Arabidopsis genome, 11 are targeted by miR156 (Rhoades *et al.*, 2002; Schwab *et al.*, 2005). SPL1, 7, 8, 12, 14 and possibly 16 are not sensitive to miR156, and might therefore bind to *FUL* during vegetative development to inhibit its expression (Guo *et al.*, 2008; Rhoades *et al.*, 2002). SPL7 has been implicated in plant adaptation to copper deprivation and is phylogenetically distinct from all other SPL transcription factors (Garcia-Molina *et al.*, 2014; Guo *et al.*, 2008; Preston & Hileman, 2013). SPL8 is mainly involved in the development of the gynoecium and pollen sac, and does not clearly contribute to flowering in SD conditions (Fig 4.14; Unte *et al.*, 2003; Xing *et al.*, 2010, 2013). Therefore, and based on their expression patterns, SPL7 and SPL8 are less likely to be regulators of *FUL* expression during vegetative development.

SPL1, 12, 14 and 16 are all relatively large SPL proteins and are related in sequence (Preston & Hileman, 2013) . SPL16 is not likely to regulate *FUL*, because it does not contain the SPL-specific SBP DNA-binding

domain (Guo *et al.*, 2008; Preston & Hileman, 2013). SPL1 and 12 function in inflorescence thermotolerance, suggesting that they are expressed after the floral transition (Chao *et al.*, 2017). However, *SPL12* is expressed in the vegetative SAM, and decreases over time (Jorgensen & Preston, 2014). This indicates that SPL12 might also have a function earlier in plant development. Moreover, the *spl1-1*/*spl12-1* double mutant was also slightly early flowering in LD conditions, suggesting that SPL1 and SPL12 inhibit the floral transition (Schwarz, 2006). Since the *mGTAC* promoter mutants of *FUL* also flowered earlier in LD conditions, SPL1 and SPL12 might be the SPLs that normally bind to the *FUL* promoter to inhibit *FUL* expression. Lastly, SPL14 is involved in sensing the fungal toxin Fumonisin B1 and in regulating plant architecture in Arabidopsis (Stone *et al.*, 2005). SPL14 affects vegetative development, suggesting it is expressed early and might regulate *FUL* expression. However, *spl14* mutants flower late in LD conditions, which makes it unlikely that SPL14 represses *FUL* expression (Stone *et al.*, 2005).

I used my LD-transcriptome data to determine whether any *SPL* genes are expressed during vegetative development in Col-0 (at about 3- and 6LD). I found that *SPL1, 2, 3, 6, 10, 11, 12, 13B* and *SPL15* were expressed highly at 3 LD compared to later time points (Fig. 5.4). In addition, *SPL8, 13A* and *16* were quite highly expressed at 6LD (Fig. 5.4).

The qRT-PCR data for *FUL* expression revealed large differences in *FUL* expression between Col-0, wild-type control lines and the *mGTAC* mutant lines at 6LDs already (Fig. 3.11A). Combining the expression patterns in the RNAseq at 3 and 6LDs with the previous knowledge of SPLs described above, suggests that particularly SPL1 and 12 and 14 are candidates that might inhibit *FUL* expression during early development. In particular, SPL1 and 12 are good candidates because the double mutant flowers slightly earlier in LD conditions and *spl14* mutants were later flowering (Schwarz, 2006; Stone *et al.*, 2005). Because both SPL1 and 12 cluster phylogenetically together with SPL14, mutation of *spl14* potentially enhances the early-flowering phenotype of *spl1-1/12-1* double mutants. If during vegetative development, non-miR156-targeted SPLs repress *FUL,* this would mean that SPL transcription factors that promote flowering, such as SPL15, are repressed during early development both through post-transcriptional repression by miR156 and by competition on their target genes by repressive SPLs.

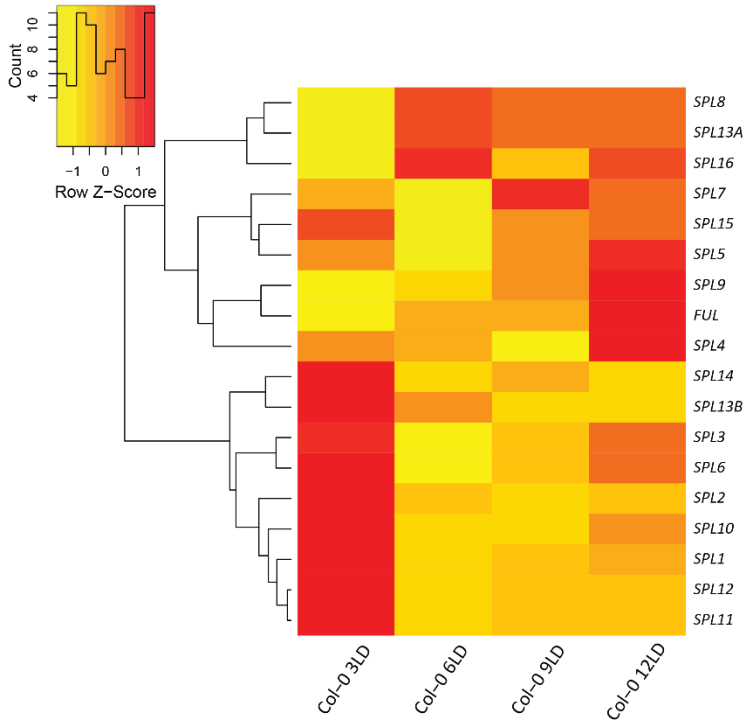

Figure 5.3. Heatmap of *SPLs* in apices Col-0 over time. Heatmap showing the expression of *SPL* genes over time in Col-0 in the LD-transcriptome dataset. Gene expression was calculated from log_2-transformed FPKM values normalised over the whole data set, which were transformed into the Z-score for each gene.

Approaches to test for the negative regulation of *FUL* by SPLs

To test whether *FUL* expression is inhibited during vegetative development, it would be useful to analyse mutants for SPL1, SPL12 and SPL14 under LD conditions. The single, double and triple mutant combinations of *SPL1, 12* and *14* could be grown in LD conditions and their flowering-time compared to that of *mGTAC* mutant lines and Col-0 plants. Moreover, *FUL* expression could be quantified in these *spl* mutants over time to determine whether *FUL* is expressed earlier or at a higher level, as would be expected. In addition, crossing the wild type and mutant *mGTAC* transgenic lines to these backgrounds could help determine if FUL protein expressed from the wild-type promoter is present in the meristem as early as in the *mGTAC* mutant lines in these backgrounds.

An unbiased approach would be to test whether the wild-type and mutant *mGTAC FUL* constructs are bound by SPLs in a yeast one-hybrid (Y1H) assay. Candidate SPL proteins from this Y1H assay could be further tested for their ability to bind to the *FUL* promoter, using EMSA or microscale thermophoresis. In these assays, binding of the wild-type *FUL* promoter could be compared to that of the *mGTAC* mutant promoter to determine whether binding by these SPLs is lost upon mutagenesis.

Lastly, because most of the data in chapter 3 is derived from transgenic lines that express *FUL* from a wild-type or mutated promoter, one confounding effect might be the position-dependent expression of the transgenes. Although different independent lines containing the mutated *FUL* promoter consistently show an earlier flowering phenotype in LD conditions, these transgenes might show expression that is dependent on their position of insertion in the genome. Therefore, clustered regularly interspaced short palindromic repeats (CRISPR)-CRISPR associated protein 9 (Cas9) technology could be used to induce targeted mutations at specific genomic loci, such as at the *FUL* promoter. The open chromatin region in the *FUL* promoter that contains the highly conserved SPL-binding site might be accessible for this approach and could yield mutations in the targeted region. If plants are identified where the conserved region X in *FUL* is partially deleted (Figs. 3.4-3.6), then these plants could be used to study their flowering-time phenotype. In this native background, one can avoid any potential confounding effects with regard to the location of the transgene position. Moreover, in contrast to the transgenic lines, these CRISPR lines could be used for ChIP-qPCR. Using this method one can confirm that SPL15 can no longer bind the mutated region, but also to test whether any other SPL has lost the ability to bind there, and how this affects MEDIATOR complex formation and RNA-polymerase II loading at the native *FUL* locus.

Perspectives

SPL15 is required for timely flowering in non-inductive conditions, and is sufficient to induce early flowering in LD conditions upon overexpression. In this thesis I set out to study how the floral integrator SPL15 regulates the floral transition.

I first genetically characterised the contribution of two known SPL15-targets *FUL* and *MIR172B* to floral induction by SPL15. I found that these two genes contribute to for floral induction in LD and that they are required for the SPL15-mediated floral induction pathway in SD conditions. *FUL* is dependent on SPL15 for its timely expression in SD conditions, whereas *MIR172B* expression seemed to be only partly dependent on SPL15.

Next, I examined how SPL15 regulates *FUL* expression by mutating the putative SPL15 binding sites in the *FUL* promoter. This showed that in SD conditions, SPL15 can indirectly regulate *FUL* expression and does not require direct binding to the *FUL* promoter. Notably, I found that in LD conditions, mutagenesis of the *FUL* promoter led to earlier flowering, suggesting that during vegetative development in LD conditions, *FUL* is normally repressed by SPLs. I hypothesised that particularly SPL1 and SPL12 might be involved in the repression of *FUL* during vegetative development. SPL1 and SPL12 might compete as repressors with other activating SPLs such as SPL15, for binding to the *FUL* promoter during the floral transition. Future studies should make use of genetics and expression analyses to determine whether SPL1 and SPL12 are responsible for transcriptional repression of *FUL.*

Lastly, I identified novel high confidence putative target genes of SPL15 by analysing the transcriptomes of plant overexpressing SPL15 in LD conditions and plants mutated in *spl15* in SD conditions. These candidate target genes of SPL15 included *SOC1, AGL42, SPL4* and *TFS1,* which are known to play roles in floral induction. I also found several genes with a role in cell proliferation such as *AN3* and *CKX3,* and proposed that these genes are involved in SPL15-mediated floral induction but also in SPL15-mediated primary inflorescence elongation. Additional genetic analyses will be needed to characterise the function of these novel putative target genes in floral induction mediated by SPL15. Moreover, I propose that SPL15 might cooperate with other MADS-domain transcription factors such as AGL42, in the transcriptional activation of target genes. I therefore suggest to use Y2H, ChIP-qPCR, Co-IP and mass spectrometry to define if SPL15 indeed binds to other MADS-domain transcription factors and how this affects transcriptional activation.

Taken together, this thesis has contributed to a better understanding of SPL15-mediated flowering and provides novel insights into how SPL15 regulates this transition in Arabidopsis.

Chapter 6:

Materials and methods

Plant material and growth conditions

Plant material

All mutant lines and generated transgenic lines are in the Col-0 ecotype background. Col-0 was used as a control genotype; often referred to as "wild-type". Mutant lines used are listed in Table 6.1. Primers that were used to genotype the mutant lines are listed in Table 6.15.

Table 6.1. Table with mutant and transgenic lines used in this work.

Mutant/transgenic line	Reference
spl15-1	(Hyun *et al.*, 2016)
ful-2	(Ferrándiz, Gu, *et al.*, 2000)
soc1-2	(H. Lee *et al.*, 2000)
spl8-1	(Unte *et al.*, 2003)
tfs1-1	(Richter *et al.*, 2019)
***spl4* CRISPR mutant**	Generated in the Coupland lab by Youbong Hyun
mir172a-2, mir172b-3, mir172c-1, mir172d-3	(O'Maoileidigh *et al.,* in review)
pSPL15::VENUS::9A::SPL15/Col-0	(Hyun *et al.*, 2016)
pSPL15::VENUS::9A::rSPL15/Col-0	(Hyun *et al.*, 2016)
pFUL::FUL::9A::VENUS/*ful-2*	Generated in this work (described below)
pFULmGTAC::FUL::9A::VENUS/*ful-2*	Generated in this work (described below)
pFULmCArG::FUL::9A::VENUS/*ful-2*	Generated in this work (described below)
pFULmCArG-mGTAC::FUL::9A::VENUS/*ful-2*	Generated in this work (described below)
pMIR172A::MIR172A::VENUS::GUS/Col-0	(O'maoileidigh *et al.*, in review)
pMIR172B::MIR172B::VENUS::GUS/Col-0	(O'maoileidigh *et al.*, in review)
pMIR172D::MIR172D::VENUS::GUS/Col-0	(O'maoileidigh *et al.*, in review)
pAP2::AP2::VENUS/Col-0	Generated in the Coupland lab by Qing Sang
pAP2::rAP2::VENUS/Col-0	Generated in the Coupland lab by Qing Sang
pTFS1::TFS1::9A::VENUS/*tfs1-1*	(Richter *et al.*, 2019)
pSOC1::SOC1::GFP/Col-0	(Immink *et al.*, 2012)
pSPL15::HA::GR::SPL15/*spl15-1*	Generated in this work (described below)
pSPL15::SPL15::GR::HA/*spl15-1*	Generated in this work (described below)
pSPL4::SPL4::9A::VENUS/Col-0	Generated in the Coupland lab by Rafael Martinez Gallegos

Growth conditions

Prior to every experiment, seeds were imbibed in tubes with water or on wet soil at 4°C in the dark for 3 days. Plants were germinated and grown under LD conditions (16 h light, 8 h dark) or SD conditions (8 h light, 16 h dark) under photosynthetic photon flux density (PPFD) of 180 µmol/s/m^2. Plants grown on plates

were sown on full-strength Murashige and Skoog (MS) medium containing 1% sucrose and were stratified on plates at 4°C for 3 days (*FT* and *TSF* expression analysis, chapter 3). For selection for Basta-resistance, seeds were sterilised with chlorine gas. For this sterilisation, seeds were put in tubes with an open lid and placed in a rack inside a desiccator. A large beaker was filled with 100 mL sodium hypochlorite solution (12% Cl; Carl ROTH, Cat. # 9062.3) solution to which 10 mL 37% HCl was added before closing the desiccator. Seeds were sterilised for 4–5 h, after which they were sown on full-strength MS medium with 1% sucrose and 12 µg/mL phosphinothricin (PPT). Seeds were imbibed on plates as described above and transferred to LD conditions for the germination and selection of resistant, surviving plants.

Molecular cloning

PIPE cloning

The Polymerase Incomplete Primer Extension (PIPE) cloning method was used to create all cloning vectors in this thesis (Klock & Lesley, 2009). This technique is based on amplifying insert (I) and vector (V) fragments with overlapping ends, and directly transforming these fragments into *Escherichia coli* to allow them to fuse into the desired plasmid. For *FUL* constructs, an existing construct containing the *FUL* promoter (complete upstream intergenic region including 5' UTR; 5,182 bp), the *FUL* genic region including the 9×Alanine::VENUS fusion and the complete downstream intergenic region (including 3' UTR; 1,241 bp) in the *p*STB205 plasmid (modified pDONR205 plasmid) was used as a template for all mutant constructs. Insert fragments were PCR-amplified with Phusion® High-Fidelity DNA Polymerase (New England Biolabs, Cat. # M0530S) according to the manufacturer's recommended protocol and contained part of the *FUL* promoter with the mutagenized sites (mGTAC or mCArG; Fig. 3.6) at the ends of the fragments, immediately before the overlapping ends. Vector fragments were PCR-amplified using PrimeSTAR® GXL DNA Polymerase (TaKaRa, Cat # R050B) and contained the rest of the *FUL* promoter, the genic region, the *VENUS*-fusion, as well as the downstream region and the complete *p*STB205 backbone.

The *SPL15* promoter and genic region with overlapping ends were PCR-amplified from the existing *pSPL15::9A::VENUS::SPL15/pDONR201* plasmid with Phusion® High-Fidelity DNA Polymerase (New England Biolabs) as described above (Hyun *et al.*, 2016). Similarly, the *GR* sequence with overlapping ends was PCR-amplified from *pML::BART::35S::GR::LhG4* (Eshed *et al.*, 2001; Ó'Maoiléidigh *et al.*, 2015) and *HA* was attached to *GR* by fusing its sequence into the *GR* primers with overhang. The generated insert thus contained *GR* fused to *HA* with overhangs and the vector contained the *SPL15* promoter, genic region, downstream region and the *p*DONR201 backbone.

For each insert and vector fragment, 5 µL PCR product was checked for its size on 1% agarose gel after which it was digested with *Dpn*I in Cutsmart buffer according to the manufacturer's recommended protocol, to destroy the original plasmid templates (New England Biolabs, Cat. # R0176S). After digestion, PCR products were purified by adding 150 µL TE buffer (pH 8.0; Table 6.13) to 50–70 µL PCR product and adding an additional 100 µL PEG solution (30% polyethylene glycol 8000 (Merck Cat. # P5413-1KG)/30 mM $MgCl_2$). This mixture was directly centrifuged at full speed (14,000 rpm) for 30 min at room temperature. After centrifugation, the supernatant was carefully removed and the pellet was dissolved in 18 µL dH_2O. For each fragment, the DNA concentration was measured with a NanoDrop 1000 spectrophotometer and for each generated construct, the purified insert and vector fragments were combined in a 20:200 (V:I) femtomolar ratio and directly transformed into chemically competent *E.coli* cells. Details on vectors used

can be found in Table 6.7, primer sequences used for cloning are listed in Table 6.16 and PCR protocols can be found in Tables 6.2–6.6 and Table 6.9.

Table 6.2. PCR mixture for Phusion PCR.

Reagent	Volume/amount
dH_2O	54 µL
5× HF buffer (provided by manufacturer)	15 µL
dNTP (10 mM)	1.5 µL
FW primer	1.5 µL
REV primer	1.5 µL
Phusion High-Fidelity DNA Polymerase (New England Biolabs, Cat. # M0530S)	0.75 µL
Template DNA/plasmid	60 ng

Table 6.3. PCR program for Phusion PCR.

PCR step		Temperature	Time
Initiation		98°C	30 seconds
35 cycles	Denaturation	98°C	10 seconds
	Annealing	60°C	30 seconds
	Extending	72°C	3 minutes
Final extension		No final extension	
Hold		4°C	∞

Table 6. 4. PCR mixture for Primestar PCR.

Reagent	Volume/amount
dH_2O	30 µL
5× Primestar GXL buffer (provided by manufacturer)	10 µL
dNTP (2.5 mM each; provided by manufacturer)	4.0 µL
FW primer	1.5 µL
REV primer	1.5 µL
PrimeSTAR GXL DNA polymerase (TaKaRa, Cat # R050B)	2.0 µL
Template DNA/plasmid	60 ng

Table 6.5. PCR program for Takara PCR.

PCR-step		Temperature	Time
Initiation		98°C	30 seconds
15 cycles	Denaturation	98°C	10 seconds
	Annealing	60°C	15 seconds
	Extension	68°C	12 minutes
Final extension		No final extension	
Hold		4°C	∞

Gateway LR-reactions

Gateway LR reactions with Gateway LR Clonase II Enzyme Mix (Invitrogen, Cat # 11791-020) were used to transfer constructs from the cloning vector into the *p*EarleyGate301 expression vector (Invitrogen Gateway; Earley *et al.*, 2006). LR-reactions were performed according to the manufacturer's protocol. In short: 1–2 µL cloning vector was combined with 1 µL expression vector and up to 10 µL TE buffer (pH 8.0) on ice. To this mixture, 2 µL pre-thawed Gateway LR Clonase II Enzyme Mix was added and the mixture was vortexed and incubated at 25°C for 2 h. After incubation, the complete mixture was directly transformed into chemically competent *E.coli* cells. Generated vectors can be found in Table 6.7 and antibiotic concentrations in Table 6.14.

Chemical transformation *E. coli*

Chemically competent DH5α TSSGT *E. coli* cells (50 µL) were thawed on ice for 10 min and then the DNA was gently added to the cell mixture. Cells were incubated with DNA for 30 min on ice and were then heat-shocked for 3 min on 37°C on a thermal block. After heat-shock treatment, the cells were kept on ice for an additional 3 min, after which 450 µL of liquid Lysogeny Broth (LB) culture medium was added. The transformed cells were placed in a shaking incubator at 37°C for 1.5 h for recovery. After recovery, the whole mixture was spread onto an LB-agarose plate containing the appropriate selective antibiotics and grown overnight. A selection (~10) of recovered colonies was grown on liquid culture overnight and plasmids were purified using a plasmid purification kit (Macherey Nagel, Cat. # 740588.50. Plasmids were tested by PCR, enzyme digestion and sequencing to obtain the final correct plasmids. Correct expression clones were transformed into *Agrobacterium tumefaciens.*

Table 6.6. PCR mixture colony PCR.

Reagent	Volume/amount
dH_2O	14.9 µL
10× buffer (provided by manufacturer)	2.0 µL
$MgCl_2$ (50 mM; provided by manufacturer)	0.6 µL
dNTP (10 mM)	0.4 µL
FW primer	1.0 µL
REV primer	1.0 µL
Taq Polymerase (6 U/µL Invitrogen/ThermoFisher: Cat. #: 18038018)	0.1 µL

Agrobacterium tumefaciens transformation

Electrocompetent GV3101 *p*SOUP *A. tumefaciens* cells (50 µL) were thawed on ice for 10 min and then 100 ng DNA was gently added to the cell mixture. Cells were electroporated in 1-mm cuvettes with a pulse of 2.20 kV. After electroporation, 450 µL LB liquid culture medium was added and the cells were incubated at 28°C in a shaking incubator for 2 h to recover. After recovery, the whole mixture was spread onto an LB-agarose plate containing the appropriate selective antibiotics (for *A. tumefaciens*: rifampicin, tetracycline, gentamycin and the vector-specific antibiotic (Table 6.7 and 6.14)) and grown for 48 h at 28°C.

Plant transformation

A pre-culture of *A. tumefaciens* (2 mL, 48 h, 28°C) was used to inoculate a 250-mL culture containing the appropriate antibiotics and was grown overnight in a shaking incubator at 28°C. The large overnight culture was mixed with 250 mL 20% sucrose (w/v) and 0.1% Silwet L-77 (Loveland Industries LTD). Plants of the desired genotype with open flowers were dipped into the mixture for 1 min, after which they were covered with plastic and kept in the dark for 12 h at room temperature (Clough & Bent, 1998). At least 54 plants were transformed per construct.

Table 6.7. Generated and used vectors and their descriptions.

Name	Vector type	Description	Resistance
pDONR201	Cloning vector	Standard Gateway® entry vector used for taking up DNA fragments for cloning	Kanamycin
pSTB205	Cloning vector	Modified Gateway® entry vector (pDONR205) used for taking up DNA fragments for cloning	Kanamycin
pEarleyGate301	Binary vector	Gateway compatible binary vector used for LR-reaction with donor vector	Kanamycin
pFUL::FUL:: VENUS pSTB205	Donor vector	pSTB205 vector containing the whole wild-type genomic region of *FUL,* with *VENUS* fused at the C-terminus.	Kanamycin
pFUL::FUL:: VENUS pEarleyGate301	Expression vector	pEarleyGate301 vector containing the whole wild-type genomic region of *FUL,* with *VENUS* fused at the C-terminus.	Kanamycin
pFUL_mGTAC:: FUL::VENUS pSTB205	Donor vector	pSTB205 vector containing the whole genomic region of *FUL* with *mGTAC* mutations in the promoter and *VENUS* fused at the C-terminus.	Kanamycin
pFUL_mGTAC:: FUL::VENUS pEarleyGate301	Expression vector	pEarleyGate301 vector containing the whole genomic region of FUL with mGTAC mutations in the promoter and VENUS fused at the C-terminus.	Kanamycin
pFUL_mCArG:: FUL::VENUS pSTB205	Donor vector	pSTB205 vector containing the whole genomic region of *FUL* with *mCArG* mutations in the promoter and *VENUS* fused at the C-terminus.	Kanamycin
pFUL-mCArG:: FUL::VENUS pEarleyGate301	Expression vector	pEarleyGate301 vector containing the whole genomic region of FUL with mCArG mutations in the promoter and VENUS fused at the C-terminus.	Kanamycin
pFUL_mCArG_mGTAC:: FUL::VENUS pSTB205	Donor vector	pSTB205 vector containing the whole genomic region of *FUL* with *mCArG* + *mGTAC* mutations in the promoter and *VENUS* fused at the C-terminus.	Kanamycin
pFUL-mCArG_mGTAC:: FUL::VENUS pEarleyGate301	Expression vector	pEarleyGate301 vector containing the whole genomic region of FUL with mCArG + mGTAC mutations in the promoter and VENUS fused at the C-terminus.	Kanamycin
pSPL15::HA::GR::SPL15 pDONR201	Donor vector	pDONR201 vector containing the whole wild-type genomic region of *SPL15,* with *HA::GR* fused at the N-terminus.	Kanamycin
pSPL15::HA::GR::SPL15 pEarleyGate301	Expression vector	pEarleyGate301 vector containing the whole wild-type genomic region of SPL15, with HA::GR fused at the N-terminus.	Kanamycin
pSPL15::SPL15::GR::HA pDONR201	Donor vector	pDONR201 vector containing the whole wild-type genomic region of *SPL15,* with *GR::HA* fused at the C-terminus.	Kanamycin
pSPL15::SPL15::GR::HA pEarleyGate301	Expression vector	pEarleyGate301 vector containing the whole wild-type genomic region of SPL15, with GR::HA fused at the C-terminus.	Kanamycin

DNA extraction and genotyping

Genotyping of mutant lines and mutant combinations was performed on single leaves (c. 0.5 × 0.5 cm) from F_2-generation plants. DNA was extracted either manually using a modified Edward's DNA extraction protocol (below) or using the Biosprint 96 with RLT buffer according to the manufacturer's protocol for 100 µL reactions (Qiagen: Cat. #: 941557; Edwards *et al.*, 1991).

Edward's DNA extraction

The collected leaf samples were ground in 390 µL extraction buffer (Table 6.13) without SDS and with two tungsten beads using the Qiagen TissueLyser II. After disruption, 10 µL 20% SDS (Merck; Cat. # 11667289001) was added to each tube and the samples were centrifuged for 3 min at 14,000 rpm. 300 µL of supernatant was transferred to a fresh 1.5-mL Eppendorf tube and mixed with 300 µL isopropanol. This mixture was centrifuged for 5 min at 14,000, the supernatant was gently removed, and the pellet was washed with 850 µL 70% ethanol (3 min, 14,000 rpm). Again, the supernatant was removed and the pellets were dried in a SpeedVac for 15 min at 30°C while spinning under vacuum. After drying, the pellet was dissolved in 100 µL dH_2O.

Genotyping PCRs

For all genotyping PCRs, standard lab PCR protocols were employed (Tables 6.8 and 6.9) and Taq-DNA Polymerase (Invitrogen/ThermoFisher: Cat. #: 18038018) was used for amplification. 1 µL Edward's-isolated DNA or 2 µL Biosprint 96-isolated DNA was added to each 20-µL reaction mixture. PCR amplicons were visualised on a 1% agarose gel, except for those used to genotype the *mir172* mutant. *mir172* mutants were genotyped only using Edward's isolated DNA, and the PCR products for *mir172a-2, mir172b-3, mir172c-1, mir172e-1* were directly electrophoresed on a 3% agarose gel, because the wild-type fragments were only ~50–100 bp longer than the mutant fragments. The *mir172d-3* PCR product was first digested with 1 µL *Pst*I (New England Biolabs, Cat # R0140S) for 3 h at 37°C. This enzyme digests the wild-type fragment and not the mutant fragment. The restriction product was electrophoresed on a 3% agarose gel to analyse the restriction pattern. Primer pairs are indicated in Table 6.15.

Table 6.8. Genotyping PCR mixture.

Reagent	Volume/amount
dH_2O	Up to 20 µL
10× buffer (provided by manufacturer)	2.0 µL
$MgCl_2$ (50mM; provided by manufacturer)	0.6 µL
dNTP (10mM)	0.4 µL
FW primer	1.0 µL
REV primer	1.0 µL
Taq Polymerase (6U/µL Invitrogen/ThermoFisher: Cat. #: 18038018)	0.1 µL
Template DNA	1.5–2.0 µL

Table 6.9. PCR program for colony and genotyping PCRs.

PCR-step		Temperature	Time
Initiation		94°C	3 minutes
30 cycles	Denaturation	94°C	45 seconds
	Annealing	Primer-pair specific	30 seconds
	Extending	72°C	90 seconds/kb
Final extension		72°C	10 minutes
Hold		4°C	∞

RNA extraction, qRT-PCR and transcriptome analyses

RNA extraction and qRT-PCR

Material for qRT-PCR and RNA-sequencing was harvested and directly frozen in liquid nitrogen and stored at -80°C. For all qRT-PCRs on apices (Table 6.10), except for those performed during the testing of the RNA-sequencing material, 6–12 SAMs were harvested. For the testing of *FUL* expression among independent *FUL* transgenic lines, 10–12 flowers at anthesis were harvested.

Table 6.10. Details of the dissection methods used for meristem enrichment in this thesis.

Name used in thesis	Meristem-enrichment methods
Apices	Material was enriched for meristematic tissue by removing as much leaf material as possible by eye. Meristematic tissue was clipped from the hypocotyl.
Dissected SAMs	Material was enriched for meristematic tissue by removing all leaf material under the stereo microscope with forceps. Only 2–3 leaf primordia were left on the SAM, and the SAM was precisely excised from the epicotyl (Fig 4.7B).

RNA was extracted after disrupting the frozen tissue with the Qiagen TissueLyser II and samples were returned to liquid nitrogen before further extraction. The RNeasy® Plant Mini Kit was used for extraction according to the manufacturer's recommendations (Qiagen: Cat. # 74904) and during the extraction, samples were kept at 4°C as much as possible. RNA was dissolved in 20 µL of RNAse-free dH_2O and quantified using a NanoDrop 1000 spectrophotometer (Thermo Scientific). Up to 5 µg RNA was incubated with DNaseI (TURBO DNA-free kit™, Invitrogen: Cat. # AM1907) to remove genomic DNA according to the manufacturer's protocol. For cDNA synthesis, 0.6–0.8 µg of DNA-free RNA was used in a reverse-transcription reaction (Superscript® IV; Invitrogen: Cat. # 18090010) and diluted 1:2 with dH_2O. Depending on the original RNA yield, 2 µL diluted cDNA was used in a qRT-PCR reaction with iQ™ SYBR® green supermix (Bio-Rad: Cat. # 170-8880). Relative transcript abundance was determined with a Roche LightCycler® 480 system (see Table 6.11 and Table 6.12 for programme and mixtures).

Table 6.11. PCR mixture for qRT-PCR.

Reagent	Volume/amount
dH_2O	2.0 µL
FW primer	0.5 µL
REV primer	0.5 µL
iQ™ SYBR® green supermix (Bio-Rad: Cat. # 170-8880)	5.0 µL
cDNA	2.0 µL

Table 6.12. PCR program for qRT-PCR.

Step		Temperature (Ramp rate)	Duration
Initiation		95°C	10 seconds
42 cycles	Denaturation	95°C (4°C/s)	10 seconds
	Annealing	60°C (2.2°C/s)	20 seconds
	Extension (single acquisition)	72°C (4.4°C/s)	20 seconds
Melting curve		97	5 seconds
		65	60 seconds
	5 acquisitions/°C	65-95°C (0.11°C/s)	-

qRT-PCR analysis

Relative expression differences were calculated relative to the expression of endogenous reference gene *SERINE/THREONINE PROTEIN PHOSPHATASE 2A* (*PP2A*) in each sample using the ΔΔCT method (Czechowski *et al.*, 2005; Livak & Schmittgen, 2001). As a second reference, samples were normalised against the expression of the gene of interest (normalised against *PP2A* expression) in Col-0 at the earliest time points (in time courses), or against the expression of Col-0 (such as for *FUL* or *SPL15* expression analysis in independent transgenic lines) or against Col-0 treated with a mock solution (during the DEX experiments). Calculations were done in Excel and the variation shown in all figures is the standard deviation. For all expression studies at least three independent biological replicates were used, unless indicated otherwise in the figure legends. Prior to first use, efficiency of oligonucleotides for qRT-PCR were tested using a standard curve and a dilution series up to 10-fold. Primers with an efficiency between 1.9 and 2.0 were considered good primers.

Harvesting for RNA-sequencing

For the LD RNA-sequencing experiment (Col-0 *vs*. *rSPL15*), 10–20 apices were harvested, but for the SD RNA-sequencing experiment (Col-0 *vs*. *spl15-1*), 20–25 SAMs were dissected under the microscope and all leaves bigger than 40 µm in length were removed (Table 6.10).

Transcriptome analyses

RNA for RNA-sequencing was extracted as described above, however up to 5 µg of RNA was incubated with TURBO-DNAse (Invitrogen; Cat # AM2238) as recommended by the manufacturer to remove any DNA left in the RNA samples. However, this DNAse was not inactivated, instead the samples were immediately purified and when needed concentrated (in the case of a low RNA yield), using a RNA Concentrator kit

(ZYMO Research, Cat # R1015). After purification, the RNA was stored in 5 µL aliquots at -80 °C and when samples from all independent biological replicates were isolated and purified, one of the 5 µL aliquots was send for library preparation and sequencing at the Max Planck-Genome-centre Cologne (https://mpgc.mpipz.mpg.de/). Sequencing was done with Illumina HiSeq3000 and for each sample, 15 million reads were sequenced.

After RNA-sequencing, the Illumina reads were pre-processed to remove any residual library adaptors with CutAdapt and the low-quality bases (Q<15) were trimmed from the ends with Trimmomatic (Bolger *et al.*, 2014; Martin, 2011). Only reads with a minimum length of 50nt were kept. Salmon was used to quantify the abundance of transcripts from the *Arabidopsis* reference transcriptome R2D2 (including GC-bias, unstranded samples; done by Dr. Edouard Severing) (Patro *et al.*, 2017; R. Zhang *et al.*, 2017).

Gene differential expression analysis was performed using *DESeq2*. by comparing Col-0 to either rSPL15 (LD-transcriptome) or *spl15-1* (SD-transcriptome) for each time point and using the standard settings. An adjusted *p*-value threshold of 0.05 (padj; multiple testing correction on the *p*-value) was used to identify differentially expressed genes (DEGs). The resulting lists of DEGs including the expression data are listed in Appendix 1 and 2 and can be provided upon request.

Visualisation of the data was done using the R-packages *ggplot2, VennDiagram, gplots, gridExtra* and *futile.logger* to generate plots, venn-diagrams and heatmaps, and to compare datasets. Input data used to generate all transcriptome figures are described in each figure legend. All scripts used for generating figures and calculations can be provided upon request.

Plant analyses

Flowering-time analyses

Plant age and flowering time was measured from when seeds were transferred to ambient growth conditions. Flowering time was scored as: 1) bolting time; the number of days after sowing before the inflorescence extended 0.5 mm out of the rosette; 2) flowering time; the number of days after sowing before the first flower opened anywhere on the plant and 3) total leaf number (TLN); the number of rosette leaves and the number of cauline leaves on the main inflorescence.

Confocal imaging and sample preparation

Samples for confocal laser scanning microscopy were harvested at indicated timepoints around Zeitgeber time 6, by dissecting shoot apical meristems (SAMs) under the stereo microscope. Dissected samples were directly placed in 4% paraformaldehyde dissolved in 1× phosphate-buffered saline solution (PBS; pH 7.0; Table 6.13) on ice. Samples were subsequently fixed on ice for 1 h at ~700 mbar. After fixation, samples were rinsed three times for 1 min with PBS and were then submerged in ClearSee (Table 6.13) and kept in the dark at room temperature. ClearSee reagent was prepared as described in Kurihara *et al.* (2015). One day before imaging, the ClearSee solution was exchanged with ClearSee containing 0.1% SCRI Renaissance 2200 dye for cell-wall staining (T. Musielak *et al.*, 2016). SAMs were imaged 3–4 days after sampling and were mounted in 0.8% low-melt agarose in a Petri dish (Bio-rad: Cat. # 1613113). Imaging was performed with a 20× (only in chapter 3) or 40× water-dipping lens using a confocal laser scanning microscope (Leica SP8) to image both VENUS (laser wavelength, 514 nm; detection wavelength, 517–569 nm) and the Renaissance dye (laser wavelength, 405 nm; detection wavelength, 410–503 nm) by sequential scanning. Samples within a single experiment were always imaged with the same settings although sometimes the gain was altered for the imaging of the Renaissance dye, to prevent overexposure.

Silique measurements and cauline leaf analysis

To measure the length of the siliques for different *FUL* transgenic lines (Fig. 3.8E) from three independent plants per line, siliques 5–10 (from the bottom of the inflorescence up) were removed from the plant and photographed next to a ruler (Canon EOS 600D). All image data were collected and loaded into Fiji (ImageJ 1.52p), where for every image, the scale was set using the ruler in the image. For each image, the length of the siliques was measured from the pedicel to the tip, with the *measure* function of Fiji. For the morphology of the cauline leaves (Fig. 3.8C, D), one representative leaf per plant line was photographed (Canon EOS 600D).

Dexamethasone induction

For induction experiments with Dexamethasone (DEX; Merck: Cat #D4902-25MG), 1.5 µL of DEX (10 µM dexamethasone, 0.01% EtOH and 0.015% Silwet L-77 in dH_20) or mock (0.01% EtOH and 0.015% Silwet L-77 in dH_20), solution was pipetted onto the centre of the rosette. During the trial experiment for testing and selecting functional SPL15 induction lines, solutions were applied once per week from 3wSD until plants bolted 1 cm. During the subsequent experiment for confocal imaging, solutions were applied every 2–3 days from 3wSD until 9wSD and for the last flowering time experiment, solutions were applied every 2–3 days from 3wSD until 11wSD.

Heterologous reporter assay

Transactivation reporter assay for binding of the *FUL* promoter by SPL9 and SPL15

These experiments were conducted by Dr. Jennifer Andres from the Institute of Synthetic Biology at the Heinrich Heine University in Duesseldorf.

For the quantitative transactivation reporter assay for binding of SPL9 and SPL15 to the *FUL* promoter or promoter fragments, human embryonic kidney cells (HEK293T; DSMZ, Braunschweig, Germany) were cultivated and transfected with equal amounts (w/w) of two plasmids. One plasmid contained the coding sequence of SPL9 or SPL15 fused to the VP16 herpes simplex virus-derived transactivation domain driven by a constitutive promoter (pSV40), and the second contained a construct with the wild-type or mutant *FUL* promoter or promoter fragments upstream of a minimal promoter (phCMVmin) controlling the human Secreted Alkaline Phosphatase (SEAP) reporter gene.

HEK cells were cultivated in Dulbecco´s modified Eagle´s medium (DMEM, PAN Biotech, Cat. # P04-03550) supplemented with 10% (v/v) tetracycline-free fetal bovine serum (FBS; PAN Biotech; Cat. # P30-3602; batch no. P080317TC) and 1.4% (v/v) penicillin/streptomycin (PAN Biotech; Cat. # P06-07100) at 37°C (5% $C0_2$). Transfection was carried out in 24-well plates by dropwise adding 100 µL 15-min-incubated (room temperature) transfection mixture (50 µL OptiMEM with 0.75 µg DNA (Invitrogen, Thermo Fisher Scientific) + 50 µL OptiMEM with 2.5 µL polyethylenimine solution (1 mg/mL, Polysciences Europe GmbH Cat. # 23966-1)) to each well with 500 µL HEK-cell culture (50,000 cells grown in DMEM culture medium for 24 h). Four hours after transfection, the medium was exchanged with fresh DMEM medium. Cells were incubated for 48 h after transfection at 37°C (5% $C0_2$), after which 200 µL of supernatant per sample was taken for SEAP quantification. Endogenous phosphatases were first heat-inactivated by subjecting the supernatant to 65°C for 1 h. After heat-inactivation, 80 µL supernatant per sample was transferred to a transparent 96-well assay plate to which 100 µL SEAP buffer was added (20 mM L-homoarginine, 1 mM $MgCl_2$ 21% (v/v) diethanolamine). 20 µL 120 nM para-Nitrophenylphosphate (pNPP, Sigma-Aldrich) were added to each sample prior to the measurement, after which the absorbance was measured at 405 nm for 1 h in a Berthold technologies Tristar^{2}S LB942 Multimode Plate Reader. SEAP activity (U/L) was calculated using the slope of the obtained curves [OD/min] combined with the Lambert-Beer's Law as described in (Balbas & Lorence, 2004; page 463–464; light path length 0.6 cm).

In silico analyses

Phylogenetic tree construction

The phylogenetic tree was constructed by Dr. Edouard Severing. The genomes of *Arabidopsis halleri, Arabidopsis lyrata, Capsella rubella, Capsella grandiflora, Cardamine hirsuta, Brassica oleracaea, Brassica rapa, Eutrema salsugineum* and *Cleome hassleriana* were downloaded from phytozome (Goodstein *et al.*, 2012). The *Arabis alpina* genome was downloaded from http://www.arabis-alpina.org (Willing *et al.*, 2015) and the genomes of *Camelina sativa, Brassica napus, Arabis nordmaniana, Aethionema arabicum, Leavenworthia alabamica* were downloaded from the CoGe website (https://genomevolution.org/coge/; Lyons & Freeling, 2008). The genomes of *Arabis iberica, Arabis auriculata* and *Arabis montbretiana* were previously sequenced in-house.

Exonerate was used (Slater & Birney, 2005) to identify the *FUL* gene in the genomes of these *Brassicaceae* species using the Arabidopsis *FUL* protein sequence (AT5G60910) as query. A multiple sequence alignment of the resulting *FUL* protein sequences was created using MUSCLE (Edgar, 2004). Noisy regions were subsequently removed from the alignments using TrimAl (Capella-Gutiérrez *et al.*, 2009; automated 1 mode) and a codon alignment was generated by replacing individual amino-acids by their corresponding codon triplet and each gap was multiplied by three. To build the final maximum likelihood tree, MODELTEST was first used to choose the most appropriate nucleotide substitution model (Posada & Crandall, 1998). Using this model, the tree was calculated with PhyML (Guindon *et al.*, 2009). One hundred bootstrap rounds were done to get branch support for the maximum likelihood tree, as is also depicted in the figure.

Phylogenetic shadowing of *FUL*

Phylogenetic shadowing of FUL protein was done using multiple sequence alignment software Clustal Omega (https://www.ebi.ac.uk/Tools/msa/clustalo/; Madeira *et al.*, 2019). Phylogenetic shadowing of *FUL* genic region was done with mVista (http://genome.lbl.gov/vista/mvista/submit.shtml; Frazer *et al.*, 2004; Mayor *et al.*, 2000) and regions of interest were extracted from here and re-aligned using multiple sequence alignment software MAFFT (https://www.ebi.ac.uk/Tools/msa/mafft/). All visualisations were done with Jalview (https://www.jalview.org/).

Data analysis

All data analyses and statistical calculations were done in R-studio (version 1.2.5019; https://rstudio.com/) using these packages: *ggplot2, plyr, dplyr, tidyverse, reshape2* and *multcompView.* Statistical tests were either done with one-way ANOVA and a Tukey-HSD multiple testing correction in the case of multiple

comparisons, or with students *t*-test in the case of pairwise comparisons (all described in figure legends). In flowering time analyses, all statistical test on leaf number were done on the total leaf number (TLN) unless indicated otherwise in the legend.

Table 6.13. List of buffers used and their components.

Application	Buffer / reagent	Components
PEG-purification PCR products	TE-buffer (pH 8.0)	10 mM Tris pH 7.5, 1 mM EDTA in dH_2O
Edward's DNA extraction	DNA Extraction buffer	200 mM Tris-HCl pH 7.5-8.0, 250 mM NaCl, 25 mM EDTA in dH_2O
Plant tissue fixation	10× PBS (pH 7.0)	1.5 M NaCl, 0.07M Na_2HPO_4, 0.03 M NaH_2PO_4 in dH_2O
Clearing of plant tissue	ClearSee	10% (w/v) xylitol powder, 15% (w/v) sodium deoxycholate and 25% (w/v) urea in dH_2O

Table 6.14. List of the antibiotics used and their final concentrations.

Antibiotic	Concentration used
Kanamycin	25 µg/mL
Rifampicin	50 µg/mL
Tetracycline	10 µg/mL
Gentamycin	8 µg/mL

Table 6.15. List of oligonucleotides used for genotyping in this thesis.

Oligo number	Oligo name	Oligo sequence	Oligo used for:
B112	spl15-1_F (DM)	TGCATCACTGATCTTGCGGTTG	Genotyping spl15-1 (Use with B113 for SPL15)
B113	spl15-1_R (DM)	GGAGTTGTTAATGTGTTCGGGTCAG	Genotyping spl15-1 (Use with B054 for *spl15-1*)
B054	GtF_LBb1_SALK	GCGTGGACCGCTTGCTGCAACT	Left border primer b1 for SALK lines (Genotyping *spl15-1)*
B034	Gt_FW_SOC1-2	TTCTTCTCCCTCCAGTAATGC	Genotyping *soc1-2* (Use with B035 for SOC1 and with B036 for *soc1-2*)
B035	Gt_REV_SOC1-2	GAGTTTTGCCCCTCACCATA	Genotyping *soc1-2*
B036	Gt_FW_Lba1_SALK	TGGTTCACGTAGTGGGCCATCG	Left border primer a1 for SALK lines (Genotyping *soc1-2)*
B209	GtF-spl8-1	AGAAGCACGACGGCTGTAGAATAGGA	Genotyping *spl8-1* (Unte *et al.*, 2003)
B210	GtR-spl8-1	AACAACGACCGCCGTCACATCACC	Genotyping *spl8-1* (Unte *et al.*, 2003)
B198	Gt_FWmir172a-2	TCGACTATTCCGCCATGTTTG	Primer Diarmuid for genotyping *mir172a-2* oDM-277
B199	Gt_REVmir172a-2	ACCTACCTGAAGAAGATCTGGATG	Primer Diarmuid for genotyping *mir172a-2* oDM-278
B200	Gt_FWmir172b-3	TCAGCCCTTGGATTCGTGAGG	Primer Diarmuid for genotyping *mir172b-3* oDM-199
B201	Gt_REVmir172b-3	TAACGCCCTAATCCGTCATTGACC	Primer Diarmuid for genotyping *mir172b-3* oDM-200
oDM-194	miR172c_T7E1.2_F	tgacctgagtatctgagatctcag	Primer Diarmuid for genotyping *mir172c-1*
oDM-195	miR172c_T7E1.2_R	cctccgatctgtgaattcctac	Primer Diarmuid for genotyping *mir172c-1*
oDM-247	miR172d1_T7E2.1_F	cttcaccctaaatctcttcctctccttcag	Primer Diarmuid for genotyping mir172d-3
oDM-248	miR172d1_T7E2.1_R	cacctcaagttatcatatcggagg	Primer Diarmuid for genotyping mir172d-3
oDM-251	miR172e1_T7E2.1_F	gtctgaatcctcttgctttcctctttgc	Primer Diarmuid for genotyping *mir172e-1*
oDM-252	miR172e1_T7E2.1_R	tcacagcatgtgcatgatcaag	Primer Diarmuid for genotyping *mir172e-1*
B272	Gt_FW_ful-2_seq	TTGGCCGAGACGTTTCACAA	Genotyping *ful-2*
B273	Gt_REV_ful-2_seq	TTGTTGGGACTCTGAAGCGG	Genotyping *ful-2*
B274	Gt_sq_rev_ful-2	attagaagtttgtatgtgcgaccc	Sequencing 3,517-nt PCR fragment (B272+B273) for *ful-2* mutation

Table 6.16. List of oligonucleotides used for cloning in this thesis.

Oligo number	Oligo name	Oligo sequence	Oligo used for:
B005	ClFW_pFUL_mCArG_I	cacaagtggcaatgcccaaacAATAAAATTtcaatgatattctttcttatatattttcgttatcaaaaccc	PCR for PIPE cloning to create mutations in 3 CArG boxes in *pFUL*, insert
B006	ClREV_pFUL_mCArG_I	tatcctgTTAAATTTTaaggaaaaaaaTTAAAATTatgtccttttcttcaatttcaagttaagtatcgatct	PCR for PIPE cloning to create mutations in 3 CArG boxes in *pFUL*, insert
B007	ClFW_pFUL_mCArG_V	aggacatAATTTTAAttttttttccttAAAATTTAAcaggataaaatattgtaaaatgttccgtgttatttttg	PCR for PIPE cloning to create mutations in 3 CArG boxes in *pFUL*, vector
B008	ClREV_pFUL_mCArG_V	aaatatataagaaagaatatcattgaAATTTTATTgtttgggcattgccacttgtgatc	PCR for PIPE cloning to create mutations in 3 CArG boxes in *pFUL*, vector
B009	ClFW_pFUL_mSBP_Ia	aatttatgtgtttatgatcaattaagATAAgaacataattaagagcaacataaacaaatttacgtcg	PCR for PIPE to create mutations in 2 SBP boxes in *pFUL*, insert 1a (combined with B012 for final insert)
B010	ClREV_pFUL_mSBP_Ia	tctgataccaaacataaactagttttTTAAactaacaaaataagaatgaaatatcaaattttgtaagaattggtaa	PCR for PIPE to create mutations in 2 SBP boxes in *pFUL*, insert 1a
B011	ClFW_pFUL_mSBP_Ib	tgatatttcattcttattttgttagtTTAAaaaactagtttatgtttggtatcagactatcagttatcaattcat	PCR for PIPE to create mutations in 2 SBP boxes in *pFUL*, insert 1b
B012	ClREV_pFUL_mSBP_Ib	cctttagcttacattgtttccTTATcTTATggacttttgttattgtttttaaggttaagaaatcagacc	PCR for PIPE to create mutations in 2 SBP boxes in *pFUL*, insert 1b (combined with B009 for final insert)
B013	ClFW_pFUL_mSBP_V	taaaaacaataacaaaagtccATAAgATAAggaaacaatgtaagctaaagggaggca	PCR for PIPE to create mutations in 4 SBP boxes in *pFUL*, Vector
B014	ClREV_pFUL_mSBP_V	tgtttatgttgctcttaattatgttcTTATcttaattgatcataaacacataaattttagtgattccttatgtc	PCR for PIPE to create mutations in 4 SBP boxes in *pFUL*, Vector
B037	ClF_GR_SPL15_I	tctgagtaagaggaagccaaaaccataATGGAAGCTCGAAAAACAAAGAAAAAAATCAAAG	FW insert for fusing GR to SPL15 protein N-terminally
B038	ClR_GR_SPL15_I	CGCTGCCGCAGCGGCAGCAGCCGCAGCGCCTTTTTGATGAAACAGAAGCTTTTTGATATTTCC	REV insert for fusing GR to SPL15 protein N-terminally AND REV insert for fusing HA and GR to SPL15 protein N-terminally
B039	ClF_GR_SPL15_V	GGCGCTGCGGCTGCTGCCGCTGCGGCAGCGATGGAGTTGTTAATGTGTTCGGGTCA	FW Vector for fusing GR to SPL15 protein N-terminally AND FW vector for fusing HA and GR to SPL15 protein N-terminally
B040	ClR_GR_SPL15_V	GATTTTTTTCTTTGTTTTTCGAGCTTCCATtatggttttggcttcctcttactcagaca	REV Vector for fusing GR to SPL15 protein N-terminally
B041	ClF_HGR_SPL15-I	ATGtacccatacgatgttccagattacgctGAAGCTCGAAAAACAAAGAAAAAAATCAAAG	FW insert for fusing HA and GR to SPL15 protein N-terminally
B042	ClR_HGR_SPL15-V	agcgtaatctggaacatcgtatgggtaCATtatggttttggcttcctcttactcagacag	FW vector for fusing HA and GR to SPL15 protein N-terminally
B043	ClF_SPL15_GR-I	GCTGCGGCTGCTGCCGCTGCGGCAGCGGGCATGGAAGCTCGAAAAACAAAGAAAAAAATCAAAG	FW insert for fusing GR to SPL15 protein C-terminally AND FW insert for fusing GR and HA to SPL15 protein C-terminally
B044	ClR_SPL15_GR-I	gatcttaaaaggtgaaagagattagacTCATTTTTGATGAAACAGAAGCTTTTTGATATTTCC	REV insert for fusing GR to SPL15 protein C-terminally
B045	ClF_SPL15_GR-V	ATCAAAAAGCTTCTGTTTCATCAAAAATGAgtctaatctctttcacctttaagatcttcatcagttt	FW Vector for fusing GR to SPL15 protein C-terminally
B046	ClR_SPL15_GR-V	GCCCGCTGCCGCAGCGGCAGCAGCCGCAGCAAGAGACCAATTGAAATGTTGAGGAGAGG	REV Vector for fusing GR to SPL15 protein C-terminally AND REV vector for fusing GR and HA to SPL15 protein C-terminally
B047	ClR_SPL15_GRH-I	TCAagcgtaatctggaacatcgtatgggtaTTTTTGATGAAACAGAAGCTTTTTGATATTTCC	REV insert for fusing GR and HA to SPL15 protein C-terminally
B048	ClF_SPL15_GRH-V	tacccatacgatgttccagattacgctTGAgtctaatctctttcacctttaagatcttcatcagttt	FW vector for fusing GR and HA to SPL15 protein C-terminally

Table 6.17. List of oligonucleotides used for qRT-PCR in this thesis.

Oligo number	Oligo name	Oligo sequence	Oligo used for:
B137	QF-FUL	TTGCAAGATCACAACAATTCGCTTCTC	Amplifying FUL cDNA
B138	QR-FUL	GAGAGTTTGGTTCCGTCAACGACGATG	Amplifying FUL cDNA
B153	QF-SPL15_Rene	CAAAGTTTGTTGCATTCACTCTAAA	Amplifying SPL15 cDNA
B154	QR-SPL15_Rene	CAAACTCAGAAAGCTGGTGAAA	Amplifying SPL15 cDNA
T009	AGL42-F	TCATGAAACCAGCAATCACGACTCA	Amplifying AGL42 cDNA
T010	AGL42-R	AGCCTTTCTTTCTCGGACCTTTCC	Amplifying AGL42 cDNA
T001	SPL4-F	GTAGCATCAATCGTGGTGGC	Amplifying SPL4 cDNA
T002	SPL4-R	CTTCGCTCATTGTGTCCAGC	Amplifying SPL4 cDNA
B225	SOC1_qLP	AACAACTCGAAGCTTCTAAACGTAA	Amplifying SOC1 cDNA
B226	SOC1_qRP	CCTCGATTGAGCATGTTCCT	Amplifying SOC1 cDNA
B151	QF-PP2AsubA3	AAGCGGTTGTGGAGAACATGATACG	Amplifying PP2A cDNA (Czechowski *et al.*, 2005)
B152	QR-PP2AsubA3	TGGAGAGCTTGATTTGCGAAATACCG	Amplifying PP2A cDNA (Czechowski *et al.*, 2005)

Abbreviations

°C	Degree celsius
µg	microgram
µm	micrometer
ABA	Absciscic acid
ACR4	ACT DOMAIN REPEAT 4
AG	Agamous
AGL15	AGAMOUS-LIKE 15
AGL42	*AGAMOUS-LIKE 42*
AN3	ANGUSTIFOLIA 3
AP1	APETALA1
AP2	APETALA 2
AP2-Ls	APETALA2-LIKEs
ARF	AUXIN RESPONSE FACTOR
At	Arabidopsis thaliana
BFT	BROTHER OF FT
BiFC	Bimolecular Fluorescence Complementation
bp	Base pair(s)
bZIP	basic LEUCINE ZIPPER DOMAIN
BZR1	BRASSINOZOLE-RESISTANT1
CAL	CAULIFLOWER
CAS9	CRISPR associated protein 9
CDKB2;1	CYCLIN DEPENDENT KINASE B2;1
cDNA	Complementary DNA
CER1-L1	ECERIFERUM1-LIKE1
ChIP	Chromatin immuno precipitation
CKX3	CYTOKININ OXIDASE 3
CO	CONSTANS
Co-IP	Co-immuno precipitation
COP1	CONSTITUTIVE PHOTOMORPHOGENIC 1
CRISPR	clustered regularly interspaced short palindromic repeats
C-terminal	Carboxy-terminal
DAP-seq	DNA affinity-purification sequencing
DEGs	Differentially Expressed Genes
DEX	Dexamethasone
dH2O	distilled, deionized water
DHS	DNAse I-hypersensitive sites
DMEM	Dulbecco´s modified Eagle´s medium
DNA	Deoxyribonucleic acid
DNase	deoxynucleosidetriphosphate
dNTP	deoxyribonuclease

DUF581	DOMAINS of UNKNOWN FUNCTION 581
ELF4	*EARLY FLOWERING 4*
EMSA	electrophoretic mobility shift assay
FBS	tetracycline-free fetal bovine serum
FCA	FLOWERING CONTROL LOCUS A
FD	FLOWERING LOCUS D
FLC	FLOWERING LOCUS C
FLD	FLOWERING LOCUS D
FLK	FLOWERING LOCUS K
FLM	FLOWERING LOCUS M
FPKM	Fragments Per Kilobase Million
FT	FLOWERING LOCUS T
FUL	FRUITFULL
FW	Forward
GA	Gibberellin (Gibberellic acid)
GAI	GIBBERELLIC ACID INSENSITIVE
GFP	GREEN FLUORESCENT PROTEIN
GI	GIGANTEA
GID1	GIBBERELLIN INSENSITIVE DWARF 1
GRN	Gene regulatory network
h	hour(s)
HEK-cells	human embryonic kidney cells
HSD	Honestly Significant Difference
I	Insert
IP	Immunoprecipitation
kb	Kilo base(s)
KNAT	KNOTTED-like from Arabidopsis thaliana
L1	Cell layer 1 of the SAM (epidermis)
L2	Cell layer 2 of the SAM, below L1
L3	Cell layer 3 of the SAM, all cells below L3 until the rib meristem
LB	Lysogeny Broth
LC-MS/MS	liquid chromatography to tandem mass spectrometry
LD	Long days
LD	LUMINIPENDENS
LFY	LEAFY
LHY	*LATE ELONGATED HYPOCOTYL*
M	molar
MADS-domain	MCM1 AGAMOUNS DEFICIENS SRF-domain
MED	MEDIATOR
mg	milligram
MIKC	MADS Intervening K-box Carboxy
MIM156	Mimicry target for miR156
min	minute(s)

MIR156	MICRORNA 156
MIR172	MICRORNA 172
miRNA	microRNA
mRNA	Messenger Ribonucleic acid
MS	Murashige and Skoog
msc	more and smaller cells
ng	nanogram
NLS	Nuclear localisation sequence
nt	Nucleotide(s)
N-terminal	Amino-terminal
OMT1	O-METHYL TRANSFERASE 1
PBS	Phosphate-buffered Saline
PCA	Principal Component Analysis
PCR	Polymerase chain reaction
PEG	Polyethylene glycol
PEP1	PERPETUAL FLOWERING 1
pH	negative decimal logarithm of the H+ concentration
PIF4	PHYTOCHROME INTERACTING FACTOR 4
PIPE	Polymerase Incomplete Primer Extension
pNPP	para-Nitrophenylphosphate
PP2A	*SERINE/THREONINE PROTEIN PHOSPHATASE 2A*
PPT	phosphinothricin
PRC2	POLYCOMB REPRESSIVE COMPLEX 2
PRR	*PSEUDO-RESPONSE REGULATOR 5*
qRT-PCR	quantitative real time-PCR
rAP2	AP2 resistant to miR172
REV	Reverse
RGA	REPRESSOR OF GA1-3
RNA	Ribonucleic acid
RNAseq	RNA-sequencing
rpm	rotations per minute
rSPL15	SPL15 resistant to miR156
SA	Salicylic acid
SAM	Shoot apical meristem
SBP	QSQUAMOSA PROMOTER BINDING
SBP	SQUAMOSA BINDING PROTEIN
SD	Short days
SEAP	SECRETED ALKALINE PHOSPHATASE
SMZ	SCHLAFMUETZE
SNZ	SCHNARCHZAPFEN
SOC1	SUPPRESSOR OF OVEREXPRESSION OF CONSTANS a
SPA1	SUPPRESSOR OF PHYTOCHROME A 1
SPL	SQUAMOSA PROMOTER BINDING PROTEIN-LIKE

SPL15	SQUAMOSA PROMOTER BINDING PROTEIN-LIKE 15
STM	SHOOT MERISTEMLESS
SUC2	*SUCROSE PROTON SYMPORTER 2*
SVP	SHORT VEGETATIVE PHASE
TE	TRIS-EDTA
TF	Transcription factor
TFS1	*TARGET OF FLC AND SVP 1*
TLN	Total leaf number
TOC1	*TIMING OF CAB EXPRESSION 1*
TOE1	TARGET OF EARLY ACTIVATION TAGGED (EAT) 1
TOE2	Target of EAT 2
TOE3	Target of EAT 3
TSF	TWINSISTER OF FT
TZF1	A. THALIANA TANDEM ZINC FINGER PROTEIN 1
V	Vector
VAL1	VIVIPAROUS1/ABSCISIC ACID INSENSITIVE3-LIKE1
VPC	Vegetative phase change
wSD	Weeks in short days
WUS	WUSCHEL
XTH7	XYLOGLUCAN ENDOTRANSGLUCOSYLASE/HYDROLASE 7
Y1H	Yeast-one-hybrid
Y2H	Yeast-two-hybrid

References

Abe, M., Kobayashi, Y., Yamamoto, S., Daimon, Y., Yamaguchi, A., Ikeda, Y., Ichinoki, H., Notaguchi, M., Goto, K., & Araki, T. (2005). FD, a bZIP protein mediating signals from the floral pathway integrator FT at the shoot apex. *Science*. https://doi.org/10.1126/science.1115983

Abe, M., Kosaka, S., Shibuta, M., Nagata, K., Uemura, T., Nakano, A., & Kaya, H. (2019). Transient activity of the florigen complex during the floral transition in arabidopsis thaliana. *Development (Cambridge)*. https://doi.org/10.1242/dev.171504

Achard, P., Cheng, H., De Grauwe, L., Decat, J., Schoutteten, H., Moritz, T., Van Der Straeten, D., Peng, J., & Harberd, N. P. (2006). Integration of plant responses to environmentally activated phytohormonal signals. *Science*. https://doi.org/10.1126/science.1118642

Albani, M. C., Castaings, L., Wötzel, S., Mateos, J. L., Wunder, J., Wang, R., Reymond, M., & Coupland, G. (2012). PEP1 of Arabis alpina Is Encoded by Two Overlapping Genes That Contribute to Natural Genetic Variation in Perennial Flowering. *PLoS Genetics*. https://doi.org/10.1371/journal.pgen.1003130

Amasino, R. (2004). Vernalization, competence, and the epigenetic memory of winter. In *Plant Cell*. https://doi.org/10.1105/tpc.104.161070

Andrés, F., & Coupland, G. (2012). The genetic basis of flowering responses to seasonal cues. In *Nature Reviews Genetics*. https://doi.org/10.1038/nrg3291

Angel, A., Song, J., Dean, C., & Howard, M. (2011). A Polycomb-based switch underlying quantitative epigenetic memory. *Nature*. https://doi.org/10.1038/nature10241

Aoyama, T., & Chua, N. H. (1997). A glucocorticoid-mediated transcriptional induction system in transgenic plants. *Plant Journal*. https://doi.org/10.1046/j.1365-313X.1997.11030605.x

Armenta-Medina, A., Lepe-Soltero, D., Xiang, D., Datla, R., Abreu-Goodger, C., & Gillmor, C. S. (2017). Arabidopsis thaliana miRNAs promote embryo pattern formation beginning in the zygote. *Developmental Biology*. https://doi.org/10.1016/j.ydbio.2017.09.009

Arribas-Hernández, L., Kielpinski, L. J., & Brodersen, P. (2016). mRNA decay of most arabidopsis miRNA targets requires slicer activity of AGO1. *Plant Physiology*. https://doi.org/10.1104/pp.16.00231

Auge, G. A., Blair, L. K., Karediya, A., & Donohue, K. (2018). The autonomous flowering-time pathway pleiotropically regulates seed germination in Arabidopsis thaliana. *Annals of Botany*. https://doi.org/10.1093/aob/mcx132

Aukerman, M. J., & Sakai, H. (2003). Regulation of Flowering Time and Floral Organ Identity by a MicroRNA and lts APETALA2-Like Target Genes. *Plant Cell*. https://doi.org/10.1105/tpc.016238

Baena-González, E., Rolland, F., Thevelein, J. M., & Sheen, J. (2007). A central integrator of transcription networks in plant stress and energy signalling. *Nature*. https://doi.org/10.1038/nature06069

Bailey, T. L., & Elkan, C. (1994). Fitting a mixture model by expectation maximization to discover motifs in biopolymers. *Proceedings / ... International Conference on Intelligent Systems for Molecular Biology ; ISMB. International Conference on Intelligent Systems for Molecular Biology*.

Bak, S., Beisson, F., Bishop, G., Hamberger, B., Höfer, R., Paquette, S., & Werck-Reichhart, D. (2011). The Arabidopsis Book - Cytochromes P450. *American Society of Plant Biologists*. https://doi.org/10.1199/tab.0144

Balanzà, V., Martínez-Fernández, I., & Ferrándiz, C. (2014). Sequential action of FRUITFULL as a modulator of the activity of the floral regulators SVP and SOC1. *Journal of Experimental Botany*. https://doi.org/10.1093/jxb/ert482

Balanzà, V., Martínez-Fernández, I., Sato, S., Yanofsky, M. F., & Ferrándiz, C. (2019). Inflorescence Meristem Fate Is Dependent on Seed Development and FRUITFULL in Arabidopsis thaliana. *Frontiers in Plant Science*. https://doi.org/10.3389/fpls.2019.01622

Balanzà, V., Martínez-Fernández, I., Sato, S., Yanofsky, M. F., Kaufmann, K., Angenent, G. C., Bemer, M., & Ferrándiz, C. (2018). Genetic control of meristem arrest and life span in Arabidopsis by a FRUITFULL-APETALA2 pathway. *Nature Communications*. https://doi.org/10.1038/s41467-018-03067-5

Balasubramanian, S., Sureshkumar, S., Lempe, J., & Weigel, D. (2006). Potent induction of Arabidopsis thaliana flowering by elevated growth temperature. *PLoS Genetics*. https://doi.org/10.1371/journal.pgen.0020106

Balbas, P., & Lorence, A. (2004). Recombinant Gene Expression. In *Recombinant Gene Expression*. https://doi.org/10.1385/1592597742

Bao, S., Hua, C., Shen, L., & Yu, H. (2020). New insights into gibberellin signaling in regulating flowering in Arabidopsis. In *Journal of Integrative Plant Biology*. https://doi.org/10.1111/jipb.12892

Barrera-Rojas, C. H., Rocha, G. H. B., Polverari, L., Pinheiro Brito, Di. A., Batista, Di. S., Notini, M. M., Da Cruz, A. C. F., Morea, E. G. O., Sabatini, S., Otoni, W. C., & Nogueira, F. T. S. (2020). MiR156-targeted SPL10 controls Arabidopsis root meristem activity and root-derived de novo shoot regeneration via cytokinin responses. *Journal of Experimental Botany*. https://doi.org/10.1093/jxb/erz475

Bartel, D. P. (2004). MicroRNAs: Genomics, Biogenesis, Mechanism, and Function. In *Cell*. https://doi.org/10.1016/S0092-8674(04)00045-5

Bartrina, I., Otto, E., Strnad, M., Werner, T., & Schmülling, T. (2011). Cytokinin regulates the activity of reproductive meristems, flower organ size, ovule formation, and thus seed yield in Arabidopsis thaliana. *Plant Cell*. https://doi.org/10.1105/tpc.110.079079

Bastow, R., Mylne, J. S., Lister, C., Lippman, Z., Martienssen, R. A., & Dean, C. (2004). Vernalization requires epigenetic silencing of FLC by histone methylation. *Nature*. https://doi.org/10.1038/nature02269

Bäurle, I., & Dean, C. (2008). Differential interactions of the autonomous pathway RRM proteins and chromatin regulators in the silencing of arabidopsis targets. *PLoS ONE*. https://doi.org/10.1371/journal.pone.0002733

Bemer, M., Van Mourik, H., Muiño, J. M., Ferrándiz, C., Kaufmann, K., & Angenent, G. C. (2017). FRUITFULL controls SAUR10 expression and regulates Arabidopsis growth and architecture. *Journal of Experimental Botany*. https://doi.org/10.1093/jxb/erx184

Bertheloot, J., Barbier, F., Boudon, F., Perez-Garcia, M. D., Péron, T., Citerne, S., Dun, E., Beveridge, C., Godin, C., & Sakr, S. (2020). Sugar availability suppresses the auxin-induced strigolactone pathway to promote bud outgrowth. *New Phytologist*. https://doi.org/10.1111/nph.16201

Bhogale, S., Mahajan, A. S., Natarajan, B., Rajabhoj, M., Thulasiram, H. V., & Banerjee, A. K. (2014). MicroRNA156: A potential graft-transmissible microrna that modulates plant architecture and tuberization in Solanum tuberosum ssp. andigena. *Plant Physiology*. https://doi.org/10.1104/pp.113.230714

Birkenbihl, R. P., Jach, G., Saedler, H., & Huijser, P. (2005). Functional dissection of the plant-specific SBP-domain: Overlap of the DNA-binding and nuclear localization domains. *Journal of Molecular Biology*. https://doi.org/10.1016/j.jmb.2005.07.013

Blázquez, M. A., Green, R., Nilsson, O., Sussman, M. R., & Weigel, D. (1998). Gibberellins promote flowering of Arabidopsis by activating the LEAFY promoter. *Plant Cell*. https://doi.org/10.1105/tpc.10.5.791

Blazquez, M. A., & Weigel, D. (2000). Integration of floral inductive signals in Arabidopsis. *Nature*. https://doi.org/10.1038/35009125

Boachon, B., Burdloff, Y., Ruan, J. X., Rojo, R., Junker, R. R., Vincent, B., Nicolè, F., Bringel, F., Lesot, A., Henry, L., Bassard, J. E., Mathieu, S., Allouche, L., Kaplan, I., Dudarev, N., Vuilleumier, S., Miesch, L., André, F., Navrot, N., … Werck-Reichharta, D. (2019). A promiscuous CYP706A3 reduces terpene volatile emission from arabidopsis flowers, affecting florivores and the floral microbiome[OPEN]. *Plant Cell*. https://doi.org/10.1105/tpc.19.00320

Boer, D. R., Freire-Rios, A., Van Den Berg, W. A. M., Saaki, T., Manfield, I. W., Kepinski, S., López-Vidrieo, I., Franco-Zorrilla, J. M., De Vries, S. C., Solano, R., Weijers, D., & Coll, M. (2014). Structural basis for DNA binding specificity by the auxin-dependent ARF transcription factors. *Cell*. https://doi.org/10.1016/j.cell.2013.12.027

Bolger, A. M., Lohse, M., & Usadel, B. (2014). Trimmomatic: A flexible trimmer for Illumina sequence data. *Bioinformatics*. https://doi.org/10.1093/bioinformatics/btu170

Borges, F., Pereira, P. A., Slotkin, R. K., Martienssen, R. A., & Becker, J. D. (2011). MicroRNA activity in the Arabidopsis male germline. In *Journal of Experimental Botany*. https://doi.org/10.1093/jxb/erq452

Borner, R., Kampmann, G., Chandler, J., Gleißner, R., Wisman, E., Apel, K., & Melzer, S. (2000). A MADS domain gene involved in the transition to flowering in Arabidopsis. *Plant Journal*. https://doi.org/10.1046/j.1365-313X.2000.00906.x

Bowman, J. L., Smyth, D. R., & Meyerowitz, E. M. (1991). Genetic interactions among floral homeotic genes of Arabidopsis. *Development*.

Boyle, A. P., Davis, S., Shulha, H. P., Meltzer, P., Margulies, E. H., Weng, Z., Furey, T. S., & Crawford, G. E. (2008). High-Resolution Mapping and Characterization of Open Chromatin across the Genome. *Cell*. https://doi.org/10.1016/j.cell.2007.12.014

Brand, L., Hörler, M., Nüesch, E., Vassalli, S., Barrell, P., Yang, W., Jefferson, R. A., Grossniklaus, U., & Curtis, M. D. (2006). A versatile and reliable two-component system for tissue-specific gene induction in Arabidopsis. *Plant Physiology*. https://doi.org/10.1104/pp.106.081299

Brenner, W. G., & Schmülling, T. (2015). Summarizing and exploring data of a decade of cytokinin-related transcriptomics. *Frontiers in Plant Science*. https://doi.org/10.3389/fpls.2015.00029

Busch, M. A., Bomblies, K., & Weigel, D. (1999). Activation of a floral homeotic gene in Arabidopsis. *Science*. https://doi.org/10.1126/science.285.5427.585

Capella-Gutiérrez, S., Silla-Martínez, J. M., & Gabaldón, T. (2009). trimAl: A tool for automated alignment trimming in large-scale phylogenetic analyses. *Bioinformatics*. https://doi.org/10.1093/bioinformatics/btp348

Capovilla, G., Schmid, M., & Posé, D. (2015). Control of flowering by ambient temperature. *Journal of Experimental Botany*. https://doi.org/10.1093/jxb/eru416

Capovilla, G., Symeonidi, E., Wu, R., & Schmid, M. (2017). Contribution of major FLM isoforms to temperature-dependent flowering in Arabidopsis thaliana. *Journal of Experimental Botany*. https://doi.org/10.1093/jxb/erx328

Cardon, G. H., Höhmann, S., Nettesheim, K., Saedler, H., & Huijser, P. (1997). Functional analysis of the Arabidopsis thaliana SBP-box gene SPL3: A novel gene involved in the floral transition. *Plant Journal*. https://doi.org/10.1046/j.1365-313X.1997.12020367.x

Cardon, G., Höhmann, S., Klein, J., Nettesheim, K., Saedler, H., & Huijser, P. (1999). Molecular characterisation of the Arabidopsis SBP-box genes. *Gene*. https://doi.org/10.1016/S0378-1119(99)00308-X

Chang, T. C., Pertea, M., Lee, S., Salzberg, S. L., & Mendell, J. T. (2015). Genome-wide annotation of microRNA primary transcript structures reveals novel regulatory mechanisms. *Genome Research*. https://doi.org/10.1101/gr.193607.115

Chao, L. M., Liu, Y. Q., Chen, D. Y., Xue, X. Y., Mao, Y. B., & Chen, X. Y. (2017). Arabidopsis Transcription Factors SPL1 and SPL12 Confer Plant Thermotolerance at Reproductive Stage. *Molecular Plant*. https://doi.org/10.1016/j.molp.2017.03.010

Chen, D., Yan, W., Fu, L. Y., & Kaufmann, K. (2018). Architecture of gene regulatory networks controlling flower development in Arabidopsis thaliana. *Nature Communications*. https://doi.org/10.1038/s41467-018-06772-3

Chen, M. K., Hsu, W. H., Lee, P. F., Thiruvengadam, M., Chen, H. I., & Yang, C. H. (2011). The MADS box gene, FOREVER YOUNG FLOWER, acts as a repressor controlling floral organ senescence and abscission in Arabidopsis. *Plant Journal*. https://doi.org/10.1111/j.1365-313X.2011.04677.x

Chen, R., Zhang, S., Sun, S., Chang, J., & Zuo, J. (2005). Characterization of a new mutant allele of the Arabidopsis Flowering Locus D (FLD) gene that controls the flowering time by repressing FLC. *Chinese Science Bulletin*. https://doi.org/10.1360/982005-1104

Chen, Xiaobo, Zhang, Z., Liu, D., Zhang, K., Li, A., & Mao, L. (2010). SQUAMOSA promoter-binding protein-like transcription factors: Star players for plant growth and development. In *Journal of Integrative Plant Biology*. https://doi.org/10.1111/j.1744-7909.2010.00987.x

Chen, Xuemei. (2004). A MicroRNA as a Translational Repressor of APETALA2 in Arabidopsis Flower Development. *Science*. https://doi.org/10.1126/science.1088060

Chiang, G. C. K., Barua, D., Kramera, E. M., Amasino, R. M., & Donohue, K. (2009). Major flowering time gene, FLOWERING LOCUS C, regulates seed germination in Arabidopsis thaliana. *Proceedings of the National Academy of Sciences of the United States of America*. https://doi.org/10.1073/pnas.0901367106

Clarke, J. H., & Dean, C. (1994). Mapping FRI, a locus controlling flowering time and vernalization response in Arabidopsis thaliana. *MGG Molecular & General Genetics*. https://doi.org/10.1007/BF00277351

Clough, S. J., & Bent, A. F. (1998). Floral dip: A simplified method for Agrobacterium-mediated transformation of Arabidopsis thaliana. *Plant Journal*. https://doi.org/10.1046/j.1365-313X.1998.00343.x

Collani, S., Neumann, M., Yant, L., & Schmid, M. (2019). FT modulates genome-wide DNA-binding of the bZIP transcription factor FD. *Plant Physiology*. https://doi.org/10.1104/pp.18.01505

Corbesier, L., Vincent, C., Jang, S., Fornara, F., Fan, Q., Searle, I., Giakountis, A., Farrona, S., Gissot, L., Turnbull, C., & Coupland, G. (2007). FT protein movement contributes to long-distance signaling in floral induction of Arabidopsis. *Science*. https://doi.org/10.1126/science.1141752

Craft, J., Samalova, M., Baroux, C., Townley, H., Martinez, A., Jepson, I., Tsiantis, M., & Moore, I. (2005). New pOp/LhG4 vectors for stringent glucocorticoid-dependent transgene expression in Arabidopsis. *Plant Journal*. https://doi.org/10.1111/j.1365-313X.2005.02342.x

Csorba, T., Questa, J. I., Sun, Q., & Dean, C. (2014). Antisense COOLAIR mediates the coordinated switching of chromatin states at FLC during vernalization. *Proceedings of the National Academy of Sciences of the United States of America*. https://doi.org/10.1073/pnas.1419030111

Czechowski, T., Stitt, M., Altmann, T., Udvardi, M. K., & Scheible, W. R. (2005). Genome-wide identification and testing of superior reference genes for transcript normalization in arabidopsis. In *Plant Physiology*. https://doi.org/10.1104/pp.105.063743

De Lucia, F., Crevillen, P., Jones, A. M. E., Greb, T., & Dean, C. (2008). A PHD-polycomb repressive complex 2 triggers the epigenetic silencing of FLC during vernalization. *Proceedings of the National Academy of Sciences of the United States of America*. https://doi.org/10.1073/pnas.0808687105

de Reuille, P. B., Routier-Kierzkowska, A. L., Kierzkowski, D., Bassel, G. W., Schüpbach, T., Tauriello, G., Bajpai, N., Strauss, S., Weber, A., Kiss, A., Burian, A., Hofhuis, H., Sapala, A., Lipowczan, M., Heimlicher, M. B., Robinson, S., Bayer, E. M., Basler, K., Koumoutsakos, P., … Smith, R. S. (2015). MorphoGraphX: A platform for quantifying morphogenesis in 4D. *ELife*. https://doi.org/10.7554/eLife.05864

Delaney, T. P., Uknes, S., Vernooij, B., Friedrich, L., Weymann, K., Negrotto, D., Gaffney, T., Gut-Rella, M., Kessmann, H., Ward, E., & Ryals, J. (1994). A central role of salicylic acid in plant disease resistance. *Science*. https://doi.org/10.1126/science.266.5188.1247

Deng, W., Ying, H., Helliwell, C. A., Taylor, J. M., Peacock, W. J., & Dennis, E. S. (2011). FLOWERING LOCUS C (FLC) regulates development pathways throughout the life cycle of Arabidopsis. *Proceedings of the National Academy of Sciences of the United States of America*. https://doi.org/10.1073/pnas.1103175108

Dill, A., Thomas, S. G., Hu, J., Steber, C. M., & Sun, T. P. (2004). The arabidopsis F-box protein SLEEPY1 targets gibberellin signaling repressors for gibberellin-induced degradation. *Plant Cell*. https://doi.org/10.1105/tpc.020958

Dinh, T. T., Girke, T., Liu, X., Yant, L., Schmid, M., & Chen, X. (2012). The floral homeotic protein APETALA2 recognizes and acts through an AT-rich sequence element. *Development*. https://doi.org/10.1242/dev.077073

Dong, Z., Danilevskaya, O., Abadie, T., Messina, C., Coles, N., & Cooper, M. (2012). A gene regulatory network model for Floral transition of the shoot apex in maize and its dynamic modeling. *PLoS ONE*. https://doi.org/10.1371/journal.pone.0043450

Dorca-Fornell, C., Gregis, V., Grandi, V., Coupland, G., Colombo, L., & Kater, M. M. (2011). The Arabidopsis SOC1-like genes AGL42, AGL71 and AGL72 promote flowering in the shoot apical and axillary meristems. *Plant Journal*. https://doi.org/10.1111/j.1365-313X.2011.04653.x

Duan, E., Wang, Y., Li, X., Lin, Q., Zhang, T., Wang, Y., Zhou, C., Zhang, H., Jiang, L., Wang, J., Lei, C., Zhang, X., Guo, X., Wang, H., & Wan, J. (2019). Osshi1 regulates plant architecture through modulating the transcriptional activity of ipa1 in rice. *Plant Cell*. https://doi.org/10.1105/tpc.19.00023

Earley, K. W., Haag, J. R., Pontes, O., Opper, K., Juehne, T., Song, K., & Pikaard, C. S. (2006). Gateway-compatible vectors for plant functional genomics and proteomics. In *Plant Journal*. https://doi.org/10.1111/j.1365-313X.2005.02617.x

Edgar, R. C. (2004). MUSCLE: Multiple sequence alignment with high accuracy and high throughput. *Nucleic Acids Research*. https://doi.org/10.1093/nar/gkh340

Edwards, K., Johnstone, C., & Thompson, C. (1991). A simple and rapid method for the preparation of plant genomic DNA for PCR analysis. In *Nucleic Acids Research*. https://doi.org/10.1093/nar/19.6.1349

Ercoli, M. F., Ferela, A., Debernardi, J. M., Perrone, A. P., Rodriguez, R. E., & Palatnik, J. F. (2018). GIF transcriptional coregulators control root meristem homeostasis. *Plant Cell*. https://doi.org/10.1105/tpc.17.00856

Eriksson, S., Böhlenius, H., Moritz, T., & Nilsson, O. (2006). GA4 is the active gibberellin in the regulation of LEAFY transcription and Arabidopsis floral initiation. *Plant Cell*. https://doi.org/10.1105/tpc.106.042317

Eshed, Y., Baum, S. F., Perea, J. V., & Bowman, J. L. (2001). Establishment of polarity in lateral organs of plants. *Current Biology*. https://doi.org/10.1016/S0960-9822(01)00392-X

Ferjani, A., Horiguchi, G., Yano, S., & Tsukaya, H. (2007). Analysis of leaf development in fugu mutants of Arabidopsis reveals three compensation modes that modulate cell expansion in determinate organs. *Plant Physiology*. https://doi.org/10.1104/pp.107.099325

Fernández, V., Takahashi, Y., Le Gourrierec, J., & Coupland, G. (2016). Photoperiodic and thermosensory pathways interact through CONSTANS to promote flowering at high temperature under short days. *The Plant Journal : For Cell and Molecular Biology*. https://doi.org/10.1111/tpj.13183

Ferrándiz, C., Gu, Q., Martienssen, R., & Yanofsky, M. F. (2000). Redundant regulation of meristem identity and plant architecture by FRUITFULL, APETALA1 and CAULIFLOWER. *Development*.

Ferrándiz, C., Liljegren, S. J., & Yanofsky, M. F. (2000). Negative regulation of the SHATTERPROOF genes by FRUITFULL during Arabidopsis fruit development. *Science*. https://doi.org/10.1126/science.289.5478.436

Ferrándiz, C., Pelaz, S., & Yanofsky, M. F. (1999). Control of Carpel and Fruit Development in Arabidopsis. *Annual Review of Biochemistry*. https://doi.org/10.1146/annurev.biochem.68.1.321

Franco-Zorrilla, J. M., Valli, A., Todesco, M., Mateos, I., Puga, M. I., Rubio-Somoza, I., Leyva, A., Weigel, D., García, J. A., & Paz-Ares, J. (2007). Target mimicry provides a new mechanism for regulation of microRNA activity. *Nature Genetics*. https://doi.org/10.1038/ng2079

Frazer, K. A., Pachter, L., Poliakov, A., Rubin, E. M., & Dubchak, I. (2004). VISTA: Computational tools for comparative genomics. *Nucleic Acids Research*. https://doi.org/10.1093/nar/gkh458

Galvão, Vinicius C., Horrer, D., Küttner, F., & Schmid, M. (2012). Spatial control of flowering by DELLA proteins in Arabidopsis thaliana. *Development (Cambridge)*. https://doi.org/10.1242/dev.080879

Galvão, Vinicius Costa, Collani, S., Horrer, D., & Schmid, M. (2015). Gibberellic acid signaling is required for ambient temperature-mediated induction of flowering in Arabidopsis thaliana. *Plant Journal*. https://doi.org/10.1111/tpj.13051

Gandikota, M., Birkenbihl, R. P., Höhmann, S., Cardon, G. H., Saedler, H., & Huijser, P. (2007). The miRNA156/157 recognition element in the 3' UTR of the Arabidopsis SBP box gene SPL3 prevents early flowering by translational inhibition in seedlings. *Plant Journal*. https://doi.org/10.1111/j.1365-313X.2006.02983.x

Gao, R., Wang, Y., Gruber, M. Y., & Hannoufa, A. (2018). MiR156/SPL10 modulates lateral root development, branching and leaf morphology in arabidopsis by silencing AGAMOUS-LIKE 79. *Frontiers in Plant Science*. https://doi.org/10.3389/fpls.2017.02226

Garcia-Molina, A., Xing, S., & Huijser, P. (2014). Functional characterisation of Arabidopsis SPL7 conserved protein domains suggests novel regulatory mechanisms in the Cu deficiency response. *BMC Plant Biology*. https://doi.org/10.1186/s12870-014-0231-5

Gehrke, A. R., & Shubin, N. H. (2016). Cis-regulatory programs in the development and evolution of vertebrate paired appendages. In *Seminars in Cell and Developmental Biology*. https://doi.org/10.1016/j.semcdb.2016.01.015

Geng, X., & Mackey, D. (2011). Dose-response to and systemic movement of dexamethasone in the GVG-inducible transgene system in Arabidopsis. *Methods in Molecular Biology (Clifton, N.J.)*. https://doi.org/10.1007/978-1-61737-998-7_6

Gómez-Mena, C., de Folter, S., Costa, M. M. R., Angenent, G. C., & Sablowski, R. (2005). Transcriptional program controlled by the floral homeotic gene AGAMOUS during early organogenesis. *Development*. https://doi.org/10.1242/dev.01600

Goodstein, D. M., Shu, S., Howson, R., Neupane, R., Hayes, R. D., Fazo, J., Mitros, T., Dirks, W., Hellsten, U., Putnam, N., & Rokhsar, D. S. (2012). Phytozome: A comparative platform for green plant genomics. *Nucleic Acids Research*. https://doi.org/10.1093/nar/gkr944

Goslin, K., Zheng, B., Serrano-Mislata, A., Rae, L., Ryan, P. T., Kwaśniewska, K., Thomson, B., Ó'Maoiléidigh, D. S., Madueño, F., Wellmer, F., & Graciet, E. (2017). Transcription factor interplay between LEAFY and APETALA1/CAULIFLOWER during floral initiation. *Plant Physiology*. https://doi.org/10.1104/pp.17.00098

Goujon, T., Sibout, R., Pollet, B., Maba, B., Nussaume, L., Bechtold, N., Lu, F., Ralph, J., Mila, I., Barrière, Y., Lapierre, C., & Jouanin, L. (2003). A new Arabidopsis thaliana mutant deficient in the expression of O-methyltransferase impacts lignins and sinapoyl esters. *Plant Molecular Biology*. https://doi.org/10.1023/A:1023022825098

Gras, D. E., Vidal, E. A., Undurraga, S. F., Riveras, E., Moreno, S., Dominguez-Figueroa, J., Alabadi, D., Blázquez, M. A., Medina, J., & Gutiérrez, R. A. (2018). SMZ/SNZ and gibberellin signaling are required for nitrate-elicited delay of flowering time in Arabidopsis thaliana. *Journal of Experimental Botany*. https://doi.org/10.1093/jxb/erx423

Gregis, V., Sessa, A., Colombo, L., & Kater, M. M. (2006). AGL24, SHORT VEGETATIVE PHASE, and APETALA1 redundantly control AGAMOUS during early stages of flower development in Arabidopsis. *Plant Cell*. https://doi.org/10.1105/tpc.106.041798

Gregis, V., Sessa, A., Dorca-Fornell, C., & Kater, M. M. (2009). The Arabidopsis floral meristem identity genes AP1, AGL24 and SVP directly repress class B and C floral homeotic genes. *Plant Journal*. https://doi.org/10.1111/j.1365-313X.2009.03985.x

Griffiths, J., Murase, K., Rieu, I., Zentella, R., Zhang, Z. L., Powers, S. J., Gong, F., Phillips, A. L., Hedden, P., Sun, T. P., & Thomas, S. G. (2006). Genetic characterization and functional analysis of the GID1 gibberellin receptors in Arabidopsis. *Plant Cell*. https://doi.org/10.1105/tpc.106.047415

Gu, Q., Ferrándiz, C., Yanofsky, M. F., & Martienssen, R. (1998). The FRUITFULL MADS-box gene mediates cell differentiation during Arabidopsis fruit development. *Development*.

Guindon, S., Delsuc, F., Dufayard, J. F., & Gascuel, O. (2009). Estimating maximum likelihood phylogenies with PhyML. *Methods in Molecular Biology*. https://doi.org/10.1007/978-1-59745-251-9_6

Guo, A. Y., Zhu, Q. H., Gu, X., Ge, S., Yang, J., & Luo, J. (2008). Genome-wide identification and evolutionary analysis of the plant specific SBP-box transcription factor family. *Gene*, *418*(1–2), 1–8. https://doi.org/10.1016/j.gene.2008.03.016

Guo, C., Xu, Y., Shi, M., Lai, Y., Wu, X., Wang, H., Zhu, Z., Scott Poethig, R., & Wu, G. (2017). Repression of miR156 by miR159 regulates the timing of the juvenile-to-adult transition in arabidopsis. *Plant Cell*. https://doi.org/10.1105/tpc.16.00975

Guo, X., Liu, J., Hao, G., Zhang, L., Mao, K., Wang, X., Zhang, D., Ma, T., Hu, Q., Al-Shehbaz, I. A., & Koch, M. A. (2017). Plastome phylogeny and early diversification of Brassicaceae. *BMC Genomics*. https://doi.org/10.1186/s12864-017-3555-3

Hauvermale, A. L., Ariizumi, T., & Steber, C. M. (2012). Gibberellin signaling: A theme and variations on DELLA repression. *Plant Physiology*. https://doi.org/10.1104/pp.112.200956

Hayama, R., Sarid-Krebs, L., Richter, R., Fernández, V., Jang, S., & Coupland, G. (2017). PSEUDO RESPONSE REGULATORs stabilize CONSTANS protein to promote flowering in response to day length. *The EMBO Journal*. https://doi.org/10.15252/embj.201693907

He, Y., & Amasino, R. M. (2005). Role of chromatin modification in flowering-time control. In *Trends in Plant Science*. https://doi.org/10.1016/j.tplants.2004.11.003

Helliwell, C. A., Wood, C. C., Robertson, M., James Peacock, W., & Dennis, E. S. (2006). The Arabidopsis FLC protein interacts directly in vivo with SOC1 and FT chromatin and is part of a high-molecular-weight protein complex. *Plant Journal*. https://doi.org/10.1111/j.1365-313X.2006.02686.x

Hellman, L. M., & Fried, M. G. (2007). Electrophoretic mobility shift assay (EMSA) for detecting protein-nucleic acid interactions. *Nature Protocols*. https://doi.org/10.1038/nprot.2007.249

Hisamatsu, T., & King, R. W. (2008). The nature of floral signals in Arabidopsis. II. Roles for FLOWERING LOCUS T (FT) and gibberellin. *Journal of Experimental Botany*. https://doi.org/10.1093/jxb/ern232

Hoecker, U., & Quail, P. H. (2001). The Phytochrome A-specific Signaling Intermediate SPA1 Interacts Directly with COP1, a Constitutive Repressor of Light Signaling in Arabidopsis. *Journal of Biological Chemistry*. https://doi.org/10.1074/jbc.M103140200

Hohmann, N., Wolf, E. M., Lysak, M. A., & Koch, M. A. (2015). A time-calibrated road map of brassicaceae species radiation and evolutionary history. *Plant Cell*. https://doi.org/10.1105/tpc.15.00482

Howard, M. L., & Davidson, E. H. (2004). cis-Regulatory control circuits in development. In *Developmental Biology*. https://doi.org/10.1016/j.ydbio.2004.03.031

Hsieh, M. H., & Goodman, H. M. (2002). Molecular characterization of a novel gene family encoding ACT domain repeat proteins in Arabidopsis. *Plant Physiology*. https://doi.org/10.1104/pp.007484

Huala, E., & Sussex, I. M. (1992). LEAFY interacts with floral homeotic genes to regulate arabidopsis floral development. *Plant Cell*. https://doi.org/10.2307/3869458

Huang, Z., Shi, T., Zheng, B., Yumul, R. E., Liu, X., You, C., Gao, Z., Xiao, L., & Chen, X. (2017). APETALA2 antagonizes the transcriptional activity of AGAMOUS in regulating floral stem cells in Arabidopsis thaliana. *New Phytologist*. https://doi.org/10.1111/nph.14151

Huijser, P., Klein, J., Lonnig, W. E., Meijer, H., Saedler, H., & Sommer, H. (1992). Bracteomania, an inflorescence anomaly, is caused by the loss of function of the MADS-box gene squamosa in Antirrhinum majus. *EMBO Journal*. https://doi.org/10.1002/j.1460-2075.1992.tb05168.x

Hyun, Y., Richter, R., Vincent, C., Martinez-Gallegos, R., Porri, A., & Coupland, G. (2016). Multi-layered Regulation of SPL15 and Cooperation with SOC1 Integrate Endogenous Flowering Pathways at the Arabidopsis Shoot Meristem. *Developmental Cell*. https://doi.org/10.1016/j.devcel.2016.04.001

Hyun, Y., Vincent, C., Tilmes, V., Bergonzi, S., Kiefer, C., Richter, R., Martinez-Gallegos, R., Severing, E., & Coupland, G. (2019). Plant science: A regulatory circuit conferring varied flowering response to cold in annual and perennial plants. *Science*. https://doi.org/10.1126/science.aau8197

Immink, R. G. H., Posé, D., Ferrario, S., Ott, F., Kaufmann, K., Valentim, F. L., de Folter, S., van der Wal, F., van Dijk, A. D. J., Schmid, M., & Angenent, G. C. (2012). Characterization of SOC1's central role in flowering by the identification of its upstream and downstream regulators. *Plant Physiology*. https://doi.org/10.1104/pp.112.202614

Iñigo, S., Alvarez, M. J., Strasser, B., Califano, A., & Cerdán, P. D. (2012). PFT1, the MED25 subunit of the plant Mediator complex, promotes flowering through CONSTANS dependent and independent mechanisms in Arabidopsis. *Plant Journal*. https://doi.org/10.1111/j.1365-313X.2011.04815.x

Jaeger, K. E., & Wigge, P. A. (2007). FT Protein Acts as a Long-Range Signal in Arabidopsis. *Current Biology*. https://doi.org/10.1016/j.cub.2007.05.008

Jang, S., Marchal, V., Panigrahi, K. C. S., Wenkel, S., Soppe, W., Deng, X. W., Valverde, F., & Coupland, G. (2008). Arabidopsis COP1 shapes the temporal pattern of CO accumulation conferring a photoperiodic flowering response. *EMBO Journal*. https://doi.org/10.1038/emboj.2008.68

Jaradat, M. R., Ruegger, M., Bowling, A., Butler, H., & Cutler, A. J. (2014). A comprehensive transcriptome analysis of silique development and dehiscence in Arabidopsis and Brassica integrating genotypic, interspecies and developmental comparisons. *GM Crops & Food*. https://doi.org/10.4161/21645698.2014.947827

Jeong, D. H., Thatcher, S. R., Brown, R. S. H., Zhai, J., Park, S., Rymarquis, L. A., Meyers, B. C., & Green, P. J. (2013). Comprehensive investigation of microRNAs enhanced by analysis of sequence variants, expression patterns, ARGONAUTE loading, and target cleavage. *Plant Physiology*. https://doi.org/10.1104/pp.113.219873

Jeong, H. L., Seong, J. Y., Soo, H. P., Hwang, I., Jong, S. L., & Ji, H. A. (2007). Role of SVP in the control of flowering time by ambient temperature in Arabidopsis. *Genes and Development*. https://doi.org/10.1101/gad.1518407

Johanson, U., West, J., Lister, C., Michaels, S., Amasino, R., & Dean, C. (2000). Molecular analysis of FRIGIDA, a major determinant of natural variation in Arabidopsis flowering time. *Science*. https://doi.org/10.1126/science.290.5490.344

Jorgensen, S. A., & Preston, J. C. (2014). Differential SPL gene expression patterns reveal candidate genes underlying flowering time and architectural differences in Mimulus and Arabidopsis. *Molecular Phylogenetics and Evolution*. https://doi.org/10.1016/j.ympev.2014.01.029

Jung, J. H., Ju, Y., Seo, P. J., Lee, J. H., & Park, C. M. (2012). The SOC1-SPL module integrates photoperiod and gibberellic acid signals to control flowering time in Arabidopsis. *Plant Journal*. https://doi.org/10.1111/j.1365-313X.2011.04813.x

Jung, J. H., Lee, H. J., Ryu, J. Y., & Park, C. M. (2016). SPL3/4/5 Integrate Developmental Aging and Photoperiodic Signals into the FT-FD Module in Arabidopsis Flowering. *Molecular Plant*. https://doi.org/10.1016/j.molp.2016.10.014

Jung, J. H., Lee, S., Yun, J., Lee, M., & Park, C. M. (2014). The miR172 target TOE3 represses AGAMOUS expression during Arabidopsis floral patterning. *Plant Science*. https://doi.org/10.1016/j.plantsci.2013.10.010

Jung, J. H., Seo, P. J., Kang, S. K., & Park, C. M. (2011). miR172 signals are incorporated into the miR156 signaling pathway at the SPL3/4/5 genes in Arabidopsis developmental transitions. *Plant Molecular Biology*. https://doi.org/10.1007/s11103-011-9759-z

K, M. J., & Laxmi, A. (2014). DUF581 is plant specific FCS-like zinc finger involved in protein-protein interaction. *PLoS ONE*. https://doi.org/10.1371/journal.pone.0099074

Kardailsky, I., Shukla, V. K., Ahn, J. H., Dagenais, N., Christensen, S. K., Nguyen, J. T., Chory, J., Harrison, M. J., & Weigel, D. (1999). Activation tagging of the floral inducer FT. *Science*. https://doi.org/10.1126/science.286.5446.1962

Katoh, K., Misawa, K., Kuma, K. I., & Miyata, T. (2002). MAFFT: A novel method for rapid multiple sequence alignment based on fast Fourier transform. *Nucleic Acids Research*. https://doi.org/10.1093/nar/gkf436

Kaufmann, K., Muiño, J. M., Østerås, M., Farinelli, L., Krajewski, P., & Angenent, G. C. (2010). Chromatin immunoprecipitation (ChIP) of plant transcription factors followed by sequencing (ChIP-SEQ) or hybridization to whole genome arrays (ChIP-CHIP). *Nature Protocols*. https://doi.org/10.1038/nprot.2009.244

Kaufmann, K., Pajoro, A., & Angenent, G. C. (2010). Regulation of transcription in plants: Mechanisms controlling developmental switches. In *Nature Reviews Genetics*. https://doi.org/10.1038/nrg2885

Kawade, K., Horiguchi, G., Usami, T., Hirai, M. Y., & Tsukaya, H. (2013). ANGUSTIFOLIA3 signaling coordinates proliferation between clonally distinct cells in leaves. *Current Biology*. https://doi.org/10.1016/j.cub.2013.03.044

Kebrom, T. H. (2017). A growing stem inhibits bud outgrowth – The overlooked theory of apical dominance. *Frontiers in Plant Science*. https://doi.org/10.3389/fpls.2017.01874

Kiefer, C., Willing, E. M., Jiao, W. B., Sun, H., Piednoël, M., Hümann, U., Hartwig, B., Koch, M. A., & Schneeberger, K. (2019). Interspecies association mapping links reduced CG to TG substitution rates to the loss of gene-body methylation. *Nature Plants*. https://doi.org/10.1038/s41477-019-0486-9

Kim, J. H., & Tsukaya, H. (2015). Regulation of plant growth and development by the GROWTH-REGULATING FACTOR and GRF-INTERACTING FACTOR duo. In *Journal of Experimental Botany*. https://doi.org/10.1093/jxb/erv349

Kim, J. J., Lee, J. H., Kim, W., Jung, H. S., Huijser, P., & Ahn, J. H. (2012). The microrNA156-SQUAMOSA promoter binding protein-like3 module regulates ambient temperature-responsive flowering via flowering locus in Arabidopsis. *Plant Physiology*. https://doi.org/10.1104/pp.111.192369

Kim, S. G., Kim, S. Y., & Park, C. M. (2007). A membrane-associated NAC transcription factor regulates salt-responsive flowering via FLOWERING LOCUS T in Arabidopsis. *Planta*. https://doi.org/10.1007/s00425-007-0513-3

Kim, S. G., Lee, A. K., Yoon, H. K., & Park, C. M. (2008). A membrane-bound NAC transcription factor NTL8 regulates gibberellic acid-mediated salt signaling in Arabidopsis seed germination. *Plant Journal*. https://doi.org/10.1111/j.1365-313X.2008.03493.x

Kinoshita, A., & Richter, R. (2020). Genetic and molecular basis of floral induction in Arabidopsis thaliana. *Journal of Experimental Botany*. https://doi.org/10.1093/jxb/eraa057

Kinoshita, A., Vayssieres, A., Richter, R., Sang, Q., Roggen, A., Van Driel, A.D., Smith, R., Coupland, G., (*in preparation).* Regulation of shoot meristem shape by photoperiodic signaling and phytohormones during floral induction in Arabidopsis.

Klein, J., Saedler, H., & Huijser, P. (1996). A new family of DNA binding proteins includes putative transcriptional regulators of the Antirrhinum majus floral meristem identity gene SQUAMOSA. *Molecular and General Genetics*. https://doi.org/10.1007/s004380050046

Klock, H. E., & Lesley, S. A. (2009). The polymerase incomplete primer extension (PIPE) method applied to high-throughput cloning and site-directed mutagenesis. *Methods in Molecular Biology*. https://doi.org/10.1007/978-1-59745-196-3_6

Kobayashi, Y., Kaya, H., Goto, K., Iwabuchi, M., & Araki, T. (1999). A pair of related genes with antagonistic roles in mediating flowering signals. *Science*. https://doi.org/10.1126/science.286.5446.1960

Koini, M. A., Alvey, L., Allen, T., Tilley, C. A., Harberd, N. P., Whitelam, G. C., & Franklin, K. A. (2009). High Temperature-Mediated Adaptations in Plant Architecture Require the bHLH Transcription Factor PIF4. *Current Biology*. https://doi.org/10.1016/j.cub.2009.01.046

Kolář, J., & Seňková, J. (2008). Reduction of mineral nutrient availability accelerates flowering of Arabidopsis thaliana. *Journal of Plant Physiology*. https://doi.org/10.1016/j.jplph.2007.11.010

Koornneef, M., Hanhart, C. J., & van der Veen, J. H. (1991). A genetic and physiological analysis of late flowering mutants in Arabidopsis thaliana. *MGG Molecular & General Genetics*. https://doi.org/10.1007/BF00264213

Korves, T. M., & Bergelson, J. (2003). A developmental response to pathogen infection in Arabidopsis. *Plant Physiology*. https://doi.org/10.1104/pp.103.027094

Krogan, N. T., Hogan, K., & Long, J. A. (2012). APETALA2 negatively regulates multiple floral organ identity genes in Arabidopsis by recruiting the co-repressor TOPLESS and the histone deacetylase HDA19. *Development (Cambridge)*. https://doi.org/10.1242/dev.085407

Kumar, S. V., Lucyshyn, D., Jaeger, K. E., Alós, E., Alvey, E., Harberd, N. P., & Wigge, P. A. (2012). Transcription factor PIF4 controls the thermosensory activation of flowering. *Nature*. https://doi.org/10.1038/nature10928

Kurihara, D., Mizuta, Y., Sato, Y., & Higashiyama, T. (2015). ClearSee: A rapid optical clearing reagent for whole-plant fluorescence imaging. *Development (Cambridge)*. https://doi.org/10.1242/dev.127613

Kwiatkowska, D. (2008). Flowering and apical meristem growth dynamics. In *Journal of Experimental Botany*. https://doi.org/10.1093/jxb/erm290

Lai, X., Daher, H., Galien, A., Hugouvieux, V., & Zubieta, C. (2019). Structural Basis for Plant MADS Transcription Factor Oligomerization. In *Computational and Structural Biotechnology Journal*. https://doi.org/10.1016/j.csbj.2019.06.014

Lang, A. (1957). THE EFFECT OF GIBBERELLIN UPON FLOWER FORMATION. *Proceedings of the National Academy of Sciences*. https://doi.org/10.1073/pnas.43.8.709

Laubinger, S., Marchal, V., Gentillhomme, J., Wenkel, S., Adrian, J., Jang, S., Kulajta, C., Braun, H., Coupland, G., & Hoecker, U. (2006). Arabidopsis SPA proteins regulate photoperiodic flowering and interact with the floral inducer CONSTANS to regulate its stability. *Development*. https://doi.org/10.1242/dev.02481

Lee, B H, Ko, J. H., Lee, S., Lee, Y., Pak, J. H., & Kim, J. H. (2009). The Arabidopsis GRF-INTERACTING FACTOR Gene Family Performs an Overlapping Function in Determining Organ Size as Well as Multiple Developmental Properties. *PLANT PHYSIOLOGY*.

Lee, Byung Ha, Wynn, A. N., Franks, R. G., Hwang, Y. sic, Lim, J., & Kim, J. H. (2014). The arabidopsis thaliana GRF-interacting factor gene family plays an essential role in control of male and female reproductive development. *Developmental Biology*. https://doi.org/10.1016/j.ydbio.2013.12.009

Lee, H. J., Jung, J. H., Cortés Llorca, L., Kim, S. G., Lee, S., Baldwin, I. T., & Park, C. M. (2014). FCA mediates thermal adaptation of stem growth by attenuating auxin action in Arabidopsis. *Nature Communications*. https://doi.org/10.1038/ncomms6473

Lee, H., Suh, S. S., Park, E., Cho, E., Ahn, J. H., Kim, S. G., Lee, J. S., Kwon, Y. M., & Lee, I. (2000). The AGAMOUS-lIKE 20 MADS domain protein integrates floral inductive pathways in Arabidopsis. *Genes and Development*. https://doi.org/10.1101/gad.813600

Lee, I., Aukerman, M. J., Gore, S. L., Lohman, K. N., Michaels, S. D., Weaver, L. M., John, M. C., Feldmann, K. A., & Amasino, R. M. (1994). Isolation of LUMINIDEPENDENS: A gene involved in the control of flowering time in Arabidopsis. *Plant Cell*. https://doi.org/10.1105/tpc.6.1.75

Lee, J. H., Hong, S. M., Yoo, S. J., Park, O. K., Lee, J. S., & Ahn, J. H. (2006). Integration of floral inductive signals by flowering locus T and suppressor of overexpression of Constans 1. In *Physiologia Plantarum*. https://doi.org/10.1111/j.1399-3054.2006.00619.x

Lee, J. H., Ryu, H. S., Chung, K. S., Posé, D., Kim, S., Schmid, M., & Ahn, J. H. (2013). Regulation of temperature-responsive flowering by MADS-box transcription factor repressors. *Science*. https://doi.org/10.1126/science.1241097

Lee, J., & Lee, I. (2010). Regulation and function of SOC1, a flowering pathway integrator. In *Journal of Experimental Botany*. https://doi.org/10.1093/jxb/erq098

Lee, J., Oh, M., Park, H., & Lee, I. (2008). SOC1 translocated to the nucleus by interaction with AGL24 directly regulates LEAFY. *Plant Journal*. https://doi.org/10.1111/j.1365-313X.2008.03552.x

Lepe-Soltero, D., Armenta-Medina, A., Xiang, D., Datla, R., Gillmor, C. S., & Abreu-Goodger, C. (2017). Annotating and quantifying pri-miRNA transcripts using RNA-Seq data of wild type and serrate-1 globular stage embryos of Arabidopsis thaliana. *Data in Brief*. https://doi.org/10.1016/j.dib.2017.10.019

Levine, M., & Davidson, E. H. (2005). Gene regulatory networks for development. In *Proceedings of the National Academy of Sciences of the United States of America*. https://doi.org/10.1073/pnas.0408031102

Li, C., & Lu, S. (2014). Molecular characterization of the SPL gene family in Populus trichocarpa. *BMC Plant Biology*. https://doi.org/10.1186/1471-2229-14-131

Liang, G., He, H., & Yu, D. (2012). Identification of Nitrogen Starvation-Responsive MicroRNAs in Arabidopsis thaliana. *PLoS ONE*. https://doi.org/10.1371/journal.pone.0048951

Liang, X., Nazarenus, T. J., & Stone, J. M. (2008). Identification of a consensus DNA-binding site for the Arabidopsis thaliana SBP domain transcription factor, AtSPL14, and binding kinetics by surface plasmon resonance. *Biochemistry*. https://doi.org/10.1021/bi701431y

Lim, M. H., Kim, J., Kim, Y. S., Chung, K. S., Seo, Y. H., Lee, I., Kim, J., Hong, C. B., Kim, H. J., & Park, C. M. (2004). A new arabidopsis gene, FLK, encodes an RNA binding protein with K homology motifs and regulates flowering time via Flowering Locus C. *Plant Cell*. https://doi.org/10.1105/tpc.019331

Lin, P. C., Pomeranz, M. C., Jikumaru, Y., Kang, S. G., Hah, C., Fujioka, S., Kamiya, Y., & Jang, J. C. (2011). The Arabidopsis tandem zinc finger protein AtTZF1 affects ABA- and GA-mediated growth, stress and gene expression responses. *Plant Journal*. https://doi.org/10.1111/j.1365-313X.2010.04419.x

Lincoln, C., Long, J., Yamaguchi, J., Serikawa, K., & Hake, S. (1994). A knotted1-like homeobox gene in Arabidopsis is expressed in the vegetative meristem and dramatically alters leaf morphology when overexpressed in transgenic plants. *Plant Cell*. https://doi.org/10.1105/tpc.6.12.1859

Liu, C., Chen, H., Er, H. L., Soo, H. M., Kumar, P. P., Han, J. H., Liou, Y. C., & Yu, H. (2008). Direct interaction of AGL24 and SOC1 integrates flowering signals in Arabidopsis. *Development*. https://doi.org/10.1242/dev.020255

Liu, C., Xi, W., Shen, L., Tan, C., & Yu, H. (2009). Regulation of Floral Patterning by Flowering Time Genes. *Developmental Cell*. https://doi.org/10.1016/j.devcel.2009.03.011

Liu, C., Zhou, J., Bracha-Drori, K., Yalovsky, S., Ito, T., & Yu, H. (2007). Specification of Arabidopsis floral meristem identity by repression of flowering time genes. *Development*, *134*(10), 1901–1910. https://doi.org/10.1242/dev.003103

Liu, H. H., Xiong, F., Duan, C. Y., Wu, Y. N., Zhang, Y., & Li, S. (2019). Importinβ4 mediates nuclear import of grf-interacting factors to control ovule development in arabidopsis. *Plant Physiology*. https://doi.org/10.1104/pp.18.01135

Liu, K., Li, Y., Chen, X., Li, L., Liu, K., Zhao, H., Wang, Y., & Han, S. (2018). ERF72 interacts with ARF6 and BZR1 to regulate hypocotyl elongation in Arabidopsis. *Journal of Experimental Botany*. https://doi.org/10.1093/jxb/ery220

Livak, K. J., & Schmittgen, T. D. (2001). Analysis of relative gene expression data using real-time quantitative PCR and the 2-ΔΔCT method. *Methods*. https://doi.org/10.1006/meth.2001.1262

Long, J. A., Moan, E. I., Medford, J. I., & Barton, M. K. (1996). A member of the KNOTTED class of homeodomain proteins encoded by the STM gene of Arabidopsis. *Nature*. https://doi.org/10.1038/379066a0

Lu, Z., Yu, H., Xiong, G., Wang, J., Jiao, Y., Liu, G., Jing, Y., Meng, X., Hu, X., Qian, Q., Fu, X., Wang, Y., & Li, J. (2013). Genome-wide binding analysis of the transcription activator IDEAL PLANT ARCHITECTURE1 reveals a complex network regulating rice plant architecture. *Plant Cell*. https://doi.org/10.1105/tpc.113.113639

Lyons, E., & Freeling, M. (2008). How to usefully compare homologous plant genes and chromosomes as DNA sequences. *Plant Journal*. https://doi.org/10.1111/j.1365-313X.2007.03326.x

Madeira, F., Park, Y. M., Lee, J., Buso, N., Gur, T., Madhusoodanan, N., Basutkar, P., Tivey, A. R. N., Potter, S. C., Finn, R. D., & Lopez, R. (2019). The EMBL-EBI search and sequence analysis tools APIs in 2019. *Nucleic Acids Research*. https://doi.org/10.1093/nar/gkz268

Mandáková, T., Hloušková, P., German, D. A., & Lysak, M. A. (2017). Monophyletic origin and evolution of the largest crucifer genomes. *Plant Physiology*. https://doi.org/10.1104/pp.17.00457

Mandel, M. A., & Yanofsky, M. F. (1995a). A gene triggering flower formation in Arabidopsis. In *Nature*. https://doi.org/10.1038/377522a0

Mandel, M. A., & Yanofsky, M. F. (1995b). The Arabidopsis AGL8 MADS Box Gene Is Expressed in Inflorescence Meristems and Is Negatively Regulated by APETALA1. *The Plant Cell*. https://doi.org/10.2307/3870185

Marín, I. C., Loef, I., Bartetzko, L., Searle, I., Coupland, G., Stitt, M., & Osuna, D. (2011). Nitrate regulates floral induction in Arabidopsis, acting independently of light, gibberellin and autonomous pathways. *Planta*. https://doi.org/10.1007/s00425-010-1316-5

Martin, A., Adam, H., Díaz-Mendoza, M., Żurczak, M., González-Schain, N. D., & Suárez-López, P. (2009). Graft-transmissible induction of potato tuberization by the microRNA miR172. *Development*. https://doi.org/10.1242/dev.031658

Martin, M. (2011). Cutadapt removes adapter sequences from high-throughput sequencing reads. *EMBnet.Journal*. https://doi.org/10.14806/ej.17.1.200

Martin, R. C., Asahina, M., Liu, P. P., Kristof, J. R., Coppersmith, J. L., Pluskota, W. E., Bassel, G. W., Goloviznina, N. A., Nguyen, T. T., Martínez-Andújar, C., Arun Kumar, M. B., Pupel, P., & Nonogaki, H. (2010). The regulation of post-germinative transition from the cotyledon- to vegetative-leaf stages by microRNA-targeted squamosa promoter-binding protein like13 in Arabidopsis. *Seed Science Research*. https://doi.org/10.1017/S0960258510000073

Martínez, C., Pons, E., Prats, G., & León, J. (2004). Salicylic acid regulates flowering time and links defence responses and reproductive development. *Plant Journal*. https://doi.org/10.1046/j.1365-313X.2003.01954.x

Mateos, J. L., Tilmes, V., Madrigal, P., Severing, E., Richter, R., Rijkenberg, C. W. M., Krajewski, P., & Coupland, G. (2017). Divergence of regulatory networks governed by the orthologous transcription factors FLC and PEP1 in Brassicaceae species. *Proceedings of the National Academy of Sciences of the United States of America*. https://doi.org/10.1073/pnas.1618075114

Mathieu, J., Yant, L. J., Mürdter, F., Küttner, F., & Schmid, M. (2009). Repression of flowering by the miR172 target SMZ. *PLoS Biology*. https://doi.org/10.1371/journal.pbio.1000148

Mayor, C., Brudno, M., Schwartz, J. R., Poliakov, A., Rubin, E. M., Frazer, K. A., Pachter, L. S., & Dubchak, I. (2000). Vista: Visualizing global DNA sequence alignments of arbitrary length. *Bioinformatics*. https://doi.org/10.1093/bioinformatics/16.11.1046

McCarthy, E. W., Mohamed, A., & Litt, A. (2015). Functional divergence of APETALA1 and FRUITFULL is due to changes in both regulation and coding sequence. *Frontiers in Plant Science*. https://doi.org/10.3389/fpls.2015.01076

Melzer, S., Lens, F., Gennen, J., Vanneste, S., Rohde, A., & Beeckman, T. (2008). Flowering-time genes modulate meristem determinacy and growth form in Arabidopsis thaliana. *Nature Genetics*. https://doi.org/10.1038/ng.253

Michaels, S. D., & Amasino, R. M. (2000). Memories of winter: Vernalization and the competence to flower. In *Plant, Cell and Environment*. https://doi.org/10.1046/j.1365-3040.2000.00643.x

Michaels, Scott D., & Amasino, R. M. (1999). FLOWERING LOCUS C encodes a novel MADS domain protein that acts as a repressor of flowering. *Plant Cell*. https://doi.org/10.1105/tpc.11.5.949

Michaels, Scott D., Ditta, G., Gustafson-Brown, C., Pelaz, S., Yanofsky, M., & Amasino, R. M. (2003). AGL24 acts as a promoter of flowering in Arabidopsis and is positively regulated by vernalization. *Plant Journal*. https://doi.org/10.1046/j.1365-313X.2003.01671.x

Michaels, Scott D., He, Y., Scortecci, K. C., & Amasino, R. M. (2003). Attenuation of FLOWERING LOCUS C activity as a mechanism for the evolution of summer-annual flowering behavior in Arabidopsis. *Proceedings of the National Academy of Sciences of the United States of America*. https://doi.org/10.1073/pnas.1531467100

Moinuddin, S. G. A., Jourdes, M., Laskar, D. D., Ki, C., Cardenas, C. L., Kim, K. W., Zhang, D., Davin, L. B., & Lewis, N. G. (2010). Insights into lignin primary structure and deconstruction from Arabidopsis thaliana COMT (caffeic acid O-methyl transferase) mutant Atomt1. *Organic and Biomolecular Chemistry*. https://doi.org/10.1039/c004817h

Moon, J., Suh, S. S., Lee, H., Choi, K. R., Hong, C. B., Paek, N. C., Kim, S. G., & Lee, I. (2003). The SOC1 MADS-box gene integrates vernalization and gibberellin signals for flowering in Arabidopsis. *Plant Journal*. https://doi.org/10.1046/j.1365-313X.2003.01833.x

Mouradov, A., Cremer, F., & Coupland, G. (2002). Control of flowering time: Interacting pathways as a basis for diversity. *Plant Cell*. https://doi.org/10.1105/tpc.001362

Murase, K., Hirano, Y., Sun, T. P., & Hakoshima, T. (2008). Gibberellin-induced DELLA recognition by the gibberellin receptor GID1. *Nature*. https://doi.org/10.1038/nature07519

Musielak, T., Bürgel, P., Kolb, M., & Bayer, M. (2016). Use of SCRI Renaissance 2200 (SR2200) as a Versatile Dye for Imaging of Developing Embryos, Whole Ovules, Pollen Tubes and Roots. *BIO-PROTOCOL*. https://doi.org/10.21769/bioprotoc.1935

Musielak, T. J., Schenkel, L., Kolb, M., Henschen, A., & Bayer, M. (2015). A simple and versatile cell wall staining protocol to study plant reproduction. *Plant Reproduction*. https://doi.org/10.1007/s00497-015-0267-1

Mylne, J., Greb, T., Lister, C., & Dean, C. (2004). Epigenetic regulation in the control of flowering. *Cold Spring Harbor Symposia on Quantitative Biology*. https://doi.org/10.1101/sqb.2004.69.457

Nguyen, S. T. T., Greaves, T., & McCurdy, D. W. (2017). Heteroblastic development of transfer cells is controlled by the microRNA miR156/SPL module. *Plant Physiology*. https://doi.org/10.1104/pp.16.01741

Nietzsche, M., Schießl, I., & Börnke, F. (2014). The complex becomes more complex: Protein-protein interactions of SnRK1 with DUF581 family proteins provide a framework for cell- and stimulus type-specific SnRK1 signaling in plants. *Frontiers in Plant Science*. https://doi.org/10.3389/fpls.2014.00054

Nikolov, L. A., Shushkov, P., Nevado, B., Gan, X., Al-Shehbaz, I. A., Filatov, D., Bailey, C. D., & Tsiantis, M. (2019). Resolving the backbone of the Brassicaceae phylogeny for investigating trait diversity. *New Phytologist*. https://doi.org/10.1111/nph.15732

Nolan, T. M., Vukasinović, N., Liu, D., Russinova, E., & Yin, Y. (2020). Brassinosteroids: Multidimensional regulators of plant growth, development, and stress responses. *Plant Cell*. https://doi.org/10.1105/tpc.19.00335

O'Malley, R. C., Huang, S. S. C., Song, L., Lewsey, M. G., Bartlett, A., Nery, J. R., Galli, M., Gallavotti, A., & Ecker, J. R. (2016). Cistrome and Epicistrome Features Shape the Regulatory DNA Landscape. *Cell*. https://doi.org/10.1016/j.cell.2016.04.038

Ó'Maoiléidigh, D. S., Thomson, B., Raganelli, A., Wuest, S. E., Ryan, P. T., Kwaśniewska, K., Carles, C. C., Graciet, E., & Wellmer, F. (2015). Gene network analysis of Arabidopsis thaliana flower development through dynamic gene perturbations. *Plant Journal*. https://doi.org/10.1111/tpj.12878

Ó'Maoiléidigh, D. S., Wuest, S. E., Rae, L., Raganelli, A., Ryan, P. T., Kwaśniewska, K., Das, P., Lohan, A. J., Loftus, B., Graciet, E., & Wellmer, F. (2013). Control of reproductive floral organ identity specification in arabidopsis by the C function regulator AGAMOUS. *Plant Cell*. https://doi.org/10.1105/tpc.113.113209

Ó'Maoiléidigh, D. S., Van Driel, A.D., Singh, A., Sang, Q., Le Bec, N., Vincent, C., Romera-Branchat, M., Severing, E., Martinez Gallegos, R., Coupland, C. (*in preparation*) Analysis of the *MIR172* family defines transcriptional and post-transcriptional mechanisms that coordinately regulate APETALA2 to control floral transition of Arabidopsis.

Oakenfull, R. J., & Davis, S. J. (2017). Shining a light on the Arabidopsis circadian clock. In *Plant, cell & environment*. https://doi.org/10.1111/pce.13033

Olas, J. J., Van Dingenen, J., Abel, C., Działo, M. A., Feil, R., Krapp, A., Schlereth, A., & Wahl, V. (2019). Nitrate acts at the Arabidopsis thaliana shoot apical meristem to regulate flowering time. *New Phytologist*. https://doi.org/10.1111/nph.15812

Ori, N., Eshed, Y., Chuck, G., Bowman, J. L., & Hake, S. (2000). Mechanisms that control knox gene expression in the Arabidopsis shoot. *Development*.

Østergaard, L., Kempin, S. A., Bies, D., Klee, H. J., & Yanofsky, M. F. (2006). Pod shatter-resistant Brassica fruit produced by ectopic expression of the FRUITFULL gene. *Plant Biotechnology Journal*. https://doi.org/10.1111/j.1467-7652.2005.00156.x

Padmanabhan, M. S., Ma, S., Burch-Smith, T. M., Czymmek, K., Huijser, P., & Dinesh-Kumar, S. P. (2013). Novel Positive Regulatory Role for the SPL6 Transcription Factor in the N TIR-NB-LRR Receptor-Mediated Plant Innate Immunity. *PLoS Pathogens*. https://doi.org/10.1371/journal.ppat.1003235

Para, A., Farré, E. M., Imaizumi, T., Pruneda-Paz, J. L., Harmon, F. G., & Kay, S. A. (2007). PRR3 is a vascular regulator of TOC1 stability in the Arabidopsis circadian clock. *Plant Cell*. https://doi.org/10.1105/tpc.107.054775

Parcy, F., Bomblies, K., & Weigel, D. (2002). Interaction of LEAFY, AGAMOUS and TERMINAL FLOWER1 in maintaining floral meristem identity in Arabidopsis. *Development*.

Pařenicová, L., De Folter, S., Kieffer, M., Horner, D. S., Favalli, C., Busscher, J., Cook, H. E., Ingram, R. M., Kater, M. M., Davies, B., Angenent, G. C., & Colombo, L. (2003). Molecular and phylogenetic analyses of the complete MADS-Box transcription factor family in Arabidopsis: New openings to the MADS world. *Plant Cell*. https://doi.org/10.1105/tpc.011544

Pascal, S., Bernard, A., Deslous, P., Gronnier, J., Fournier-Goss, A., Domergue, F., Rowland, O., & Joubès, J. (2019). Arabidopsis CER1-LIKE1 functions in a cuticular very-long-chain alkane-forming complex. *Plant Physiology*. https://doi.org/10.1104/pp.18.01075

Patro, R., Duggal, G., Love, M. I., Irizarry, R. A., & Kingsford, C. (2017). Salmon: fast and bias-aware quantification of transcript expression using dual-phase inference. *Nature Methods*. https://doi.org/10.1038/NMETH.4197

Peng, J., Carol, P., Richards, D. E., King, K. E., Cowling, R. J., Murphy, G. P., & Harberd, N. P. (1997). The Arabidopsis GAI gene defines a signaling pathway that negatively regulates gibberellin responses. *Genes and Development*. https://doi.org/10.1101/gad.11.23.3194

Plotnikova, A., Kellner, M., Mosiolek, M., Schon, M., & Nodine, M. (2019). MicroRNA Dynamics and Functions During Arabidopsis Embryogenesis. *BioRxiv*. https://doi.org/10.1101/633735

Poethig, R. S. (2013). Vegetative phase change and shoot maturation in plants. In *Current Topics in Developmental Biology*. https://doi.org/10.1016/B978-0-12-396968-2.00005-1

Porri, A., Torti, S., Romera-Branchat, M., & Coupland, G. (2012). Spatially distinct regulatory roles for gibberellins in the promotion of flowering of arabidopsis under long photoperiods. *Development (Cambridge)*. https://doi.org/10.1242/dev.077164

Posada, D., & Crandall, K. A. (1998). MODELTEST: Testing the model of DNA substitution. *Bioinformatics*. https://doi.org/10.1093/bioinformatics/14.9.817

Posé, D., Verhage, L., Ott, F., Yant, L., Mathieu, J., Angenent, G. C., Immink, R. G. H., & Schmid, M. (2013). Temperature-dependent regulation of flowering by antagonistic FLM variants. *Nature*. https://doi.org/10.1038/nature12633

Preston, J. C., & Hileman, L. C. (2013). Functional evolution in the plant SQUAMOSA-PROMOTER BINDING PROTEIN-LIKE (SPL) gene family. In *Frontiers in Plant Science*. https://doi.org/10.3389/fpls.2013.00080

Puranik, S., Acajjaoui, S., Conn, S., Costa, L., Conn, V., Vial, A., Marcellin, R., Melzer, R., Brown, E., Hart, D., Theißen, G., Silva, C. S., Parcy, F., Dumas, R., Nanao, M., & Zubieta, C. (2014). Structural basis for the oligomerization of the MADS domain transcription factor SEPALLATA3 in Arabidopsis. *Plant Cell*. https://doi.org/10.1105/tpc.114.127910

Purugganan, M. D., Rounsley, S. D., Schmidt, R. J., & Yanofsky, M. F. (1995). Molecular evolution of flower development: Diversification of the plant MADS-box regulatory gene family. *Genetics*.

Putterill, J., Robson, F., Lee, K., Simon, R., & Coupland, G. (1995). The CONSTANS gene of arabidopsis promotes flowering and encodes a protein showing similarities to zinc finger transcription factors. *Cell*. https://doi.org/10.1016/0092-8674(95)90288-0

Qu, J., Kang, S. G., Wang, W., Musier-Forsyth, K., & Jang, J. C. (2014). The Arabidopsis thaliana tandem zinc finger 1 (AtTZF1) protein in RNA binding and decay. *Plant Journal*. https://doi.org/10.1111/tpj.12485

Qüesta, J. I., Song, J., Geraldo, N., An, H., & Dean, C. (2016). Arabidopsis transcriptional repressor VAL1 triggers Polycomb silencing at FLC during vernalization. *Science*. https://doi.org/10.1126/science.aaf7354

Reece-Hoyes, J. S., & Marian Walhout, A. J. (2012). Yeast one-hybrid assays: A historical and technical perspective. In *Methods*. https://doi.org/10.1016/j.ymeth.2012.07.027

Reeves, P. H., & Coupland, G. (2001). Analysis of flowering time control in Arabidopsis by comparison of double and triple mutants. *Plant Physiology*. https://doi.org/10.1104/pp.126.3.1085

Reinhart, B. J., Weinstein, E. G., Rhoades, M. W., Bartel, B., & Bartel, D. P. (2002). MicroRNAs in plants. *Genes and Development*. https://doi.org/10.1101/gad.1004402

Rhoades, M. W., Reinhart, B. J., Lim, L. P., Burge, C. B., Bartel, B., & Bartel, D. P. (2002). Prediction of plant microRNA targets. *Cell*. https://doi.org/10.1016/S0092-8674(02)00863-2

Riboni, M., Galbiati, M., Tonelli, C., & Conti, L. (2013). GIGANTEA enables drought escape response via abscisic acid-dependent activation of the florigens and SUPPRESSOR of OVEREXPRESSION of CONSTANS11[c][w]. *Plant Physiology*. https://doi.org/10.1104/pp.113.217729

Riboni, M., Test, A. R., Galbiati, M., Tonelli, C., & Conti, L. (2016). ABA-dependent control of GIGANTEA signalling enables drought escape via up-regulation of FLOWERING LOCUS T in Arabidopsis thaliana. *Journal of Experimental Botany*. https://doi.org/10.1093/jxb/erw384

Richter, R., Kinoshita, A., Vincent, C., Martinez-Gallegos, R., Gao, H., van Driel, A. D., Hyun, Y., Mateos, J. L., & Coupland, G. (2019). Floral regulators FLC and SOC1 directly regulate expression of the B3-type transcription factor TARGET of FLC and SVP 1 at the Arabidopsis shoot apex via antagonistic chromatin modifications. *PLoS Genetics*. https://doi.org/10.1371/journal.pgen.1008065

Rodriguez, R. E., Mecchia, M. A., Debernardi, J. M., Schommer, C., Weigel, D., & Palatnik, J. F. (2010). Control of cell proliferation in Arabidopsis thaliana by microRNA miR396. *Development*. https://doi.org/10.1242/dev.043067

Roig-Villanova, I., Bou, J., Sorin, C., Devlin, P. F., & Martínez-García, J. F. (2006). Identification of primary target genes of phytochrome signaling. Early transcriptional control during shade avoidance responses in arabidopsis. *Plant Physiology*. https://doi.org/10.1104/pp.105.076331

Romanel, E. A. C., Schrago, C. G., Couñago, R. M., Russo, C. A. M., & Alves-Ferreira, M. (2009). Evolution of the B3 DNA binding superfamily: New insights into REM family gene diversification. *PLoS ONE*. https://doi.org/10.1371/journal.pone.0005791

Romera-Branchat, M., Edouard, S., Chloe, P., Hyonhwa, O., Coral, V., Guillaume, N., Rafael, M.-G., Seonghoe, J., Fernando, A. L., Pedro, M., & George, C. (2020). Functional Divergence of the Arabidopsis Florigen-Interacting bZIP Transcription Factors FD and FDP. *Cell Reports*, *31*(9).

Rose, J. K. C., Braam, J., Fry, S. C., & Nishitani, K. (2002). The XTH family of enzymes involved in xyloglucan endotransglucosylation and endohydrolysis: Current perspectives and a new unifying nomenclature. In *Plant and Cell Physiology*. https://doi.org/10.1093/pcp/pcf171

Ruiz-García, L., Madueño, F., Wilkinson, M., Haughn, G., Saunas, J., & Martínez-Zapater, J. M. (1997). Different roles of flowering-time genes in the activation of floral initiation genes in Arabidopsis. *Plant Cell*. https://doi.org/10.1105/tpc.9.11.1921

Ryu, J. Y., Lee, H. J., Seo, P. J., Jung, J. H., Ahn, J. H., & Park, C. M. (2014). The arabidopsis floral repressor BFT delays flowering by competing with FT for FD binding under high salinity. *Molecular Plant*. https://doi.org/10.1093/mp/sst114

Samach, A., Onouchi, H., Gold, S. E., Ditta, G. S., Schwarz-Sommer, Z., Yanofsky, M. F., & Coupland, G. (2000). Distinct roles of constans target genes in reproductive development of Arabidopsis. *Science*. https://doi.org/10.1126/science.288.5471.1613

Sanda, S. L., & Amasino, R. M. (1996). Interaction of FLC and late-flowering mutations in Arabidopsis thaliana. *Molecular and General Genetics*. https://doi.org/10.1007/BF02174346

Schmid, M., Uhlenhaut, N. H., Godard, F., Demar, M., Bressan, R., Weigel, D., & Lohman, J. U. (2003). Dissection of floral induction pathways using global expression analysis. *Development*. https://doi.org/10.1242/dev.00842

Schoof, H., Lenhard, M., Haecker, A., Mayer, K. F. X., Jürgens, G., & Laux, T. (2000). The stem cell population of Arabidopsis shoot meristems is maintained by a regulatory loop between the CLAVATA and WUSCHEL genes. *Cell*. https://doi.org/10.1016/S0092-8674(00)80700-X

Schulten, A., Bytomski, L., Quintana, J., Bernal, M., & Krämer, U. (2019). Do Arabidopsis Squamosa promoter binding Protein-Like genes act together in plant acclimation to copper or zinc deficiency? . *Plant Direct*. https://doi.org/10.1002/pld3.150

Schwab, R., Palatnik, J. F., Riester, M., Schommer, C., Schmid, M., & Weigel, D. (2005). Specific effects of microRNAs on the plant transcriptome. *Developmental Cell*. https://doi.org/10.1016/j.devcel.2005.01.018

Schwarz, S. (2006). *Molecular and Functional Analysis of SBP-Box Transcription Factors in Arabidopsis thaliana.* University of Cologne.

Schwarz, S., Grande, A. V., Bujdoso, N., Saedler, H., & Huijser, P. (2008). The microRNA regulated SBP-box genes SPL9 and SPL15 control shoot maturation in Arabidopsis. *Plant Molecular Biology*. https://doi.org/10.1007/s11103-008-9310-z

Searle, I., He, Y., Turck, F., Vincent, C., Fornara, F., Kröber, S., Amasino, R. A., & Coupland, G. (2006). The transcription factor FLC confers a flowering response to vernalization by repressing meristem competence and systemic signaling in Arabidopsis. *Genes and Development*. https://doi.org/10.1101/gad.373506

Serrano-Mislata, A., Goslin, K., Zheng, B., Rae, L., Wellmer, F., Graciet, E., & Madueño, F. (2017). Regulatory interplay between LEAFY, APETALA1/CAULIFLOWER and TERMINAL FLOWER1: New insights into an old relationship. *Plant Signaling and Behavior*. https://doi.org/10.1080/15592324.2017.1370164

Shikata, M., Koyama, T., Mitsuda, N., & Ohme-Takagi, M. (2009). Arabidopsis SBP-Box genes SPL10, SPL11 and SPL2 control morphological change in association with shoot maturation in the reproductive phase. *Plant and Cell Physiology*. https://doi.org/10.1093/pcp/pcp148

Shim, J. S., Kubota, A., & Imaizumi, T. (2017a). Circadian clock and photoperiodic flowering in arabidopsis: CONSTANS is a Hub for Signal integration. *Plant Physiology*. https://doi.org/10.1104/pp.16.01327

Shim, J. S., Kubota, A., & Imaizumi, T. (2017b). Update on Circadian Clock and Photoperiodic Flowering Circadian Clock and Photoperiodic Flowering in Arabidopsis: CONSTANS Is a Hub for Signal Integration 1[OPEN]. *Plant Physiology*. https://doi.org/10.1104/pp.16.01327

Shimada, A., Ueguchi-Tanaka, M., Nakatsu, T., Nakajima, M., Naoe, Y., Ohmiya, H., Kato, H., & Matsuoka, M. (2008). Structural basis for gibberellin recognition by its receptor GID1. *Nature*. https://doi.org/10.1038/nature07546

Siligato, R., Wang, X., Yadav, S. R., Lehesranta, S., Ma, G., Ursache, R., Sevilem, I., Zhang, J., Gorte, M., Prasad, K., Wrzaczek, M., Heidstra, R., Murphy, A., Scheres, B., & Mähönen, A. P. (2016). Multisite gateway-compatible cell type-specific gene-inducible system for plants. *Plant Physiology*. https://doi.org/10.1104/pp.15.01246

Silverstone, A. L., Jung, H. S., Dill, A., Kawaide, H., Kamiya, Y., & Sun, T. P. (2001). Repressing a repressor: Gibberellin-induced rapid reduction of the RGA protein in Arabidopsis. *Plant Cell*. https://doi.org/10.1105/tpc.13.7.1555

Simon, R., Igeno, M. I., & Coupland, G. (1996). Activation of floral meristem identity genes in Arabidopsis. *Nature*. https://doi.org/10.1038/384059a0

Simpson, G. G. (2004). The autonomous pathway: Epigenetic and post-transcriptional gene regulation in the control of Arabidopsis flowering time. In *Current Opinion in Plant Biology*. https://doi.org/10.1016/j.pbi.2004.07.002

Skopelitis, D. S., Hill, K., Klesen, S., Marco, C. F., von Born, P., Chitwood, D. H., & Timmermans, M. C. P. (2018). Gating of miRNA movement at defined cell-cell interfaces governs their impact as positional signals. *Nature Communications*. https://doi.org/10.1038/s41467-018-05571-0

Skylar, A., & Wu, X. (2011). Regulation of Meristem Size by Cytokinin Signaling. In *Journal of Integrative Plant Biology*. https://doi.org/10.1111/j.1744-7909.2011.01045.x

Slater, G. S. C., & Birney, E. (2005). Automated generation of heuristics for biological sequence comparison. *BMC Bioinformatics*. https://doi.org/10.1186/1471-2105-6-31

Song, Y. H., Kubota, A., Kwon, M. S., Covington, M. F., Lee, N., Taagen, E. R., Laboy Cintrón, D., Hwang, D. Y., Akiyama, R., Hodge, S. K., Huang, H., Nguyen, N. H., Nusinow, D. A., Millar, A. J., Shimizu, K. K., & Imaizumi, T. (2018). Molecular basis of flowering under natural long-day conditions in Arabidopsis. *Nature Plants*. https://doi.org/10.1038/s41477-018-0253-3

Stone, J. M., Liang, X., Nekl, E. R., & Stiers, J. J. (2005). Arabidopsis AtSPL14, a plant-specific SBP-domain transcription factor, participates in plant development and sensitivity to fumonisin B1. *Plant Journal*. https://doi.org/10.1111/j.1365-313X.2005.02334.x

Suárez-López, P., Wheatley, K., Robson, F., Onouchi, H., Valverde, F., & Coupland, G. (2001). CONSTANS mediates between the circadian clock and the control of flowering in Arabidopsis. *Nature*. https://doi.org/10.1038/35074138

Sun, L. R., Hao, F. S., Lu, B. S., & Ma, L. Y. (2010). AtNOA1 modulates nitric oxide accumulation and stomatal closure induced by salicylic acid in arabidopsis. *Plant Signaling and Behavior*. https://doi.org/10.4161/psb.5.8.12293

Sung, S., & Amasino, R. M. (2004). Vernalization in Arabidopsis thaliana is mediated by the PHD finger protein VIN3. *Nature*. https://doi.org/10.1038/nature02195

Sureshkumar, S., Dent, C., Seleznev, A., Tasset, C., & Balasubramanian, S. (2016). Nonsense-mediated mRNA decay modulates FLM-dependent thermosensory flowering response in Arabidopsis. *Nature Plants*. https://doi.org/10.1038/NPLANTS.2016.55

Tao, Z., Shen, L., Liu, C., Liu, L., Yan, Y., & Yu, H. (2012). Genome-wide identification of SOC1 and SVP targets during the floral transition in Arabidopsis. *Plant Journal*. https://doi.org/10.1111/j.1365-313X.2012.04919.x

Teper-Bamnolker, P., & Samach, A. (2005). The flowering integrator FT regulates SEPALLATA3 and FRUITFULL accumulation in Arabidopsis leaves. *Plant Cell*. https://doi.org/10.1105/tpc.105.035766

Todesco, M., Rubio-Somoza, I., Paz-Ares, J., & Weigel, D. (2010). A collection of target mimics for comprehensive analysis of MicroRNA function in Arabidopsis thaliana. *PLoS Genetics*. https://doi.org/10.1371/journal.pgen.1001031

Torti, S., Fornara, F., Vincent, C., Andrés, F., Nordström, K., Göbel, U., Knoll, D., Schoof, H., & Coupland, G. (2012). Analysis of the Arabidopsis shoot meristem transcriptome during floral transition identifies distinct regulatory patterns and a leucine-rich repeat protein that promotes flowering. *Plant Cell*. https://doi.org/10.1105/tpc.111.092791

Tripathi, R. K., Bregitzer, P., & Singh, J. (2018). Genome-wide analysis of the SPL/miR156 module and its interaction with the AP2/miR172 unit in barley. *Scientific Reports*. https://doi.org/10.1038/s41598-018-25349-0

Truernit, E., & Sauer, N. (1995). The promoter of the Arabidopsis thaliana SUC2 sucrose-H+ symporter gene directs expression of β-glucuronidase to the phloem: Evidence for phloem loading and unloading by SUC2. *Planta: An International Journal of Plant Biology*. https://doi.org/10.1007/BF00203657

Unte, U. S., Sorensen, A. M., Pesaresi, P., Gandikota, M., Leister, D., Saedler, H., & Huijser, P. (2003). SPL8, an SBP-box gene that affects pollen sac development in Arabidopsis. *Plant Cell*. https://doi.org/10.1105/tpc.010678

Usami, T., Horiguchi, G., Yano, S., & Tsukaya, H. (2009). The more and smaller cells mutants of Arabidopsis thaliana identify novel roles for SQUAMOSA PROMOTER BINDING PROTEIN-LIKE genes in the control of heteroblasty. *Development*. https://doi.org/10.1242/dev.028613

Valverde, F., Mouradov, A., Soppe, W., Ravenscroft, D., Samach, A., & Coupland, G. (2004). Photoreceptor Regulation of CONSTANS Protein in Photoperiodic Flowering. *Science*. https://doi.org/10.1126/science.1091761

Van Dijk, A. D. J., Morabito, G., Fiers, M., Van Ham, R. C. H. J., Angenent, G. C., & Immink, R. G. H. (2010). Sequence motifs in MADS transcription factors responsible for specificity and diversification of protein-protein interaction. *PLoS Computational Biology*. https://doi.org/10.1371/journal.pcbi.1001017

Veley, K. M., & Michaels, S. D. (2008). Functional redundancy and new roles for genes of the autonomous floral-promotion pathway. *Plant Physiology*. https://doi.org/10.1104/pp.108.118927

Wang, H., Pan, J., Li, Y., Lou, D., Hu, Y., & Yu, D. (2016). The DELLA-CONSTANS transcription factor cascade integrates gibberellic acid and photoperiod signaling to regulate flowering. *Plant Physiology*. https://doi.org/10.1104/pp.16.00891

Wang, J., Mei, J., & Ren, G. (2019). Plant microRNAs: Biogenesis, homeostasis, and degradation. In *Frontiers in Plant Science*. https://doi.org/10.3389/fpls.2019.00360

Wang, J. W., Czech, B., & Weigel, D. (2009). miR156-Regulated SPL Transcription Factors Define an Endogenous Flowering Pathway in Arabidopsis thaliana. *Cell*. https://doi.org/10.1016/j.cell.2009.06.014

Wang, J. W., Schwab, R., Czech, B., Mica, E., & Weigel, D. (2008). Dual effects of miR156-targeted SPL genes and CYP78A5/KLUH on plastochron length and organ size in Arabidopsis thaliana. *Plant Cell*. https://doi.org/10.1105/tpc.108.058180

Wang, L., & Zhang, Q. (2017). Boosting Rice Yield by Fine-Tuning SPL Gene Expression. In *Trends in Plant Science*. https://doi.org/10.1016/j.tplants.2017.06.004

Wang, R., Farrona, S., Vincent, C., Joecker, A., Schoof, H., Turck, F., Alonso-Blanco, C., Coupland, G., & Albani, M. C. (2009). PEP1 regulates perennial flowering in Arabis alpina. *Nature*. https://doi.org/10.1038/nature07988

Wang, Y., Hu, Z., Yang, Y., Chen, X., & Chen, G. (2009). Function annotation of an SBP-box gene in arabidopsis based on analysis of co-expression networks and promoters. *International Journal of Molecular Sciences*. https://doi.org/10.3390/ijms10010116

Wang, Z., Wang, Y., Kohalmi, S. E., Amyot, L., & Hannoufa, A. (2016). SQUAMOSA PROMOTER BINDING PROTEIN-LIKE 2 controls floral organ development and plant fertility by activating ASYMMETRIC LEAVES 2 in Arabidopsis thaliana. *Plant Molecular Biology*. https://doi.org/10.1007/s11103-016-0536-x

Wei, H., Zhao, Y., Xie, Y., & Wang, H. (2018). Exploiting SPL genes to improve maize plant architecture tailored for high-density planting. In *Journal of experimental botany*. https://doi.org/10.1093/jxb/ery258

Wei, S., Gruber, M. Y., Yu, B., Gao, M. J., Khachatourians, G. G., Hegedus, D. D., Parkin, I. A. P., & Hannoufa, A. (2012). Arabidopsis mutant sk156 reveals complex regulation of SPL15 in a miR156-controlled gene network. *BMC Plant Biology*. https://doi.org/10.1186/1471-2229-12-169

Weigel, D., & Meyerowitz, E. M. (1993). Activation of floral homeotic genes in Arabidopsis. *Science*. https://doi.org/10.1126/science.261.5129.1723

Wigge, P. A., Kim, M. C., Jaeger, K. E., Busch, W., Schmid, M., Lohmann, J. U., & Weigel, D. (2005). Integration of spatial and temporal information during floral induction in Arabidopsis. *Science*. https://doi.org/10.1126/science.1114358

Willing, E. M., Rawat, V., Mandáková, T., Maumus, F., James, G. V., Nordström, K. J. V., Becker, C., Warthmann, N., Chica, C., Szarzynska, B., Zytnicki, M., Albani, M. C., Kiefer, C., Bergonzi, S., Castaings, L., Mateos, J. L., Berns, M. C., Bujdoso, N., Piofczyk, T., … Schneeberger, K. (2015). Genome expansion of Arabis alpina linked with retrotransposition and reduced symmetric DNA methylation. *Nature Plants*. https://doi.org/10.1038/nplants.2014.23

Wilson, R. N., Heckman, J. W., & Somerville, C. R. (1992). Gibberellin is required for flowering in Arabidopsis thaliana under short days. *Plant Physiology*. https://doi.org/10.1104/pp.100.1.403

Wollenberg, A. C., & Amasino, R. M. (2012). Natural variation in the temperature range permissive for vernalization in accessions of Arabidopsis thaliana. *Plant, Cell and Environment*. https://doi.org/10.1111/j.1365-3040.2012.02548.x

Wood, C. C., Robertson, M., Tanner, G., Peacock, W. J., Dennis, E. S., & Helliwell, C. A. (2006). The Arabidopsis thaliana vernalization response requires a polycomb-like protein complex that also includes VERNALIZATION INSENSITIVE 3. *Proceedings of the National Academy of Sciences of the United States of America*. https://doi.org/10.1073/pnas.0606385103

Wu, G., Park, M. Y., Conway, S. R., Wang, J. W., Weigel, D., & Poethig, R. S. (2009). The Sequential Action of miR156 and miR172 Regulates Developmental Timing in Arabidopsis. *Cell*. https://doi.org/10.1016/j.cell.2009.06.031

Wu, G., & Poethig, R. S. (2006). Temporal regulation of shoot development in Arabidopsis thaliana by miRr156 and its target SPL3. *Development*. https://doi.org/10.1242/dev.02521

Wu, Z., Fang, X., Zhu, D., & Dean, C. (2020). Autonomous pathway: Flowering locus c repression through an antisense-mediated chromatin-silencing mechanism. *Plant Physiology*. https://doi.org/10.1104/pp.19.01009

Wurzinger, B., Nukarinen, E., Nägele, T., Weckwerth, W., & Teige, M. (2018). The snrk1 kinase as central mediator of energy signaling between different organelles. In *Plant Physiology*. https://doi.org/10.1104/pp.17.01404

Xie, Y., Zhou, Q., Zhao, Y., Li, Q., Liu, Y., Ma, M., Wang, B., Shen, R., Zheng, Z., & Wang, H. (2020). FHY3 and FAR1 Integrate Light Signals with the miR156-SPL Module-Mediated Aging Pathway to Regulate Arabidopsis Flowering. *Molecular Plant*. https://doi.org/10.1016/j.molp.2020.01.013

Xing, S., Salinas, M., Garcia-Molina, A., Höhmann, S., Berndtgen, R., & Huijser, P. (2013). SPL8 and miR156-targeted SPL genes redundantly regulate Arabidopsis gynoecium differential patterning. *Plant Journal*. https://doi.org/10.1111/tpj.12221

Xing, S., Salinas, M., Höhmann, S., Berndtgen, R., & Huijser, P. (2010). miR156-targeted and nontargeted SBP-Box transcription factors act in concert to secure male fertility in Arabidopsis. *Plant Cell*. https://doi.org/10.1105/tpc.110.079343

Xu, F., Li, T., Xu, P. B., Li, L., Du, S. S., Lian, H. L., & Yang, H. Q. (2016). DELLA proteins physically interact with CONSTANS to regulate flowering under long days in Arabidopsis. *FEBS Letters*. https://doi.org/10.1002/1873-3468.12076

Xu, M., Hu, T., Smith, M. R., & Poethig, R. S. (2016). Epigenetic regulation of vegetative phase change in arabidopsis. *Plant Cell*. https://doi.org/10.1105/tpc.15.00854

Xu, M., Hu, T., Zhao, J., Park, M. Y., Earley, K. W., Wu, G., Yang, L., & Poethig, R. S. (2016). Developmental Functions of miR156-Regulated SQUAMOSA PROMOTER BINDING PROTEIN-LIKE (SPL) Genes in Arabidopsis thaliana. *PLoS Genetics*. https://doi.org/10.1371/journal.pgen.1006263

Yamaguchi, A., Kobayashi, Y., Goto, K., Abe, M., & Araki, T. (2005). TWIN SISTER of FT (TSF) acts as a floral pathway integrator redundantly with FT. *Plant and Cell Physiology*. https://doi.org/10.1093/pcp/pci151

Yamaguchi, A., Wu, M. F., Yang, L., Wu, G., Poethig, R. S., & Wagner, D. (2009). The MicroRNA-Regulated SBP-Box Transcription Factor SPL3 Is a Direct Upstream Activator of LEAFY, FRUITFULL, and APETALA1. *Developmental Cell*. https://doi.org/10.1016/j.devcel.2009.06.007

Yamaguchi, N., Winter, C. M., Wellmer, F., & Wagner, D. (2015). Identification of direct targets of plant transcription factors using the GR fusion technique. *Methods in Molecular Biology*. https://doi.org/10.1007/978-1-4939-2444-8_6

Yamaguchi, N., Winter, C. M., Wu, M. F., Kanno, Y., Yamaguchi, A., Seo, M., & Wagner, D. (2014). Gibberellin acts positively then negatively to control onset of flower formation in Arabidopsis. *Science*. https://doi.org/10.1126/science.1250498

Yamasaki, H., Hayashi, M., Fukazawa, M., Kobayashi, Y., & Shikanai, T. (2009). SQUAMOSA promoter binding protein-like7 is a central regulator for copper homeostasis in Arabidopsis. *Plant Cell*. https://doi.org/10.1105/tpc.108.060137

Yamasaki, K., Kigawa, T., Inoue, M., Tateno, M., Yamasaki, T., Yabuki, T., Aoki, M., Seki, E., Matsuda, T., Nunokawa, E., Ishizuka, Y., Terada, T., Shirouzu, M., Osanai, T., Tanaka, A., Seki, M., Shinozaki, K., & Yokoyama, S. (2004). A Novel Zinc-binding Motif Revealed by Solution Structures of DNA-binding Domains of Arabidopsis SBP-family Transcription Factors. *Journal of Molecular Biology*. https://doi.org/10.1016/j.jmb.2004.01.015

Yan, J., Chia, J. C., Sheng, H., Jung, H. Il, Zavodna, T. O., Zhang, L., Huang, R., Jiao, C., Craft, E. J., Fei, Z., Kochian, L. V., & Vatamaniuk, O. K. (2017). Arabidopsis pollen fertility requires the transcription factors CITF1 and SPL7 that regulate copper delivery to anthers and jasmonic acid synthesis. *Plant Cell*. https://doi.org/10.1105/tpc.17.00363

Yang, H., Berry, S., Olsson, T. S. G., Hartley, M., Howard, M., & Dean, C. (2017). Distinct phases of Polycomb silencing to hold epigenetic memory of cold in Arabidopsis. *Science*. https://doi.org/10.1126/science.aan1121

Yang, L., Xu, M., Koo, Y., He, J., & Scott Poethig, R. (2013). Sugar promotes vegetative phase change in Arabidopsis thaliana by repressing the expression of MIR156A and MIR156C. *ELife*. https://doi.org/10.7554/eLife.00260

Yant, L., Mathieu, J., Dinh, T. T., Ott, F., Lanz, C., Wollmann, H., Chen, X., & Schmid, M. (2010). Orchestration of the floral transition and floral development in arabidopsis by the bifunctional transcription factor APETALA2. *Plant Cell*. https://doi.org/10.1105/tpc.110.075606

Yao, T., Park, B. S., Mao, H. Z., Seo, J. S., Ohama, N., Li, Y., Yu, N., Mustafa, N. F. B., Huang, C. H., & Chua, N. H. (2019). Regulation of flowering time by SPL10/MED25 module in Arabidopsis. *New Phytologist*. https://doi.org/10.1111/nph.15954

Yoo, S. K., Chung, K. S., Kim, J., Lee, J. H., Hong, S. M., Yoo, S. J., Yoo, S. Y., Lee, J. S., & Ahn, J. H. (2005). CONSTANS activates SUPPRESSOR OF OVEREXPRESSION OF CONSTANS 1 through FLOWERING LOCUS T to promote flowering in Arabidopsis. *Plant Physiology*. https://doi.org/10.1104/pp.105.066928

Yu, N., Cai, W. J., Wang, S., Shan, C. M., Wang, L. J., & Chena, X. Y. (2010). Temporal control of trichome distribution by microRNA156-targeted SPL genes in Arabidopsis thaliana. *Plant Cell*. https://doi.org/10.1105/tpc.109.072579

Yu, S., Galvão, V. C., Zhang, Y. C., Horrer, D., Zhang, T. Q., Hao, Y. H., Feng, Y. Q., Wang, S., Schmid, M., & Wang, J. W. (2012). Gibberellin regulates the Arabidopsis floral transition through miR156-targeted SQUAMOSA PROMOTER BINDING-LIKE transcription factors. *Plant Cell*. https://doi.org/10.1105/tpc.112.101014

Yu, S., Li, C., Zhou, C. M., Zhang, T. Q., Lian, H., Sun, Y., Wu, J., Huang, J., Wang, G., & Wang, J. W. (2013). Sugar is an endogenous cue for juvenile-to-adult phase transition in plants. *ELife*. https://doi.org/10.7554/eLife.00269

Yuan, W., Luo, X., Li, Z., Yang, W., Wang, Y., Liu, R., Du, J., & He, Y. (2016). A cis cold memory element and a trans epigenome reader mediate Polycomb silencing of FLC by vernalization in Arabidopsis. *Nature Genetics*. https://doi.org/10.1038/ng.3712

Zhang, B., Wang, L., Zeng, L., Zhang, C., & Ma, H. (2015). Arabidopsis TOE proteins convey a photoperiodic signal to antagonize CONSTANS and regulate flowering time. *Genes and Development*. https://doi.org/10.1101/gad.251520.114

Zhang, R., Calixto, C. P. G., Marquez, Y., Venhuizen, P., Tzioutziou, N. A., Guo, W., Spensley, M., Entizne, J. C., Lewandowska, D., Have, S. Ten, Frey, N. F., Hirt, H., James, A. B., Nimmo, H. G., Barta, A., Kalyna, M., & Brown, J. W. S. (2017). A high quality Arabidopsis transcriptome for accurate transcript-level analysis of alternative splicing. *Nucleic Acids Research*. https://doi.org/10.1093/nar/gkx267

Zhang, T., Marand, A. P., & Jiang, J. (2016). PlantDHS: A database for DNase I hypersensitive sites in plants. *Nucleic Acids Research*. https://doi.org/10.1093/nar/gkv962

Zhang, Y., Song, G., Lal, N. K., Nagalakshmi, U., Li, Y., Zheng, W., Huang, P. jui, Branon, T. C., Ting, A. Y., Walley, J. W., & Dinesh-Kumar, S. P. (2019). TurboID-based proximity labeling reveals that UBR7 is a regulator of N NLR immune receptor-mediated immunity. *Nature Communications*. https://doi.org/10.1038/s41467-019-11202-z

Zhao, J., Jiang, L., Che, G., Pan, Y., Li, Y., Hou, Y., Zhao, W., Zhong, Y., Ding, L., Yan, S., Sun, C., Liu, R., Yan, L., Wu, T., Li, X., Weng, Y., & Zhanga, X. (2019). A Functional Allele of CsFUL1 regulates fruit length through repressing CsSUP and inhibiting auxin transport in cucumber. *Plant Cell*. https://doi.org/10.1105/tpc.18.00905

Zhao, X., Wang, J., Yuan, J., Wang, X. L., Zhao, Q. P., Kong, P. T., & Zhang, X. (2015). NITRIC OXIDE-ASSOCIATED PROTEIN1 (AtNOA1) is essential for salicylic acid-induced root waving in Arabidopsis thaliana. *New Phytologist*. https://doi.org/10.1111/nph.13327

Zhu, Q. H., & Helliwell, C. A. (2011). Regulation of flowering time and floral patterning by miR172. *Journal of Experimental Botany*. https://doi.org/10.1093/jxb/erq295

Zuo, J., Niu, Q. W., & Chua, N. H. (2000). An estrogen receptor-based transactivator XVE mediates highly inducible gene expression in transgenic plants. *Plant Journal*. https://doi.org/10.1046/j.1365-313X.2000.00868.x

Acknowledgements

I would very much like to Prof. Dr. George Coupland, my supervisor and promoter, for all his guidance throughout my PhD. Thanks for the opportunity to work in your lab, for all your support and the countless scientific discussions and hypothesizing meetings we've had about floral induction. I hope I haven't been too much of a burden with my Dutch rudeness.

I would also like to thank my examination committee; Prof. Dr. Ute Hoecker, Prof. Dr. Martin Huelskamp and Dr. Franziska Turck, for taking the time to evaluate my thesis and to assess my PhD defence.

Thanks to the members of my Thesis Advisory Committee for their efforts in guiding my project and taking important decisions when things did not work out as I would have wanted. Thanks to Prof. Dr. Klaus Theres for your ideas during the TAC-meetings. Especially thanks to Dr. Diarmuid O'Maoileidigh, for your tips and tricks in the lab, your guidance throughout my PhD, and the opportunity to work with the amazing materials you generated. I have learned a lot about tweaking ChIP experiments, CRISPR and bar jokes. I would also like to thank Dr. Alice Pajoro, for bringing in the practical aspects of some of my experiments, for your tips during my TAC-meetings and your views on plant sciences in Holland, I have always very much appreciated your view

Thanks Dr. Jennifer Andres and Prof. Dr. Matias Zurbriggen for the collaboration on the *FUL* promoter in mammalian cells.

Dr. Edouard Severing, wat heb ik tering veel van jou geleerd! Echt enorm bedankt voor al je hulp met R, Linux en transcriptome analysis, ik had me geen slimmere, praktischere en grappigere leermeester kunnen wensen. Fiets ze!

Thanks to Dr. René Richter and Dr. Youbong Hyun for all the work you have done on SPL15, and all the plant materials that I could directly work with. René, thank you for teaching me how to precisely do ChIPs, and how to think about all the aspects involved in transcriptional regulation.

Thanks to all former and current Coupland-group members for their advice, technical tips, scientific discussions and for all the lunches and dinners we've had. You've all contributed to making this a better thesis.

Ich möchte auch gerne die Gärtner nochmal herzlich danken für die gute Versorgung von meinem Arabidopsis Unkraut. Vielen lieben Dank Sybille, Monika, Heike, Manfred, Maxime, John, Julia und natürlich Aristeidis!

Liebe Renate und Ecki, euch muss ich auch unbedingt danken für eure Hilfe in Halle 14! Ohne euch beide würde es viel mehr Kaputte Kammern geben und würde leider viele Experimenten zerstört

werden.

Thanks to Stephan Wagner for being a great PhD coordinator and being involved with the students. I very much appreciated all your help with organising documents at UoC and thank you so much for helping out with my reviewers!

Thank you, Adrian Roggen and Enric Bertran Garcia de Olalla, for being such cool office mates and Hall-14 Gatekeepers. Special thanks to Adrian for your incredible humour, intelligent remarks, for sharing your amazing confocal images and of course for sharing cookies! I hope both of you were okay with Laserkraft's "Nein-Mann" on Friday and my disturbances with useless facts and ideas.

Thanks to Laura Trimborn, Tim Neefjes and Miguel Wente for collaborating on some of the experiments, I have learned a lot about supervising thanks to you!

Liebe Michaela, Kerstin und Brigitte, danke für eure Hilfe im Labor, mit meinem Deutsch und die tolle Gespräche über das Leben außerhalb der Arbeit.

Dear Procrastinators Anonymous members, let's stop being anonymous. Thanks Leo, Ale, Beta, Ivo, Lennert, Chloé, Nora, Kees and Marco for all the trips, hikes, jokes, beers and mental support during the past years. By the way, let's not stop doing all these things:)

I would also like to thank Dr. Marcel Proveniers for inspiring me to follow-up on my curiosity and to continue doing what I like. We've had many discussions about floral induction, about plant sciences and your enthusiasm has always kept me going, even after I left your lab.

Maar daar heb ik niet alleen Marcel voor te danken, Evelien Stouten, ik wil jou ook heel graag enorm bedanken voor het delen van al je skills tijdens mijn eerste jaren in het lab. Ik bakte er niet altijd wat van, en ben blij dat je me dat niet kwalijk genomen hebt. Je hebt er aan bijgedragen dat ik het labwerk nog altijd ontzettend leuk vind, zelfs als het niet helemaal loopt zoals ik zou willen.

Thanks beste vriendinnetje Bel, in Sydney en op Christmas Island, voor het aanhoren van mijn geklaag over mijn PhD en voor alle daar op volgende bemoedigende toespraken. Nu ben jij aan de beurt, you can do it!

Roos, Ren, Piet, mama, Margo, papa, Willeke, Ger, Robert, Joachim, Max en Aad, bedankt voor jullie bezoekjes en belletjes om het hier tijdens onaangename tijden beter te maken, en het delen van jullie verhalen uit Nederland.

Lieve Jor, jij mag als laatste, maar hoort eigenlijk bovenaan. Bedankt voor al je hulp en je steun door dik en dun. Wat hebben we samen veel kutte en toffe tijden beleefd. Wat fantastisch dat we al onze wetenschappelijke inzichten konden delen en verbeteren. Eens kijken of we deze samenwerkingsskills ook kunnen toepassen in ons volgende avontuur.

Erklärung zur Dissertation

"Ich versichere, dass ich die von mir vorgelegte Dissertation selbständig angefertigt, die benutzten Quellen und Hilfsmittel vollständig angegeben und die Stellen der Arbeit − einschließlich Tabellen, Karten und Abbildungen −, die anderen Werken im Wortlaut oder dem Sinn nach entnommen sind, in jedem Einzelfall als Entlehnung kenntlich gemacht habe; dass diese Dissertation noch keiner anderen Fakultät oder Universität zur Prüfung vorgelegen hat; dass sie − abgesehen von unten angegebenen Teilpublikationen − noch nicht veröffentlicht worden ist, sowie, dass ich eine solche Veröffentlichung vor Abschluss des Promotionsverfahrens nicht vornehmen werde. Die Bestimmungen der Promotionsordnung sind mir bekannt. Die von mir vorgelegte Dissertation ist von Prof. Dr. George Coupland betreut worden."

13. July 2020

*Erklärung zur Dissertation gemäß der Promotionsordnung vom 02. Februar 2006 mit den Änderungsordnungen vom 10. Mai 2012, 16. Januar 2013 und 21. Februar 2014